Dissecting the molecular responses of *Sorghum bicolor* to *Macrophomina phaseolina* infection

by

Y. M. Ananda Yapa Bandara

B.S., University of Peradeniya, Sri Lanka, 2008
M.S., University of Peradeniya, Sri Lanka, 2010

AN ABSTRACT OF A DISSERTATION

Submitted in partial fulfillment of the requirements for the degree

DOCTOR OF PHILOSOPHY

Department of Plant Pathology
College of Agriculture

KANSAS STATE UNIVERSITY
Manhattan, Kansas

2017

Abstract

Charcoal rot, caused by the necrotrophic fungus, *Macrophomina phaseolina* (Tassi) Goid., is an important disease in sorghum (*Sorghum bicolor* (L.) Moench). The molecular interactions between sorghum and *M. phaseolina* are poorly understood. In this study, a large-scale RNA-Seq experiment and four follow-up functional experiments were conducted to understand the molecular basis of charcoal rot resistance and/or susceptibility in sorghum.

In the first experiment, stalk mRNA was extracted from charcoal-rot-resistant (SC599) and susceptible (Tx7000) genotypes and subjected to RNA sequencing. Upon *M. phaseolina* inoculation, 8560 genes were differentially expressed between the two genotypes, out of which 2053 were components of 200 known metabolic pathways. Many of these pathways were significantly up-regulated in the susceptible genotype and are thought to contribute to enhanced pathogen nutrition and virulence, impeded host basal immunity, and reactive oxygen (ROS) and nitrogen species (RNS)-mediated host cell death. The paradoxical hormonal regulation observed in pathogen-inoculated Tx7000 was characterized by strongly upregulated salicylic acid and down-regulated jasmonic acid pathways. These findings provided useful insights into induced host susceptibility in response to this necrotrophic fungus at the whole-genome scale.

The second experiment was conducted to investigate the dynamics of host oxidative stress under pathogen infection. Results showed *M. phaseolina*'s ability to significantly increase the ROS and RNS content of two charcoal-rot-susceptible genotypes, Tx7000 and BTx3042. Over-accumulation of nitric oxide (NO) in stalk tissues in the pathogen-inoculated susceptible genotypes was confirmed using a NO-specific fluorescent probe and confocal microscopy. Significantly increased malondialdehyde content confirmed the enhanced oxidative stress experienced by the susceptible genotypes after pathogen inoculation. These findings suggested the contribution of oxidative stress-associated induced cell death on charcoal rot susceptibility under infection.

In the third functional experiment, the behavior of the sorghum antioxidant system after pathogen inoculation was investigated. *M. phaseolina* significantly increased the glutathione s-

transferase (GST), glutathione peroxidase (GPX), glutathione reductase (GR), and peroxidase activities of the susceptible genotypes (Tx7000, BTx3042) but not in the resistant genotypes (SC599, SC35). Increased activities of these enzymes in susceptible genotypes may contribute to reduced oxidative stress thus lowering charcoal rot susceptibility.

The fourth functional experiment was designed to quantify induced host-derived cell wall degrading enzymes (CWDEs) using crude enzyme mixtures from stalks. A gel diffusion assay revealed significantly increased pectinesterase activity in pathogen-inoculated Tx7000 and BTx3042 while significantly increased polygalacturonase activity was determined by absorbance. Fluorimetric determination of cell extracts revealed significantly increased cellulose degrading enzyme activity in *M. phaseolina*-inoculated Tx7000 and BTx3042. These findings revealed the pathogen's ability to promote charcoal rot susceptibility in grain sorghum through induced host CWDEs.

The last functional study was designed to profile the stalk tissue lipidome of Tx7000 and SC599 after *M. phaseolina* inoculation using automated direct infusion electrospray ionization-triple quadrupole mass spectrometry (ESI-MS/MS). *M. phaseolina* significantly decreased the phytosterol, phosphatidylserine, and ox-lipid contents in Tx7000 while significantly increasing stigmasterol:sitosterol ratio. Except for ox-lipid content, none of the above was significantly affected in resistant SC599. Results suggested the lethal impacts of *M. phaseolina* inoculation on plastid- and cell- membrane integrity and the lipid-based signaling capacity of Tx7000. Findings shed light on the host lipid classes that contribute to induced charcoal rot susceptibility in grain sorghum.

Dissecting the molecular responses of *Sorghum bicolor* to *Macrophomina phaseolina* infection

by

Y. M. Ananda Yapa Bandara

B.S., University of Peradeniya, Sri Lanka, 2008
M.S., University of Peradeniya, Sri Lanka, 2010

A DISSERTATION

Submitted in partial fulfillment of the requirements for the degree

DOCTOR OF PHILOSOPHY

Department of Plant Pathology
College of Agriculture

KANSAS STATE UNIVERSITY
Manhattan, Kansas

2017

Approved by:

Major Professor
Dr. Christopher R. Little

Copyright

Abstract

Charcoal rot, caused by the necrotrophic fungus, *Macrophomina phaseolina* (Tassi) Goid., is an important disease in sorghum (*Sorghum bicolor* (L.) Moench). The molecular interactions between sorghum and *M. phaseolina* are poorly understood. In this study, a large-scale RNA-Seq experiment and four follow-up functional experiments were conducted to understand the molecular basis of charcoal rot resistance and/or susceptibility in sorghum.

In the first experiment, stalk mRNA was extracted from charcoal-rot-resistant (SC599) and susceptible (Tx7000) genotypes and subjected to RNA sequencing. Upon *M. phaseolina* inoculation, 8560 genes were differentially expressed between the two genotypes, out of which 2053 were components of 200 known metabolic pathways. Many of these pathways were significantly up-regulated in the susceptible genotype and are thought to contribute to enhanced pathogen nutrition and virulence, impeded host basal immunity, and reactive oxygen (ROS) and nitrogen species (RNS)-mediated host cell death. The paradoxical hormonal regulation observed in pathogen-inoculated Tx7000 was characterized by strongly upregulated salicylic acid and down-regulated jasmonic acid pathways. These findings provided useful insights into induced host susceptibility in response to this necrotrophic fungus at the whole-genome scale.

The second experiment was conducted to investigate the dynamics of host oxidative stress under pathogen infection. Results showed *M. phaseolina*'s ability to significantly increase the ROS and RNS content of two charcoal-rot-susceptible genotypes, Tx7000 and BTx3042. Over-accumulation of nitric oxide (NO) in stalk tissues in the pathogen-inoculated susceptible genotypes was confirmed using a NO-specific fluorescent probe and confocal microscopy. Significantly increased malondialdehyde content confirmed the enhanced oxidative stress experienced by the susceptible genotypes after pathogen inoculation. These findings suggested the contribution of oxidative stress-associated induced cell death on charcoal rot susceptibility under infection.

In the third functional experiment, the behavior of the sorghum antioxidant system after pathogen inoculation was investigated. *M. phaseolina* significantly increased the glutathione s-

transferase (GST), glutathione peroxidase (GPX), glutathione reductase (GR), and peroxidase activities of the susceptible genotypes (Tx7000, BTx3042) but not in the resistant genotypes (SC599, SC35). Increased activities of these enzymes in susceptible genotypes may contribute to reduced oxidative stress thus lowering charcoal rot susceptibility.

The fourth functional experiment was designed to quantify induced host-derived cell wall degrading enzymes (CWDEs) using crude enzyme mixtures from stalks. A gel diffusion assay revealed significantly increased pectinesterase activity in pathogen-inoculated Tx7000 and BTx3042 while significantly increased polygalacturonase activity was determined by absorbance. Fluorimetric determination of cell extracts revealed significantly increased cellulose degrading enzyme activity in *M. phaseolina*-inoculated Tx7000 and BTx3042. These findings revealed the pathogen's ability to promote charcoal rot susceptibility in grain sorghum through induced host CWDEs.

The last functional study was designed to profile the stalk tissue lipidome of Tx7000 and SC599 after *M. phaseolina* inoculation using automated direct infusion electrospray ionization-triple quadrupole mass spectrometry (ESI-MS/MS). *M. phaseolina* significantly decreased the phytosterol, phosphatidylserine, and ox-lipid contents in Tx7000 while significantly increasing stigmasterol:sitosterol ratio. Except for ox-lipid content, none of the above was significantly affected in resistant SC599. Results suggested the lethal impacts of *M. phaseolina* inoculation on plastid- and cell- membrane integrity and the lipid-based signaling capacity of Tx7000. Findings shed light on the host lipid classes that contribute to induced charcoal rot susceptibility in grain sorghum.

Table of Contents

List of Figures

List of Tables

Acknowledgements

I wish to express my most sincere gratitude and appreciation to my major professor, Dr. Christopher R. Little for accepting me into his research program, providing all the financial assistance, and granting with me the academic freedom to thrive as a scholar and a researcher during my graduate career. I am grateful to my advisory committee Drs. William Bockus, Tesfaye Tesso, and Sanzhen Liu for their invaluable advice and assistance during the period. I'm also grateful to Dr. Loretta Johnson for serving as the outside chair of my thesis committee. I would also like to gratefully acknowledge the Kansas Grain Sorghum Commission and Center for Sorghum Improvement (CSI) for funding our research.

I would like to extend my acknowledgements to Drs. Philine Wangemann, Donghai Wang, Scott Bean, Floyd Dowell, Ruth Welti, and Ramasamy Perumal for providing various facilities and services and collaborating with us in various research projects. Drs. Shantha Peiris, Dereje Gobena, K. Zhang, Messrs. Joel Sanneman, Daniel J. Hopper, Chad Brady, Lance Noll, and Ms. Natalie Waite are also acknowledged for their technical assistance.

My hearty gratitude goes to my mother, B.M.I. Kumaratilaka and father, Y.M.P. Yapa for their incessant support and being exemplary in teaching me the value of dedication, organization, assertiveness, honesty, and simplicity. I am grateful to my beloved wife, Dr. Dilooshi Weerasooriya for her patience, love, and constant encouragement in the journey of life and being together with me on my mundane and supramundane achievements and goals. My sisters, W.Y. Bandara, A.Y. Bandara, and B.Y. Bandara and brothers-in-law, Layantha Bandara, Prabhath Gorockgahagoda, and Damith Abeykoon are also gratefully appreciated for their support. I'm thankful to my uncles, Dr. Mahinda Ekanayaka, Mr. Hemachandra Karunathilaka and Mr. Wijekoon Bandara and aunts, Mrs. Premalatha Tikirikumarihami, Mrs. Sunethra Kumarihami, and Dr. Nilmini Ekanayaka as well as my parents-in-law, Mrs. Rohini Moragolla and Mr. Cyril Bandara for their assistance extended to me during past years. A word of thanks goes to all my teachers from kindergarten to university for their contribution to who I am today.

I also wish to thank the faculty and office staff members of the Plant Pathology Department for their kind and friendly support during past years. The Department of Plant Pathology at Kansas State University is greatly admired for the quality graduate education and research excellence.

Dedication

With the utmost gratitude, I dedicate this work to the "Noble Triple Gem" for bestowing me with the rationale, path, guidance, and fortitude to elude the "world" and be free from "presence" and "absence."

Chapter 1 - Literature Review

Sorghum bicolor (L) Moench

Sorghum [*Sorghum bicolor* (L) Moench] is the fifth most important cereal crop grown worldwide (FAO, 2007). It is a staple for many nations in sub-Saharan African region. Around the world, sorghum is utilized as an important source of food, feed, sugar, and fiber. With the recent interest in bioenergy feedstocks, sorghum has been recognized as a promising alternative for sustainable biofuel production. The United States Department of Agriculture's Prospective Plantings report revealed that 6.69 million acres of land were under sorghum cultivation in 2016. Its comparative advantages include drought tolerance, resistance to mycotoxins and fungi, and survivability in relatively harsher climatic conditions. Adding tremendous value to the American economy, U.S. sorghum exports were valued at more than $2.1 billion in 2015. Although sorghum is grown as feed and industrial grain in the Americas and Australia, Africa and Asia grow it as a food (Dykes et al., 2005, Rooney and Waniska, 2000). However, sorghum is becoming more popular as a food in the United States with the discovery of the health-associated benefits of sorghum, including its gluten-free characteristics, low glycemic index, cholesterol-lowering properties, anti-inflammatory, and anti-carcinogenic properties (Bralley et al., 2008; Burdette et al., 2010; Moraes et al., 2012; Turner et al., 2006; Yang et al., 2009).

The sorghum genome (line BTx623) was sequenced and reported by Paterson et al. (2009). Availability of the sorghum genome sequence has laid the foundation towards coupling sorghum genes to their functions and to perform powerful comparative genomics analyses. The size of the sorghum genome is 732.2 Mb, which is larger than that of rice (430 Mb) and ~ 3- fold smaller than that of maize (2400 Mb) (Arumuganathan and Earle, 1991). The sorghum genome includes 34,211 loci containing protein-coding transcripts and 47,205 protein-coding transcripts (*Sorghum bicolor* v3.1 DOE-JGI, http://phytozome.jgi.doe.gov/). Its comparatively small genome makes sorghum an attractive model for functional genomics of the Saccharinae and other C4 grasses. Sorghum is an important target for plant genomics due to its adaptation to harsh environments and wide genetic diversity (Menz et al., 2002). Sorghum is a diverse genus which contains both cultivated and wild species, many of which are inter-fertile. Among these, *Sorghum bicolor* (2n

= 20) is the most important taxon that includes the cultivated races. Sorghum is predominantly self-pollinated and is functionally diploid.

Sorghum stalk rot diseases

Stalk rots are among the most ubiquitous diseases of sorghum (Zummo 1984; Jardine 2006). These diseases show a wide geographic distribution and consequently occur in both tropical and temperate environments (Tarr 1962). Stalk rots are a common problem in the sorghum growing areas of the United States particularly in the southern states and in the central Great Plains (Duncan 1983; Edmunds 1964; Edmunds & Zummo 1975, Reed et al. 1983). Most stalk rot pathogens colonize the stalk and cause disease during the post-flowering stages (Ilyas et al. 1976; Reed et al. 1983). Stalk rot diseases cause degradation of the pith tissue at or near the base of the stalk (Edmunds 1964). Infection often results in damaged vascular and cortical tissues in both the stalk and root system which results in reduced water and nutrient uptake and translocation (Hundekar & Anahosur 1994). Stalk rot disease, under severe circumstances, may result in complete disintegration of root and stalk tissues, which leads to lodging (Zummo 1984). Based upon the responsible causal organisms, there are two sorghum stalk rot diseases. Charcoal rot caused by *Macrophomina phaseolina* (Tassi) Goidanich and Fusarium stalk rot, caused by different *Fusarium* spp. (Tarr 1962). These are the most widespread stalk rot pathogens in tropical, subtropical, and temperate regions, although several other pathogens such as *Colletotrichum sublineolum* and *C. graminicola* can also cause stalk rots (Tarr 1962). Among *Fusarium* spp., *F. thapsinum* Klittich, Leslie, Nelson & Marasas is one of the most aggressive stalk rot pathogens of sorghum (Leslie et al. 2005; Tesso et al. 2005; Tesso et al. 2010; Tesso & Ejeta 2011). *F. thapsinum* is capable of infecting certain sorghum hybrids as early as 30 days after planting (Khune et al. 1984). *Fusarium andiyazi* Marasas, Rheeder, Lampr, Zeller & Leslie and *F. proliferatum* (Matsush.) Nirenberg, Gerlach & Nirenberg are also considered as important stalk rotting *Fusarium* species. Charcoal rot incidences are more pronounced when plants are exposed to prolonged drought and high temperature stress during the grain development stage (Edmunds 1964; Tesso et al. 2012). Fusarium stalk rot is generally more severe when drought and high temperature occur during grain development followed by wet and cool conditions near physiological maturity (Zummo 1980).

The symptoms of stalk rot disease are visible to the naked eye when an infected sorghum stalk is longitudinally split. Fusarium infection is characterized by a reddish to pink colored lesion in a split open stem. The characteristic lesion color is commonly attributed to infection-associated host anthocyanin (primarily 3-deoxyanthocyanidin) production although no published reports are available that exclusively demonstrate host anthocyanin profiles under disease pressure. Lesions may be visible in uppermost internodes and the peduncle particularly in highly susceptible genotypes. *Fusarium* stalk rot signs include premature plant death and grain ripening, or impeded grain filling (Tarr, 1962). Stalk infection by *M. phaseolina* is characterized by distinctive grey to black color pigmentation in the infected area. Often, as the infected plant matures and reaches senescence phase, bundles of small, black microsclerotia are observed in the infected area. These are important internal signs of the disease.

Impact of stalk rot diseases on grain sorghum yield components

Poor standability and reduced grain weight are the major stalk rot-mediated yield losses in grain sorghum (Tesso et al., 2012). Zummo (1980) reported that stalk rots impede or inhibit the grain-filling process and result in shriveled seeds. However, varying levels of lodging have been identified by Anahosur and Patil (1983) as the major contributor to charcoal rot-mediated sorghum seed weight losses. Seetharama et al. (1991) reported that there were no simple correlations between charcoal rot disease incidence and sorghum yield or yield components. However, their conclusions remain doubtful as the findings were based upon a study conducted in a field where *M. phaseolina* was supposed to be present based on historical data. Therefore, no controlled inoculation was adopted which questions the uniformity of infection. Moreover, the observed stalk rot incidences were attributed to *M. phaseolina*, just based on symptomatology. Authors have never isolated the causal organism from symptomatic stalk tissues to confirm the species identity. Moreover, a few publications have provided information concerning the plant growth stage at which stalk rot infections occur and possible impacts they could have on yield. For example, Reed et al. (1983) and Jardine and Leslie (1992) reported that most stalk rot pathogens colonize the stalk and incite disease during the “post-flowering” stages whereas Khune et al. (1984) indicated that stalk rot pathogens are found in host tissues at various sorghum growth stages.

Sorghum yield components are comprised of the number of panicles per square meter, number of seeds per panicle, and seed weight, which are defined as the first, second, and third yield components, respectively (Maman et al., 2004). A simple development stage terminology for describing yield and yield components of grain sorghum was put forward by Eastin and Sullivan (1974) according to the following growth stages: (i) the vegetative period from planting to panicle initiation (GS1); (ii) the reproductive period from panicle initiation to flowering (GS2); and (iii) grain filling from flowering to physiological maturity (GS3). The number of seeds per panicle is physiologically determined during GS2 when floret number is set in the developing panicle (Eastin et al., 1999; Maiti and Bidinger, 1981). As the second yield component directly relates to GS2, any biotic and/or abiotic stress that prevails before or at the onset of this stage could have adverse effects on the second yield component. Similarly, since seed filling is largely related with GS3, stresses occurring at this stage may influence the third yield component.

When stalk inoculations were performed at GS1 and GS3, Bandara et al. (2017a) showed the ability of stalk rot pathogens (*F. thapsinum*, *F. proliferatum*, *F. andiyazi*, and *M. phaseolina*) to significantly reduce total seed weight per panicle (TSWP) at both stages (in comparison to control). The four pathogens, on average, caused greater TSWP reduction when inoculated at GS1 (52%) than at GS3 (37%). All pathogens significantly reduced total seeds per panicle upon GS1 inoculation and 100-seed weight upon GS3 inoculation. Although inoculations at GS3 did not have a significant impact, all pathogens significantly reduced percent seed set when inoculations were performed at GS1. GS1 inoculation was also found to significantly decrease total number of reproductive sites per panicle, demonstrating pathogen interference with head formation resulting in smaller heads than control. This study appeared to be the first systematic investigation which revealed inoculation stage-specific effects of stalk rot pathogens on yield components of grain sorghum under controlled inoculations. Bandara et al. (2017a) also provided insights into key yield traits to be emphasized in sorghum breeding programs to produce stalk rot tolerant sorghum genotypes.

Impact of stalk rot diseases on sweet sorghum

Sweet sorghum (*Sorghum bicolor* (L.) Moench) is a prospective feedstock for bioethanol production. Like sugarcane (*Saccharum* spp.), sweet sorghum juice can be directly fermented

into ethanol. Moreover, unlike sugarcane, sweet sorghum can be widely cultivated across the United States (Keeney and DeLuca 1992; Smith et al., 1987). Sweet sorghum stalks contain sugar and biomass in high amounts (20 to 30 dry tons/ha) (Wang et al., 2008; Barbanti et al., 2006). In comparison to maize and sugarcane, sweet sorghum has higher tolerance to abiotic stresses such as drought and waterlogging and is well adapted to marginal soils (Reddy and Reddy 2003; Ali et al., 2008). As it needs less water than sugarcane (-33%) and corn (-50%) and requires lower nutrient amendments, sweet sorghum is appropriate for low-input agricultural production systems (Smith and Frederiksen 2000). The aforementioned attributes make sweet sorghum an ideal feedstock for bioethanol production.

Although several reports demonstrated the impacts of stalk rots on grain sorghum yields, quality, and biomass (Bandara et al., 2017a; Bandara et al., 2017b; Bean et al., 2013; Funnell-Harris et al., 2014; Miron et al., 2005; Rajewski and Francis 1991; Tesso et al., 2005), a few reports are available for their effects on sweet sorghum (Funnell-Harris et al., 2016, Bandara et al., 2017c). Stalk rot-mediated lodging is a major concern with sweet sorghum cultivation. Using lesion length measurements in inoculated peduncles, sweet sorghum lines 'Rio' and 'M81E' have been shown to be resistance to *F. thapsinum* and *M. phaseolina*, respectively while, the line 'Colman' has been identified as susceptible to both pathogens (Funnell-Harris et al., 2016).

Bandara et al. (2017c) reported the impacts of Fusarium stalk rot (*F. thapsinum*) and charcoal rot (*M. phaseolina*) diseases on sweet sorghum biofuel traits using stalk inoculations. On average, *F. thapsinum* and *M. phaseolina* reduced grain weight and dried bagasse weight by 17.4 and 17.6%, respectively, across genotypes. Depending on the genotype, pathogens reduced juice weight, BRIX, and total soluble sugars per plant in the ranges of 11.3 to 25.9, 0.2 to 16.7, and 21.2 to 33.3%, respectively. Moreover, their estimations revealed that dried bagasse and grain weight reductions can lead up to 1050 and 800 L ethanol yield loss per hectare, respectively. The ability of stalk rot diseases to reduce the juice weight and BRIX (up to 25.9 and 16.7%, respectively) was also demonstrated. These reductions are estimated to cause reductions in juice (sugar)-based ethanol yields in the range of 424 to 1460 L ha^{-1}, depending on the hybrid. Therefore, Bandara et al. (2017c) demonstrated the negative impacts of these diseases on lignocellulosic-, starch-, and juice-based bioethanol yields. Their results also revealed non-significant general and specific

combining abilities (for stalk rot resistance) of the parental sorghum genotypes used in the study. This indicated the lack of comparative advantage of using a given parent over the others to produce a hybrid with significantly higher resistance to Fusarium stalk rot and charcoal rot diseases. Therefore, identifying new parents with better combining ability for producing hybrids with superior resistance to stalk rot disease is pivotal for the sustainability of a sweet sorghum-based bioethanol industry.

Relationship between stalk rot resistance and tolerance with staygreen trait

As it improves the ability to adapt to post-flowering drought stress (particularly when the crop depends on residual soil moisture for grain development and maturity), staygreen (or delayed senescence) in sorghum is commonly accepted as a valuable trait (Rosenow et al. 1977). Greater green-leaf-area duration during grain filling is the result of different combinations of three factors: green leaf area at flowering, senescence onset time, and rate of senescence (Borrell et al. 2000a; van Oosterom et al. 1996). Soil and plant analytical development (SPAD) meter values measured with leaves at physiological maturity is a direct indicator of the staygreen trait (Xu et al., 2000). Staygreen is reported to be associated with decreased lodging (Mughogho and Pande 1984) and reduced susceptibility to charcoal rot disease (Mughogho and Pande 1984; Tenkouano et al. 1993). Therefore, selection for the staygreen trait could help minimizing the charcoal rot incidence in the field.

Through a two-year field study conducted using staygreen and non-staygreen sorghum lines (SC599, BTx3042) and hybrids (84G62, DKD37-07), Bandara et al. (2016) investigated the relationship between SPAD and disease severity after inoculation with *F. thapsinum*, *F. proliferatum*, *F. andiyazi*, and *M. phaseolina* inoculation. SPAD readings were obtained at soft-dough, hard-dough, and physiological maturity. Results revealed the ability of all pathogens to significantly reduce SPAD of the genotypes over the mock-inoculated control at three developmental stages. The stalk-rot-resistant and staygreen check line, SC599, exhibited a remarkable feature of negative senescence from soft dough to physiological maturity under disease pressure. Demonstrating the potential beneficial impact of the staygreen trait on stalk rot resistance, Bandara et al. (2016) revealed a significant and negative linear correlation between disease severity and SPAD at all developmental stages. Moreover, the difference between control

and pathogen treated SPAD at physiological maturity was significantly and positively correlated with the difference between control and pathogen-treated total seed weight per panicle (i.e., tolerance). This demonstrated the capacity of the staygreen trait to enhance stalk rot tolerance under stalk rot disease pressure.

Using fourteen genotypic groups derived from the Tx642 × Tx7000 (Tx642, Fusarium stalk rot and charcoal-rot-resistant; Tx7000, Fusarium stalk rot and charcoal-rot-susceptible) recombinant inbred line (RIL) population carrying a combination of staygreen (stg) QTL, a multi-environmental experiment was conducted by Adeyanju et al. (2016). The objective was to determine the effects of major staygreen (stg) quantitative trait loci (QTL) in response to infection by two stalk rot pathogens, *M. phaseolina* and *F. thapsinum*. Their results revealed that stg QTL have variable effects on severity of stalk rot diseases. Genotypes carrying either stg1 or stg3, or their combination (stg1+3) was found to express a greater level of resistance against *M. phaseolina* while resistance to *F. thapsinum* required a combination of stg1 and stg3. They further revealed that the other stg QTL blocks such as stg2 and stg4, did not affect resistance to either pathogen.

Staygreen is an important trait that needs a constant attention in breeding programs that particularly focus on producing hybrids that yield better under predicted, intensified future drought conditions and associated stalk rot incidence. Moreover, staygreen may also be instrumental in reducing yield losses associated with various foliar diseases caused by numerous pathogens for many economically important crops. For instance, one of the consistently found key compounds in staygreen genotypes is the cyanogenic glucoside, dhurrin. Cyanogenic glycosides including dhurrin are instrumental in providing chemical defense against fungal pathogens and insects (Siebert et al., 1996; Zagrobelny et al., 2004). Therefore, staygreen trait may be considered as a morphological marker for foliar disease resistance. On the other hand, staygreen may directly contribute to yield tolerance as well. Given its various physiological benefits, staygreen should remain a key attribute to be pursued in sorghum given the climatic changes, increased disease occurrence, rapid population growth, and threatened food security predicted for our future.

Macrophomina phaseolina

The anamorphic fungus, *M. phaseolina* belongs to the ascomycete family Botryosphaeriaceae (Slippers et al., 2013). Despite its broad host range, *M. phaseolina* is a monotypic genus and contains only one species: *M. phaseolina* (Sutton, 1980). It can survive in the form of conidia (in pycnidia), microsclerotia, and mycelia in crop residuals and act as the primary inocula upon overwintering. However, in nature, pycnidia are rarely formed on certain hosts but can be induced in vitro by altering the incubation conditions (Mihail and Taylor, 1995; Gaetan et al., 2006). *M. phaseolina*'s ability to produce pycnidia depends on the specific nature of the fungal isolate and the host species, which determine the epidemiological role of conidia in the disease cycle (Ahmed and Ahmed, 1969). For example, pycnidia formation on sorghum has not been reported while certain *M. phaseolina* isolates do form them on jute (Sarkar et al., 2010). Therefore, microsclerotia can be considered as the primary source of inoculum to initiate the disease cycle. Microsclerotia can remain viable in soil and crop residues for more than four years (Short et al., 1980). The survival of microsclerotia is significantly decreased by the high soil moisture content, repeated freezing and thawing of soil, and low soil carbon to nitrogen ratio (Dhingra and Sinclair, 1975). Enhanced production of microsclerotia under low water potentials that occurs during drought has been documented (Dhingra and Sinclair, 1977; Olaya and Abawi, 1996). Due to the longevity of microsclerotia, *M. phaseolina* competes well with other soil pathogens particularly when the soil temperature is above 30ºC and soil nutrient levels are low.

Post-flowering stress conditions such as drought, heat, and nutrient imbalance predispose plants to *M. phaseolina* infection. However, unlike Fusarium stalk rot, wet and cooler soil conditions after the occurrence of stress are not necessary to manifest charcoal rot disease (Dodd 1980; Seetharama et al. 1987; Zummo 1980). In fact charcoal rot is more conspicuous when soil temperature is > 32 ºC (Edmunds, 1964), thus continuous high soil temperature is conducive for charcoal rot outbreaks. Overwintering microsclerotia germinate from a few cells at a time on the root surface, or near the roots in the presence of host root exudates. Germination results in the production of many germ tubes which give rise to appressoria. The appressoria penetrate the root epidermal cell walls by enzymatic digestion and mechanical pressure or via wounds and natural openings (Gupta et al., 2012). Appressoria are microscopically visible at the tip of the primary hyphae on the root surface as early as 3 days after inoculation (Ammon et al., 1975). Hyphae

penetrate the root epidermis and are primarily restricted to the intercellular spaces of the cortex of the primary roots during the initial stages of infection. Subsequently, adjacent cells collapse and heavily infected plants may die prematurely due to the production of fungal toxins such as phaseolinone or botryodiplodin (Ramezani et al., 2007). Branching mycelia colonize the vascular tissue by growing through the cortex and then entering the xylem vessels (Abawi and Pastor-Corrales, 1990). Upon entering the vascular tissues, the fungus spreads through the tap root and blocks the vessels resulting in wilting of the plant (Wyllie, 1988). Enzymatic degradation and toxin production may also contribute to wilting (Jones and Wang, 1997; Kuti et al., 1997). Plugging of host vessels due to the profuse growth of mycelia can also contribute to premature host death. As the plant dies, microsclerotia are produced from mycelia and the cycle continues. Lesion nematodes are reported to contribute to enhanced charcoal rot incidences in sorghum as they provide entry points to the pathogen (Norton, 1958). However, the growing hyphae can infect the roots only when the plants undergo moisture and temperature stresses (Odvody and Dunkle 1979). Upon root invasion, the pathogen rapidly moves to above ground basal stalk portions, attacking the lower internodes. Like in *Fusarium* stalk rot, the disease symptoms of the charcoal rot can also be observed in upper internodes (even in the peduncle) of highly susceptible sorghum genotypes. However, unlike *Fusarium* spp., reports that demonstrate the vertical transmission of *M. phaseolina* is limited. The seed-borne nature and seed-to-seedling transmission of *M. phaseolina* has been documented in infected okra seeds (Pun et al., 1998).

Host range, geographic distribution, and economic importance of *M. phaseolina*

M. phaseolina infects more than 500 plant species around the world (Ali and Dennis, 1992). It causes many plant diseases including damping-off, seedling blight, leaf blight, stem blight, collar rot, stem rot, charcoal rot, basal stem rot, root rot, stem canker, and wilt (Babu et al., 2007; Songa and Hillocks, 1996; Singh et al., 1990; McCain and Scharpf, 1989). Increased incidences of the pathogen on diverse crop species has recently been reported worldwide highlighting the importance of this pathogen to global crop production (Aviles et al., 2008; Khangura and Aberra, 2009; Mahmoud and Budak, 2011; Sharifi and Mahdavi, 2012; da Silva and Clark, 2013). The hosts affected by *M. phaseolina* include major food crops (maize, sorghum; Su et al., 2001),

pulse crops (common bean; Mayek-Perez et al., 2001: green gram; Raguchander et al., 1997), oil crops (soybean; Ali and Dennis, 1992: sunflower; Khan, 2007: sesame; Dinakaran and Mohammed, 2001), and fiber crops (jute; De and Chattopadhyay, 1992: cotton; Aly et al., 2007). Other hosts include forest trees such as *Abies*, *Pinus*, *Pseudotsuga*, *Cassia*, and softwood trees (Lodha et al., 1986; McCain and Scharpf, 1989), fruit trees (*Citrus* spp., *Cocos nucifera*, *Coffea* spp., *Ziziphus mauritiana*, *Leucaena* spp.), medicinal plants, and numerous weed species (Lodha et al., 1986; Songa and Hillocks, 1996).

M. phaseolina has a broad geographic distribution. It occurs in North and South America, Australia, Asia, Europe, and Africa (McGee 1991). It is particularly troublesome in tropical and subtropical countries with arid to semiarid climates in Africa, Asia, Europe, and North and South America (Abawi and Pastor-Corrales, 1990; Gray et al., 1990; Diourte et al., 1995; Wrather et al., 2001; Wrather et al., 2003).

Charcoal rot disease is a key concern in soybean and accounted for a total yield loss of $173.80 million in the United States during the 2002 crop season (Wrather et al., 2003). The mean (from 1974 to 1994) annual soybean yield losses for 16 southern states was estimated to be 8.54×10^5 tons, making charcoal rot the second most destructive disease in this region (Wrather, 1995). The estimated yield loss due to charcoal rot in soybean in the top 10 soybean-producing countries during 1994 was 1.23 million tons (Wrather et al. 1997). In 1998, Macrophomina stem canker was another high priority soybean disease causing tremendous annual economic losses in the top-ten soybean-producing countries (United States, Brazil, Argentina, China, India, Paraguay, Canada, Indonesia, Bolivia and Italy) (Wrather et al., 2001). In United States, the annual soybean yield reduction was estimated to be 1.98, 0.28, and 0.49 million metric tons in 2003, 2004 and 2005, respectively (Wrather and Koenning, 2006). The incidence of *M. phaseolina* in sorghum fields was reported to be 70% in the bay region of Somalia (Gray et al., 1991) while yield losses in *Phaseolus vulgaris* L. in semi-arid eastern Kenya was estimated to be 300 kg/ha (Wortmann and Allen, 1994). *M. phaseolina* causes severe destruction to olives in Egypt (Ghoneim et al., 1996), Tunisia (Boulila and Mahjoub, 1994), Europe, and the Mediterranean region (Sanchez-Hernandez et al., 1996, 1998). At 40% disease severity, the *M. phaseolina* infection-associated yield losses in sesame (*Sesamum indicum* L.) have been estimated up to 57% (Maiti et al., 1988).

M. phaseolina genome and virulence mechanisms

Islam et al. (2012) reported the *M. phaseolina* genome sequence. The genome size was found to be 49.3 Mb in size with 14,249 genes. The median gene length was 1265 bp. The repetitive sequences were estimated at 2.84% of the genome while 3.98% was designated as transposable elements. The large number of transposons present in the *M. phaseolina* genome is suggested to be the primary mechanism for mutagenesis and gene duplications, which may elucidate the broad host range of *M. phaseolina*. *M. phaseolina* contains many genes for secreted peroxidases, oxidases, and hydrolytic enzymes for degrading cell wall polysaccharides and lignocelluloses to penetrate the host tissue. Therefore, these enzymes appeared to be among the major virulence factors for *M. phaseolina*. The *M. phaseolina* genome contains numerous pathogen-host interaction genes including those for adhesion, cell wall breakdown, purine biosynthesis, signal transduction, and patulin biosynthesis. Moreover, carbohydrate esterases (CE) are present in *M. phaseolina*, where the CE9 and CE10 families are found in remarkably higher numbers when compared to other fungi. CEs play a key role in pathogenesis and participate in the first line of attack during host invasion (Ospina-Giraldo et al., 2010). In addition, Islam et al (2012) also reported that, in comparison to all sequenced ascomycete species, *M. phaseolina* encodes a significant number of major facilitator superfamily (MFS) type membrane transporters, P450s, transposases, glycosidases, and secondary metabolites to effectively overcome host plant defense responses.

Previous experimental evidence has validated the role of cell wall degrading enzymes (CWDEs) (Ammon and Wyllie, 1972) and phytotoxins (Bhattacharya et al., 1992) in *M. phaseolina* virulence. Endoglucanases are among the most important enzymes involved in pathogenesis caused by *M. phaseolina* (Heiler et al., 1993). A unique β-1,4-endoglucanase like those found in plants has been identified in *M. phaseolina* by Wang and Jones (1995). This similarity may elucidate the effectiveness of *M. phaseolina* in penetrating the plant cell walls. Several other CWDEs such as amylases, proteases, hemicellulases, pectinases, and phosphatidases also play a central role in pathogenesis (Amadioha, 2000). Several phytotoxins produced by *M. phaseolina* have been identified and attributed to the virulence of individual isolates (Bhattacharya et al., 1992). These phytotoxins include asperlin, isoasperlin, phomalactone, phaseolinic acid, phomenon, and phaseolinone (Dhar et al., 1982; Mahato et al., 1987). Among these,

phaseolinone is a heat-resistant, non-host-specific exotoxin that reported to inhibit seed germination in black gram (*Phaseolus mungo*) at concentrations as low as 25 µg/ml (Bhattacharya, 1987). UV-mutated non-toxigenic mutants of *M. phaseolina* were reported to be avirulent on black gram seedlings while infectivity was restored in the presence of phaseolinone (Sett et al., 2000). These findings confirmed the involvement of phaseolinone as a major phytotoxic substance in disease initiation. Phaseolinone also causes wilting in seedlings and necrotic lesions on leaves (Bilgrami et al., 1979). Infection of *Corchorus capsularis* (jute) plants with *M. phaseolina* resulted in elevated nitric oxide, reactive nitrogen species and S-nitrosothiols production in infected tissues leading to enhanced charcoal rot disease susceptibility (Sarkar et al., 2014). Therefore, the ability of this pathogen to manipulate host metabolic pathways such as nitrate reduction I (nitric oxide production) seem to be an important aspect of virulence thus induced disease susceptibility.

Genetic basis of charcoal rot resistance in sorghum

Understanding the complexity of disease resistance at the molecular level is critical to develop charcoal-rot-resistant sorghum lines and hybrids. Towards this end, only two efforts have been reported so far. Reddy et al (2008) reported a study based upon QTL mapping approach to investigate the genetic basis of charcoal rot resistance in sorghum. In this study (conducted in two environments), by using a population of F9 generation recombinant inbred lines (RILs), derived from IS22380 (susceptible) × E36-1 (resistant), along with parents, a total of 85 polymorphic marker loci (62 nuclear and 4 genic SSRs, 19 RAPDs) were identified for the construction of a genetic map, spanning 650.3 cM in all ten linkage groups. Through the mapping analysis, five QTLs at one environment and four QTLs at the other environment were identified for the component traits of charcoal rot disease resistance. QTLs for number of internodes crossed by the lesion, lesion length, and percent lodging accounted for 31.8, 10.8 and 18.9% of the phenotypic variability at one environment while the same at the second environment accounted for 14.9, 10.5 and 26.4%, respectively. Some of the QTLs for said traits were identified to be common across two environments and are likely to assist in marker-assisted selection (MAS) for charcoal rot resistance in sorghum.

Adeyanju et al. (2015) reported a genome-wide association study (GWAS) on resistance to charcoal rot and Fusarium stalk rot diseases in grain sorghum. A sorghum diversity panel consisting of 300 genotypes from different parts of the world was used. Four single nucleotide polymorphic sites (SNPs), either reside within or adjacent to two genes [*Sb09g029260* (chalcone synthase), and *Sb09g028280.1* (ROP GTPase proteins)] were found to be significantly associated with charcoal rot resistance. However, each associated SNP had relatively small effect on the traits accounting for low of phenotypic variation (maximum of 16%). Although the associated allele frequency estimations revealed enriched charcoal rot resistance alleles in durra and caudatum sub-populations, their results suggest complex molecular mechanisms underlying resistance to *M. phaseolina*.

The genetic control of resistance to necrotrophic pathogens in general and *M. phaseolina* in particular, is poorly understood. Although *M. phaseolina* affects more than 500 plant species, its impact on the genome wide host transcription profile has not been reported in any of its host species. Large scale gene expression studies such as RNA sequencing can provide a broader view and better understanding of the disease resistance mechanisms and would help to devise better disease control strategies.

REFERENCES

Abawi GS, Pastor-Corrales MA. 1990. Root rot of beans in Latin America and Africa: Diagnosis, research methodologies and management strategies. *Centro International de Agricultura Tropical*, pp. 114. Cali, Colombia.

Adeyanju A, Little C, Yu J, Tesso T. 2015. Genome-wide association study on resistance to stalk rot diseases in grain sorghum. *G3: Genes| Genomes| Genetics* 5: 1165-1175.

Adeyanju A, Yu J, Little C, Rooney W, Klein P, Burke J, Tesso T. 2016. Sorghum RILs segregating for stay-green QTL and leaf dhurrin content show differential reaction to stalk rot diseases. *Crop Science* 56: 2895-2903.

Ahmed N, Ahmed QA. 1969. Physiologic specialization in *Macrophomina phaseolina* (Maubl.) Ashby, causing stem rot of jute, *Corchorus* species. *Mycopathologia* 39: 129-138.

Ali SM, Dennis J. 1992. Host range and physiological specialization of *Macrophomina phaseolina* isolated from field peas in South-Australia. *Australian Journal of Experimental Agriculture* 32: 1121-1125.

Ali M, Rajewski J, Baenziger P, Gill KS, Eskridge KM, Dweikat I. 2008. Assessment of genetic diversity and relationship among a collection of US sweet sorghum germplasm by SSR markers. *Molecular Breeding* 21: 497-509.

Aly AA, Abdel-Sattar MA, Omar MR, Abd-Elsalam KA. 2007. Differential antagonism of *Trichoderma* sp. against *Macrophomina phaseolina*. *Journal of Plant Protection Research* 47: 91-102.

Amadioha AC. 2000. The production and activity of extracellular amylase by *Rhizoctonia bataticola*. *Archives of Phytopathology and Plant Protection* 33: 1-9.

Ammon V, Wyllie TD. 1972. Penetration and host-parasite relationships of *Macrophomina phaseolina* on *Glycine max*. *Phytopathology* 62: 743-744.

Ammon V, Wyllie TD, Brown MF. 1975. Investigation of infection process of *Macrophomina phaseolina* on surface of soybean roots using scanning electron-microscopy. *Mycopathologia* 55: 77-81.

Anahosur KH, Patil SH. 1983. Assessment of losses in sorghum seed weight due to charcoal rot. *Indian Phytopathology* 36: 85-88.

Arumuganathan K, Earle E.D. 1991. Nuclear DNA content of some important plant species. *Plant Molecular Biology Reporter* 9: 208-218.

Aviles M, Castillo S, Bascon J, Zea-Bonilla T, Martin-Sanchez PM, Perez-Jimenez RM. 2008. First report of *Macrophomina phaseolina* causing crown and root rot of strawberry in Spain. *Plant Pathology* 57: 382-382.

Babu BK, Saxena AK, Srivastava AK, Arora DK. 2007. Identification and detection of *Macrophomina phaseolina* by using species-specific oligonucleotide primers and probe. *Mycologia* 99: 797-803.

Bandara YMAY, Weerasooriya DK, Tesso TT, Little CR. 2016. Stalk rot fungi affect leaf greenness (SPAD) of grain sorghum in a genotype-and growth-stage-specific manner. *Plant Disease* 100: 2062-2068.

Bandara YMAY, Weerasooriya DK, Tesso TT, Prasad PVV, Little CR. 2017a. Stalk rot fungi affect grain sorghum yield components in an inoculation stage-specific manner. *Crop Protection* 94: 97-105.

Bandara YMAY, Tesso TT, Bean SR, Dowell FE, Little CR. 2017b. Impacts of fungal stalk rot pathogens on physicochemical properties of sorghum grain. *Plant Disease* https://doi.org/10.1094/PDIS-02-17-0238-RE

Bandara YMAY, Weerasooriya DK, Tesso TT, Little CR. 2017c. Impacts of stalk rot diseases on sweet sorghum biofuel traits. *BioEnergy research* 10: 26-35.

Barbanti L, Grandi S, Vecchi A, Venturi G. 2006. Sweet and fibre sorghum (*Sorghum bicolor* (L.) Moench), energy crops in the frame of environmental protection from excessive nitrogen loads. *European Journal of Agronomy* 25:30-39.

Bean BW, Baumhardt RL, McCollum FT III, McCuistion KC. 2013. Comparison of sorghum classes for grain and forage yield and forage nutritive value. *Field Crops Research* 142: 20-26.

Bhattacharya G, Dhar TK, Bhattacharyya FK, Siddiqui KA. 1987. Mutagenic action of phaseolinone, a mycotoxin isolated from *Macrophomina phaseolina*. *Australian Journal of Biological Sciences* 40: 349-353.

Bhattacharya D, Siddiqui KAI, Ali E. 1992. Phytotoxic metabolites of *Macrophomina phaseolina*. *Indian Journal of Mycology and Plant Pathology* 22: 54-57.

Bilgrami KS, Jamaluddin, Rizvi MA. 1979. The fungi of India. Part I. New Delhi, India: Today and Tomorrow's Printers and Publishers.

Borrell AK, Hammer GL, Douglas ACL. 2000. Does maintaining green leaf area in sorghum improve yield under drought? I. Leaf growth and senescence. *Crop Science* 40:1026-1037.

Boulila M, Mahjoub M. 1994. Inventory of olive disease in Tunisia. *Bulletin-OEPP* 31: 111-112.

Bralley E, Greenspan P, Hargrove JL, Hartle DK. 2008. Inhibition of hyaluronidase activity by select sorghum brans. *Journal of Medicinal Food* 11: 307-312.

Burdette A, Garner PL, Mayer EP, Hargrove JL, Hartle DK, Greenspan P. 2010. Anti-inflammatory activity of select sorghum (*Sorghum bicolor*) brans. *Journal of Medicinal Food* 13: 879-887.

da Silva WL, Clark CA. 2013. Infection of sweet potato by *Fusarium solani* and *Macrophomina phaseolina* prior to harvest. *Plant Disease* 97: 1636-1644.

De BK, Chattopadhyay SB. 1992. Effect of potash on stem rot disease of jute caused by *Macrophomina phaseolina*. *Journal of Mycopathological Research* 30: 51-55.

Dhar TK, Siddiqui KAI, Ali E. 1982. Structure of phaseolinone, a novel phytotoxin from *Macrophomina phaseolina*. *Tetrahedron Letters* 23: 5459-5462.

Dhingra OD, Sinclair JB. 1975. Survival of *Macrophomina phaseolina* sclerotia in soil: Effect of soil moisture, carbon: nitrogen ratio, carbon sources, and nitrogen concentrations. *Phytopathology* 65: 236-240.

Dhingra OD, Sinclair JB. 1977. An annotated bibliography of *Macrophomina phaseolina* 1905–1975. Universidade Federal Viçosa, Viçosa, Brazil. 244.

Dinakaran D, Mohammed SEN. 2001. Identification of resistant sources to root rot of sesame caused by *Macrophomina phaseolina* (Tassi.) Goid. *Sesame and Safflower Newsletter* 16: 68-71.

Diourte M, Starr JL, Jeger MJ, Stack JP, Rosenow DT. 1995. Charcoal rot (*Macrophomina phaseolina*) resistance and the effects of water stress on disease development in sorghum. *Plant Pathology* 44: 196-202.

Dodd J.L. 1980. The photosynthetic stress translocation balance concept of sorghum stalk rot. In *Proceedings of International Workshop of Sorghum Diseases*, pp 300-305. 11-15 December 1978, Hyderabad, India. Texas A&M University/ICRISAT Press.

Duncan RR. 1983. Anthracnose-*Fusarium* disease complex on sorghum in southeastern USA. *Sorghum Newsletter* 26: 121-122.

Dykes L., Rooney LW, Waniska RD, Rooney WL. 2005. Phenolic compounds and antioxidant activity of sorghum grains of varying genotypes. *Journal of Agricultural and Food Chemistry* 53: 6813-6818.

Edmunds LK. 1964. Combined relation of plant maturity, temperature and soil moisture to charcoal stalk rot development in grain sorghum. *Phytopathology* 54: 514-517.

Edmunds LK, Zummo N. 1975. Sorghum diseases in the United States and their control. Agriculture Handbook, United States Department of Agriculture 468.

Eastin JD, Sullivan CY. 1974. Yield consideration in selected cereals. In *Mechanisms of regulation of plant growth* (ed. R.L. Bielski et al.), pp. 871–877. Bull. 12. Royal Society of New Zealand, Wellington, New Zealand.

Eastin J.D, Petersen CL, Zavala-Garcia F, Dhopte A, Verma PK, Ounguela VB, Wit MW, Hernandez VG, Munoz ML, Gerik TJ, Gandoul GI, Hovney MRA, Onofre LM. 1999. Potential heterosis associated with developmental and metabolic processes in sorghum and maize. In *The genetics and exploitation of heterosis in crops* (ed. J.G. Coors, S. Pandey), pp. 205–229. ASA, CSSA, and SSSA, Madison, WI.

Funnell-Harris DL, Sattler SE, Pedersen JF. 2014. Response of *Fusarium thapsinum* to sorghum *brown midrib* lines and to phenolic metabolites. *Plant Disease* 98: 1300-1308.

Funnell-Harris DL, O'Neill PM, Sattler SE, Yerka MK. 2016. Response of sweet sorghum lines to stalk pathogens *Fusarium thapsinum* and *Macrophomina phaseolina*. *Plant Disease* 100: 896-903.

Gaetan SA, Fernandez L, Madia M. 2006. Occurrence of charcoal rot caused by *Macrophomina phaseolina* on canola in Argentina. *Plant Disease* 90: 524-524.

Ghoneim SSH, Abdel-Massih MI, Mahmoud FAF. 1996. Interaction between root-knot nematode and root rot on olive trees. *Annals of Agricultural Sciences* 41: 445-461.

Gray FA, Kolp BJ, Mohamed MA. 1990. A disease survey of crops grown in the Bay Region of Somalia, East Africa. *FAO Plant Protection Bulletin* 38: 39-47.

Gray FA, Mihail JD, Lavigne RJ, Porter PM. 1991. Incidence of charcoal rot of sorghum and soil populations of *Macrophomina phaseolina* associated with sorghum and native vegetation in Somalia. *Mycopathologia* 114: 145-151.

Gupta GK, Sharma SK, Ramteke R. 2012. Biology, epidemiology and management of the pathogenic Fungus *Macrophomina phaseolina* (Tassi) Goid with special reference to charcoal rot of soybean (*Glycine max* (L.) Merrill). *Journal of Phytopathology* 160: 167-180.

Heiler S, Mendgen K, Deising H. 1993. Cellulolytic enzymes of the obligately biotrophic rust fungus *Uromyces viciae-fabae* are regulated differentiation-specifically. *Mycological Research* 97: 77-85.

Hundekar AR, Anahosur KH, 1994. Pathogenicity of fungi associated with sorghum stalk rot. *Karnataka Journal of Agricultural Science* 7: 291-295.

Ilyas MB, Ellis MA, Sinclair JB. 1976. Effect of soil fungicides on *Macrophomina phaseolina* sclerotium viability in soil and in soybean stem pieces. *Phytopathology 66*: 355-359.

Islam MS, Haque MS, Islam MM, Emdad EM, Halim A, Hossen QM, Hossain MZ, Ahmed B, Rahim S, Rahman MS, Alam MM, Hou S, Wan X, Saito JA, Alam M. 2012. Tools to kill: genome of one of the most destructive plant pathogenic fungi *Macrophomina phaseolina*. *BMC Genomics* 13: 1.

Jardine DJ, Leslie JF. 1992. Aggressiveness of *Gibberella fujikuroi* (*Fusarium moniliforme*) isolates to grain sorghum under greenhouse conditions. *Plant Disease* 76: 897-900.

Jardine D. 2006. Stalk Rots of Corn and Sorghum. Agricultural Research Station and Cooperative Extension Service, Kansas State University, USA.

Jones RW, Wang HY. 1997. Immunolocalization of a beta-1,4-endoglucanase from *Macrophomina phaseolina* expressed in planta. *Canadian Journal of Microbiology* 43: 491-495.

Keeney DR, DeLuca TH. 1992. Biomass as an energy source for the midwestern US. *American Journal of Alternative Agriculture* 7: 137-144.

Khan SN. 2007. *Macrophomina phaseolina* as causal agent for charcoal rot of sunflower. *Mycopathologia* 5: 111-118.

Khangura R, Aberra M. 2009. First report of charcoal rot on canola caused by *Macrophomina phaseolina* in western Australia. *Plant Disease* 93: 666-667.

Khune NN, Kurhekar DE, Raut JG, Wangikar PD, 1984. Stalk rot of sorghum caused by *Fusarium moniliforme*. *Indian Phytopathology* 37: 316-319.

Kuti JO, Schading RL, Latigo GV, Braford JM. 1997. Differential responses of guayule (*Parthenium argentatum* Gray) genotypes to culture filtrate and toxin from *Macrophomina phaseolina* (Tassi) Goidanich. *Journal of Phytopathology* 145: 305-311.

Leslie JF, Zeller KA, Lamprecht SC, Rheeder JP, Marasas FO. 2005. Toxicity, pathogenicity and genetic differentiation of five species of *Fusarium* from sorghum and millet. *Phytopathology* 95: 275-283.

Lodha S, Gupta GK, Singh S. 1986. Crop disease situation and some new records in Indian arid zone. *Annals of Arid Zone* 25: 311-320.

Mahato SB, Siddiqui KAI, Bhattacharya G, Ghosa T, Miyahara K, Sholichin M, Kawasaki T. (1987). Structure and stereochemistry of phaseolinic acid: A new acid from *Macrophomina phaseolina*. *Journal of Natural Products* 50: 245-247.

Mahmoud A, Budak H. 2011. First report of charcoal rot caused by *Macrophomina phaseolina* in sunflower in Turkey. *Plant Disease* 95: 223-223.

Maiti RK, Bidinger FR. 1981. Growth and development of pearl millet plant. *ICRISAT Research Bulletin* 6. Hyderabad, India.

Maiti S, Hedge MR, Chattopadhyra SB. 1988. Handbook of annual oilseed crops. New Delhi, India: Oxford and IBH Publishing.

Maman N, Mason SC, Lyon DJ, Dhungana P. 2004. Yield components of pearl millet and grain sorghum across environments in the central Great Plains. *Crop Science* 44: 2138-2145.

Mayék-Pérez N, López-Castañeda C, López-Salinas E, Cumpián-Gutiérrez J, Acosta-Gallegos JA. 2001. Resistance to *Macrophomina phaseolina* (Tassi) Goid. in common bean under field conditions in Mexico. *Agrociencia (Montecillo)* 35: 649-661.

McCain AH, Scharpf RF. 1989. Effect of inoculum density of *Macrophomina phaseolina* on seedling susceptibility of six conifer species. *European Journal of Plant Pathology* 19: 119-123.

McGee DC. 1991. Soybean Diseases. A Reference Source for Seed Technologist. St Paul, MN, USA, APS Press.

Menz MA, Klein RR, Mullet JE, Obert JA, Unruh NC, Klein PE. 2002. A high-density genetic map of *Sorghum bicolor* (L.) Moench based on 2926 AFLP, RFLP and SSR markers. *Plant Molecular Biology* 48: 483-499.

Mihail JD, Taylor SJ. 1995. Interpreting variability among isolates of *Macrophomina phaseolina* in pathogenicity, pycnidium production, and chlorate utilization. *Canadian Journal of Botany* 73: 1596-1603.

Miron J, Zuckerman E, Sadeh D, Adin G, Nikbachat M, Yosef E, Ben-Ghedalia D, Carmi A, Kipnis T, Soloman R. 2005. Yield, composition and in vitro digestibility of new forage sorghum varieties and their ensilage characteristics. *Animal Feed Science and Technology* 120: 17-32.

Mughogho LK, Pande S. 1984. Charcoal rot of sorghum. In *Sorghum Root and Stalk Rots, a Critical Review.* Proceedings of the Consultative Group Discussion on Research Needs and Strategies for Control of Root and Stalk Rot Diseases (ed. G. Rosenberg), pp. 11-24. 27 Nov - 2 Dec 1983, Bellagio, Italy. ICRISAT Press, Patancheru, A.P. 502324, India.

Norton, D.C. 1958. The association of *Pratylenchus hexincisus* with charcoal rot of sorghum. *Phytopathology* 48: 355-358.

Odvody GN, Dunkle LD. 1979. Charcoal stalk rot of sorghum: Effect of environment on host parasite relations. *Phytopathology* 69: 250-254.

Olaya G, Abawi GS. 1996. Effect of water potential on mycelial growth and on production and germination of sclerotia of *Macrophomina phaseolina*. *Plant Disease* 80: 1347-1350.

Ospina-Giraldo MD, Griffith JG, Laird EW, Mingora C. 2010. The CAZyome of *Phytophthora* spp.: A comprehensive analysis of the gene complement coding for carbohydrate-active enzymes in species of the genus *Phytophthora*. *BMC Genomics* 11: 525-540.

Paterson AH, Bowers JE, Bruggmann R, Dubchak I, Grimwood J, Gundlach H, Haberer G, Hellsten U, Mitros T, Poliakov A, Schmutz J. 2009. The *Sorghum bicolor* genome and the diversification of grasses. *Nature* 457: 551-556.

Pun KB, Sabitha D, Valluvaparidasan V. 1998. Studies on seed-borne nature of *Macrophomina phaseolina* in okra. *Plant Disease Research* 13: 249-290.

Raguchander T, Rajappan K, Samiappan R. 1997. Evaluating methods of application of biocontrol agent in the control of mungbean root rot. *Indian Phytopathology* 50: 229-234.

Rajewski JF, Francis CA. 1991. Defoliation effects on grain fill, stalk rot, and lodging of grain sorghum. *Crop Science* 31: 353-359.

Ramezani M, Shier WT, Abbas HK, Tonos JL, Baird RE, Sciumbato GL. 2007. Soybean charcoal rot disease fungus *Macrophomina phaseolina* in Mississippi produces the phytotoxin (-)-botryodiplodin but no detectable phaseolinone. *Journal of Natural Products* 70: 128-129.

Reed JE, Partridge JE, Nordquist PT, 1983. Fungal colonization of stalks and roots of grain sorghum during the growing season. *Plant Disease* 64: 417-420.

Reddy PS, Fakrudin B, Punnuri SM, Arun SS, Kuruvinashetti MS, Das IK, Seetharama N, 2008. Molecular mapping of genomic regions harboring QTLs for stalk rot resistance in sorghum. *Euphytica* 159: 191-198.

Reddy B, Reddy PS. 2003. Sweet sorghum: characteristics and potential. *International Sorghum and Millets Newsletter* 44: 26-28.

Rooney LW, Waniska RD. 2000. Sorghum food and industrial utilization. In *Sorghum: Origin, History, Technology, and Production* (ed. C.W. Smith, R.A. Frederiksen), pp. 689-750. John Wiley and Sons, New York.

Rosenow DT, Johnson JW, Frederiksen RA, Miller FR. 1977. Relationship of nonsenescence to lodging and charcoal rot in sorghum. *Agronomy Abstracts* 69.

Sanchez-Hernandez ME, Perez-de-Algaba A, Blanco-Lopez MA, Trapero-Casas A. 1996. Vascular wilt of young olive trees. *Agricultura Revista-Agropecuaria* 65: 2928-2932.

Sanchez-Hernandez ME, Davila AR, Perez-de-Algaba A, Blanco-Lopez MA, Trapero-Casas A. 1998. Occurrence and etiology of death of young olive trees in Southern Spain. *European Journal of Plant Pathology* 104: 347-357.

Sarkar TS, Biswas P, Ghosh SK, Ghosh S. 2014. Nitric oxide production by necrotrophic pathogen *Macrophomina phaseolina* and the host plant in charcoal rot disease of jute: Complexity of the interplay between necrotroph–host plant interactions. *PloS one* 9(9) p.e107348.

Seetharama N, Bidinger, FR, Rao KN, Gill KS, Mulgund M, 1987. Effect of pattern and severity of moisture deficit stress on stalk rot incidence in sorghum. I. Use of line source irrigation technique, and the effect of time of inoculation. *Field Crops Research* 15: 289-308.

Seetharama N, Sachan RC, Huda AKS, Gill KS, Rao KN, Bidinger FR, Reddy DM. 1991. Effect of pattern and severity of moisture-deficit stress on stalk-rot incidence in sorghum. II. Effect of source/sink relationships. *Field Crops Research* 26: 355-374.

Sett S, Mishra SK, Siddiqui KA. 2000. Avirulent mutants of *Macrophomina phaseolina* and *Aspergillus fumigatus* initiate infection in *Phaseolus mungo* in the presence of phaseolinone; levamisole gives protection. *Journal of Biosciences* 25: 73-80.

Sharifi K, Mahdavi M. 2012. First report of strawberry crown and root rot caused by *Macrophomina phaseolina* in Iran. *Iranian Journal of Plant Pathology* 47: 479-480.

Short G, Wyllie T, Bristow P. 1980. Survival of *Macrophomina phaseolina* in soil and in residue of soybean. *Phytopathology* 70: 13-17.

Siebert M, Sommer S, Li S, Wang Z, Severin K, Heide L. 1996. Genetic engineering of plant secondary metabolism. Accumulation of 4-hydroxybenzoate glucosides as a result of the expression of the bacterial ubiC gene in tobacco. *Plant Physiology* 112: 811-819.

Singh SK, Nene YL, Reddy MV. 1990. Influence of cropping systems on *Macrophomina phaseolina* populations in soil. *Plant Disease* 74: 812-814.

Slippers B, Boissin E, Phillips AJ, Groenewald JZ, Lombard L, Wingfield MJ, Postma A, Burgess T, Crous PW. 2013. Phylogenetic lineages in the Botryosphaeriales: a systematic and evolutionary framework. *Studies in Mycology* 76: 31-49.

Smith GA, Bagby MO, Lewellan RT, Doney DL, Moore PH, Hills FJ, Campbell LG, Hogaboam GJ, Coe GE, Freeman K. 1987. Evaluation of sweet sorghum for fermentable sugar production potential. *Crop Science* 27: 788-793.

Smith CW, Frederiksen RA. 2000. Sorghum: Origin, history, technology, and production. John Wiley & Sons.

Songa W Hillocks RJ. 1996. Legume hosts of *Macrophomina phaseolina* in Kenya and effect of crop species on soil inoculum level. *Journal of Phytopathology* 144: 387-391.

Su G, Suh SO, Schneider RW, Russin JS. 2001. Host specialization in the charcoal rot fungus, *Macrophomina phaseolina*. *Phytopathology* 91: 120-126.

Sutton, B.C. (1980). The coelomycetes, fungi imperfecti with pycnidia, acervuli and stromata. Commonwealth Mycological Institute. Kew, Surrey, UK.

Tarr SAJ, 1962. Root and stalk diseases: Red stalk rot, Colletotrichum rot, anthracnose, and red leaf spot. In *Diseases of Sorghum, Sudan Grass and Brown Corn*, pp. 58-73. Commonwealth Mycological Institute, Kew, Surrey, UK.

Tenkouano A, Miller ER, Frederiksen RA, Rosenow DT. 1993. Genetics of nonsenescence and charcoal rot resistance in sorghum. *Theoretical and Applied Genetics* 85: 644-648.

Tesso TT, Claflin LE, Tuinstra MR. 2005. Analysis of stalk rot resistance and genetic diversity among drought tolerant sorghum genotypes. *Crop Science* 45: 645-652.

Tesso TT, Ochanda N, Little CR, Claflin L, Tuinstra MR. 2010. Analysis of host plant resistance to multiple *Fusarium* species associated with stalk rot disease in sorghum [*Sorghum bicolor* (L.) Moench]. *Field Crops Research* 118: 177-182.

Tesso T, Ejita G. 2011. Stalk strength and reaction to infection by *Macrophomina phaseolina* of brown midrib maize (*Zea mays*) and sorghum (*Sorghum bicolor*). *Field Crops Research* 120: 271-275.

Tesso T, Perumal R, Little CR, Adeyanju A, Radwan GL, Prom LK, Magill CW. 2012. Sorghum pathology and biotechnology - A fungal disease perspective: Part II. Anthracnose, stalk rot, and downy mildew. *European Journal of Plant Science and Biotechnology* 6: 31-44.

Turner ND, Diaz A, Taddeo SS, Vanamala J, McDonough CM, Dykes L, Murphy ME, Carroll RJ, Rooney LW. 2006. Bran from black or brown sorghum suppresses colon carcinogenesis. *The FASEB Journal* 20: 599-599.

Van Oosterom EJ, Jayachandran R, Bidinger FR. 1996. Diallel analysis of the stay-green trait and its components in sorghum. *Crop Science* 36: 549-555.

Wang H, Jones RW. 1995. A unique endoglucanase-encoding gene cloned from the phytopathogenic fungus *Macrophomina phaseolina*. *Applied and Environmental Microbiology* 61: 2004-2006.

Wang D, Bean S, McLaren J, Seib P, Madl R, Tuinstra M, Shi Y, Lenz M, Wu X, Zhao R. 2008. Grain sorghum is a viable feedstock for ethanol production. *Journal of Industrial Microbiology and Biotechnology* 35: 313-320.

Wrather JA. 1995. Soybean disease loss estimates for the southern United States, 1974 to 1994. *Plant Disease* 79: 1076-1079.

Wrather JA, Anderson TR, Arsyad DM, Gai J, Ploper LD, Porta-Puglia A, Ram HH, Yorinori JT. 1997. Soybean disease loss estimates for the top ten soybean producing countries in 1994. *Plant Disease* 81: 107-110.

Wrather JA, Anderson TR, Arsyad DM, Tan Y, Ploper LD, Porta-Puglia A, Ram HH, Yorinori JT. 2001. Soybean disease loss estimates for the top 10 soybean producing countries in 1998. *Canadian Journal of Plant Pathology* 23: 115-121.

Wrather JA, Koenning SR, Anderson TR. 2003. Effect of diseases on soybean yields in the United States and Ontario (1999 to 2002). *Plant Health Progress* doi:10.1094/PHP-2003-0325-01-RV.

Wrather JA, Koenning SR. 2006. Estimates of disease effects on soybean yields in the United States 2003 to 2005. *Journal of Nematology* 38: 173-180.

Wortmann CS, Allen DJ. 1994. African bean production environments: Their definition, characteristics, and constraints. Network on Bean Research in Africa. Occasional paper series 11. Cali, Colombia: Centro Internacional de Agricultura Tropical.

Wyllie TD 1988. Charcoal rot of soybean-current status. In *Soybean diseases of the north central region* (ed. TD Wyllie, DH Scott), pp. 106-113. St. Paul, MN: APS Press.

Xu W, Rosenow DT, Nguyen HT. 2000. Stay green trait in grain sorghum: relationship between visual rating and leaf chlorophyll concentration. *Plant Breeding* 119: 365-367.

Yang L, Browning JD, Awika JM. 2009. Sorghum 3-deoxyanthocyanins possess strong phase II enzyme inducer activity and cancer cell growth inhibition properties. *Journal of Agricultural and Food Chemistry* 57: 1797-1804.

Zagrobelny M, Bak S, Rasmussen AV, Jorgensen B, Naumann CM, Moller BL. 2004. Cyanogenic glucosides and plant-insect interactions. *Phytochemistry* 65: 293-306.

Zummo N, 1980. *Fusarium* disease complex of sorghum in West Africa. In *Proceedings of the International Workshop on Sorghum Diseases*, pp. 11-15. ICRISAT Press, Hyderabad, India.

Zummo N. 1984. Fusarium root and stalk disease complex. In: *Sorghum Root and Stalk Rots, a Critical Review. Proceedings of the Consultative Group Discussion on Research Needs and Strategies for Control of Root and Stalk Rot Diseases* (ed. G. Rosenberg), pp. 25-29). 27 Nov - 2 Dec 1983, Bellagio, Italy. Patancheru, A.P. 502324, India: ICRISAT Press.

Chapter 2 - *Macrophomina phaseolina* induces charcoal rot susceptibility in grain sorghum: evidence from genome-wide transcriptome profiling.

ABSTRACT

Macrophomina phaseolina (MP) is an important necrotrophic pathogen that infects over 500 plant species. It causes charcoal rot in many economically important crops. However, the molecular basis of charcoal rot resistance is poorly understood. To dissect the mechanisms underlying charcoal rot resistance in grain sorghum [*Sorghum bicolor* (L.) Moench], stalk mRNA was extracted from two known resistant and susceptible genotypes at three post inoculation stages (PIS) and profiled with RNA sequencing. Upon MP inoculation, 8560 genes were differentially expressed at three PIS between two genotypes, out of which 2053 were components of 200 known metabolic pathways. Many of these pathways were significantly up-regulated in the susceptible genotype. Based on the transcriptional data, it is hypothesized that enhanced pathogen nutrition and virulence, impeded host basal immunity, and reactive oxygen and nitrogen species-mediated cell death may contribute to charcoal rot susceptibility. The complex hormonal regulation observed in the MP-inoculated susceptible genotype was characterized by the strong upregulation of salicylic acid, ethylene, gibberellin, and cytokinin biosynthetic pathways and down-regulated jasmonic acid and brassinosteroid pathways. Although host susceptibility to necrotrophs is often attributed to the phytotoxins they produce, our data provided an unprecedented level of detail about sorghum transcriptional changes during its interaction with MP and provided useful insights into induced host susceptibility against necrotrophic fungi at the whole genome scale.

Keywords: Sorghum, *Macrophomina phaseolina*, charcoal rot, RNA-Seq, transcription, induced disease susceptibility

INTRODUCTION

Macrophomina phaseolina (Fig. 2.1.A) is a soil-borne, necrotrophic fungal pathogen that causes disease in over 500 plant species (Islam et al., 2012). Despite its broad host range, *Macrophomina* is a monotypic genus and contains only one species: *M. phaseolina* (Sutton, 1980). It is widely accepted as a difficult-to-control pathogen due to its persistence as sclerotia in the soil and in plant debris (Fig. 2.1.B) and can remain viable in soil and crop residue for more than 4 years (Short et al., 1980). *M. phaseolina* is a high-temperature pathogen (Gray et al., 1991). Moreover, the diseases caused by *M. phaseolina* such as seedling blight, charcoal rot, stem rot, and root rot are also favored by higher temperatures (30-35°C) and low soil moisture (Sandhu et al., 1999). Such environmental factors emphasize the potential threat of *M. phaseolina* to crop production in drought-prone regions. In fact, increased occurrence of the pathogen on various crop species has recently been reported worldwide (Khangura and Aberra, 2009; Mahmoud and Budak, 2011). Moreover, under predicted future climatic changes, tremendous yield losses due to intensified charcoal rot incidence around the world could be expected in many crops.

M. phaseolina causes charcoal rot in many economically important crops such as sorghum, soybean, maize, alfalfa and jute (Islam et al., 2012). It prevails across wide geographic regions including both tropical and temperate environments (Tarr, 1962, Tesso et al., 2012). In the United States, charcoal rot is a common problem in the southern states and central Great Plains (Edmunds and Zummo, 1975; Janet, 1983, Tesso et al., 2012). Charcoal rot is a high priority fungal disease in sorghum [*Sorghum bicolor* (L.) Moench], causing tremendous crop losses whereever sorghum is grown (Tarr, 1962, Tesso et al., 2012). Charcoal rot in sorghum deserves much scientific attention as it can directly affect global food security. Sorghum is a staple cereal crop for many people in the marginal, semiarid environments of Africa and South Asia. The unique capability of sorghum to grow in low and variable rainfall regions reveals its suitability to enhance agricultural productivity in water-limited environments (Rosenow et al., 1983; Mann et al., 1983). Around the world, sorghum is utilized as an important source of food, feed, sugar, and fiber. With the recent interest in bioenergy feedstocks, sorghum has been recognized as a promising alternative for sustainable biofuel production (Kimber et al., 2013).

Charcoal rot in sorghum is characterized by degradation of pith tissue at or near the base of the stalk causing death of stalk pith cells (Edmunds, 1964). Infected plants often have damaged vascular and cortical tissues in both the root and stalk systems that may reduce nutrient and water absorption and translocation (Hundekar and Anahosur, 2012). Typical charcoal rot symptoms can be seen by longitudinally splitting the infected stalks. Doing so reveals distinctive grey to black pigmentation (Fig. 2.1.C) of the entire infected tissue covered with bundles of small, black microsclerotia (Fig. 2.1.B). Plant lodging, impeded grain filling, and premature ripening are the major causes of yield losses due this disease. For decades, charcoal rot has been considered among the most widespread and destructive stalk rot diseases of sorghum (Mughogho and Pande, 1984; Tesso et al., 2005) which demonstrates the formidability of disease control. Although host resistance has been deployed, the inability to achieve complete control of the disease has been partly attributed to the polygenic nature of resistance and a poor understanding of the molecular basis of the sorghum-*Macrophomina* interaction. Understanding the complexity of disease resistance at the molecular level is critical to develop charcoal-rot-resistant sorghum lines and hybrids. Towards this end, only a single study has been reported thus far. Through a genome-wide association study (GWAS), Adeyanju et al. (2015) found four single nucleotide polymorphic sites (SNPs), that either reside within or adjacent to two genes [*Sb09g029260* (chalcone synthase), and *Sb09g028280.1* (ROP GTPase proteins)], which are significantly associated with stalk rot resistance. However, the findings seemed narrow in scope as the R^2 values for the SNPs were low (maximum of 0.16). Moreover, the derivable amount of useful information for the plant-pathogen interaction is limited with GWAS, particularly when the resistance is quantitative in nature.

The genetic control of resistance to necrotrophic pathogens in general and *M. phaseolina*, in particular, is poorly understood. Large-scale gene expression studies can provide a broader view and better understanding of disease resistance mechanisms. Although *M. phaseolina* affects more than 500 plant species, its impact on the genome-wide host transcription profile has not been reported for any of its host species. Here, we characterize and compare the global transcriptome of resistant and susceptible sorghum genotypes infected with *M. phaseolina* at three post-inoculation stages (PIS) using RNA-Seq technology, the sorghum reference genome (BTx623) along with agriGO, and SorghumCyc databases.

Classically, plant scientists believed that necrotrophs kill the host using various phytotoxins secreted into the host tissues before feeding (Friesen et al., 2010; Zhang et al., 2011; Mengiste, 2012; Jia et al., 2013). More recently, effectors have been discovered that interact with specific dominant host susceptibility genes, demonstrating the reliance of certain necrotrophic fungi on a gene-for-gene mechanism to manifest disease susceptibility (Liu et al., 2009; Oliver and Solomon, 2010; Faris et al., 2010). Here, we show that *M. phaseolina* manipulates diverse aspects of the host plant's metabolism and defense responses, providing new insights into induced host susceptibility by a necrotroph at the whole genome scale. The contribution and interconnection between differentially expressed, prominent metabolic pathways towards charcoal rot susceptibility in grain sorghum are reported here.

MATERIALS AND METHODS

Plant materials, establishment, maintenance, inoculum preparation, and inoculation

Charcoal-rot-resistant (SC599R) and -susceptible (Tx7000) sorghum genotypes were used. Seeds were treated with the fungicide captan (N-trychloromethyl thio-4-cyclohexane-1,2 dicarboxamide) and were planted in 19 L Poly-Tainer pots filled with Metro-Mix 360 growing medium (Sun Gro Bellevue, WA, U.S.A). Three seeds were planted in each pot at the beginning. However, leaving the most vigorous one, the other two seedlings were thinned at three weeks after emergence. There were 18 pots per each genotype. Pots were randomly placed on a bench in the greenhouse and kept at 25-32°C with a 16-h light/8-h dark photoperiod. Plant maintenance was carried out according to the procedures described by Bandara et al. (2015). A previously characterized, highly virulent isolate of *M. phaseolina* obtained from the row crops pathology lab, Department of Plant Pathology, Kansas State University was used for the experiment. The protocol described by Bandara et al. (2015) was used to prepare *M. phaseolina* inoculum. Briefly, *M. phaseolina* was grown on potato dextrose agar at 30°C for 5 d. Subcultures from PDA were used to initiate liquid cultures in potato dextrose broth (PDB) to obtain mycelia. Mycelial suspensions were blended and filtered through four layers of sterile cheesecloth to obtain small hyphal fragments. Filtrates containing hyphal fragments were centrifuged at 3000 g for five minutes, and the resulting pellets were resuspended in 50 mL of 10 mM (pH 7.2) sterile

phosphate-buffered saline (PBS). Concentrations of hyphal fragments were determined using a hemocytometer and adjusted to 2×10^6 hyphal fragments mL^{-1} by diluting with PBS. All inoculum preparation steps were performed under aseptic conditions. Plants were inoculated at 14 days after anthesis using a 1 mL, 26 gauge, 1.5-inch needle, sterile surgical syringe by injecting 0.1 mL of inoculum into the basal node of the stalk. Phosphate-buffered saline (pH 7.2) was used as the mock-inoculated control treatment. Two inoculation treatments were randomly assigned to each experimental unit (= single plant in the pot).

Tissue collection, RNA extraction and quality check

Stalk tissues of inoculated and mock-inoculated control plants were collected from three biological replicates at 2, 7, and 30 days post-inoculation (DPI) (3 biological replicates per DPI per treatment per sorghum line = 36 plants total). From each biological replicate, a 8-10 cm long stalk piece encompassing the inoculation point was collected and immediately frozen in liquid nitrogen to prevent mRNA degradation and then stored at -80°C until RNA extraction. For consistency across replicates, approximately 1 g of stalk tissues 2 cm above the symptomatic region was used for RNA extraction. The symptomatic region is a necrotic lesion. Therefore, to ensure the quality and quantity of the RNA extract, tissue sampling was conducted 2 cm above the lesion border. RNA extraction was performed using Triazole reagent (Thermo Scientific, USA) following the manufacturer's instructions. Extracted total RNA was treated with Amplification Grade DNAse I (Invitrogen Corporation, USA). RNA quality and quantity were checked using a Nanodrop 2000 instrument (Thermo Scientific, USA). RNA samples were diluted with RNase-free water to obtain samples with a concentration of 100-200 ng/µl. RNA integrity and quantity were checked using an Agilent 2100 Bioanalyzer (Agilent Technologies Genomics, USA). RNA from biological replicates was not pooled.

cDNA library construction and Illumina sequencing

Thirty-six cDNA libraries (one from each treatment/replicate) were constructed using the Illumina TruSeq™ RNA sample preparation kit according to the manufacturer's protocol (Illumina Inc., USA). RNA from each plant was subjected to two rounds of enrichment for poly-A mRNAs using "oligodT" attached magnetic beads. Purified mRNA was chemically fragmented and converted to single-stranded cDNAs according to the manufacturer's protocol

(Illumina Inc., USA). cDNA from each library was separately barcoded with adapter indexes and pooled. Sequencing was performed on a HiSeq 2000 platform (Illumina Inc., USA) using 100 bp single-end sequencing runs at the Genome Sequencing Facility at Kansas University Medical Center, Lawrence.

Sequence processing, alignment to BTx623 reference genome, analysis for differentially expressed genes and assigning gene functions

Single-end sequencing reads obtained from HiSeq 2000 runs were subjected to adapter trimming and quality filtering with a stand-alone adapter trimmer "Cutadapt" (Martin, 2011). The *Sorghum bicolor* reference genome (Sbicolor_v1.4) (Paterson et al., 2009) was used to perform read alignment using Genomic Short-read Nucleotide Alignment Program (GSNAP) (Wu and Watanabe, 2005). An R script was used to determine the read counting per gene in each sample. The RPKM value per gene in each sample represents read counts per kilobase of transcribed region per million reads (Mortazavi et al., 2008). Differential gene expression analysis was conducted using 'DESeq2' which employs a method based on the negative binomial distribution, with variance and mean linked by local regression. A q-value (Benjamini and Hochberg, 1995) was determined for each gene to account for multiple tests. To control false discovery rate (FDR) at 5%, only the genes with q-values smaller than 0.05 were considered to be significantly differentially expressed. DESeq2 analysis was performed at two levels. First, to identify pattern of changes in differential gene expression among two treatments between two lines, analysis was performed to test the null hypothesis of no two-way interaction between line (2 levels: resistant and susceptible sorghum lines) and treatment (2 levels: *M. phaseolina*-inoculated and mock-inoculated control) for each gene within each post-inoculation stage (i.e., 2, 7, and 30 DPI). Genes with significant two-way interaction (null hypothesis rejected) at the 5% FDR were designated as significantly differentially expressed. The hypothesis tested was,

H_O: Resistant line (infected-control) = Susceptible line (infected-control)

H_A: Resistant line (infected-control) ≠ Susceptible line (infected-control)

The second round of DESeq2 analysis was performed with the whole data set to further investigate the behavior of genes with a significant two-way interaction. Here, the difference

between two treatments was considered within each sorghum line and post-inoculation stage. The hypothesis tested was,

H_O: infected = control

H_A: infected ≠ control

Genes with rejected null hypothesis at the 5% FDR were designated as significantly differentially expressed between *M. phaseolina* infection and mock-inoculated control treatment within sorghum line and post-inoculation stage. To assign putative functions for differentially expressed genes, we used the gene annotation file acquired from the "Phytozome" database (Goodstein et al., 2012).

Functional annotation of differentially expressed genes using Gene Ontology (GO) and SorghumCyc metabolic pathway enrichment analyses

Gene Ontology (GO) enrichment analysis was performed using an R software package "goseq" to identify over-represented (significantly enriched) GO terms in the differentially expressed genes. This analysis classifies gene transcripts and their products into their corresponding biological processes (BP), molecular functions (MF), and cellular components (CC). To investigate the over-represented GO terms of an individual sorghum line at each post-inoculation stage, a list of differentially expressed genes that resulted from the second round of DESeq2 analysis was used. GO functional annotations for sorghum gene products were acquired from Agrigo (http://bioinfo.cau.edu.cn/agriGO/). GO categories were considered significantly enriched based on the *P*-value cut-off of 0.05. To further narrow down and understand the role and implications of differentially expressed genes on charcoal rot disease manifestation, metabolic pathway analysis was performed. For this analysis, we used genes with significant line × treatment interaction along with SorghumCyc genome database (ftp://ftp.gramene.org/pub/gramene/pathways/sorghumcyc (v. 1.0 beta)). Moreover, metabolic pathway enrichment analysis was performed using the Z-score method described by (Dugas et al., 2011) to determine the significantly enriched metabolic pathways. Briefly, the Z-score was determined as the quantity of the number of observed genes minus the expected gene number, divided by the square root of the standard deviation of the expected genes for each pathway. The observed gene counts are

defined as the number of differentially expressed genes within a pathway. The expected counts are computed by multiplying the number of genes in the differentially expressed gene list across all pathways by the number of genes within the pathway of interest and dividing this value by the number unique genes in the collection of all pathways. This helps to derive functional annotations and infer metabolic pathways of sorghum (Youens-Clark et al., 2011) under the experimental conditions concerned. Enrichment was performed separately for the three post inoculation stages. A metabolic pathway was considered significantly enriched if the calculated Z-score for that pathway ≥ 2 and the expected number of genes for a family > 1.

RESULTS

Read count correlation between biological replicates for informative genes

The reads per kilobase of transcript per million mapped reads (RPKM) values for each informative gene were compared between replicates for correlation, within a treatment (*M. phaseolina* and control), genotype (resistant and susceptible), and PIS (2, 7, and 30 DPI) to confirm the gene expression consistency between biological replicates. High R^2 values were observed in each of the 36 correlation analyses. Figure 2.2 shows example scatter plots for one selected correlation analysis out of three (i.e. replicates 1 vs 2, 1 vs 3, and 2 vs 3) per each treatment, genotype, and PIS combination. Strong R^2 values revealed the consistency of gene expression between biological replicates and ensured the reliability of RNA-Seq data in drawing valid inferences.

Mapping transcriptome to the reference genome and differential gene expression analysis

Overall, approximately 444 million quality filtered reads were generated across 36 samples (two genotypes, two treatments, three PIS, three biological replicates). Of those, approximately 420 million reads were mapped to the sorghum reference genome while around 400 million reads were uniquely mapped. The read mapping summary for all samples used in the study is given in Table 2.1. *P*-value histograms for informative genes showed “anti-conservative” distributions (Fig. 2.3) for *M. phaseolina* vs control comparisons for two sorghum genotypes at three PIS,

where the null *P*-values along the bottom of the graphs were uniformly distributed between zero and one. The observed anti-conservative distributions confirmed the appropriateness of deploying a false discovery rate to control inflation of type I error (false positives). The first round of DESeq2 analysis was conducted to identify genes with significant genotype × treatment interaction (see Methods) and revealed 2317, 7133, and 432 differentially expressed genes (DEG) at 2, 7, and 30 DPI, respectively. Figure 2.4 shows the distribution and overlap of DEG at three PIS. Table 2.2 shows the number of informative, significant, up/down regulated genes of each genotype upon *M. phaseolina* inoculation at three PIS. Volcano plots given in Figure 2.5 show the distribution of up/down-regulated genes and their significance for each genotype at three DPI.

Gene Ontology (GO) annotation of differentially expressed genes

Appendix A contains a complete list of significantly enriched GO terms for two sorghum genotypes at each PIS. The DEG transcripts with known GO annotation were categorized into 214, 100, and 180 GO terms in the resistant genotype (SC599) at 2, 7, and 30 DPI, respectively while those of the susceptible genotype (Tx7000) were categorized into 184, 243, and 203. Forty-two, 28, and 34 GO terms were common between resistant and susceptible sorghum lines at 2, 7, and 30 DPI, respectively. In each of the six cases (two genotypes, three DPI), most of the enriched GO terms were represented by biological processes (BP) followed by molecular function (MP) category. Cellular components (CC) was the least represented category. Figure 2.6 shows the distribution of enriched GO terms among three functional categories. Figure 2.7 shows the major sub-categories of each basic GO category for significantly enriched GO terms of two sorghum genotypes at each PIS. Within the biological process category, genes involved in major sub-categories such as assembly, response to abiotic stress, catabolic process, response to ions/substances, defense response, response to biotic stress, signal transduction, response to hormone, regulation, transport, response to abiotic stimuli, metabolic process, developmental process, cellular process, and biosynthetic process were common among the three PIS, although their relative representation varied among PIS. Biosynthetic, cellular, and developmental processes were among the most represented sub-categories at all stages, revealing the sensitivity of those processes to *M. phaseolina* inoculation. Within the cellular component category, cell wall, chloroplast, and membrane sub-categories were common among three PIS and appeared to

be highly impacted by the pathogen. Within the molecular function category, sub-categories such as binding, transporter, and enzyme/protein activity were prominent among all PIS. Overall, genes that belong to the sub-categories mentioned above may play a critical role in disease reaction (either resistance or susceptibility) in response to *M. phaseolina* inoculation.

SorghumCyc metabolic pathway enrichment analysis

To further explore the broader insights obtained from GO annotation analysis, DEG were subjected to metabolic pathway enrichment analysis. Although DESeq2 analysis (concerning the genotype × inoculation treatment interaction) resolved for 2317, 7133, and 432 DEG at 2, 7, and 30 DPI, respectively, only 588, 1718, and 100 of them had assigned metabolic pathways. The 588 DEG at 2 DPI were constituents of 143 metabolic pathways. However, only 14 pathways fulfilled the enrichment criteria (see Methods). Similarly, 1718 and 100 DEG resulted at 7 and 30 DPI and were constituents of 217 and 58 metabolic pathways. Only 106 pathways were enriched at 7 DPI while no enriched pathways were observed at 30 DPI. Pathway enrichment analysis revealed the importance of expression profile differences between resistant and susceptible genotypes at 7 DPI in response to pathogen infection as the highest number of enriched pathways resulted at 7 DPI. Therefore, for interpretation purposes, we focused on data at 7 DPI. A list of significantly enriched pathways and the number of observed and expected genes involved and respective Z-scores of each pathway are given in Appendix B. Interestingly, the resistant genotype, SC599, exhibited stable gene expression in the presence of the pathogen. Therefore, in the majority of genes, there was no significant differential expression between *M. phaseolina* and control inoculations. Contrary to the resistant genotype, *M. phaseolina* inoculation resulted in significant differential expression (infected – control) in the susceptible genotype. Consequently, the significant genotype × inoculation treatment interactions (see Methods) were more influenced by the susceptible genotype, Tx7000. Moreover, most of the metabolic pathways that were upregulated in Tx7000 are hypothesized to be instrumental in inducing susceptibility. Figure 2.8 shows the interconnection between different metabolic pathways and their contribution towards enhanced susceptibility. Appendix C contains a list of differentially expressed genes at three PIS that belong to some important SorghumCyc metabolic pathways discussed in this paper. Figs. 2.9 and 2.10 show the expression behavior (in terms of log 2-fold change differential expression between mock-inoculated control and *M. phaseolina*

inoculation) of three representative SC599 and Tx7000 genes that belongs to prominent metabolic pathways discussed in this chapter.

Differentially expressed genes in relation to sugar, starch, and glycerol metabolism

Pathway enrichment analysis showed that trehalose and rhamnose biosynthesis; fructose degradation to pyruvate and lactate; sucrose degradation to ethanol and lactate; glycerol, triacylglycerol, and starch degradation; and UDP glucose conversion pathways are significantly enriched. Many genes involved in those pathways were significantly differentially expressed between susceptible and resistant genotypes in response to *M. phaseolina* infection. Compared to control treatment, most of the genes involved in these pathways were significantly upregulated in the susceptible genotype, Tx7000 (Fig. 2.8) while those of resistant line were not significantly differentially expressed.

Ten genes involved in the trehalose biosynthetic pathway were significantly up-regulated in Tx7000 upon inoculation while those of SC599 did not exhibit significant differential expression (Appendix C). These included genes such as trehalose phosphatase (*Sb02g033420*), trehalose synthase (*Sb09g025660*), and trehalose-6-phosphate synthase (*Sb07g021920*) (Fig. 2.9.A) and were found to be up-regulated (by approximately 90-, 5-, and 25-fold, respectively) compared to the control. Eight genes (*Sb03g030610*, *Sb01g028740*, *Sb02g019490*, *Sb07g002570*, *Sb10g005250*, *Sb10g025280*, *Sb01g002920*, *Sb03g027840*) involved in UDP glucose conversion pathway were significantly upregulated *M. phaseolina* inoculated Tx7000 (Appendix C, Fig. 2.9.B). Another eight genes (*Sb01g038050*, *Sb01g039220*, *Sb01g043370*, *Sb02g029130*, *Sb08g022850*, *Sb09g018070*, and *Sb10g024490*) involved in the dTDP-L-rhamnose biosynthetic pathway were also significantly upregulated in Tx7000 after *M. phaseolina* inoculation (Appendix C, Fig. 2.9.C). Forty-four genes involved in fructose degradation to pyruvate and lactate metabolic pathway were significantly upregulated in *M. phaseolina*-inoculated Tx7000 while those of SC599 showed non-significant differential expression (Appendix C). These included two 6-phosphofructokinase encoding genes, four aspartic proteinase nepenthesin-2 precursor genes, one aspartic proteinase gene, six dirigent protein genes, two enolase genes, two glyceraldehyde-3-phosphate dehydrogenase genes, two hexokinase genes, four lactate/malate dehydrogenase genes, one phosphofructokinase gene, three pyruvate kinase genes, five

transporter family protein genes, and one triosephosphate isomerase gene. Fold up-regulation of these genes ranged from 1.4 to 113. Figure 2.9.D shows the expression pattern of three representative genes. Further, two genes (*Sb03g013420*, neutral/alkaline invertase; *Sb04g022350*, plant neutral invertase domain containing protein) in sucrose degradation I pathway and eight genes (*Sb01g006480,* glucose-6-phosphate isomerase; *Sb02g009280*, *Sb02g036310*, *Sb02g037570*, *Sb03g007080*, *Sb08g016530*, *Sb09g028810*, transporter family proteins; *Sb07g003750*, transporter, major facilitator family) in sucrose degradation to ethanol and lactate pathways were significantly upregulated in *M. phaseolina*-inoculated Tx7000. Figure 2.9.E shows the expression pattern of three representative genes involved in the sucrose degradation I pathway. Except *Sb02g037570* and *Sb09g028810* (which were significantly down-regulated), other genes of SC599 were not significant differential expressed.

Nineteen genes involved in starch degradation were significantly upregulated in Tx7000 including those encoding for alpha-amylase precursor (*Sb03g032830*, *Sb02g023250*, *Sb02g023790*), *glycosyltransferase* (*Sb03g007960*, *Sb10g018300*, *Sb10g002800*, *Sb03g008010*, *Sb04g035100*), and *transferase* family protein (*Sb02g031580, Sb10g005760, Sb10g005770*). These genes were up-regulated between 1.6- to 104-fold. Figure 2.9.F shows the typical expression pattern of three representative genes encode for each of the above-mentioned enzymes. Moreover, we observed a strong down-regulation of the starch biosynthesis genes in Tx7000 after *M. phaseolina* inoculation. For instance, three genes encoding *starch synthase* (*Sb06g029050*, *Sb02g009870*, *Sb09g026570*) were significantly down-regulated in Tx7000 (Fig. 2.9.G).

Expression behavior of the selected representative genes in the glycerol and triacylglycerol degradation pathways is shown in Fig. 2.9.H and I. Ten genes involve in glycerol degradation showed significant upregulation in Tx7000, out of which six genes encode for glycerophosphoryl diester phosphodiesterase family protein (*Sb04g021010*, *Sb06g014320*, *Sb07g026000*, *Sb01g015000*, *Sb03g035370*, *Sb04g024440*). These genes were up-regulated between 2.3- to 86-fold. The former four genes were significantly down-regulated in SC599 while the latter two were not significantly differentially expressed. Seven genes involved in triacylglycerol degradation were significantly up-regulated in Tx7000, out of which two genes encode for lipase

(*Sb04g019260*, *Sb03g009750*) and lipase precursor (*Sb02g042310*, *Sb05g025890*), one gene for *lipase* class 3 family protein (*Sb08g017740*), and another for *hydrolase* (*Sb03g039170*). The genes were up-regulated between 2.5- to 208-fold.

Differentially expressed genes in relation to host cell wall composition/degradation and phytoalexin biosynthesis

M. phaseolina significantly down-regulated cellulose biosynthesis genes while significantly up-regulating the homogalacturonan degradation pathway in Tx7000 (Fig. 2.8). Genes encode for cellulose synthase (*Sb02g010110*, *Sb02g025020*, *Sb03g034680*, *Sb01g019720*), CSLF6 (cellulose synthase-like family F, *Sb02g035980*), and CSLH1 (cellulose synthase-like family H, *Sb07g004110*) were significantly down-regulated while a cellulase gene (*Sb01g024390*) was significantly up-regulated (Fig. 2.9.J). Moreover, one gene encodes for endoglucanase, eight genes encode for glycosyl hydrolases family 17*,* and two genes encode for glucan endo-1,3-beta-glucosidase precursor were significantly up-regulated in *M. phaseolina*-inoculated Tx7000. Many genes encode for invertase (*Sb06g000550*, *Sb07g000850*, *Sb07g000860*, *Sb07g000870*), pectinesterase (*Sb01g022290*, *Sb02g012560*, *Sb03g012820*, *Sb03g036790*, *Sb09g017920*), and polygalacturonase (*Sb02g025730*, *Sb02g028280*, *Sb03g042350*, *Sb07g000740*, *Sb09g027150*) found to be significantly up-regulated in Tx7000 and were involved in homogalacturonan degradation metabolic pathway (Fig. 2.9.K). None of those genes were differentially expressed in SC599.

The genes involved in phenylalanine (*Sb08g004880*, *Sb06g000430*, *Sb01g038740*), phenylpropanoid (*Sb04g026560*, *Sb04g017460*), and isoflavonoid biosynthesis (*Sb07g025010*, *Sb03g005590*, *Sb03g005570*, *Sb01g005720*, *Sb01g040580*, encode gibberellin receptor GID1L2) were significantly up-regulated in *M. phaseolina* inoculated Tx7000 (Fig. 2.8). However, two genes involved in the coumarin biosynthesis pathway were significantly down-regulated (*Sb06g022510*) while many O-methyltransferases genes (*Sb04g036900*, *Sb04g037820*, *Sb07g005970*) were also strongly down-regulated.

Differentially expressed genes related to host aerobic respiration and nitric oxide biosynthetic pathways

Aerobic respiration-electron donor II/III pathways were significantly enriched in *M. phaseolina*-inoculated Tx7000. Twenty-one genes involved in the aerobic respiration-electron donor II pathway were significantly up-regulated, out of which four genes encode for cytochrome b-c_1 complex subunits (*Sb01g004390*, *Sb01g008560*, *Sb10g005110*, *Sb05g002090*). Another four genes encode for cytochrome c oxidase (*Sb08g018180*, *Sb03g027710*, *Sb02g039590*, *Sb01g006750*) (Fig. 2.9.L). These enzymes play a critical role in biochemical generation of ATP via oxidative phosphorylation. Out of seventeen significantly up-regulated genes that were involved in the aerobic respiration-electron donor III pathway, five genes encode for potassium transporter (*Sb02g042430*, *Sb10g009770*, *Sb07g006000*, *Sb03g044780*, *Sb03g044790*), while seven genes encode for a transmembrane 9 superfamily member protein (*Sb08g004730*, *Sb01g041650*, *Sb02g032530*, *Sb07g016310*, *Sb04g029560*, *Sb10g025700*, *Sb10g025690*). Interestingly, although not significant, most of these genes in SC599 were down-regulated after pathogen inoculation.

The nitrate reduction I pathway, involved in nitric oxide (NO) synthesis, was significantly up-regulated in Tx7000 upon *M. phaseolina* infection (Fig. 2.8). Three Tx7000 genes (*Sb08g011530*, *Sb04g027860* [encode laccase precursor protein], *Sb05g000680* [laccase-23]) involved in NO biosynthesis were strongly upregulated (Fig. 2.10.A). These genes were up-regulated approximately 650-, 180-, and 16-fold compared to the mock-inoculated control, respectively. Although not significant, these genes were down regulated in SC599 (Fig. 2.10.A).

Genes involved in chlorophyll degradation and Calvin cycle are differentially expressed

A gene that encodes chlorophyllase-2 (*Sb02g012300*) was up-regulated 200-fold in Tx7000 after *M. phaseolina* inoculation. Differential expression of this gene was not apparent in SC599. Moreover, thirteen genes involved in Calvin cycle showed significant up-regulation in *M. phaseolina*-inoculated Tx7000 and all of them encode for a ras-related protein (Fig. 2.10.B).

Differentially expressed genes related to host antioxidant system

We observed significant up-regulations of the genes involved in gamma-glutamyl cycle and glutathione-mediated detoxification pathways in Tx7000 upon *M. phaseolina* inoculation (Fig. 2.8). Figure 2.10.C and D, respectively, show the typical expression behavior of genes involved in those pathways. In total, twenty Tx7000 genes involved in the gamma-glutamyl cycle were significantly up-regulated (Appendix C). This cycle is the major glutathione (GSH) synthetic pathway in plants. Thirty-three Tx7000 genes involved in the glutathione-mediated detoxification pathway were significantly upregulated and encoded glutathione S-transferase (GST) (Appendix C). In the case of SC599, the majority of these genes were non-significantly down-regulated while some showed significant down-regulation.

Sb04g001460 (AMP-binding enzyme)*, Sb07g022040* (AMP-binding domain containing protein), *Sb05g020160*, *Sb05g020220*, and *Sb05g020230* (chalcone synthase) involved in flavonoid biosynthesis were significantly up-regulated in Tx7000 upon *M. phaseolina* inoculation while those of SC599 were not significantly differentially expressed (Fig. 2.10.E).

Forty genes involved in the betanidin degradation pathway were significantly up-regulated in Tx7000, out of which fourteen genes encoded for peroxidase precursors (*Sb05g001030*, *Sb09g004650*, *Sb09g004660*, *Sb10g028500*, *Sb03g036760*, *Sb09g020960*, *Sb03g046760*, *Sb06g030940*, *Sb05g001000*, *Sb09g021000*, *Sb01g020830*, *Sb03g013200*, *Sb03g013210*, *Sb01g041760*). Four genes each encoded MYB family transcription factor and ubiquitin-conjugating enzyme, and five genes encoded transporter family protein. These also showed a significant up-regulation in Tx7000. Figure 2.10.F shows the differential expression patterns of three representative genes involved in the betanidin degradation pathway.

Differentially expressed genes involved in host hormonal pathways

We observed strong evidence for enhanced salicylic acid (SA) production in *M. phaseolina*-inoculated Tx7000 (Fig. 2.8). Two phenylalanine ammonia-lyase genes (*Sb06g022750*, *Sb04g026560*) were significantly up-regulated in Tx7000 after *M. phaseolina* inoculation. Moreover, twelve genes involved in the chorismate biosynthesis including chorismate synthase-2

(*Sb10g002230*, *Sb03g018040*, *Sb01g040790*, *Sb10g028720*, *Sb09g004240*, *Sb05g003930*, *Sb05g003920*, *Sb01g033590*, *Sb02g039660*, *Sb05g024910*, *Sb01g019150*, *Sb02g037520*) (Fig. 2.10.G) and eighteen genes involved in the tetrahydrofolate biosynthesis (*Sb06g024530*, *Sb07g023030*, *Sb09g021540*, *Sb04g027180*, *Sb01g031140*, *Sb10g001620*, *Sb08g004260*, *Sb06g024355*, *Sb02g012630*, *Sb02g026140*, *Sb06g031800*, *Sb01g020570*, *Sb06g002560*, *Sb06g002800*, *Sb01g020580*, *Sb07g023780*, *Sb02g032700*, *Sb01g020990*) (Fig. 2.10.H) were significantly up-regulated in Tx7000.

Strong up-regulation of ethylene biosynthesis from methionine and methionine biosynthetic pathways was observed in *M. phaseolina*-inoculated Tx7000 (Fig. 2.8). Four significantly up-regulated genes (*Sb02g026280*, *Sb09g003800*, *Sb09g003790*, encode for 1-aminocyclopropane-1-carboxylate oxidase; *Sb01g026350*, encode for 26S proteasome non-ATPase regulatory subunit 4) may have contributed to enhanced ethylene biosynthesis in Tx7000 (Fig. 2.10.I). Further, nine genes (*Sb03g036040*, *Sb01g042580*, *Sb03g025740*, *Sb04g008020*, *Sb03g032590*, *Sb01g023070*, *Sb04g031870*, *Sb02g037580*, *Sb01g042690*) involved in methionine biosynthesis were also significantly up-regulated in Tx7000, and could have contributed to enhanced ethylene biosynthesis.

Although twelve genes in the brassinosteroid biosynthetic pathway (*Sb06g030800*, *Sb06g018830*, *Sb09g029490*, *Sb02g033270*, *Sb06g029550*, *Sb06g028720*, *Sb05g022890*, *Sb10g025740*, *Sb02g038530*, *Sb01g021890*, *Sb02g038520*, *Sb01g035380*; the latter seven genes encode for a NAD dependent epimerase/dehydratase family protein) (Fig. 2.10.J) were significantly up-regulated in Tx7000, two steroid 22-alpha hydroxylase genes (*Sb03g002870* and *Sb05g002580*) were significantly down-regulated in Tx7000 after pathogen inoculation. Another two 3-oxo-5-alpha-steroid 4-dehydrogenase encoding genes (*Sb03g040050* and *Sb02g003510*) were also found to be significantly down-regulated in pathogen-inoculated Tx7000. None of these four genes were significantly differentially expressed in SC599 in response to pathogen inoculation. Moreover, the sterol and trans, trans-farnesyl diphosphate biosynthetic pathways were significantly down-regulated in *M. phaseolina*-inoculated Tx7000. Genes involved in the sterol biosynthesis such as cycloartenol synthase (*Sb06g015960*, *Sb08g019310*, *Sb08g019300*, *Sb08g019290*), cycloartenol-C-24-methyltransferase 1 (*Sb01g004300*), cycloeucalenol

cycloisomerase (*Sb09g002170*), and cytochrome P450 51 (*Sb05g022370*, *Sb08g002250*) and three genes involved in the trans, trans-farnesyl diphosphate biosynthesis pathway (prenyltransferase, *Sb01g044560*; para-hydroxybenzoate polyprenyltransferase, *Sb04g038180*; polyprenyl synthetase, *Sb07g005530*) were significantly down-regulated in Tx7000.

Eleven genes involved in gibberellin biosynthetic pathway were significantly up-regulated in *M. phaseolina*-inoculated Tx7000 (Fig 2.10.K), out of which three genes encoded flavonol synthase/flavanone 3-hydroxylase (*Sb10g004340*, *Sb03g038880*, *Sb01g029140*) and naringenin, 2-oxoglutarate 3-dioxygenase (*Sb06g026350*, *Sb06g026330*, *Sb06g026340*). One gene encoded gibberellin 20 oxidase 2 (*Sb02g012470*) and another encoded gibberellin 3-beta-dioxygenase 2-2 (*Sb03g004020*).

Twenty-six genes involved in the latter steps of jasmonic acid (JA) biosynthesis (such as cytochrome P450 74A3 and 12-oxophytodienoate reductase) were significantly up-regulated in the susceptible genotype, Tx7000, after *M. phaseolina* inoculation (Appendix C, Fig 2.10.L) out of which seven genes each encode for 12-oxophytodienoate reductase and no apical meristem protein. However, genes such as phospholipase A2 (*Sb07g028890*, *Sb01g010640*, *Sb03g037150*, *Sb01g040430*, *Sb06g021680*) and lypoxygenase (*Sb06g031350*, *Sb01g011040*) (needed for the initial steps in JA biosynthesis) were significantly down-regulated in *M. phaseolina* inoculated Tx7000.

The cytokinin biosynthetic pathway (38 genes) was significantly up-regulated in Tx7000 after *M. phaseolina* inoculation (Appendix C, Fig. 2.8). Genes encoding anthocyanidin glucosyltransferases (seven genes), cytokinin glucosyltransferases (seven genes), UDP-glucoronosyl/UDP-glucosyl transferase (two genes), UDP-glucoronosyl and UDP-glucosyl transferase domain containing protein (seven genes), indole-3-acetate beta-glucosyltransferase (two genes), flavonol-3-O-glycoside-7-O-glucosyltransferase 1 (two genes) were significantly up-regulated in pathogen inoculated Tx7000. Moreover, three genes involved in cytokinin degradation (cytokinin dehydrogenase precursor) were significantly down-regulated in Tx7000 after *M. phaseolina* inoculation.

DISCUSSION

The current study provided transcriptional-data-based evidences on induced charcoal rot susceptibility in grain sorghum. Although functional studies are essential to validate this hypothesis, this study serves the purpose of providing new insights into potential mechanisms that underlie induced susceptibility using gene expression data. For the interpretation purpose, we assume that transcriptional data reflect the translational changes. Chapters 3-6 of this thesis provide information about the additional functional investigations conducted on selected metabolic pathways to prove the concept of induced charcoal rot susceptibility.

Altered sorghum sugar/starch/glycerol metabolism, enhanced pathogen nourishment and virulence, and increased disease susceptibility.

The multifunctional nature of trehalose is well known (Fernandez et al., 2010). It can elicit plant defense, particularly against biotrophic/hemi-biotrophic fungi (Bae et al., 2005a; Bae et al., 2005b; Renard-Merlier et al., 2007). Trehalose-mediated defense elicitation seems less important against necrotrophs such as *M. phaseolina*. Trehalose is a key compound of virulence in certain fungal pathogens (Foster et al., 2003; Wilson et al., 2007; Puttikamonkul et al., 2010; Djonović et al., 2013). It is accumulated in *Plasmodiophora brassicae*-infected *Arabidopsis thaliana* roots, hypocotyls, stem, and leaves (Brodmann et al., 2002). However, Brodmann et al. (2002) believe that this increase is most probably due to the synthesis of trehalose by the pathogen and not by *Arabidopsis*. Moreover, trehalose 6-phosphate is required for the onset of tobacco leaf senescence (Wingler et al., 2012). Therefore, upregulated trehalose biosynthesis in Tx7000 may play a role in the onset of stalk senescence, which in turn enhances susceptibility to *M. phaseolina*. Although trehalose production by *M. phaseolina* has not been previously demonstrated, our data show that it can induce trehalose production in the susceptible sorghum host. From the standpoint of biosynthesis, trehalose-6-phosphate (T6P) is synthesized using UDP-glucose and glucose-6-phosphate as substrates, and then directly converted to trehalose (Foster et al., 2003). Interestingly, we observed a strong upregulation of the UDP-glucose conversion (into UDP-galactose) pathway in Tx7000 (Appendix C, Figs. 2.8, 2.9.B). Although UDP-glucose conversion contributes to lowered trehalose biosynthesis, reduced amounts of

UDP-glucose in stalks could contribute to the enhanced stalk senescence (Craig and Hooker, 1961), increasing Tx7000's susceptibility to the fungus.

Rhamnose has been reported to be a potent inducer of endopolygalacturonase gene expression in *Colletotrichum lindemuthianum*, which ultimately contributes to its enhanced virulence (Hugouvieux et al., 1997). Involvement of rhamnose in enhanced virulence in certain animal pathogenic fungi has also been reported (Fernandes et al., 1999). Therefore, host-derived rhamnose could be a virulence factor for *M. phaseolina*. Genotypes such as Tx7000, which tends to produce more rhamnose in the presence of *M. phaseolina*, appear to be more susceptible to charcoal rot disease.

The upregulated fructose degradation to pyruvate and lactate, sucrose degradation I, and sucrose degradation to ethanol and lactate pathways in Tx7000 may lead to less available stalk sugar content and in turn contributes to faster stalk senescence and increases susceptibility to the pathogen. Although evidence from sorghum is lacking, some studies have shown that the amount of reducing sugar and sucrose present in the lower stalk of susceptible maize genotypes is less than that of resistant genotypes and pith cell senescence occurs more quickly in susceptible plants (Craig and Hooker, 1961). Therefore, sorghum genotypes with lower stalk sugar content along with high sugar degradation under pathogen infection may be more susceptible to charcoal rot disease.

Upregulated starch degradation in Tx7000 may also contribute to stalk senescence. As the major storage substance, starch biosynthesis is important for the plants as it is the major source for the respiration at night. Further, starch provides a buffer against irradiance changes during the day (Lunn and Hatch, 1995). Therefore, down-regulated biosynthesis and up-regulated degradation of starch can affect normal plant function and in turn contribute to enhanced stalk senescence.

Significantly up-regulated glycerol and triacylglycerol degradation pathways in Tx7000 may contribute to an enhanced nutritional status for the pathogen and contribute to enhanced disease susceptibility (Fig. 2.8). Triacylglycerol is degraded in to glycerol. Glycerol is then degraded into glycerol-3-phosphate and subsequently converted in to dihydroxy-acetone-phosphate

(http://pathway.gramene.org). Glycerol, glycerol-3-phosphate, and dihydroxy-acetone-phosphate may be utilized by *M. phaseolina* to fulfil its carbon requirement. Use of glycerol and its derivatives as the sole carbon and energy source by both bacteria and fungi is documented (Wei et al., 2004). Moreover, through targeted gene disruption of glycerol-3-phosphate dehydrogenase in *Colletotrichum gloeosporioides*, glycerol has been shown to be a nutrient transferred from host plant to fungal pathogen (Wei et al., 2004). The glycerol acquired from the host can in turn contribute to appressorium turgor generation, facilitating increased infection and subsequent spread. Although such a phenomenon is not reported for *M. phaseolina*, this has been demonstrated *in Magnaporthe grisea* (Thines et al., 2000). *M. phaseolina* contains 839 transporter genes comprising 106 families (Islam et al., 2012). The presence of transporters in vast quantities reveals the pathogen's ability to uptake different carbon and other sources from the host and to use a diverse array of carbon sources.

Altered cell wall related metabolic pathways may contribute to impeded host basal immunity

The presence of pre-formed barriers is often claimed to be the first line of plant defense (Thordal-Christensen, 2003). These could be structural, chemical, or enzymatic. Among structural barriers, plant cell walls play a critical role in limiting pathogen entrance to the host cell environment. Cellulose, hemicellulose, and pectin substances such as homogalacturonan are the major components of the primary cell wall. Cellulase, endoglucanase, and glycosyl hydrolases are major enzymes responsible for cellulose hydrolysis (Wilson, 2009). Fungi that possess these enzymes can use cellulose as an energy source (Wood et al., 1989). Two-hundred and nineteen glycosyl hydrolases including 25 putative endoglucanases, seven exocellobiohydrolases, and 28 β-glucosidases have been identified in *M. phaseolina* that facilitate the hydrolysis of host cellulose (Islam et al., 2012). Moreover, Glucan endo-1,3-beta-glucosidase is secreted by certain other fungi to degrade cellulose in plant cell walls (Do Vale et al., 2012). It has also been shown to be up-regulated in host plants infected with viruses (Beffa et al., 1993). In the current study, *M. phaseolina* appeared to reduce cellulose biosynthesis while increasing the depletion of existing cellulose via enhanced cellulose degradation. This, while impeding the structural resistance of the host, may contributes to enhanced stalk senescence, both of which facilitate the susceptibility to this necrotrophic pathogen. Moreover, inhibition of

cellulose biosynthesis can result in induced jasmonic acid (JA) and salicylic acid (SA) biosynthesis (Hamann et al., 2009). Further, mutations of certain cellulose synthase genes result in activation of JA and ethylene (ET) signaling (Ellis and Turner, 2001; Ellis et al., 2002a; Ellis et al., 2002b). Cellulose synthase mutant cev1 displays constitutively high JA levels (Ellis et al., 2002b). Therefore, cellulose synthases in the plant cell wall seem to be involved in regulation of JA levels. The significantly down-regulated cellulose synthase in the susceptible genotype, Tx7000 could potentially contribute to the up-regulation of JA biosynthetic pathway.

Typically, necrotrophs use their own cell wall–degrading enzymes (CWDEs) to induce host cell necrosis and cause leakage of nutrients (Mengiste, 2012). Here, we present evidence for the induction of host-derived CWDEs in the presence of a necrotrophic fungus. Furthermore, homogalacturonan degradation results in oligogalacturonides (OGs) release (Galletti et al., 2008). OGs released from *Arabidopsis* cell walls during infection by the necrotrophic fungus, *Botrytis cinerea* has been shown to trigger a robust NADPH oxidase (AtrbohD)-dependent oxidative burst (Galletti et al., 2008). Therefore, up-regulated host homogalacturonan degradation in the presence of *M. phaseolina* not only impedes the structural resistance of the host, but possibly amplifies disease associated-cell death. This in turn increases host susceptibility to *M. phaseolina*.

Lignin is a phenolic polymer covalently attached to the cellulose and hemicellulose components of cell walls of certain specialized cells such as the xylem tracheary elements, sclerenchyma and phloem fibers (Balakshin et al., 2008). It provides structural support to the wall and aids transporting water and nutrients within xylem (Harada and Cote, 1985). In addition, pathogen attack can trigger lignification of plant tissue (Dixon, 2001). However, in the current study, we found some indirect evidence for the *M. phaseolina*'s ability to impede cell wall lignification. O-methyltransferases (OMTs), one of the major groups of methyltransferases in plants, methylate the oxygen atom of a variety of secondary metabolites including phenylpropanoids, flavonoids, coumarin, and some alkaloids (Ibrahim et al., 1998; Ibrahim and Muzac, 2000). These phenolic compounds are formed from L-phenylalanine (Bureau et al., 2007). The methylated products of these secondary metabolites play a critical role as precursors in lignin biosynthesis (Bohm, 1998; Wink, 2003). OMTs have been shown to participate in lignin biosynthesis in herbacious tobacco

plants (Zhong et al., 1998), woody poplar plants (Zhong et al., 2000), and wheat (Ma and Xu, 2008) through their methylation activity. The strongly down-regulated OMTs in pathogen-inoculated TX700, could limit the formation of methylated forms of phenylpropanoids, and isoflavonoids, leading to less lignification of vascular tissues causing structural weakness. This, while facilitating the colonization and rapid spread of *M. phaseolina*, can also contribute to impeded water and nutrient transportation.

Up-regulated aerobic respiration aids reactive oxygen species (ROS) production and disease-associated cell death

Based upon gene expression data, Tx7000 appeared to have enhanced cellular respiration after *M. phaseolina* inoculation. Enhanced cellular respiration increases the ROS synthesis potential. In plant cells, the mitochondrial electron transport chain is a key site of ROS production (Møller, 2001). Increased respiratory electron transport and oxygen uptake resulted in increased production of ROS, and in turn amplified the oxidative stress in *Arabidopsis*, leading to enhanced programmed cell death (Tiwari et al., 2002). On the other hand, ROS associated hypertensive response (HR) or program cell death is a major plant resistance mechanism against plant pathogens. It provides resistance to biotrophic pathogens that obtain their energy from living cells (Kumar et al., 2001). Cell death also occurs during infection by necrotrophs and is indicative of successful infection (Govrin et al., 2006; van Kan, 2006). Activation of cell death augments colonization by necrotrophic pathogens (Govrin and Levine, 2000). Like HR-associated cell death, disease-associated cell death is moderated by host factors, including plant hormones and ROS (Desmond et al., 2008; Rossi et al., 2011). Therefore, ROS is a virulence factor for necrotrophs. Pathogenicity of *B. cinerea* and *S. sclerotiorum* has been shown to be directly dependent upon the level of superoxide and hydrogen peroxide (Govrin and Levine, 2000). Moreover, *B. cinerea* actively triggers an oxidative burst during cuticle penetration and primary lesion formation (Govrin and Levine, 2000; Tenberge et al., 2002; Tenberge, 2007). Therefore, findings of the current study indicated the potential contribution of enhanced host cellular respiration in ROS mediated charcoal rot susceptibility augmentation.

Nitric oxide is an integral component of oxidative burst-mediated cell death

In nature, plant-borne NO plays a key role in controlling cell differentiation and lignification, root and shoot development, flowering, growth and reorientation of pollen tubes, senescence and maturation, stomatal movement, plant-pathogen interactions, and programmed cell death (Malolepsza, 2007). HR-associated cell death is dependent upon balanced production of NO and ROS (Delledonne et al., 2001). Therefore, at low concentrations, NO can function as a signaling molecule that provides resistance against biotrophic or hemi-biotrophic pathogens via HR. However, a strong NO burst can facilitate necrotroph infection owing to NO mediated plant cell death. Induced NO production by the jute plant (*Corchorus capsularis*) in response to *M. phaseolina* infection has been demonstrated by Sarkar et al. (2014). Hence, taken together, strong induction of ROS and NO by *M. phaseolina* in Tx7000 appeared to enhance its susceptibility to the pathogen.

Potential role of upregulated chlorophyll degradation and Calvin cycle in charcoal rot disease reaction

Other than mitochondria, a major source of ROS in plants resides in the thylakoid membranes of chloroplasts (Zimmermann and Zentgraf, 2005; Foyer et al., 1994). Several forms of biotic and abiotic stress, such as pathogen attack or excess light, can result in the release of chlorophyll from the thylakoid membranes (Karpinski et al., 2003). Unless these released chlorophylls are quickly degraded, the photodynamic action of free chlorophyll can result in enhanced ROS generation and cause cellular damage (Takamiya et al., 2000). Chlorophyllase-1 (encoded by AtCLH1) of *Arabidopsis* is rapidly induced after tissue damage caused by the bacterial necrotroph *Erwinia carotovora* or the necrotrophic fungus *Alternaria brassicicola* and is instrumental in swiftly degrading free chlorophylls (Kariola et al., 2005). Upregulated chlorophyllase expression in pathogen-inoculated Tx7000 provides evidence for *M. phaseolina* infection-mediated-chlorophyll release and the enhanced ROS synthesis capacity in this genotype. Through upregulated chlorophyllase-2, Tx7000 may minimize the ROS generation and subsequent ROS-mediated cell death. However, the accumulation of chlorophyll breakdown products could also induce cell death, possibly by contributing to ROS biosynthesis (Mach et al., 2001; Pruzinska et al., 2003; Yao and Greenberg, 2006). Therefore, the fate of upregulated

chlorophyllase-2 may be enhanced charcoal rot susceptibility through increased ROS production associated stalk senescence.

The impact of pathogen infection on reduced RUBP regeneration in various crops is widely reported (Bowden et al., 1990; Pennypacker et al., 1995; Yang et al., 2014). However, as transcriptional data suggested, the enhanced RUBP regeneration capacity observed in the current study could contribute to enhanced Calvin cycle efficiency. This is important to minimize the host energy deficit and maintain housekeeping cellular functions as *M. phaseolina* inoculation may resulted in increased aerobic respiration in the susceptible genotype.

Potential role of strong antioxidant responses in charcoal rot disease reaction

GSH and GST are strong antioxidants that prevent oxidative damage to cells. As there was a strong upregulation in NO and ROS biosynthetic genes, upregulated GSH and GST could be instrumental in minimizing the oxidative damages due to NO (Airaki et al., 2011) and ROS (Noctor and Foyer, 1998), thus reducing cell death, and decreasing susceptibility of Tx7000 to *M. phaseolina*. However, some studies have shown that elevated GSH, instead of preventing oxidative damage, can potentially induce cell death (Creissen et al., 1999; de Pinto et al., 2002). Down-regulation of GSH genes in the resistant line, SC599, suggested the possibility of the latter phenomenon for the *M. phaseolina*-sorghum interaction, although functional studies are needed to deduce the exact role of GSH in this interaction.

Fungal elicitors and GSH have been shown to activate the transcription of certain chalcone synthase genes such as CHS15 (Dron et al., 1988; Choudhary et al., 1990; Harrison et al., 1991). As mentioned above, we observed a strong up-regulation of the gamma glutamyl cycle in *M. phaseolina*-infected Tx7000, which is responsible for GSH biosynthesis. Glutathione may contribute to the upregulation of flavonoid biosynthesis through transcriptional activation of the three chalcone synthase genes mentioned in the Results section. Flavonoids are known to be effective scavengers of reactive oxygen species (ROS) (Landry et al., 1995; Ryan et al., 2002; Tattini et al., 2004; Tattini et al., 2005; Lillo et al., 2008; Agati et al., 2009; Agati et al., 2011) and the up-regulation of its synthesis in Tx7000 would help lowering its susceptibility to *M. phaseolina*.

The up-regulated betanidin degradation pathway in *M. phaseolina*-infected Tx7000 (Fig. 2.8) may contribute to decreased disease susceptibility. Peroxidase genes involved in this pathway reduce cellular H_2O_2 levels (Hammond-Kosack and Jones, 1996) and helps to reduce ROS-mediated cell death, which in turn contributes to decreased susceptibility to *M. phaseolina*. The *Arabidopsis* gene *BOS1* that encodes for a MYB transcription factor protein is required to restrict the spread of necrotrophic pathogens, *Botrytis cinerea* and *Alternaria brassicicola* (Mengiste et al., 2003). Therefore, the up-regulated MYB family transcription factor in Tx7000 may also play a vital role in decreasing susceptibility to *M. phaseolina*.

Susceptibility is augmented by complex hormonal regulation

The gene expression data suggested a complex hormonal interplay in Tx7000 in response to *M. phaseolina* inoculation that may ultimately resulted in enhanced susceptibility to charcoal rot disease. Necrotrophic fungal pathogens can manipulate host phytohormone pathways, enabling them to kill and feed on dead cells (Kazan and Lyons, 2014). The gene expression data suggested the potential for strong upregulation in salicylic acid (SA), ethylene (ET), gibberellin, and cytokinin biosynthetic pathways and down-regulated JA and brassinosteroid pathways in Tx7000 due to *M. phaseolina* infection. SA (Draper, 1997; Van Camp et al., 1998), ethylene (Crowell et al., 1992; Rao et al., 2002), brassinosteroid (Yamamoto et al., 2001; Xia et al., 2009; Zhang et al., 2010), and gibberellin (Achard et al., 2008; Ishibashi et al., 2012) can trigger ROS production, which results in oxidative burst-mediated cell death. Therefore, up-regulation of these hormone biosynthetic pathway genes in Tx7000 after *M. phaseolina* inoculation may enhances susceptibility to this necrotrophic fungus.

The potential for enhanced salicylic acid (SA) production in *M. phaseolina* inoculated Tx7000 was observed. Although elevated SA promotes resistance to biotrophs and hemibiotrophs, it enhances susceptibility to necrotrophs (Veronese et al., 2004; Veronese et al., 2006). Further, SA is synthesized in the plastid from chorismate via the isochorismate pathway (Wildermuth et al., 2001; Dempsey et al., 2011) and in the cytosol through the phenylalanine ammonia-lyase pathway (Dempsey et al., 2011). Of these, the former is the major source of both basal and pathogen-induced SA production (Dempsey et al., 2011). Further, phenylalanine is derived from

the precursor chorismate (Dao et al., 2011). As mentioned earlier, the phenylalanine biosynthetic genes were also significantly up-regulated in Tx7000 (Fig. 2.8). This presumably contributed by up-regulated chorismate biosynthesis. Hence, the potential contribution of induced chorismate production in SA synthesis through phenylalanine ammonia-lyase pathway was also evident in this study. Moreover, chorismate is an essential substrate for para-amino benzoic acid (PABA) synthesis in plants (Haslam, 1993) and PABA is a direct precursor for folic acid synthesis (Wittek et al., 2015). On the other hand, enhanced tetrahydrofolate biosynthesis can yield more folic acid. Folic acid is an inducer of salicylic acid-dependent immunity in *Arabidopsis* and enhances susceptibility to *Alternaria brassicicola* (Wittek et al., 2015). Moreover, application of folic acid itself increased the susceptibility to this necrotrophic fungus (Wittek et al., 2015). As *M. phaseolina* is a necrotroph, we speculate that potentially up-regulated host folic acid production could enhance the susceptibility of Tx7000 to this pathogen.

In addition to its role as a ROS synthesis inducer, ethylene is a known senescence inducer (Bleecker and Patterson, 1997). Both these phenomena are in favor of promoting host susceptibility to necrotrophs. Hence upregulated ethylene biosynthetic genes could mean that Tx7000 is more vulnerable to *M. phaseolina*.

Although many genes involved in the brassinosteroid biosynthetic pathway were significantly up-regulated in Tx7000 after *M. phaseolina inoculation*, some key genes (steroid 22-alpha hydroxylase and 3-oxo-5-alpha-steroid 4-dehydrogenase) of this pathway were significantly down-regulated. Therefore, brassinosteroid production could be constrained in Tx7000 upon pathogen inoculation. Brassinosteroids are plant growth-regulating steroids (Grove et al., 1979) and are synthesized from trans-farnesyl diphosphate and sterols (http://pathway.gramene.org). Therefore, the down-regulated trans-farnesyl diphosphate and sterol biosynthetic genes observed in Tx7000 upon pathogen inoculation could also negatively affect the rate of brassinosteroid biosynthesis. Other than its involvement in enhanced ROS generation, upregulated brassinosteroid biosynthesis can result in higher ethylene concentrations in the infected area as it triggers ethylene biosynthesis (Schlagnhaufer et al., 1984; Vardhini and Rao, 2002). Moreover, brassinosteroids induce nitric oxide production (Cui et al., 2011). Therefore, if brassinosteroids are overproduced, it could be detrimental to Tx7000 in the presence of necrotrophic fungi like *M.*

phaseolina. Therefore, restricted brassinosteroids production could be advantageous for Tx7000. However, brassinosteroids have been shown to increase the antioxidant capacity of different plant systems (Cheng et al., 2014; Li et al., 2016), suggesting the protective role of brassinosteroids against oxidative stress. Therefore, further investigations are needed to determine the role of constrained brassinosteroid synthesis in the *M. phaseolina*-sorghum interaction.

In the current study, we observed transcriptional evidence for up-regulated gibberellin biosynthesis in pathogen-inoculated Tx7000. Exogenous application of gibberellin resulted in enhanced susceptibility to *Alternaria brassicicola* in *Arabidopsis* (Bari and Jones, 2009). This indicates the potential of gibberellin as a virulence factor for necrotrophic pathogens. Moreover, gibberellin is shown to be a negative regulator of defense against necrotrophs (Achard et al., 2008; Navarro et al., 2008). Therefore, it may be possible that gibberellin induces charcoal rot susceptibility in Tx7000. However, the isoflavonoid biosynthetic pathway (genes of which were found to be upregulated in Tx7000 in the current study) contains genes that encode for a gibberellin receptor *GID1L2*. This shows that gibberellin is essential for isoflavonoid biosynthesis. Earlier in the discussion, the role of isoflavonoids in charcoal rot disease resistance was discussed. Therefore, contrary to the above-mentioned hypothesis, upregulated gibberellin biosynthesis could indirectly contribute to reduced charcoal rot susceptibility in Tx7000. Therefore, further functional experiments are needed to deduce the exact function of host-derived gibberellin in the charcoal rot disease reaction.

In general, there is a cross-talk between SA and JA biosynthetic pathways in plants and their signaling tends to be mutually antagonistic (Clarke et al., 1998; Gupta et al., 2000; Petersen et al., 2000; Clarke et al., 2001; Jirage et al., 2001; Glazebrook, 2005; Bernsdorff et al., 2016). Although evidences for simultaneous up-regulation of both SA and JA are rare, Salzman et al. (2005) have shown that increased SA could lead to increased endogenous JA production in sorghum. Moreover, Schenk et al. (2000) have shown the synergism between SA and JA signaling. In the current study, although the genes involved in the latter steps of JA biosynthesis were upregulated, down-regulation of the genes involved in the initial steps of JA biosynthesis suggested that Tx7000 has limited JA biosynthetic capacity under *M. phaseolina* inoculation. JA-

mediated host resistance against necrotrophic pathogens is well documented (Thomma et al., 1998; Thomma et al., 1999; McDowell and Dangl, 2000). Furthermore, exogenous application of JA has been shown to confer resistance to necrotrophs, while loss of JA synthesis or response can compromise defense against fungal and oomycete necrotrophs (Vijayan et al., 1998; Thomma et al., 1999; Abuqamar et al., 2008). Therefore, the impeded JA biosynthetic capacity of Tx7000 could increase its susceptibility to charcoal rot. Interestingly, JA and ET have also been shown to promote susceptibility to the necrotrophic fungal pathogen, *Alternaria alternata* f. sp. *lycopersici* (AAL) through toxin- induced cell death in tomato (Zhang et al., 2011; Jia et al., 2013). Typically, necrotrophs use diverse phytotoxic compounds such as toxins to induce cell necrosis (Mengiste, 2012). *M. phaseolina* also produces a variety of phytotoxins including asperlin, isoasperlin, phomalactone, phomenon, phaseolinone (Dhar et al., 1982; Bhattacharya et al., 1992), and botryodiplodin (Ramezani et al., 2007). We suspect that, as in the case of AAL, the potency of phytotoxins (one, several or all) produced by *M. phaseolina* could be enhanced by JA, so that instead conferring resistance, JA is instrumental in increasing the charcoal rot susceptibility. Therefore, impeded JA biosynthetic capacity of Tx7000 could potentially decrease its susceptibility to charcoal rot disease. More functional experiments are essential to rule out the precise function of host-derived JA in the reaction of sorghum to *M. phaseolina*.

As indicated by the transcriptional data, the potentially up-regulated host cytokinin biosynthesis in Tx7000 upon *M. phaseolina* inoculation may also have complex implications on the charcoal rot disease reaction. For instance, its role in delaying senescence (Gan and Amasino, 1995; Wingler et al., 1998; Chang et al., 2003; Guo and Gan, 2011) and decreasing host susceptibility, particularly against viruses (Masuta et al., 1995; Pogány et al., 2004; Gális et al., 2004) are well documented. This suggests that cytokinins help reduce susceptibility against necrotrophic pathogens. However, cytokinin has also been shown to induce SA-mediated defense responses that confer resistance to biotrophs and hemi-biotrophs (Choi et al., 2010; Choi et al., 2011; Argueso et al., 2012). Furthermore, the application of cytokinin induces NO accumulation in *Arabidopsis* (Tun et al., 2008), demonstrating the potential involvement of cytokinin in stimulating hypersensitive reaction (HR) and R protein-mediated programmed cell death. In this study, NO biosynthetic genes were significantly up-regulated in the susceptible genotype after *M. phaseolina* inoculation. Therefore, although cytokinin may play a critical role in conferring

resistance against biotrophs or hemi-biotrophs, it could be a virulence factor for necrotrophic pathogens. Therefore, more functional investigations are needed to understand the precise role of cytokinin in the *M. phaseolina*-sorghum interaction. Moreover, extracellular invertase is essential for the delay of cytokinin-mediated senescence in tobacco (Balibrea Lara et al., 2004). As mentioned earlier, a significant up-regulation of four invertase encoding genes was observed in *M. phaseolina* inoculated Tx7000 and were attributed to enhanced homogalacturonan degradation. Unless invertase is not an essential element for delays in cytokinin-mediated senescence in sorghum as opposed to tobacco, invertases appeared to play a dual role in sorghum that results in two antagonistic outcomes under *M. phaseolina* infection. On one hand, it is involved in impeded structural immunity and disease-associated cell death that promotes susceptibility to *M. phaseolina*. On the other hand, up-regulated invertase synthesis could promote cytokinin-mediated delays in senescence, decreasing the susceptibility to this necrotrophic pathogen. The potential dual actions of invertase in relation to the predisposition of charcoal rot also deserves further investigations.

CONCLUSIONS

In this study, we examined the stalk transcriptomes of known charcoal-rot-resistant (SC599) and susceptible (Tx7000) sorghum genotypes in response to *M. phaseolina* inoculation. Differential gene expression and subsequent metabolic pathway analyses indicated that a considerable number of metabolic pathways are significantly up-regulated in the *M. phaseolina* inoculated susceptible genotype and in turn contributed to enhanced charcoal rot susceptibility. These pathways were broadly related to host basal immunity, pathogen nutrition and virulence, and reactive oxygen/ nitrogen species-mediated host cell death. The paradoxical hormonal regulation observed in pathogen-inoculated Tx7000 was characterized by strongly up-regulated salicylic acid and down-regulated jasmonic acid pathways. The majority of the SC599 genes were not significantly differentially expressed. This indicated the stable gene expression behavior of the resistant genotype, despite pathogen inoculation. Although further functional investigations are needed to prove the concept, findings of the current study provided exciting insights into induced host susceptibility to charcoal rot disease at the whole-genome scale.

REFERENCES

Abuqamar S, Chai MF, Luo H, Song F, Mengiste T. 2008. Tomato protein kinase 1b mediates signaling of plant responses to necrotrophic fungi and insect herbivory. *Plant Cell* 20: 1964-1983.

Achard P, Renou J, Berthomé R, Harberd NP, Genschik P. 2008. Plant DELLAs restrain growth and promote survival of adversity by reducing the levels of reactive oxygen species. *Current Biology* 18: 656-660.

Adeyanju A, Little C, Yu J, Tesso T. 2015. Genome-wide association study on resistance to stalk rot diseases in grain sorghum. *G3: Genes| Genomes| Genetics* 5: 1165-1175

Agati G, Biricolti S, Guidi L, Ferrini F, Fini A, Tattini M. 2011. The biosynthesis of flavonoids is enhanced similarly by UV radiation and root zone salinity in *L. vulgare* leaves. *Journal of Plant Physiology* 168: 204-212.

Agati G, Stefano G, Biricolti S, Tattini M. 2009. Mesophyll distribution of 'antioxidant' flavonoid glycosides in *Ligustrum vulgare* leaves under contrasting sunlight irradiance. *Annals of Botany* 104: 853-861.

Airaki M, Sanchez-Moreno L, Leterrier M, Barroso JB, Palma JM, Corpas FJ. 2011. Detection and quantification of S-nitrosoglutathione (GSNO) in pepper (*Capsicum annuum* L.) plant organs by LC-ES/MS. *Plant and Cell Physiology* 52: 2006-2015.

Argueso CT, Ferreira FJ, Epple P, To JP, Hutchison CE, Schaller GE, Dangl JL, Kieber JJ. 2012. Two-component elements mediate interactions between cytokinin and salicylic acid in plant immunity. *PLoS Genetics* 8: p.e1002448.

Bae H, Herman E, Bailey B, Bae H, Sicher R. 2005a. Exogenous trehalose alters *Arabidopsis* transcripts involved in cell wall modification, abiotic stress, nitrogen metabolism, and plant defense. *Physiologia Plantarum* 125: 114-126.

Bae H, Herman E, Sicher R. 2005b. Exogenous trehalose promotes non-structural carbohydrate accumulation and induces chemical detoxification and stress response proteins in *Arabidopsis thaliana* grown in liquid culture. *Plant Science* 168: 1293-1301.

Balakshin MY, Capanema EA, Chang H. 2007. MWL fraction with a high concentration of lignin-carbohydrate linkages: Isolation and 2D NMR spectroscopic analysis. *Holzforschung* 61: 1-7.

Bandara YMAY, Perumal R, Little CR. 2015. Integrating resistance and tolerance for improved evaluation of sorghum lines against Fusarium stalk rot and charcoal rot. *Phytoparasitica* 43: 485-99.

Bari R, Jones JD. 2009. Role of plant hormones in plant defence responses. *Plant Molecular Biology* 69: 473-488.

Beffa RS, Neuhaus JM, Meins F. 1993. Physiological compensation in antisense transformants: specific induction of an "ersatz" glucan endo-1,3-beta-glucosidase in plants infected with necrotizing viruses. *Proceedings of the National Academy of Sciences*, USA 90: 8792-8796.

Benjamini Y, Hochberg Y. 1995. Controlling the false discovery rate: a practical and powerful approach to multiple testing. *Journal of the Royal Statistical Society. series B (Methodological)* 289-300.

Bernsdorff F, Doring AC, Gruner K, Schuck S, Brautigam A, Zeier J. 2016. Pipecolic acid orchestrates plant systemic acquired resistance and defense priming via salicylic acid-dependent and -independent pathways. *Plant Cell* 28: 102-129.

Bhattacharya D, Siddiqui KA, Ali E. 1992. Phytotoxic metabolites of *Macrophomina phaseolina*. *Indian Journal of Mycology and Plant Pathology* 22: 54-57.

Bleecker AB, Patterson SE. 1997. Last exit: senescence, abscission, and meristem arrest in *Arabidopsis*. *Plant Cell* 9: 1169-1179.

Bohm BA. 1998. Introduction to flavonoids: Chemistry and biochemistry of organic natural products. Harwood Academic Publishers, Amsterdam 2: 339-364.

Bowden RL, Rouse DI, Sharkey TD. 1990. Mechanism of photosynthesis decrease by *Verticillium dahliae* in potato. *Plant Physiology* 94: 1048-1055.

Brodmann D, Schuller A, Ludwig-Müller J, Aeschbacher RA, Wiemken A, Boller T, Wingler A. 2002. Induction of trehalase in *Arabidopsis* plants infected with the trehalose-producing pathogen *Plasmodiophora brassicae*. *Molecular Plant-Microbe Interactions* 15: 693-700.

Bureau T, Lam KC, Ibrahim RK, Behdad B, Dayanandan S. 2007. Structure, function, and evolution of plant *O-methyltransferases*. *Genome* 50: 1001-1013.

Chang H, Jones ML, Banowetz GM, Clark DG. 2003. Overproduction of cytokinins in petunia flowers transformed with P(SAG12)-IPT delays corolla senescence and decreases sensitivity to ethylene. *Plant Physiology* 132: 2174-2183.

Cheng F, Zhou YH, Xia XJ, Shi K, Zhou J, Yu JQ. 2014. Chloroplastic thioredoxin-f and thioredoxin-m1/4 play important roles in brassinosteroids-induced changes in CO_2 assimilation and cellular redox homeostasis in tomato. *Journal of Experimental Botany* 65: 4335-4347.

Choi J, Huh SU, Kojima M, Sakakibara H, Paek K, Hwang I. 2010. The cytokinin-activated transcription factor ARR2 promotes plant immunity via TGA3/NPR1-dependent salicylic acid signaling in *Arabidopsis*. *Developmental Cell* 19: 284-295.

Choi J, Choi D, Lee S, Ryu C, Hwang I. 2011. Cytokinins and plant immunity: old foes or new friends? *Trends in Plant Science* 16: 388-394.

Choudhary AD, Lamb CJ, Dixon RA. 1990. Stress Responses in Alfalfa (*Medicago sativa* L.): VI. Differential responsiveness of chalcone synthase induction to fungal elicitor or glutathione in electroporated protoplasts. *Plant Physiology* 94: 1802-1807.

Clarke JD, Aarts N, Feys BJ, Dong X, Parker JE. 2001. Constitutive disease resistance requires EDS1 in the *Arabidopsis* mutants cpr1 and cpr6 and is partially EDS1-dependent in cpr5. *Plant Journal* 26: 409-420.

Clarke JD, Liu Y, Klessig DF, Dong X. 1998. Uncoupling PR gene expression from NPR1 and bacterial resistance: characterization of the dominant *Arabidopsis* cpr6-1 mutant. *Plant Cell* 10: 557-569.

Craig J, Hooker AL. 1961. Relation of sugar trends and pith density to *Diplodia* stalk rot in dent Corn. *Diplodia* root and stalk rot of dent corn. *Phytopathology* 51: 376-382.

Creissen G, Firmin J, Fryer M, Kular B, Leyland N, Reynolds H, Pastori G, Wellburn F, Baker N, Wellburn A, Mullineaux P. 1999. Elevated glutathione biosynthetic capacity in the chloroplasts of transgenic tobacco plants paradoxically causes increased oxidative stress. *Plant Cell* 11: 1277-1292.

Crowell DN, John ME, Russell D, Amasino RM. 1992. Characterization of a stress-induced, developmentally regulated gene family from soybean. *Plant Molecular Biology* 18: 459-466.

Cui J, Zhou Y, Ding J, Xia X, Shi K, Chen S, Asami T, Chen Z, Yu J. 2011. Role of nitric oxide in hydrogen peroxide-dependent induction of abiotic stress tolerance by brassinosteroids in cucumber. *Plant, Cell & Environment* 34: 347-358.

Dao T, Linthorst H, Verpoorte R. 2011. Chalcone synthase and its functions in plant resistance. *Phytochemistry Reviews* 10: 397-412.

De Pinto MC, Tommasi F, De Gara L. 2002. Changes in the antioxidant systems as part of the signaling pathway responsible for the programmed cell death activated by nitric oxide and reactive oxygen species in tobacco Bright-Yellow 2 cells. *Plant Physiology* 130: 698-708.

Delledonne M, Zeier J, Marocco A, Lamb C. 2001. Signal interactions between nitric oxide and reactive oxygen intermediates in the plant hypersensitive disease resistance response. *Proceedings of the National Academy of Sciences USA*. 98: 13454-13459.

Dempsey DA, Vlot AC, Wildermuth MC, Klessig DF. 2011. Salicylic acid biosynthesis and metabolism. The *Arabidopsis* Book e0156.

Desmond OJ, Manners JM, Stephens AE, Maclean DJ, Schenk PM, Gardiner DM, Munn AL, Kazan K. 2008. The *Fusarium* mycotoxin deoxynivalenol elicits hydrogen peroxide production, programmed cell death and defence responses in wheat. *Molecular Plant Pathology* 9: 435-445.

Dhar TK, Siddiqui KA, Ali E. 1982. Structure of phaseolinone, a novel phytotoxin from *Macrophomina phaseolina*. *Tetrahedron Letters* 23: 5459-5462.

Dixon RA. 2001. Natural products and plant disease resistance. *Nature* 411: 843-847.

Djonović S, Urbach JM, Drenkard E, Bush J, Feinbaum R, Ausubel JL, Traficante D, Risech M, Kocks C, Fischbach MA. 2013. Trehalose biosynthesis promotes *Pseudomonas aeruginosa* pathogenicity in plants. *PLoS Pathogens* 9: p.e1003217.

Do Vale LH, Gómez-Mendoza DP, Kim M, Pandey A, Ricart CA, Edivaldo Filho XF, and Sousa MV. 2012. Secretome analysis of the fungus *Trichoderma harzianum* grown on cellulose. *Proteomics* 12: 2716-2728.

Draper J. 1997. Salicylate, superoxide synthesis and cell suicide in plant defence. *Trends in Plant Science* 2: 162-165.

Dron M, Clouse SD, Dixon RA, Lawton MA, Lamb CJ. 1988. Glutathione and fungal elicitor regulation of a plant defense gene promoter in electroporated protoplasts. *Proceedings of the National Academy of Sciences USA* 85: 6738-6742.

Dugas DV, Monaco MK, Olsen A, Klein RR, Kumari S, Ware D, Klein PE. 2011. Functional annotation of the transcriptome of *Sorghum bicolor* in response to osmotic stress and abscisic acid. *BMC Genomics* 12: 514.

Edmunds LK, Zummo N. 1975. Sorghum diseases in the United States and their control. Agriculture Handbook, United States Department of Agriculture 468.

Edmunds L. 1964. Combined relation of plant maturity temperature soil moisture to charcoal stalk rot development in grain sorghum. *Phytopathology* 54: 514.

Ellis C, Karafyllidis I, Turner JG. 2002a. Constitutive activation of jasmonate signaling in an *Arabidopsis* mutant correlates with enhanced resistance to *Erysiphe cichoracearum*, *Pseudomonas syringae*, and *Myzus persicae*. *Molecular Plant-Microbe Interactions 15: 1025-1030.*

Ellis C, Turner JG. 2001. The *Arabidopsis* mutant cev1 has constitutively active jasmonate and ethylene signal pathways and enhanced resistance to pathogens. *Plant Cell* 13: 1025-1033.

Ellis C, Karafyllidis I, Wasternack C, Turner JG. 2002b. The *Arabidopsis* mutant cev1 links cell wall signaling to jasmonate and ethylene responses. *Plant Cell* 14: 1557-1566.

Faris JD, Zhang Z, Lu H, Lu S, Reddy L, Cloutier S, Fellers JP, Meinhardt SW, Rasmussen JB, Xu SS, Oliver RP. 2010. A unique wheat disease resistance-like gene governs effector-triggered susceptibility to necrotrophic pathogens. *Proceedings of the National Academy of Sciences USA* 107: 13544–13549.

Fernandes KS, Mathews HL, Bezerra LML. 1999. Differences in virulence of *Sporothrix schenckii* conidia related to culture conditions and cell-wall components. *Journal of Medical Microbiology* 48: 195-203.

Fernandez O, Béthencourt L, Quero A, Sangwan RS, Clément C. 2010. Trehalose and plant stress responses: friend or foe? *Trends in Plant Science* 15: 409-417.

Foster AJ, Jenkinson JM, Talbot NJ. 2003. Trehalose synthesis and metabolism are required at different stages of plant infection by *Magnaporthe grisea*. *EMBO Journal* 22: 225-235.

Foyer CH, Lelandais M, Kunert, KJ. 1994. Photooxidative stress in plants. *Physiologia Plantarum* 92: 696-717.

Friesen TL, Chu CG, Liu ZH, Xu SS, Halley S, Faris JD. 2009. Host-selective toxins produced by *Stagonospora nodorum* confer disease susceptibility in adult wheat plants under field conditions. *Theoretical and Applied Genetics* 118: 1489–1497.

Gális I, Smith JL, Jameson PE. 2004. Salicylic acid-, but not cytokinin-induced, resistance to WClMV is associated with increased expression of SA-dependent resistance genes in *Phaseolus vulgaris*. *Journal of Plant Physiology* 161: 459-466.

Galletti R, Denoux C, Gambetta S, Dewdney J, Ausubel FM, De Lorenzo G, Ferrari S. 2008. The AtrbohD-mediated oxidative burst elicited by oligogalacturonides in *Arabidopsis* is dispensable for the activation of defense responses effective against *Botrytis cinerea*. *Plant Physiology* 148, 1695-1706.

Gan S, Amasino RM. 1995. Inhibition of leaf senescence by autoregulated production of cytokinin. *Science* 270: 1986-1988.

Glazebrook J. 2005. Contrasting mechanisms of defense against biotrophic and necrotrophic pathogens. *Annual Review of Phytopathology* 4: 205-227.

Goodstein DM, Shu S, Howson R, Neupane R, Hayes RD, Fazo J, Mitros T, Dirks W, Hellsten U, Putnam N, Rokhsar DS. 2012. Phytozome: a comparative platform for green plant genomics. *Nucleic Acids Research* 40:1178-1186.

Govrin EM, Levine A. 2000. The hypersensitive response facilitates plant infection by the necrotrophic pathogen *Botrytis cinerea*. *Current Biology* 10: 751-757.

Govrin EM, Rachmilevitch S, Tiwari BS, Solomon M, Levine A. 2006. An elicitor from *Botrytis cinerea* induces the hypersensitive response in *Arabidopsis thaliana* and other plants and promotes the gray mold disease. *Phytopathology* 96: 299-307.

Gray F, Mihail J, Lavigne R, Porter P. 1991. Incidence of charcoal rot of sorghum and soil populations of *Macrophomina phaseolina* associated with sorghum and native vegetation in Somalia. *Mycopathologia* 114: 145-151.

Grove MD, Spencer GF, Rohwedder WK, Mandava N, Worley JF, Warthen JD, Steffens GL, Flippen-Anderson JL, Cook JC. 1979. Brassinolide, a plant growth-promoting steroid isolated from *Brassica napus* pollen. *Nature* 281: 216-217.

Guo Y, Gan S. 2011. AtMYB2 regulates whole plant senescence by inhibiting cytokinin-mediated branching at late stages of development in *Arabidopsis*. *Plant Physiology* 156: 1612-1619.

Gupta V, Willits MG, Glazebrook J. 2000. *Arabidopsis thaliana* EDS4 contributes to salicylic acid (SA)-dependent expression of defense responses: evidence for inhibition of jasmonic acid signaling by SA. *Molecular Plant-Microbe Interactions* 13: 503-511.

Hamann T, Bennett M, Mansfield J, Somerville C. 2009. Identification of cell-wall stress as a hexose-dependent and osmosensitive regulator of plant responses. *Plant Journal* 57: 1015-1026.

Hammond-Kosack KE, Jones JD. 1996. Resistance gene-dependent plant defense responses. *Plant Cell* 8: 1773-1791.

Harada T, Cote WA. 1985. Structure of wood. In *Biosynthesis and Biodegradation of Wood Components* (ed. T. Higuchi), pp. 1-42. San Diego, Academic Press.

Harrison MJ, Lawton MA, Lamb CJ, Dixon RA. 1991. Characterization of a nuclear protein that binds to three elements within the silencer region of a bean chalcone synthase gene promoter. *Proceedings of the National Academy of Sciences USA* 88: 2515-2519.

Haslam E. 1993. Shikimic acid: metabolism and metabolites. Wiley Chichester, UK.

Hugouvieux V, Centis S, Lafitte C, Esquerre-Tugaye M. 1997. Induction by (alpha)-L-arabinose and (alpha)-L-rhamnose of endopolygalacturonase gene expression in *Colletotrichum lindemuthianum*. *Applied and Environmental Microbiology* 63: 2287-2292.

Hundekar A, Anahosur K. 2012. Pathogenicity of fungi associated with sorghum stalk rot. *Karnataka Journal of Agricultural Sciences* 7: 291-295.

Ibrahim RK, Bruneau A, Bantignies B. 1998. Plant *O-methyltransferases*: molecular analysis, common signature and classification. *Plant Molecular Biology* 36: 1-10.

Ibrahim RK, Muzac I. 2000. The *methyltransferase* gene superfamily: a tree with multiple branches. *Recent Advances in Phytochemistry* 34: 349-384.

Ishibashi Y, Tawaratsumida T, Kondo K, Kasa S, Sakamoto M, Aoki N, Zheng SH, Yuasa T, Iwaya-Inoue M. 2012. Reactive oxygen species are involved in gibberellin/abscisic acid signaling in barley aleurone cells. *Plant Physiology* 158: 1705-1714.

Islam MS, Haque MS, Islam MM, Emdad EM, Halim A, Hossen QM, Hossain MZ, Ahmed B, Rahim S, Rahman MS, Alam MM, Hou S, Wan X, Saito JA, Alam M. 2012. Tools to kill:

genome of one of the most destructive plant pathogenic fungi *Macrophomina phaseolina*. *BMC Genomics* 13: 1.

Janet E. 1983. Fungal colonization of stalks and roots of grain sorghum during the growing season. *Plant Disease* 67: 417-420.

Jia C, Zhang L, Liu L, Wang J, Li C, Wang Q. 2013. Multiple phytohormone signalling pathways modulate susceptibility of tomato plants to *Alternaria alternata* f. sp. *lycopersici*. *Journal of Experimental Botany* 64: 637-650.

Jirage D, Zhou N, Cooper B, Clarke JD, Dong X, Glazebrook J. 2001. Constitutive salicylic acid-dependent signaling in cpr1 and cpr6 mutants requires PAD4. *Plant Journal* 26: 395-407.

Kariola T, Brader G, Li J, Palva ET. 2005. *Chlorophyllase* 1, a damage control enzyme, affects the balance between defense pathways in plants. *Plant Cell* 17: 282-294.

Karpinski S, Gabrys H, Mateo A, Karpinska B, Mullineaux PM. 2003. Light perception in plant disease defence signalling. *Current Opinion in Plant Biology* 6: 390-396.

Kazan K, Lyons R. 2014. Intervention of phytohormone pathways by pathogen effectors. *Plant Cell* 26: 2285-2309.

Khangura R, Aberra M. 2009. First report of charcoal rot on canola caused by *Macrophomina phaseolina* in Western Australia. *Plant Disease* 93: 666-666.

Kimber CT, Dahlberg JA, Kresovich S. 2013. The gene pool of *Sorghum bicolor* and its improvement. In: Genomics of the Saccharinae, Springer pp. 23-41.

Kumar J, Hückelhoven R, Beckhove U, Nagarajan S, Kogel K. 2001. A compromised Mlo pathway affects the response of barley to the necrotrophic fungus *Bipolaris sorokiniana* (teleomorph: *Cochliobolus sativus*) and its toxins. *Phytopathology* 91: 127-133.

Landry LG, Chapple CC, Last RL. 1995. *Arabidopsis* mutants lacking phenolic sunscreens exhibit enhanced ultraviolet-B injury and oxidative damage. *Plant Physiology* 109: 1159-1166.

Lara MEB, Garcia MCG, Fatima T, Ehneß R, Lee TK, Proels R, Tanner W. Roitsch T. 2004. Extracellular invertase is an essential component of cytokinin-mediated delay of senescence. *Plant Cell* 16: 1276-1287.

Li X, Guo X, Zhou Y, Shi K, Zhou J, Yu J, Xia X. 2016. Overexpression of a brassinosteroid biosynthetic gene Dwarf enhances photosynthetic capacity through activation of Calvin cycle enzymes in tomato. *BMC plant biology* 16: 33.

Lillo C, Lea US, Ruoff P. 2008. Nutrient depletion as a key factor for manipulating gene expression and product formation in different branches of the flavonoid pathway. *Plant, Cell & Environment* 31: 587-601.

Liu Z, Faris JD, Oliver RP, Tan KC, Solomon PS, McDonald MC, McDonald BA, Nunez A, Lu S, Rasmussen JB, Friesen TL. 2009. SnTox3 acts in effector triggered susceptibility to induce disease on wheat carrying the Snn3 gene. *PLoS Pathogens* 5(9): p.e1000581.

Lunn JE, Hatch MD. 1995. Primary partitioning and storage of photosynthate in sucrose and starch in leaves of C4 plants. *Planta* 197: 385-391.

Ma Q, Xu Y. 2008. Characterization of a caffeic acid 3-O-methyltransferase from wheat and its function in lignin biosynthesis. *Biochimie* 90: 515-524.

Mach JM, Castillo AR, Hoogstraten R, Greenberg JT. 2001. The *Arabidopsis*-accelerated cell death gene ACD2 encodes red chlorophyll catabolite reductase and suppresses the spread of disease symptoms. *Proceedings of the National Academy of Sciences USA* 98:771-776.

Mahmoud A, Budak H. 2011. First report of charcoal rot caused by *Macrophomina phaseolina* in sunflower in Turkey. *Plant Disease* 95: 223-223.

Malolepsza U. 2007. Nitric oxide production in plants. *Postepy Biochemii* 53, 263-271.

Mann JA, Kimber CT, Miller FR. 1983. The Origin and Early Cultivation of Sorghums in Africa. Texas FARMER Collection.

Martin M. 2011. Cutadapt removes adapter sequences from high-throughput sequencing reads. *EMBnet Journal* 17: 10-12.

Masuta C, Tanaka H, Uehara K, Kuwata S, Koiwai A, Noma M. 1995. Broad resistance to plant viruses in transgenic plants conferred by antisense inhibition of a host gene essential in S-adenosylmethionine-dependent transmethylation reactions. *Proceedings of the National Academy of Sciences USA* 92: 6117-6121.

McDowell JM, Dangl JL. 2000. Signal transduction in the plant immune response. *Trends in Biochemical Sciences* 25: 79-82.

Mengiste T. 2012. Plant immunity to necrotrophs. *Annual Review of Phytopathology* 50: 267-294.

Mengiste T, Chen X, Salmeron J, Dietrich R. 2003. The BOTRYTIS SUSCEPTIBLE1 gene encodes an R2R3MYB transcription factor protein that is required for biotic and abiotic stress responses in *Arabidopsis*. *Plant Cell* 15: 2551-2565.

Møller IM. 2001. Plant mitochondria and oxidative stress: electron transport, NADPH turnover, and metabolism of reactive oxygen species. *Annual Review of Plant Biology* 52: 561-591.

Mortazavi A, Williams BA, McCue K, Schaeffer L, Wold B. 2008. Mapping and quantifying mammalian transcriptomes by RNA-Seq. *Nature Methods* 5: 621-628.

Mughogho LK, Pande S. 1984. Charcoal rot of sorghum, in: Rosenberg, G. (Ed), Sorghum Root and Stalk Rots, a Critical Review. Proceedings of the Consultative Group Discussion on

Research Needs and Strategies for Control of Root and Stalk Rot Diseases. 27 Nov - 2 Dec 1983, Bellagio, Italy. Patancheru, A.P. 502324, India: ICRISAT Press. pp. 11–24.

Navarro L, Bari R, Achard P, Lisón P, Nemri A, Harberd NP, Jones JD. 2008. DELLAs control plant immune responses by modulating the balance of jasmonic acid and salicylic acid signaling. *Current Biology* 18: 650-655.

Noctor G, Foyer CH. 1998. Ascorbate and glutathione: keeping active oxygen under control. *Annual Review of Plant Biology* 49: 249-279.

Oliver RP, Solomon PS. 2010. New developments in pathogenicity and virulence of necrotrophs. *Current Opinion in Plant Biology* 13: 415–419.

Paterson AH, Bowers JE, Bruggmann R, Dubchak I, Grimwood J, Gundlach H, Haberer G, Hellsten U, Mitros T, Poliakov A. 2009. The *Sorghum bicolor* genome and the diversification of grasses. *Nature* 457: 551-556.

Pennypacker B, Knievel D, Risius M, Leath K. 1995. Impact of *Verticillium albo-atrum* and photosynthetic photon flux density on ribulose-1, 5-bisphosphate carboxylase/oxygenase in resistant alfalfa. *Phytopathology* 85: 132-138.

Petersen M, Brodersen P, Naested H, Andreasson E, Lindhart U, Johansen B, Nielsen HB, Lacy M, Austin MJ, Parker JE. 2000. *Arabidopsis MAP kinase 4* negatively regulates systemic acquired resistance. *Cell* 103: 1111-1120.

Pogány M, Koehl J, Heiser I, Elstner EF, Barna B. 2004. Juvenility of tobacco induced by cytokinin gene introduction decreases susceptibility to Tobacco necrosis virus and confers tolerance to oxidative stress. *Physiological and Molecular Plant Pathology* 65: 39-47.

Pruzinska A, Tanner G, Anders I, Roca M, Hortensteiner S. 2003. Chlorophyll breakdown: pheophorbide a oxygenase is a Rieske-type iron-sulfur protein, encoded by the accelerated cell death 1 gene. *Proceedings of the National Academy of Sciences USA* 100: 15259-15264.

Puttikamonkul S, Willger SD, Grahl N, Perfect JR, Movahed N, Bothner B, Park S, Paderu P, Perlin DS, Cramer Jr, RA. 2010. *Trehalose 6-phosphate phosphatase* is required for cell wall integrity and fungal virulence but not trehalose biosynthesis in the human fungal pathogen *Aspergillus fumigatus*. *Molecular Microbiology* 77: 891-911.

Ramezani M, Shier WT, Abbas HK, Tonos JL, Baird RE, Sciumbato GL. 2007. Soybean charcoal rot disease fungus *Macrophomina phaseolina* in Mississippi produces the phytotoxin (-)-botryodiplodin but no detectable phaseolinone. *Journal of Natural Products* 70: 128-129.

Rao MV, Lee H, Davis KR. 2002. Ozone-induced ethylene production is dependent on salicylic acid, and both salicylic acid and ethylene act in concert to regulate ozone-induced cell death. *Plant Journal* 32: 447-456.

Renard-Merlier D, Randoux B, Nowak E, Farcy F, Durand R, Reignault P. 2007. Iodus 40, salicylic acid, heptanoyl salicylic acid and trehalose exhibit different efficacies and defence targets during a wheat/powdery mildew interaction. *Phytochemistry* 68: 1156-1164.

Rosenow D, Quisenberry J, Wendt C, Clark L. 1983. Drought tolerant sorghum and cotton germplasm. *Agricultural Water Management* 7: 207-222.

Rossi FR, Gárriz A, Marina M, Romero FM, Gonzalez ME, Collado IG, Pieckenstain FL. 2011. The sesquiterpene botrydial produced by *Botrytis cinerea* induces the hypersensitive response on plant tissues and its action is modulated by salicylic acid and jasmonic acid signaling. *Molecular Plant-Microbe Interactions* 24: 888-896.

Ryan KG, Swinny EE, Markham KR, Winefield C. 2002. Flavonoid gene expression and UV photoprotection in transgenic and mutant *Petunia* leaves. *Phytochemistry* 59: 23-32.

Salzman RA, Brady JA, Finlayson SA, Buchanan CD, Summer EJ, Sun F, Klein PE, Klein RR, Pratt LH, Cordonnier-Pratt MM, Mullet JE. 2005. Transcriptional profiling of sorghum induced by methyl jasmonate, salicylic acid, and aminocyclopropane carboxylic acid reveals cooperative regulation and novel gene responses. *Plant Physiology* 138: 352-368.

Sandhu A, Singh R, Sandhu A. 1999. Factors influencing susceptibility of cowpea to *M. phaseolina*. *Journal of Mycology and Plant Pathology* 29: 421-424.

Sarkar TS, Biswas P, Ghosh SK, Ghosh S. 2014. Nitric oxide production by necrotrophic pathogen *Macrophomina phaseolina* and the host plant in charcoal rot disease of Jute: complexity of the interplay between necrotroph–host plant interactions. *PloS one* 9: e107348

Schenk PM, Kazan K, Wilson I, Anderson JP, Richmond T, Somerville SC, and Manners JM. 2000. Coordinated plant defense responses in *Arabidopsis* revealed by microarray analysis. *Proceedings of the National Academy of Sciences USA* 97: 11655-11660.

Schlagnhaufer C, Arteca RN, Yopp JH. 1984. Evidence that brassinosteroid stimulates auxin-induced ethylene synthesis in mung bean hypocotyls between S-adenosylmethionine and 1-aminocyclopropane-1-carboxylic acid. *Physiologia Plantarum* 61: 555-558.

Short G. Wyllie T, Bristow P. 1980. Survival of *Macrophomina phaseolina* in soil and in residue of soybean. *Phytopathology* 70: 13-17.

Sutton BC. 1980. The coelomycetes, fungi imperfecti with pycnidia, acervuli and stromata. Commonwealth Mycological Institute. Kew, Surrey, UK.

Takamiya K, Tsuchiya T, Ohta H. 2000. Degradation pathway (s) of chlorophyll: what has gene cloning revealed? *Trends in Plant Science* 5: 426-431.

Tarr SAJ, 1962. Root and stalk diseases: Red stalk rot, Colletotrichum rot, anthracnose, and red leaf spot, in: Diseases of Sorghum, Sudan Grass and Brown Corn. Commonwealth Mycological Institute, Kew, Surrey, UK, pp. 58–73.

Tattini M, Galardi C, Pinelli P, Massai R, Remorini D, Agati G. 2004. Differential accumulation of flavonoids and hydroxycinnamates in leaves of *Ligustrum vulgare* under excess light and drought stress. *New Phytologist* 163: 547-561.

Tattini M, Guidi L, Morassi-Bonzi L, Pinelli P, Remorini D, Degl'Innocenti E, Giordano C, Massai R, Agati G. 2005. On the role of flavonoids in the integrated mechanisms of response of *Ligustrum vulgare* and *Phillyrea latifolia* to high solar radiation. *New Phytologist* 167: 457-470.

Tenberge KB, Beckedorf M, Hoppe B, Schouten A, Solf M, von den Driesch M. 2002. In situ localization of AOS in host-pathogen interactions. *Microscopy and Microanalysis* 8: 250-251.

Tenberge KB. 2007. Morphology and cellular organization in *Botrytis* interactions with plants. In: Botrytis: Biology, Pathology and Control. Springer Netherlands, pp. 67-84.

Tesso TT, Claflin LE, Tuinstra MR. 2005. Analysis of stalk rot resistance and genetic diversity among drought tolerant sorghum genotypes. *Crop Science* 45: 645-652.

Tesso T, Perumal R, Little CR, Adeyanju A, Radwan GL, Prom LK, Magill CW. 2012. Sorghum pathology and biotechnology-a fungal disease perspective: Part II. Anthracnose, stalk rot, and downy mildew. *European Journal of Plant Science and Biotechnology* 6: 31-44.

Thines E, Weber RW, Talbot NJ. 2000. MAP kinase and protein kinase A-dependent mobilization of triacylglycerol and glycogen during appressorium turgor generation by *Magnaporthe grisea*. *Plant Cell* 12: 1703-1718.

Thomma BP, Eggermont K, Penninckx IA, Mauch-Mani B, Vogelsang R, Cammue BP, Broekaert WF. 1998. Separate jasmonate-dependent and salicylate-dependent defense-response

pathways in *Arabidopsis* are essential for resistance to distinct microbial pathogens. *Proceedings of the National Academy of Sciences USA* 95: 15107-15111.

Thomma BP, Eggermont K, Tierens KF, Broekaert WF. 1999. Requirement of functional ethylene-insensitive 2 gene for efficient resistance of *Arabidopsis* to infection by *Botrytis cinerea*. *Plant Physiology* 121: 1093-1102.

Thordal-Christensen H. 2003. Fresh insights into processes of nonhost resistance. *Current Opinion in Plant Biology* 6: 351-357.

Tiwari BS, Belenghi B, Levine A. 2002. Oxidative stress increased respiration and generation of reactive oxygen species, resulting in ATP depletion, opening of mitochondrial permeability transition, and programmed cell death. *Plant Physiology* 128: 1271-1281.

Tun NN, Livaja M, Kieber JJ, Scherer GF. 2008. Zeatin-induced nitric oxide (NO) biosynthesis in *Arabidopsis thaliana* mutants of NO biosynthesis and of two-component signaling genes. *New Phytologist* 178: 515-531.

Van Camp W, Van Montagu M, Inzé D. 1998. H_2O_2 and NO: redox signals in disease resistance. *Trends in Plant Science* 3: 330-334.

Van Kan JA. 2006. Licensed to kill: the lifestyle of a necrotrophic plant pathogen. *Trends in Plant Science* 11: 247-253.

Vardhini BV, Rao SSR. 2002. Acceleration of ripening of tomato pericarp discs by brassinosteroids. *Phytochemistry* 61: 843-847.

Veronese P, Chen X, Bluhm B, Salmeron J, Dietrich R, Mengiste T. 2004. The BOS loci of *Arabidopsis* are required for resistance to *Botrytis cinerea* infection. *Plant Journal* 40: 558-574.

Veronese P, Nakagami H, Bluhm B, Abuqamar S, Chen X, Salmeron J, Dietrich RA, Hirt H, Mengiste T. 2006. The membrane-anchored BOTRYTIS-INDUCED KINASE1 plays distinct roles in *Arabidopsis* resistance to necrotrophic and biotrophic pathogens. *Plant Cell* 18: 257-273.

Vijayan P, Shockey J, Levesque CA, Cook RJ, Browse J. 1998. A role for jasmonate in pathogen defense of *Arabidopsis*. *Proceedings of the National Academy of Sciences USA* 95: 7209-7214.

Wei Y, Shen W, Dauk M, Wang F, Selvaraj G, Zou J. 2004. Targeted gene disruption of *glycerol-3-phosphate dehydrogenase* in *Colletotrichum gloeosporioides* reveals evidence that glycerol is a significant transferred nutrient from host plant to fungal pathogen. *The Journal of Biological Chemistry* 279: 429-435.

Wildermuth M.C, Dewdney J, Wu G, Ausubel FM. 2001. Isochorismate synthase is required to synthesize salicylic acid for plant defence. *Nature* 414: 562-565.

Wilson DB. 2009. Cellulases and biofuels. *Current Opinion in Biotechnology*. 20: 295-299.

Wilson RA, Jenkinson JM, Gibson RP, Littlechild JA, Wang ZY, Talbot NJ. 2007. Tps1 regulates the pentose phosphate pathway, nitrogen metabolism and fungal virulence. *EMBO Journal* 26: 3673-3685.

Wingler A, von Schaewen A, Leegood RC, Lea PJ, Quick WP. 1998. Regulation of leaf senescence by cytokinin, sugars, and light effects on NADH-dependent hydroxypyruvate reductase. *Plant Physiology* 116: 329-335.

Wingler A, Delatte TL, O'Hara LE, Primavesi LF, Jhurreea D, Paul MJ, Schluepmann H. 2012. Trehalose 6-phosphate is required for the onset of leaf senescence associated with high carbon availability. *Plant Physiology* 158: 1241-1251.

Wink M. 2003. Evolution of secondary metabolites from an ecological and molecular phylogenetic perspective. *Phytochemistry* 64: 3-19.

Wittek F, Kanawati B, Wenig M, Hoffmann T, Franz-Oberdorf K, Schwab W, Schmitt-Kopplin P, Vlot AC. 2015. Folic acid induces salicylic acid-dependent immunity in *Arabidopsis* and enhances susceptibility to *Alternaria brassicicola*. *Molecular Plant Pathology* 16: 616-622.

Wood TM, McCrae SI, Bhat KM. 1989. The mechanism of fungal cellulase action. Synergism between enzyme components of *Penicillium pinophilum* cellulase in solubilizing hydrogen bond-ordered cellulose. *Biochemical Journal* 260: 37-43.

Wu TD, Watanabe CK. 2005. GMAP: a genomic mapping and alignment program for mRNA and EST sequences. *Bioinformatics* 21: 1859-1875.

Xia XJ, Wang YJ, Zhou YH, Tao Y, Mao WH, Shi K, Asami T, Chen Z, Yu JQ. 2009. Reactive oxygen species are involved in brassinosteroid-induced stress tolerance in cucumber. *Plant Physiology* 150: 801-814.

Yamamoto R, Fujioka S, Demura T, Takatsuto S, Yoshida S, Fukuda H. 2001. Brassinosteroid levels increase drastically prior to morphogenesis of tracheary elements. *Plant Physiology* 125: 556-563.

Yang C, Zhang Z, Gao H, Liu M, Fan X. 2014. Mechanisms by which the infection of *Sclerotinia sclerotiorum* (Lib.) de Bary affects the photosynthetic performance in tobacco leaves. *BMC Plant Biology* 14: 240.

Yao N, Greenberg JT. 2006. Arabidopsis ACCELERATED CELL DEATH2 modulates programmed cell death. *Plant Cell* 18: 397-411.

Youens-Clark K, Buckler E, Casstevens T, Chen C, Declerck G, Derwent P, Dharmawardhana P, Jaiswal P, Kersey P, Karthikeyan AS, Lu J, McCouch SR, Ren L, Spooner W, Stein JC, Thomason J, Wei S, Ware D. 2011. Gramene database in 2010: updates and extensions. *Nucleic Acids Research* 39: D1085-D1094.

Zhang A, Zhang J, Ye N, Cao J, Tan M, Zhang J, Jiang M. (2010). ZmMPK5 is required for the NADPH oxidase-mediated self-propagation of apoplastic H_2O_2 in brassinosteroid-induced antioxidant defence in leaves of maize. *Journal of Experimental Botany* 61: 4399-4411.

Zhang L, Jia C, Liu L, Zhang Z, Li C, Wang Q. 2011. The involvement of jasmonates and ethylene in *Alternaria alternata* f. sp. *lycopersici* toxin-induced tomato cell death. *Journal of Experimental Botany* 62: 5405-5418.

Zhong R, Morrison WH, Negrel J, Ye ZH, (1998). Dual methylation pathways in lignin biosynthesis. *Plant Cell* 10: 2033-2046.

Zhong R, Morrison WH, Himmelsbach DS, Poole FL, Ye ZH. 2000. Essential role of *caffeoyl coenzyme A O-methyltransferase* in lignin biosynthesis in woody poplar plants. *Plant Physiology* 124: 563-578.

Zimmermann P, Zentgraf U. 2005. The correlation between oxidative stress and leaf senescence during plant development. *Cellular and Molecular Biology Letters* 10: 515-534.

TABLES AND FIGURES

Table 2.1. Read mapping summary of the RNA-Seq data across three biological replicates.

Genotype	Treatment	Days post inoculation (DPI)	Quality filtered reads	Mapped reads	Mapped (%)	Uniquely Mapped	Uniquely Mapped (%)
SC599	Control	2	34338650	32355187	94.5	30561986	89.2
SC599	Control	7	39626136	38071028	96.1	35802653	90.3
SC599	Control	30	37433599	33931178	90.8	31948671	85.5
SC599	MP†	2	40617949	38041287	93.9	35783682	88.4
SC599	MP	7	37252891	35083073	94.1	33048830	88.6
SC599	MP	30	34395442	30266999	88.1	28568688	83.2
Tx7000	Control	2	37469203	36320193	96.9	34289683	91.5
Tx7000	Control	7	34075052	33118766	97.2	31309546	91.9
Tx7000	Control	30	39197941	37675198	96.2	35600718	90.9
Tx7000	MP	2	37162153	35671059	96.1	33557987	90.4
Tx7000	MP	7	33515204	32491470	97.0	30613203	91.4
Tx7000	MP	30	39058205	37828405	96.9	35594845	91.2

†MP = *Macrophomina phaseolina*

Table 2.2. Quantitative summary of the differential gene expression between *Macrophomina phaseolina* (MP) and control (CON) treatments (MP - CON) for two genotypes at three post inoculation stages (DPI).

Genotype	DPI	Informative genes	Significant genes	Up-regulated				Down-regulated			
				1-2fc[†]	2-4fc	>4fc	Total	1-2fc	2-4fc	>4fc	Total
SC599	2	19918	2849	365	586	505	1456	416	708	269	1393
SC599	7	16877	381	22	126	69	217	26	94	44	164
SC599	30	19843	1307	58	226	263	547	21	180	559	760
Tx7000	2	18847	3194	622	807	508	1937	572	522	163	1257
Tx7000	7	21026	8857	1097	1477	2062	4636	859	1547	1815	4221
Tx7000	30	19556	1716	139	373	280	792	54	229	641	924

[†]fc = fold change

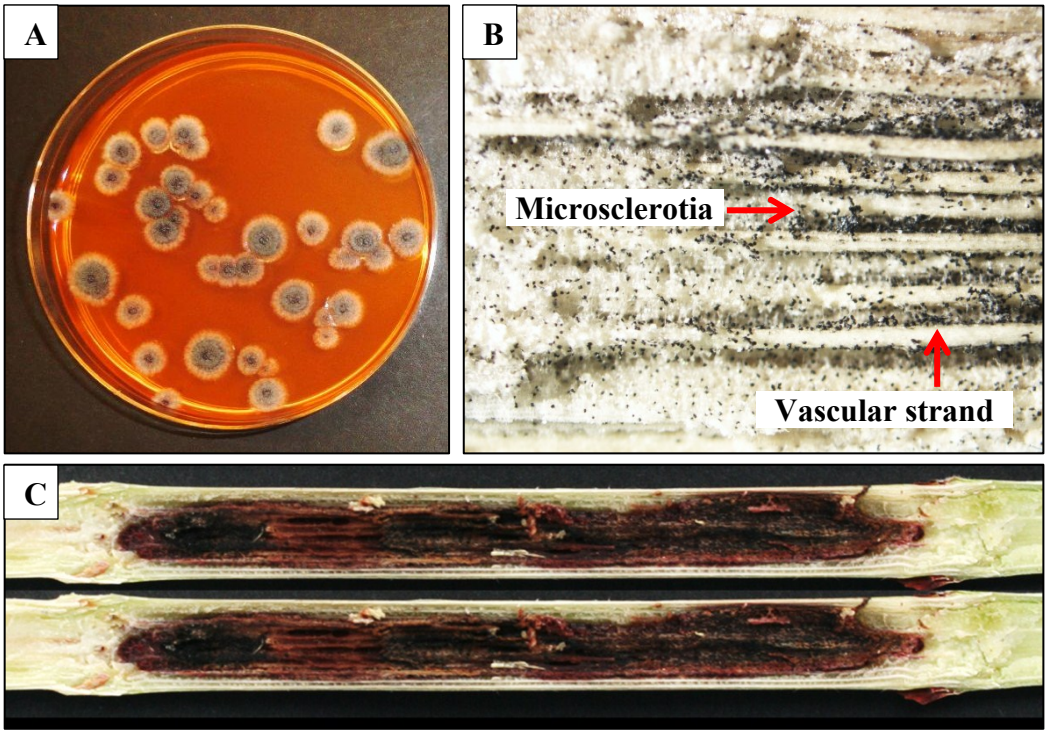

Figure 2.1. Typical colony characteristics of *Macrophomina phaseolina* on rifampicin supplemented semi selective potato dextrose agar medium (A); *M. phaseolina* microsclerotia present in the longitudinally split, infected *Sorghum bicolor* (L.) Moench stalks (B); and typical symptoms observed in *S. bicolor* stalks after inoculation with *M. phaseolina* (note stalk lesions with dark discoloration) (C).

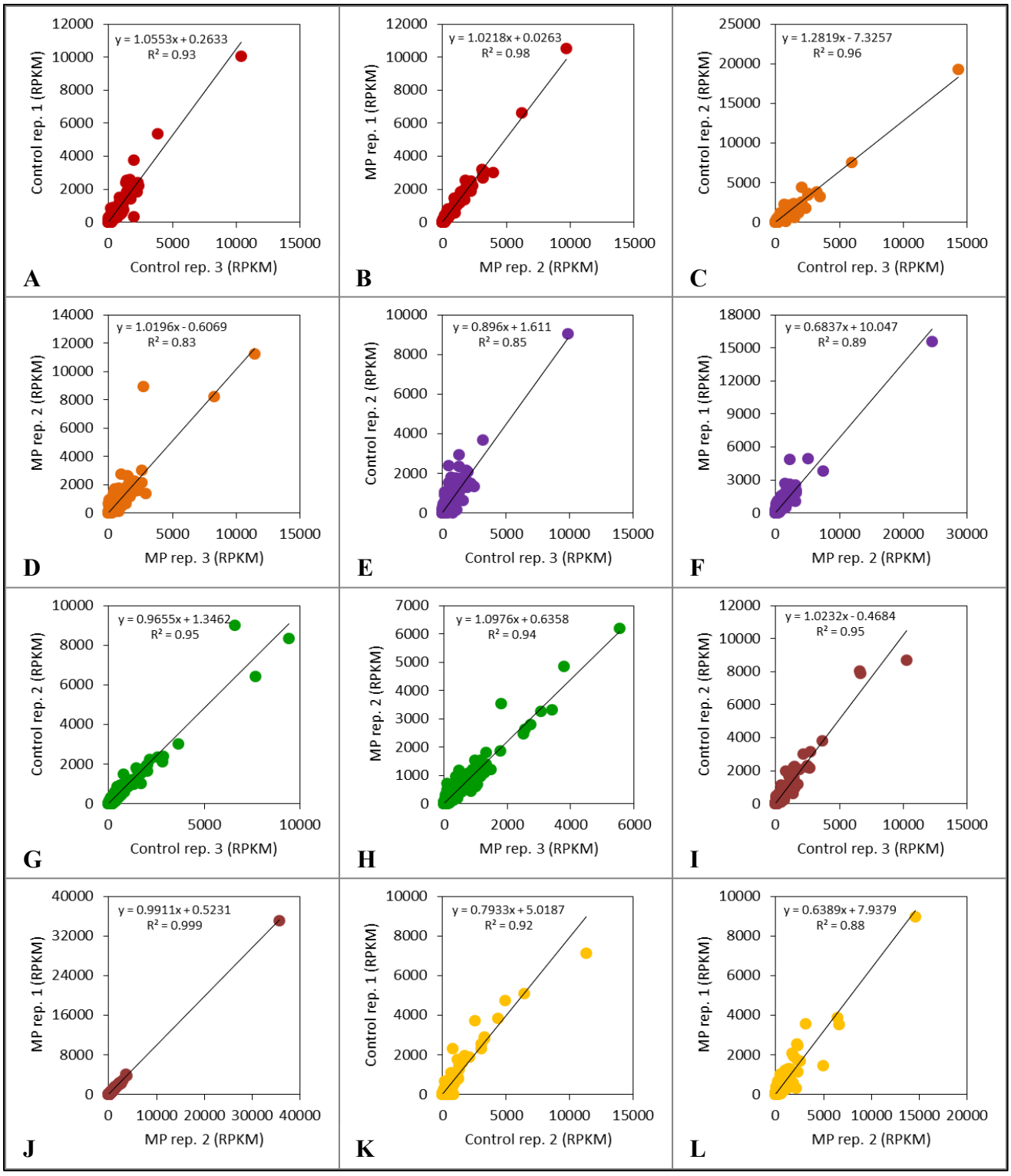
y = 1.0553x + 0.2633
R² = 0.93
Control rep. 1 (RPKM)
Control rep. 3 (RPKM)
A
y = 1.0218x + 0.0263
R² = 0.98
MP rep. 1 (RPKM)
MP rep. 2 (RPKM)
B
y = 1.2819x - 7.3257
R² = 0.96
Control rep. 2 (RPKM)
Control rep. 3 (RPKM)
C
y = 1.0196x - 0.6069
R² = 0.83
MP rep. 2 (RPKM)
MP rep. 3 (RPKM)
D
y = 0.896x + 1.611
R² = 0.85
Control rep. 2 (RPKM)
Control rep. 3 (RPKM)
E
y = 0.6837x + 10.047
R² = 0.89
MP rep. 1 (RPKM)
MP rep. 2 (RPKM)
F
y = 0.9655x + 1.3462
R² = 0.95
Control rep. 2 (RPKM)
Control rep. 3 (RPKM)
G
y = 1.0976x + 0.6358
R² = 0.94
MP rep. 2 (RPKM)
MP rep. 3 (RPKM)
H
y = 1.0232x - 0.4684
R² = 0.95
Control rep. 2 (RPKM)
Control rep. 3 (RPKM)
I
y = 0.9911x + 0.5231
R² = 0.999
MP rep. 1 (RPKM)
MP rep. 2 (RPKM)
J
y = 0.7933x + 5.0187
R² = 0.92
Control rep. 1 (RPKM)
Control rep. 2 (RPKM)
K
y = 0.6389x + 7.9379
R² = 0.88
MP rep. 1 (RPKM)
MP rep. 2 (RPKM)
L

Figure 2.2. Scatter plots showing the correlation between reads per kilobase of transcript per million mapped reads (RPKM) values for each informative gene among two selected biological replicates of the resistant genotype (SC599), receiving the control treatment at two days post-inoculation (DPI) (A), *Macrophomina phaseolina* treatment at 2 DPI (B), control treatment at 7 DPI (C), *M. phaseolina* treatment at 7 DPI (D), control treatment at 30 DPI (E), *M. phaseolina* treatment at 30 DPI (F), and of the susceptible genotype (Tx7000), receiving the control treatment at 2 DPI (G), *M. phaseolina* treatment at 2 DPI (H), control treatment at 7 DPI (I), *M. phaseolina* treatment at 7 DPI (J), control treatment at 30 DPI (K), and *M. phaseolina* treatment at 30 DPI (L).

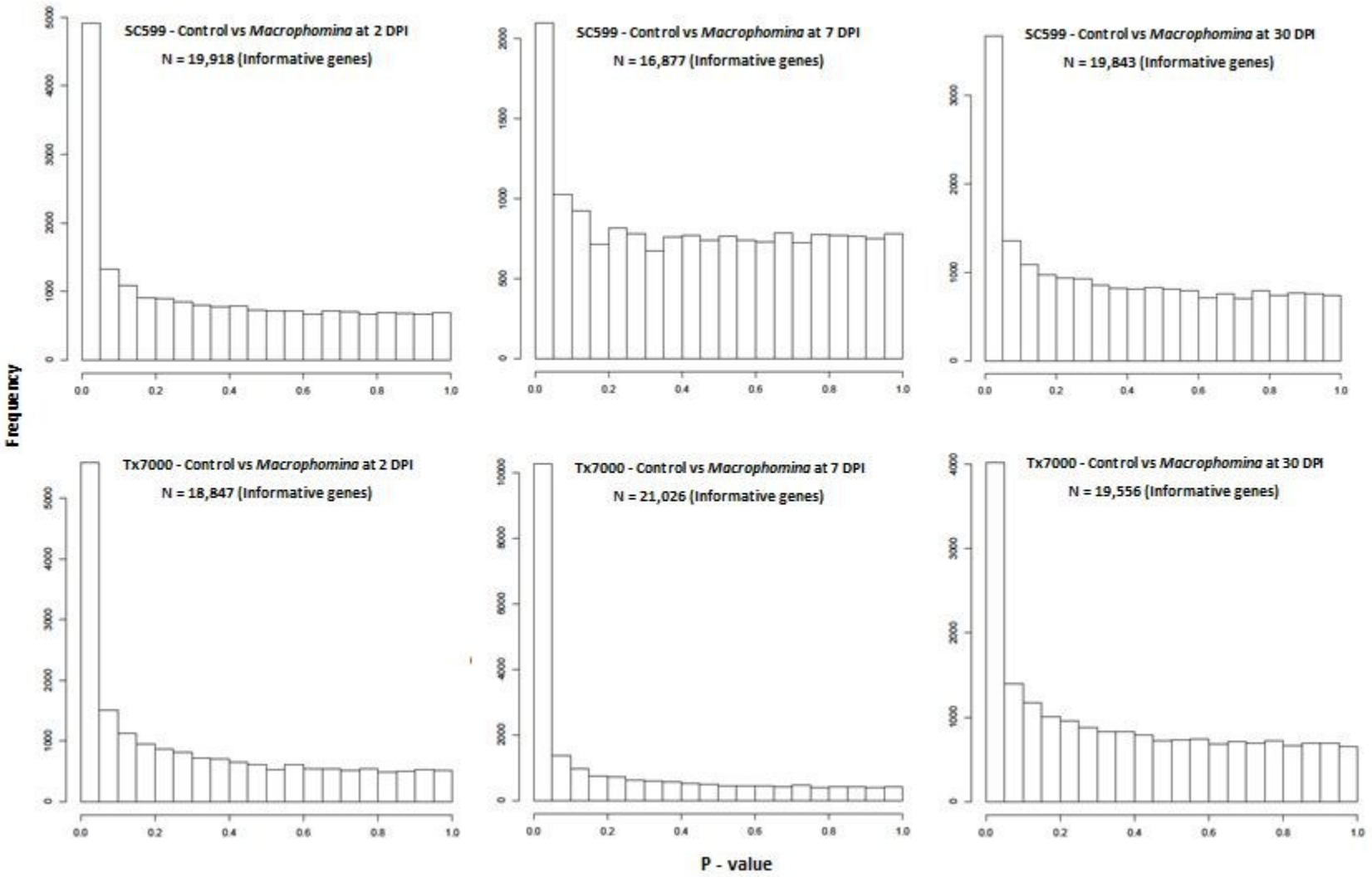

Figure 2.3. *P*-value histograms for informative genes for control and *Macrophomina phaseolina* comparisons at each post-inoculation stage.

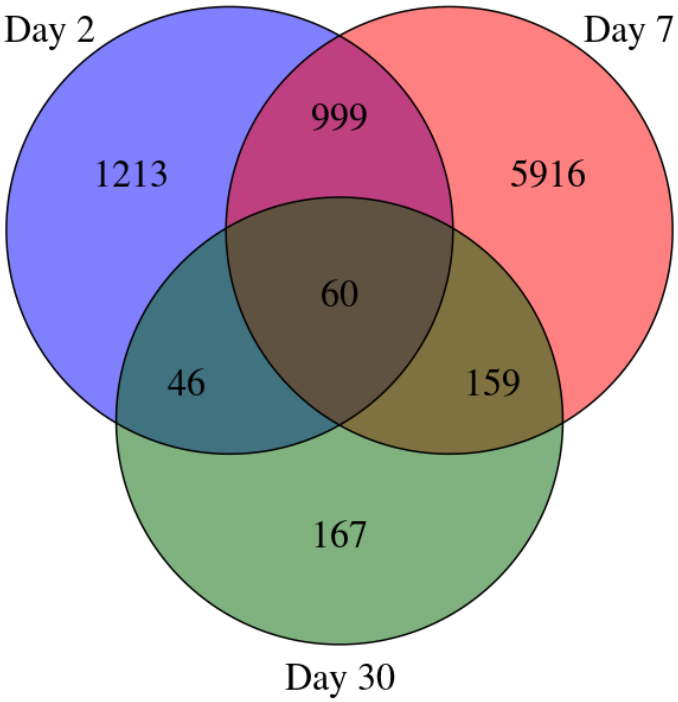

Figure 2.4. Venn diagram displaying the distribution and overlap of differentially expressed genes between resistant and susceptible sorghum genotypes in response to *Macrophomina phaseolina* inoculation at 2, 7, and 30 DPI.

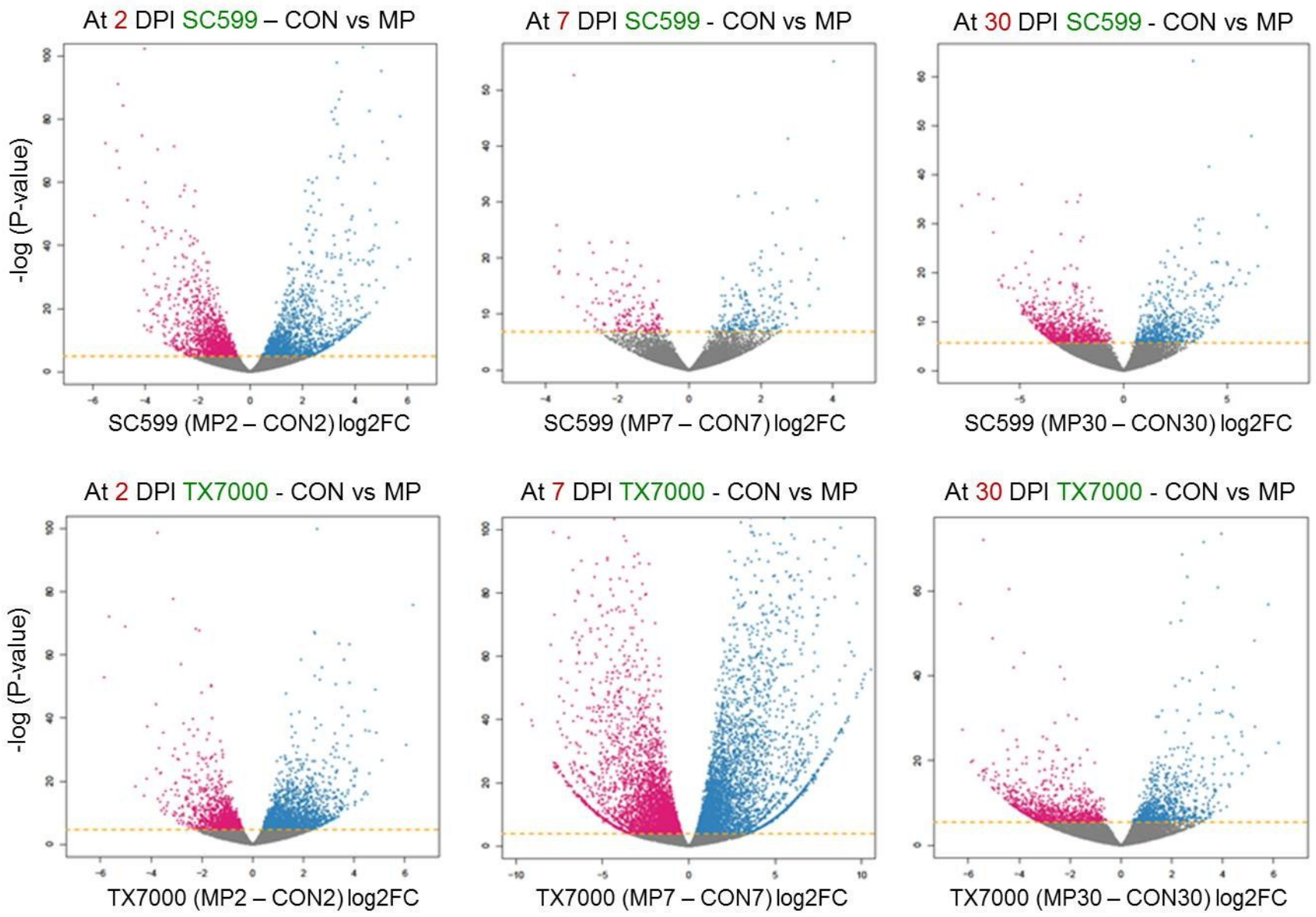
At 2 DPI SC599 – CON vs MP
At 7 DPI SC599 - CON vs MP
At 30 DPI SC599 - CON vs MP
-log (P-value)
SC599 (MP2 – CON2) log2FC
SC599 (MP7 – CON7) log2FC
SC599 (MP30 – CON30) log2FC
At 2 DPI TX7000 - CON vs MP
At 7 DPI TX7000 - CON vs MP
At 30 DPI TX7000 - CON vs MP
-log (P-value)
TX7000 (MP2 – CON2) log2FC
TX7000 (MP7 – CON7) log2FC
TX7000 (MP30 – CON30) log2FC

Figure 2.5. Volcano plots (top panel for SC599 and bottom panel for Tx7000) displaying the distribution of up- and down-regulated genes and their statistical significance. The pink dots indicate significantly down-regulated genes while the blue dots indicate the significantly up-regulated genes. The yellow dotted line in each graph indicates the cutoff *P*-value for differential expression (in negative log form). CON = control treatment, MP = *M. phaseolina* treatment. CON2 = control treatment at 2 DPI, MP2 = *M. phaseolina* treatment at 2 DPI, CON7 = control treatment at 7 DPI, MP7 = *M. phaseolina* treatment at 7 DPI, CON30 = control treatment at 30 DPI, MP30 = *M. phaseolina* treatment at 30 DPI. Log2FC = log two-fold change expression.

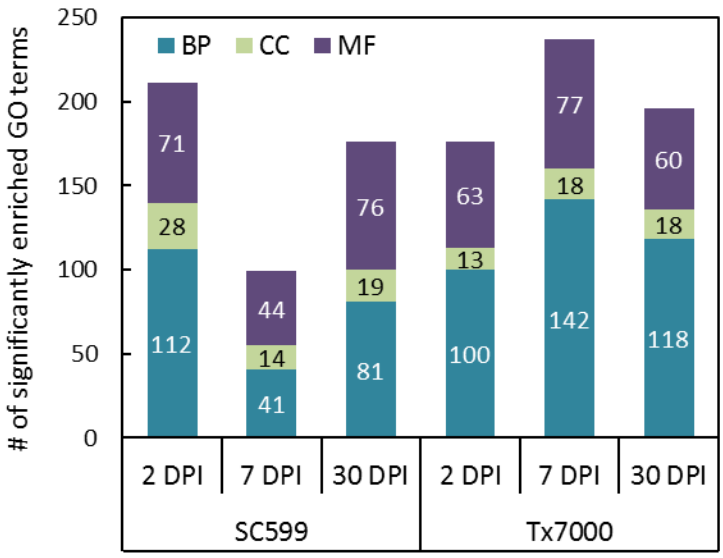

Figure 2.6. Distribution of enriched gene ontology (GO) terms for two sorghum genotypes among three functional categories (biological processes, BP; molecular functions, MF; cellular components, CC) at 2, 7, and 30 DPI.

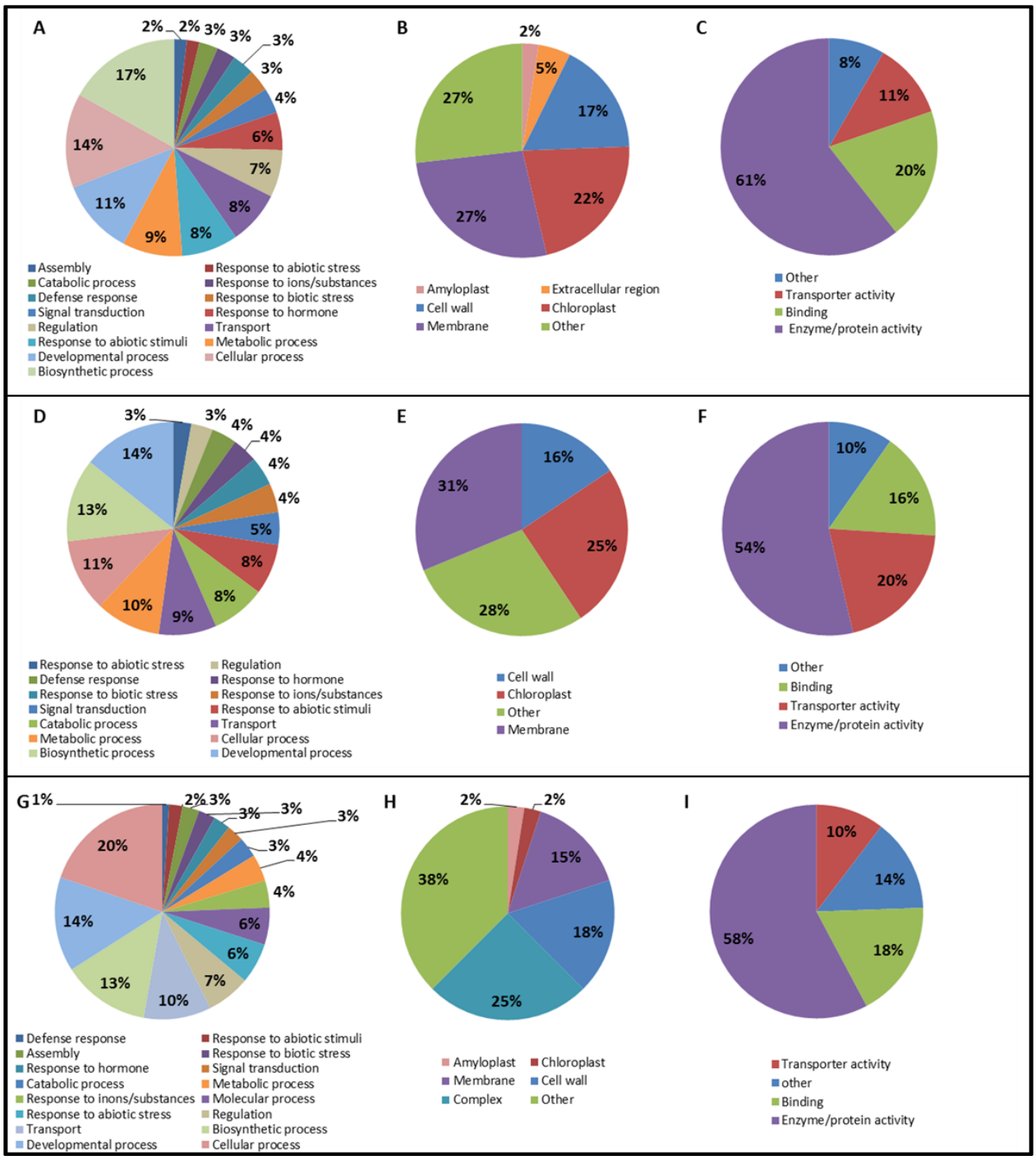
A
2%
2%
3%
3%
3%
3%
4%
6%
7%
8%
8%
9%
11%
14%
17%
Assembly
Catabolic process
Defense response
Signal transduction
Regulation
Response to abiotic stimuli
Developmental process
Biosynthetic process
Response to abiotic stress
Response to ions/substances
Response to biotic stress
Response to hormone
Transport
Metabolic process
Cellular process
B
2%
5%
17%
22%
27%
27%
Amyloplast
Cell wall
Membrane
Extracellular region
Chloroplast
Other
C
8%
11%
20%
61%
Other
Transporter activity
Binding
Enzyme/protein activity
D
3%
3%
4%
4%
4%
4%
5%
8%
8%
9%
10%
11%
13%
14%
Response to abiotic stress
Defense response
Response to biotic stress
Signal transduction
Catabolic process
Metabolic process
Biosynthetic process
Regulation
Response to hormone
Response to ions/substances
Response to abiotic stimuli
Transport
Cellular process
Developmental process
E
16%
25%
28%
31%
Cell wall
Chloroplast
Other
Membrane
F
10%
16%
20%
54%
Other
Binding
Transporter activity
Enzyme/protein activity
G
1%
2%
3%
3%
3%
3%
3%
4%
4%
6%
6%
7%
10%
13%
14%
20%
Defense response
Assembly
Response to hormone
Catabolic process
Response to inons/substances
Response to abiotic stress
Transport
Developmental process
Response to abiotic stimuli
Response to biotic stress
Signal transduction
Metabolic process
Molecular process
Regulation
Biosynthetic process
Cellular process
H
2%
2%
15%
18%
25%
38%
Amyloplast
Membrane
Complex
Chloroplast
Cell wall
Other
I
10%
14%
18%
58%
Transporter activity
other
Binding
Enzyme/protein activity

Figure 2.7. Sub-classification of the three gene ontology (GO) categories of two sorghum genotypes at three post-inoculation stages. Biological processes (A, B, C), cellular components (D, E, F), and molecular functions (G, H, I) at 2, 7, and 30 days post-inoculation, respectively.

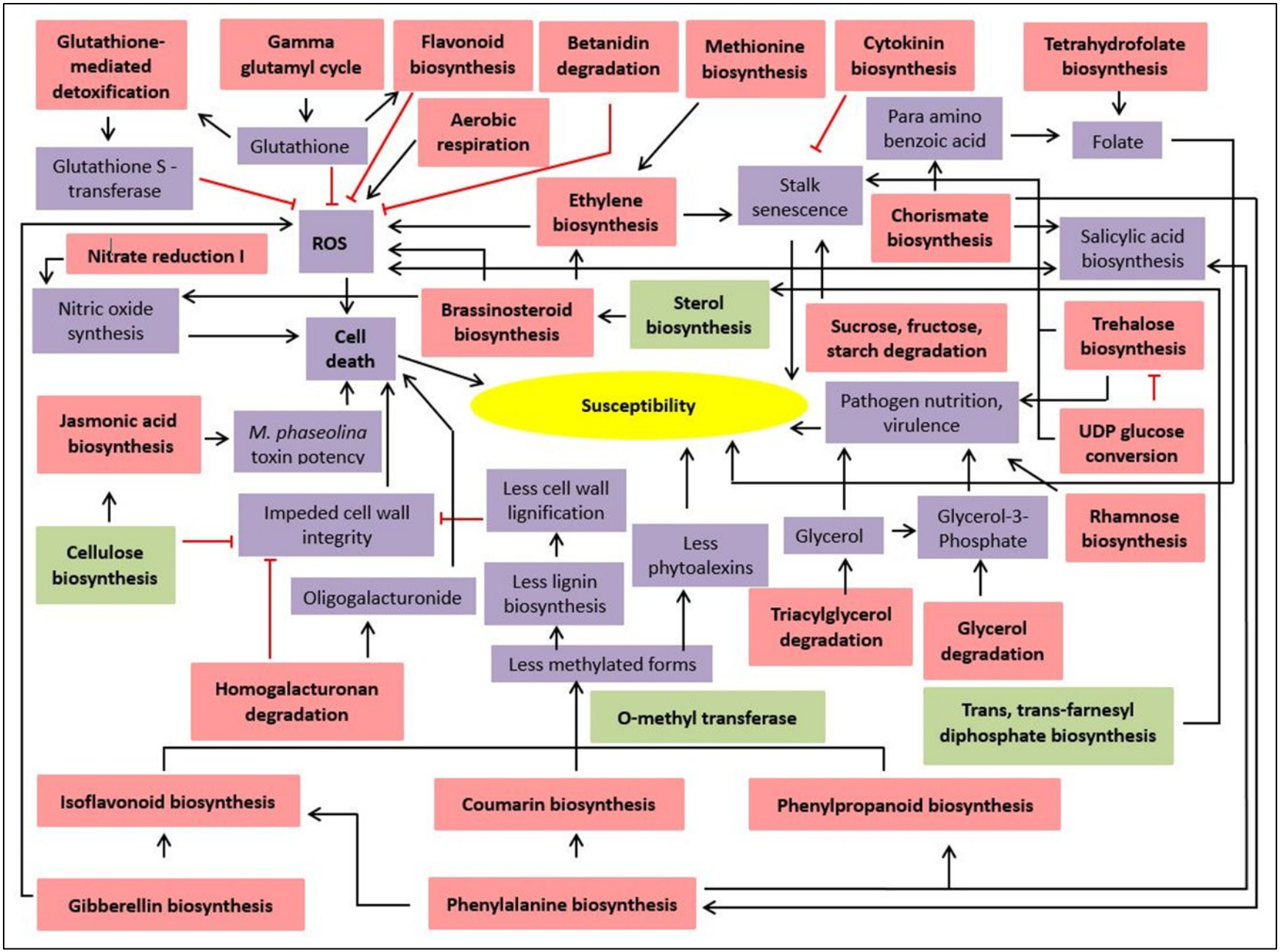
Glutathione-mediated detoxification
Gamma glutamyl cycle
Flavonoid biosynthesis
Betanidin degradation
Methionine biosynthesis
Cytokinin biosynthesis
Tetrahydrofolate biosynthesis
Glutathione
Aerobic respiration
Para amino benzoic acid
Folate
Glutathione S - transferase
Ethylene biosynthesis
Stalk senescence
Chorismate biosynthesis
Salicylic acid biosynthesis
ROS
Nitrate reduction I
Nitric oxide synthesis
Brassinosteroid biosynthesis
Sterol biosynthesis
Sucrose, fructose, starch degradation
Trehalose biosynthesis
Cell death
Susceptibility
Pathogen nutrition, virulence
UDP glucose conversion
Jasmonic acid biosynthesis
M. phaseolina toxin potency
Less cell wall lignification
Impeded cell wall integrity
Less phytoalexins
Glycerol
Glycerol-3-Phosphate
Rhamnose biosynthesis
Cellulose biosynthesis
Oligogalacturonide
Less lignin biosynthesis
Triacylglycerol degradation
Glycerol degradation
Less methylated forms
Homogalacturonan degradation
O-methyl transferase
Trans, trans-farnesyl diphosphate biosynthesis
Isoflavonoid biosynthesis
Coumarin biosynthesis
Phenylpropanoid biosynthesis
Gibberellin biosynthesis
Phenylalanine biosynthesis

Figure 2.8. Interconnection between major metabolic pathways and their contribution towards enhanced susceptibility of Tx7000 to *Macrophomina phaseolina.* Pathways in pink and green boxes indicate up- and down-regulation, respectively, while those in purple boxes indicate different biological processes and compounds.

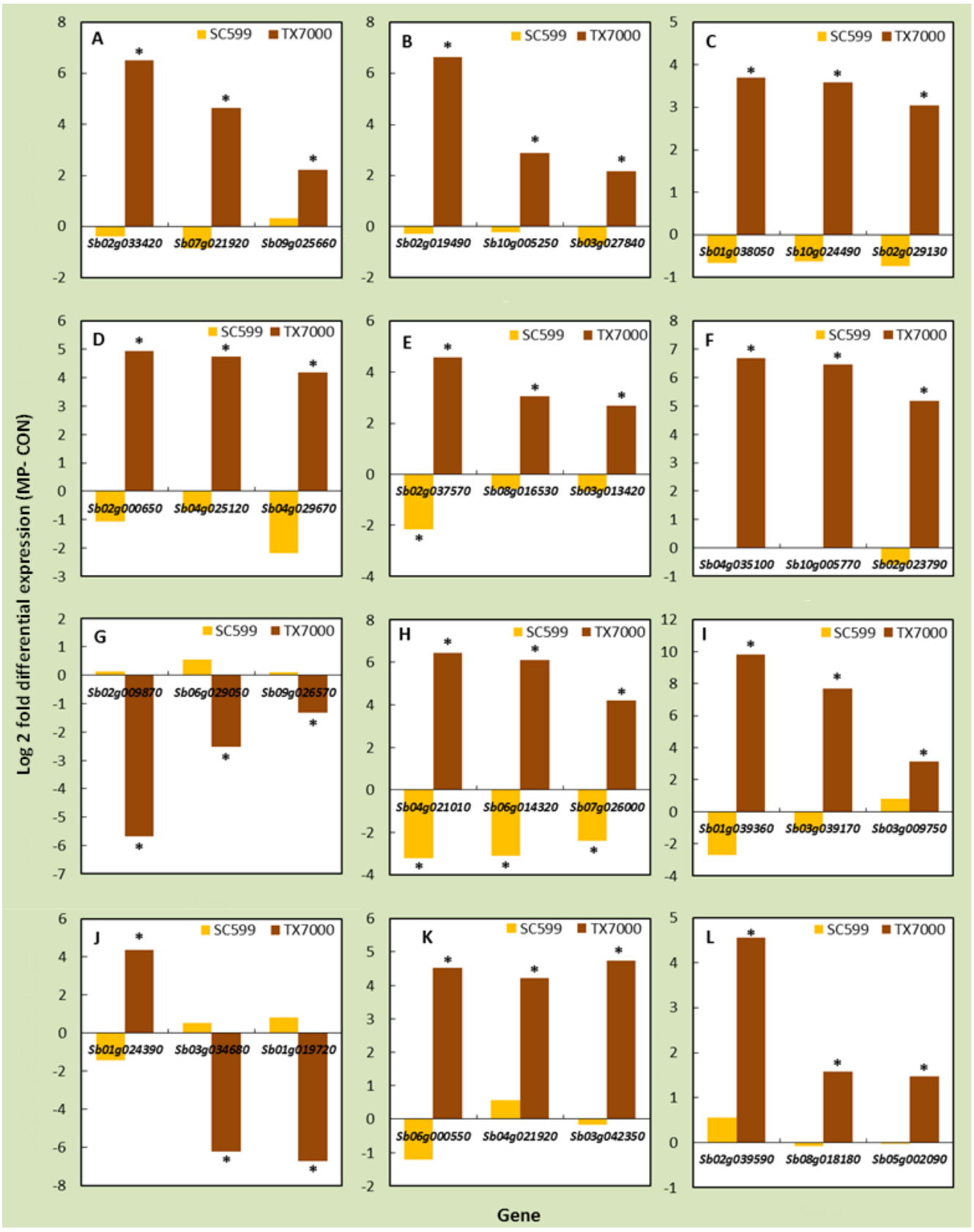
A
SC599
TX7000
Sb02g033420
Sb07g021920
Sb09g025660
B
SC599
TX7000
Sb02g019490
Sb10g005250
Sb03g027840
C
SC599
TX7000
Sb01g038050
Sb10g024490
Sb02g029130
D
SC599
TX7000
Sb02g000650
Sb04g025120
Sb04g029670
E
SC599
TX7000
Sb02g037570
Sb08g016530
Sb03g013420
F
SC599
TX7000
Sb04g035100
Sb10g005770
Sb02g023790
G
SC599
TX7000
Sb02g009870
Sb06g029050
Sb09g026570
H
SC599
TX7000
Sb04g021010
Sb06g014320
Sb07g026000
I
SC599
TX7000
Sb01g039360
Sb03g039170
Sb03g009750
J
SC599
TX7000
Sb01g024390
Sb03g034680
Sb01g019720
K
SC599
TX7000
Sb06g000550
Sb04g021920
Sb03g042350
L
SC599
TX7000
Sb02g039590
Sb08g018180
Sb05g002090
Log 2 fold differential expression (MP- CON)
Gene

Figure 2.9. Log two-fold differential expression between *Macrophomina phaseolina* (MP) and mock-inoculated control (CON) treatments for three representative SC599 and Tx7000 genes from trehalose biosynthesis (A), UDP-glucose conversion (B), dTDP-L-rhamnose biosynthesis (C), fructose degradation to pyruvate and lactate (D), sucrose degradation to ethanol and lactate (E), starch degradation (F), starch biosynthesis (G), glycerol degradation (H), triacylglycerol degradation (I), cellulose biosynthesis (J), homogalacturonan degradation (K), and aerobic respiration-electron donor II (L) metabolic pathways. Asterisks indicate significant differential expression between *Macrophomina phaseolina* and mock-inoculated control treatment.

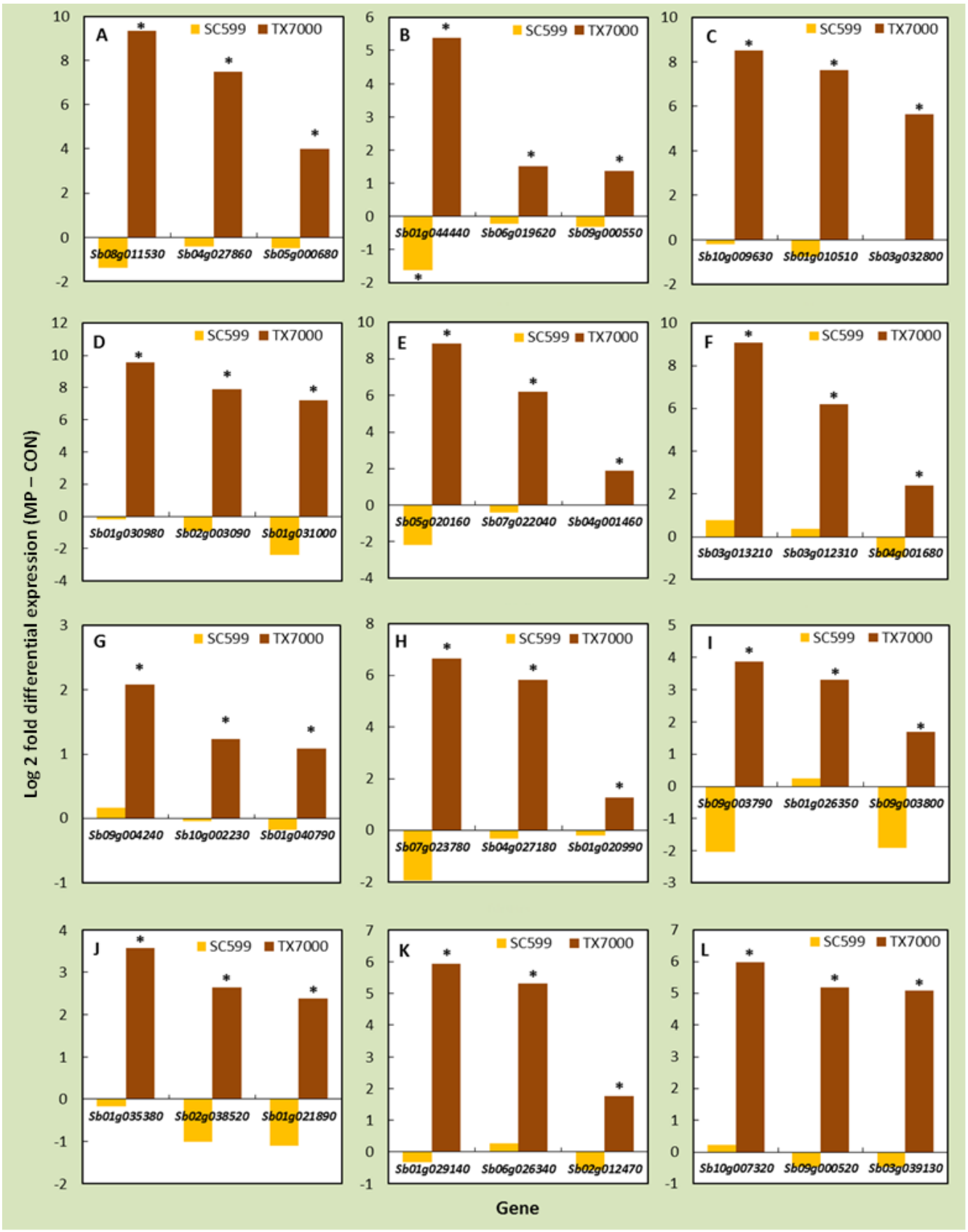
A
SC599
TX7000
Sb08g011530
Sb04g027860
Sb05g000680
B
Sb01g044440
Sb06g019620
Sb09g000550
C
Sb10g009630
Sb01g010510
Sb03g032800
D
Sb01g030980
Sb02g003090
Sb01g031000
E
Sb05g020160
Sb07g022040
Sb04g001460
F
Sb03g013210
Sb03g012310
Sb04g001680
G
Sb09g004240
Sb10g002230
Sb01g040790
H
Sb07g023780
Sb04g027180
Sb01g020990
I
Sb09g003790
Sb01g026350
Sb09g003800
J
Sb01g035380
Sb02g038520
Sb01g021890
K
Sb01g029140
Sb06g026340
Sb02g012470
L
Sb10g007320
Sb09g000520
Sb03g039130
Log 2 fold differential expression (MP – CON)
Gene

Figure 2.10. Log two-fold differential expression between *Macrophomina phaseolina* and mock inoculated control (CON) treatments for three representative SC599 and Tx7000 genes from nitrate reduction I pathway (A), calvin cycle (B), gamma glutamyl cycle (C), glutathione-mediated detoxification (D), flavonoid biosynthesis (E), betanidin degradation (F), chorismate biosynthesis (G), tetrahydrofolate biosynthesis (H), ethylene biosynthesis (I), brassinosteroid biosynthesis (J), gibberellin biosynthesis (K), and jasmonic acid biosynthesis (L) metabolic pathways. Asterisk indicates significant differential expression between *Macrophomina phaseolina* and mock inoculated control treatment.

Chapter 3 - *Macrophomina phaseolina* infection induces oxidative stress response in charcoal-rot-susceptible sorghum genotypes.

ABSTRACT

Macrophomina phaseolina is a necrotrophic fungus that causes the charcoal rot disease in sorghum [*Sorghum bicolor* (L.) Moench]. Necrotrophs are known to secrete reactive oxygen species (ROS) and induce a strong oxidative stress in the host to kill host cells and promote infection and colonization. In this study, the host transcriptional and biochemical aspects in relation to the oxidative stress of known charcoal-rot-resistant (SC599) and -susceptible (Tx7000) sorghum genotypes in response to *M. phaseolina* inoculation were investigated. RNA sequencing revealed 64 differentially expressed genes between SC599 and Tx7000 that are related to the biosynthesis of ROS and nitric oxide (NO). After *M. phaseolina* inoculation, most of these genes were significantly up-regulated in Tx7000 while they were not significantly differentially expressed in SC599. Follow-up functional experiments demonstrated *M. phaseolina*'s ability to significantly increase the ROS and reactive nitrogen species (RNS) content in charcoal-rot-susceptible genotypes, Tx7000 and Btx3042. The presence of NO in susceptible stalk tissues was confirmed using a NO-specific fluorescent probe and confocal microscopy. Enhanced oxidative stress experienced by *M. phaseolina* inoculated Tx7000 and Btx3042 was further confirmed by their significantly increased malondialdehyde content (An indicator of ROS and RNS mediated lipid peroxidation). Taken together, this study showed that *M. phaseolina* promotes host-derived oxidative stress responses in charcoal-rot-susceptible sorghum genotypes which may contribute to induced cell death associated-disease susceptibility to this important necrotrophic phytopathogen.

Keywords: sorghum, *Macrophomina phaseolina*, necrotrophic fungi, oxidative stress, reactive oxygen and nitrogen species, nitric oxide, induced disease susceptibility, antioxidant system, lipid peroxidation

INTRODUCTION

Plants are equipped with a variety of defense mechanisms to protect themselves from pathogen infection. Pathogen-associated molecular patterns (PAMPs), attributed to the basal defense of plants, are elicited by plants as a less specific recognition system to prevent pathogenic invasion and restrict pathogen growth (Jones & Dangl, 2006). Plants produce resistance proteins in response to infection by pathogens that contribute to basal defense. These proteins promote inducible defense responses often characterized by hypersensitive response (HR)-associated cell death upon pathogen recognition. HR constrains the invasion of biotrophic pathogens. Biotrophs derive their energy requirements from living host cells. On the other hand, necrotrophic pathogens actively kill host tissue as they colonize and obtain nutrients from dead or dying cells (Stone, 2001). Therefore, any mechanism that results in host cell death, including HR, is beneficial for growth and pathogenesis of necrotrophs. Cell death during HR is dependent upon the balanced production of nitric oxide (NO) and reactive oxygen species (ROS) (Delledonne et al., 2001). Many necrotrophs produce ROS as virulence factors during colonization (Shetty et al., 2008). For example, high levels of ROS contribute to the infection, colonization, and suppression of host defenses by the necrotrophic fungus, *Botrytis cinerea* (van Kan, 2006; Choquer et al., 2007). *Macrophomina phaseolina* generates a flux of NO during the infection process of the jute plant (Sarkar et al., 2014).

M. phaseolina is a globally important, soil borne, necrotrophic fungal pathogen that causes diseases in over 500 plant species (Islam et al., 2012) including major food (Su et al., 2001), pulse (Mayék-Pérez et al., 2001; Raguchander et al., 1993), fiber [jute (De et al., 1992), cotton (Aly et al., 2007)] and oil crops (Wyllie, 1998). Despite its broad host range, *M. phaseolina* is a monotypic genus and contains only one species (Sutton, 1980). *M. phaseolina* causes charcoal rot disease in many economically important crops including sorghum, soybean, maize, alfalfa, and jute (Islam et al., 2012). It occurs across wide geographic regions including both tropical and temperate environments (Tarr, 1962, Tesso et al., 2012). Charcoal rot in sorghum is characterized by degradation of pith tissue at or near the base of the stalk causing death of stalk pith cells (Edmunds, 1964). Infected plants often have damaged vascular and cortical tissues in both the root and stalk systems that may reduce nutrient and water absorption and translocation

(Hundekar and Anahosur, 2012). Sorghum is a staple cereal crop for many people in the marginal, semi-arid environments of Africa and South Asia. The unique capability of sorghum to grow in low and variable rainfall regions reveals its suitability to enhance agricultural productivity in water-limited environments (Rosenow et al., 1983). Around the world, sorghum is utilized as an important source of food, feed, sugar and fiber. With the recent interest in bioenergy feedstocks, sorghum has been recognized as a promising alternative for sustainable biofuel production (Kimber et al., 2013). Recent studies have revealed the negative impacts of charcoal rot disease on grain (Bandara et al., 2017a; Bandara et al., 2016) and sweet (Bandara et al., 2017b) sorghum. As charcoal rot is a high priority fungal disease in sorghum [*Sorghum bicolor* (L.) Moench], causing tremendous crop losses where ever sorghum is grown (Tarr, 1962, Tesso et al., 2012), more research is needed to identify charcoal rot resistance mechanisms.

Although some necrotrophic fungi use their own ROS and reactive nitrogen species (RNS) as virulence factors during infection and colonization (Shetty et al., 2008; van Kan, 2006; Choquer et al., 2007; Sarkar et al., 2014), necrotroph infection-associated upregulation of host-derived ROS and RNS is poorly described. In chapter two, we outlined the differentially expressed genes between resistant (SC599) and susceptible (Tx7000) sorghum genotypes that are associated with oxidative stress responses. In this chapter, the follow-up biochemical studies in relation to oxidative stress, nitric oxide biosynthetic capacity, and the level of lipid peroxidation of known resistant (SC599, SC35) and susceptible (Tx7000, BTx3042) sorghum genotypes in response to *M. phaseolina* inoculation are reported. Relevant gene expression data are also discussed in detail.

MATERIALS AND METHODS

Plant materials, establishment, maintenance, inoculum preparation, inoculation, and sorghum stalk tissue collection

Two charcoal-rot-resistant (SC599, SC35) and two susceptible (Tx7000, BTx3042) sorghum lines were used. Plant establishment, randomization of the treatment factors (genotype, inoculation treatment, and tissue harvest time), plant maintenance, inoculum preparation, and

inoculation were conducted according to the methods described in the Chapter 2. At 4, 7, and 10 days post- inoculation (DPI), 15 cm long stalk pieces encompassing the inoculation point were cut from five biologically replicated plants, immediately suspended in liquid nitrogen, and subsequently stored at -80°C until used in functional experiments.

Preparation of tissue lysates and measuring absorption and fluorescence

Stalk tissues were retrieved from -80°C storage and approximately 1 g of stalk tissue (1 cm away from the symptomatic region) was chopped into liquid nitrogen (in a mortar) using a sterile scalpel. The stalk pieces were ground in to a fine powder using a pestle. Approximately 200 mg of stalk tissue powder was transferred into 2 mL microcentrifuge tubes filled with 1 ml of 1X PBS with 0.5% Triton X (for in vitro ROS/RNS assay) and 1X PBS with 1X BHT (for quantification of lipid peroxidation via the thiobarbituric acid reactive substances assay; TBARS). Buffer selections were based on the instructions by assay kit manufacturers (see below). Samples were centrifuged at 10000 g for 10 min at 4°C. Supernatants were transferred into new microcentrifuge tubes and stored at -80°C until used in assays. All absorption and fluorescence measurements (as instructed by the assay kit manufacturers) were performed using a 96-well plate reader (Synergy H1 Hybrid Reader; BioTek, Winooski, VT, USA) at specified wave lengths (see below). Path length correction was performed using an option available in the plate reader during the measurements.

Quantification of total oxidative stress (free radical content)

The OxiSelect In Vitro ROS/RNS Assay Kit (Cell Biolabs, San Diego, CA, USA) was used to quantify reactive species (ROS) and reactive nitrogen species (RNS) content. The assay employs a ROS/RNS-specific fluorogenic probe, dichlorodihydrofluorescein DiOxyQ (DCFH-DiOxyQ), which is first primed with a quench removal reagent and subsequently stabilized in the highly reactive DCFH form. Various ROS and RNS such as hydrogen peroxide (H_2O_2), peroxyl radical ($ROO^{\cdot}$), nitric oxide (NO), and peroxynitrite anion ($ONOO^-$) can react with DCFH and oxidize it into the fluorescent 2′,7′-dichlorodihydrofluorescein (DCF). Fluorescence intensity is proportional to the reactive species content within the sample. Free radical molecules are representative of both ROS and RNS. The assay measures the total free radical population within a sample. In the current study, reactive species content was assayed following the protocol

described by the manufacturer. Briefly, 50 µL of the supernatant (see previous section) from each sample was transferred to a black 96-well Nunclon Delta Surface microplate (Thermo Scientific Nunc, Roskilde, Denmark) and incubated with the catalyst (1X) for 5 min at room temperature. 100 µL of freshly prepared DCFH solution was added to each well and incubated for 45 min. The plate was covered with aluminum foil to protect the reaction mix from light. After incubation, fluorescence from the samples was measured at 485 nm excitation and 535 nm emission wavelengths. A dilution series of DCF standards (in the concentration range of 0 µM – 10 µM) was prepared by diluting the 1mM DCF stock in 1X PBS and used to prepare a DCF standard curve. The DCF standard curve was used to determine the reactive species content of samples and expressed as mM DCF per 200 mg of stalk tissue (fresh weight).

Detection of nitric oxide (NO) by confocal microscopy

A fluorescent dye, 4-amino-5-methylamino-2',7'-difluorofluorescein diacetate (DAF-FM DA; Molecular Probes, Eugene, OR, USA) was used to detect NO production by sorghum genotypes in response to inoculation treatment at 7 DPI. DAF-FM DA is non-fluorescent until it reacts with NO to form DAF-FM (bright green fluorescence). DAF-FM DA passively diffuses across cellular membranes. The fluorescence quantum yield of DAF-FM increases about 160-fold after reacting with nitric oxide (Kojima et al., 1999). In the current study, sorghum stem cross sections (made 1 cm away from the symptomatic area) were incubated with 10 mM DAF-FM DA prepared in 10 mM Tris–HCl (pH 7.4) for 1 h at 25°C in darkness (Corpas et al., 2004). After incubation, samples were washed twice with 10 mM Tris–HCl buffer for 15 min each. Then the sections were examined by Carl Zeiss 700 confocal microscope. The light intensity and exposure times were kept constant for DAF-FM DA green fluorescence (excitation 495 nm; emission 515 nm), and chlorophyll autofluorescence (chlorophyll *a* and *b*, excitation 429 and 450 nm, respectively; emission 650 and 670 nm, respectively) as red. For each sorghum genotype, fluorescence of the mock-inoculated treatment (control) was used as baseline.

Quantification of lipid peroxidation

Malondialdehyde (MDA) content in stalk samples was measured using an OxiSelect thiobarbituric acid reactive substances (TBARS) assay kit (Cell Biolabs, San Diego, CA, USA) as an estimate of lipid peroxidation. Lipid peroxides are unstable indicators of oxidative stress in

cells, and they decompose in to complex end products such as MDA (Kappus, 1985). The TBARS assay is based on MDA's reactivity with thiobarbituric acid (TBA) via an acid-catalysed nucleophilic-addition reaction. The resulting pinkish-red fluorescent MDA:TBA (1:2) adduct has an absorbance maxima at 532 nm and can be measured calorimetrically (Kappus, 1985; Janero, 1990). In the present study, 100 µL of sample was incubated with 100 µL of sodium dodecyl sulfate lysis solution in a microcentrifuge tube for 5 min at room temperature. Thiobarbituric acid (250 µL) was added into each sample and incubated at 95°C for 1 h. After cooling to room temperature on ice for 5 min, samples were centrifuged at 3000 rpm for 15 min. The supernatant (200 µL) was transferred to a 96-well microplate, and the absorbance was read at 532 nm. A dilution series of MDA standards (in the concentration range of 0 - 125 µM) was prepared by diluting the MDA Standard in deionized water and used to prepare the MDA standard curve. The MDA content of the samples was determined using a MDA standard curve and expressed as µmol per 200mg of stalk tissue (fresh weight).

Statistical analysis

Data were analyzed for variance (ANOVA) using the PROC GLIMMIX procedure of SAS software version 9.2 (SAS Institute, 2008). Variance components for the two fixed factors, genotype and inoculation treatment, were estimated using restricted maximum likelihood (REML) method at each post-inoculation stage (4, 7, and 10 DPI). Studentized residual plots and Q-Q plots were used to test the assumptions of identical and independent distribution of residuals and their normality, respectively. Whenever heteroskedasticity was observed, appropriate heterogeneous variance models were fitted to meet the model assumptions by specifying a random/group statement (group = genotype or inoculation treatment) after the model statement. Bayesian information criterion (BIC) was used to determine the most parsimonious model. Means separations were carried out using the PROC GLMMIX procedure of SAS. Main effects of factors were determined with adjustments for multiple comparisons using the Tukey-Kramer test. Whenever genotype × treatment interaction was statistically significant, the simple effects of inoculation treatment were determined at each genotype level (four genotypes). As inoculation treatment comprised only two levels (control and *M. phaseolina*), there wasn't a need to adjust the critical *P*-values for multiple comparisons.

RESULTS

Genome wide transcriptome profiling

Differential gene expression analysis

As indicted in the chapter 2, the metabolic pathway enrichment analysis revealed the importance of expression profile differences between resistant and susceptible genotypes at 7 DPI. Therefore, for interpretation purposes, the transcriptional data at 7 DPI has been emphasized in this chapter. At 7 DPI, 64 oxidative stress related genes were found to be differentially expressed between charcoal-rot-resistant and susceptible genotypes in response to *M. phaseolina* inoculation (Table 3.1) and are described below.

Differentially expressed genes involved in host ROS biosynthesis

In the endoplasmic reticulum, NAD(P)H-dependent electron transport involving cytochrome P450 (CP450) produces superoxide anions ($O_2^{\bullet-}$) (Mittler, 2002). Moreover, the up-regulation of CP450 resulted in increased conversion of endogenous compounds into reactive metabolites and is a source of oxidative stress (Nebert et al., 2000). Therefore, increased CP450 expression is a direct indication of enhanced oxidative stress. In the RNA-Seq study (reported in chapter 2), a number of CP450 genes involved in known metabolic pathways such as acetone degradation (to methylglyoxal), betanidin degradation, brassinosteroid biosynthesis II, free phenylpropanoid acid biosynthesis, gibberellic acid biosynthesis, jasmonic acid biosynthesis, lactucaxanthin biosynthesis, nicotine degradation II, nicotine degradation III, phaseic acid biosynthesis, and phenylpropanoid biosynthesis were differentially expressed (Appendix C). Moreover, 38 differentially expressed CP450 genes (Table 3.1) did not have assigned metabolic pathways. They could be involved in the generation of NAD(P)H-dependent superoxide anions ($O_2^{\bullet-}$). Out of these 38, fourteen were significantly down-regulated in the susceptible genotype while 22 were significantly up-regulated, which contributed to a 42.1 log2 fold net up-regulation of CP450 in the susceptible genotype (Table 3.1).

NADPH oxidases catalyze the synthesis of $O_2^{\bullet-}$ in the apoplast (Sagi & Fluhr, 2006). A gene that encodes an NADPH oxidase (*Sb0621s002010*) was significantly down-regulated (log2 fold = 3.2) in Tx7000 after *M. phaseolina* inoculation (Table 3.1) while the gene in SC599 did not significantly differently expressed.

Copper amine oxidases and flavin-containing amine oxidases contribute to defense responses occurring in the apoplast through H_2O_2 production following pathogen invasion (Cona et al., 2006, Wimalasekera et al., 2011). In the current study, four genes that encode for flavin-containing amine oxidases were differentially expressed (Table 3.1) and two of them were significantly up-regulated in pathogen inoculated Tx7000 (*Sb06g032450*, *Sb06g032460*; log2 fold = 0.92, 4.10, respectively), while the other two were significantly down-regulated (*Sb01g044230*, *Sb07g005780*; log2 fold = -4.96, -2.04, respectively). Another gene that encodes for amine oxidase-related protein (*Sb01g006160*) was significantly down-regulated (log2 fold = -1.39) in Tx7000. Two of the three genes that encoded for a copper methylamine oxidase precursor (*Sb02g036990, Sb04g028410*) were significantly down-regulated in pathogen-inoculated Tx7000 (log2 fold = -3.71, -2.84, respectively) the other (*Sb06g020020*) was significantly up-regulated (log2 fold = 3.33).

NADH dehydrogenase is a major source of ROS production in mitochondria (Moller, 2001; Arora et al., 2002). Direct reduction of oxygen to $O_2^{\bullet-}$ occurs in the flavoprotein region of the NADH dehydrogenase segment of the respiratory chain complex I (Arora et al., 2002). In the current study, two genes that encode for NADH dehydrogenase 1 alpha sub-complex, assembly factor 1 (*Sb03g033415*, log2 fold = 2.14) and a NADH dehydrogenase iron-sulfur protein 4 (*Sb02g037780*, log2 fold = 0.97) were significantly upregulated in pathogen-inoculated Tx7000 (Table 3.1).

Differentially expressed genes involved in host NO biosynthesis

NO plays a key role in plant immune responses such as hypersensitive response (HR) cell death during incompatible plant–pathogen interactions (Delledonne et al. 1998; Durner et al. 1998; Yoshioka et al. 2011). The nitrate reduction I and citrulline-nitric oxide cycles are the major NO

biosynthetic pathways in plants (Planchet & Kaiser, 2006). In the current study, six genes (*Sb04g000530*, *Sb01g039180*, *Sb05g000240*, *Sb07g024150*, *Sb10g002510*, *Sb09g002030*) involved in the citrulline-nitric oxide cycle (encode for six isozymes of nitric oxide synthase (EC 1.14.13.39) were significantly down-regulated in Tx7000 after *M. phaseolina* inoculation (Table 3.1). Compared to mock-inoculated control, this was a 12.1 net log2 fold down-regulation (net = summation of the log2 fold values of differentially expressed genes concerned). Five genes (*Sb08g011530*, *Sb04g027860*, *Sb05g000680*, *Sb03g039960*, *Sb04g025630*) involved in the nitrate reduction I pathway were significantly up-regulated in pathogen-inoculated Tx7000 and encoded for isozymes of nitrite reductase (NO-forming) (EC 1.7.2.1), marking a 26.8 net log2 fold up-regulation in comparison to the control treatment. Moreover, three genes (*Sb07g022750*, *Sb07g026290*, *Sb04g007060*) involved in the nitrate reduction II (assimilatory) pathway (encode for NADH-cytochrome b5 reductase (EC 1.7.1.1)) were significantly down-regulated (net log2 fold = -7.61) in pathogen-inoculated Tx7000.

Functional investigations

Analysis of variance (ANOVA)

The two-way interaction between genotype and inoculation treatment was significant for ROS/RNS and TBARS assays at all three post-inoculation stages (4, 7, and 10 DPI) (Table 3.2).

M. phaseolina inoculation induces ROS/RNS accumulation in charcoal-rot-susceptible genotypes

To investigate the potential differences of oxidative stress imposed by *M. phaseolina* on charcoal-rot-resistant and susceptible sorghum genotypes, the total free radical population (representative of both ROS and RNS) in mock- and pathogen-inoculated samples at three post-inoculation stages was measured. Compared to control, *M. phaseolina* significantly increased the ROS/RNS content of both susceptible genotypes (BTx3042 and Tx7000) at all post-inoculation stages (4, 7, and 10 DPI) (Figure 3.1). *M. phaseolina* increased ROS/RNS in BTx3042 by 70.5, 52.5, and 123.8% at 4, 7, and 10 DPI, respectively. In Tx7000, increases were 185.1, 47.3, and 81.9%. *M. phaseolina* inoculation did not significantly affect the ROS/RNS content of the two resistant genotypes, SC599 and SC35. Although not statistically significant, ROS/RNS content

of *M. phaseolina*-inoculated SC599 was lower than the control at 10 DPI. The same phenomenon was observed for SC35 at 4 and 7 DPI.

M. phaseolina inoculation induces NO accumulation in charcoal-rot-susceptible genotypes

Bright green fluorescence was observed in the infected stem cross-sections of Tx7000 and BTx3042 at 7 DPI and indicated NO specific fluorescence with DAF-FM DA (Figures 3.2, 3.4). This revealed the ability of *M. phaseolina* to induce NO biosynthesis and accumulation in charcoal-rot-susceptible sorghum genotypes. NO-specific fluorescence was absent in control tissue sections (Figure 3.2), which indicated that induction of NO only after inoculation with the pathogen. Neither mock- or pathogen-inoculation produced NO-specific fluorescence in the resistant genotypes, SC599 and SC35 (Figures 3.3, 3.4). Therefore, these charcoal-rot-resistant genotypes do not undergo NO burst-mediated oxidative stress after *M. phaseolina* infection.

M. phaseolina inoculation enhances lipid peroxidation in charcoal-rot-susceptible genotypes

The severity of lipid peroxidation, as indicated by malondialdehyde (MDA) content is a direct indicator of the degree of oxidative stress that plants undergo (Sharma et al., 2012). In the current study, compared to respective controls, *M. phaseolina* inoculation significantly increased MDA content (μM) in both charcoal-rot-susceptible genotypes at all post-inoculation stages (Figure 3.5). *M. phaseolina* increased MDA in BTx3042 by 124, 54.4, and 80.6% at 4, 7, and 10 DPI, respectively. Pathogen induced increases for Tx7000 were 262.4, 70, and 75%. *M. phaseolina* inoculation did not significantly affect MDA content of the two resistant genotypes, SC599 and SC35. In general, compared to other genotypes, SC35 showed a higher MDA content at 4 and 7 DPI for both control and pathogen inoculations (Figure 3.5, error bars signify standard errors). However, there was a dramatic drop in MDA content from 7 to 10 DPI with both control and pathogen inoculations for this genotype.

DISCUSSION

The synthesis and accumulation of ROS in plants as a defense response to pathogen attack are well described (Dangl and Jones, 2001; Torres et al., 2002). Apoplastic synthesis of superoxide

($O_2^{\bullet-}$) and its dismutation product hydrogen peroxide (H_2O_2) has been reported in response to a variety of pathogens (Doke, 1983; Auh and Murphy, 1995; Grant et al., 2000). Although ROS accumulation typically correlates with effective disease resistance reactions against biotrophic or hemi-biotrophic pathogens (Vanacker et al., 2000; Allan & Fluhr, 1997), certain necrotrophs induce ROS synthesis in the infected tissue to promote cell death that facilitates subsequent infection (Govrin and Levine, 2000, Foley et al., 2016). In fact, ROS-mediated defense responses, effective against biotrophic pathogens, increase susceptibility to necrotrophic pathogens (Kliebenstein & Rowe, 2008). The current study provided transcriptional and functional evidences for the ability of necrotrophic fungus *M. phaseolina* to induce ROS and RNS in charcoal-rot-susceptible sorghum genotypes (Tx7000, BTx3042).

In the endoplasmic reticulum, the CP450 involved in NAD(P)H-dependent electron transport chain contributes to $O_2^{\bullet-}$ production (Mittler, 2002). In the current study, we observed a net up-regulation of CP450 which potentiate the NAD(P)H-dependent $O_2^{\bullet-}$ production in endoplasmic reticulum. Therefore, the endoplasmic reticulum appears to be an important ROS generating powerhouse, contributing to enhanced oxidative stress in Tx7000 after *M. phaseolina* inoculation. In the apoplast, NADPH oxidases catalyze the synthesis of $O_2^{\bullet-}$ (Sagi & Fluhr, 2006). NADPH oxidases are also involved in ROS production in response to pathogen infections (Sagi and Fluhr, 2001; Torres et al., 2002). Fungal NADPH oxidases have been shown to be required for pathogenesis of certain necrotrophic fungi such as *Sclerotinia sclerotiorum* (Kim et al., 2011), *Botrytis cinerea* (Segmueller et al., 2008), and *Alternaria alternata* (Yang & Chung, 2012). In the current study, the observed down-regulation of a host NADPH oxidase (*Sb0621s002010*) gene suggested that apoplastic $O_2^{\bullet-}$ is not a significant source of pathogen induced oxidative stress in Tx7000.

Amine oxidases are involved in apoplastic H_2O_2 production (Cona et al., 2006, Wimalasekera et al., 2011). In the current study, genes encoding amine oxidases showed a net down-regulation in Tx7000, thus amine oxidase-mediated apoplastic H_2O_2 production would remain minimal in response to *M. phaseolina* inoculation.

NADH dehydrogenases are major sources of ROS production in mitochondria (Moller, 2001; Arora et al., 2002). The significant up-regulation of two NADH dehydrogenase genes (*Sb03g033415*, *Sb02g037780*) suggested the potential contribution of mitochondria as a source of enhanced ROS production in Tx7000 in response to pathogen inoculation. Consistent with the gene expression data, the in vitro ROS/RNS functional assay revealed *M. phaseolina'*s ability to significantly increase the stalk free radical content of both susceptible genotypes (BTx3042 and Tx7000) at all three post inoculation stages (4, 7, and 10 DPI). Therefore, *M. phaseolina*'s ability to trigger a strong oxidative stress in charcoal-rot-susceptible sorghum genotypes was evident.

Along with ROS, NO plays an important role in the hypersensitive response to avirulent biotrophic pathogens (Delledonne et al., 1998; Durner et al., 1998; Yoshioka et al., 2011). The role of NO in host defense against necrotrophs is contradictory. For instance, NO is claimed to confer resistance against certain necrotrophic fungal pathogens (Asai et al., 2010; Perchepied et al., 2010). On the contrary, a strong accumulation of NO in host tissue correlated with enhanced disease susceptibility was observed in the compatible jute-*M. phaseolina* (Sarkar et al., 2014) and lily-*Botrytis elliptica* interaction (van Baarlen et al., 2004). Agreeing with the latter phenomenon, a strong NO burst was observed in susceptible sorghum stalk tissues (Tx7000, BTx3042) upon *M. phaseolina* inoculation (Figures 3.2, 3.4). NO-specific fluorescence was found to be stronger in the vascular bundle regions. As no mycelial fragments or microsclerotia were observed in the cross-sections, the observed NO was exclusively from the host. This suggested the systemic circulation of NO through the vascular tissues. Moreover, fluorescence was observed in parenchyma cells, which indicated the cell-to-cell movement of NO. The movement of NO via apoplastic and symplastic pathways has been described (Graziano & Lamattina, 2005).

The RNA sequencing experiment provided some clues on the host metabolic pathways that contributed to the surge in NO. The nitrate reduction I and citrulline-nitric oxide cycles are the major NO biosynthetic pathways in plants (Planchet & Kaiser, 2006). In citrulline-nitric oxide cycle, NO is synthesized from arginine by nitric oxide synthase, generating L-citrulline as a by-product (Planchet & Kaiser, 2006). In the current study, the down-regulated nitric oxide synthase genes in Tx7000 suggested that the citrulline-nitric oxide cycle remains inactive during *M.*

phaseolina infection and is not a significant source pathway for NO synthesis. Interestingly, the genes encoding nitrite reductase (EC 1.7.2.1) which involved in the nitrate reduction I pathway were highly up-regulated in Tx7000 after pathogen inoculation. Nitrite reductase converts nitrite in-to NO. Therefore, the nitrate reduction I pathway appeared to be the major source of host-derived NO in response to *M. phaseolina* infection. This argument is further bolstered by the observed down-regulation of the nitrate reduction II (assimilatory) pathway in Tx7000 after pathogen inoculation. In this pathway, the Tx7000 genes encode NADH-cytochrome b5 reductase (EC 1.7.1.1), which catalyzes the conversion of nitrate to nitrite, were down-regulated, limiting the nitrite to ammonia and ammonia to L-glutamine conversions in the chloroplast. Therefore, the down-regulated NADH-cytochrome b5 reductase genes increase the availability of nitrate pools for nitrate reduction I pathway where nitrate is reduced into NO. Therefore, over-accumulation of NO in the plant induced *by M. phaseolina* appeared to escalate its spread of infection and constitute a key element determining success of this necrotrophic pathogen.

In the current study, evidence for NO and $O_2^{\bullet-}$ accumulation in charcoal-rot-susceptible sorghum genotypes after *M. phaseolina* inoculation has been presented. NO can react with $O_2^{\bullet-}$ to form peroxynitrite ($ONOO^-$) (Koppenol et al., 1992). Peroxynitrite triggers a myriad of cytotoxic effects including lipid peroxidation, protein unfolding and aggregation, and DNA strand breakage (Vandelle & Delledonne, 2011; Murphy, 1999). When produced abundantly, $ONOO^-$ contributes to rapid necrosis, whereas lower quantities induce apoptosis (Bonfoco et al., 1995). Although not specifically tested, the significantly increased free radical content observed in charcoal-rot-susceptible genotypes could be indicative of the $ONOO^-$ increment in pathogen-inoculated Tx7000 and BTx3042. Therefore, plant-derived $ONOO^-$ may play a role as an endogenous virulence factor for *M. phaseolina*.

ROS/RNS-associated lipid peroxidation during pathogen infection is widely described (Jalloul et al., 2002; Göbel et al., 2003; Zoeller et al., 2012). Malondialdehyde (MDA) is one of the final products of unsaturated fatty acid peroxidation in phospholipids and is accounts for cellular and organellar membrane damage (Halliwell & Gutteridge, 1989). The oxidative stress experienced by charcoal-rot-susceptible sorghum genotypes after *M. phaseolina* inoculation was further confirmed by the enhanced lipid peroxidation observed in those genotypes.

CONCLUSIONS

In this study, we examined the genome-wide transcriptome profiles of *M. phaseolina* challenged charcoal-rot-resistant (SC599) and susceptible (Tx7000) sorghum genotypes to identify differentially expressed genes that related to host oxidative stress. The observed up-regulation of cytochrome P450, and NADH dehydrogenase genes, respectively, revealed the importance of the endoplasmic reticulum and mitochondria as ROS generating powerhouses contributing to enhanced oxidative stress in Tx7000 upon *M. phaseolina* inoculation. Pathogen inoculation-mediated oxidative stress enhancement in Tx7000 and BTx3042 was confirmed by increased ROS/RNS and malondialdehyde content. Prominent nitric oxide (NO) accumulation observed in Tx7000 and BTx3042 after *M. phaseolina* inoculation was possibly associated with the up-regulated host nitrate reduction I metabolic pathway. Overall, this study demonstrated the ability of *M. phaseolina* to trigger a strong host-derived oxidative stress response in sorghum in a genotype-specific manner. It is hypothesized that enhanced oxidative stress-associated massive host cell death promotes rapid colonization and spread of this necrotrophic fungus leading to induced charcoal rot susceptibility. Use of differentially expressed genes and *in planta* NO synthesis as potential molecular and biochemical markers in sorghum germplasm screening for charcoal rot resistance/susceptibility should be pursued in future research.

REFERENCES

Allan AC, Fluhr R. 1997. Two distinct sources of elicited reactive oxygen species in tobacco epidermal cells. *Plant Cell* 9: 1559-1572.

Aly AA, Abdel-Sattar MA, Omar MR, Abd-Elsalam KA. 2007. Differential antagonism of Trichoderma sp. against *Macrophomina phaseolina*. *Journal of Plant Protection Research* 47: 91-102.

Arora A, Sairam RK, Srivastava GC. 2002. Oxidative stress and antioxidative system in plants. *Current Science* 82: 1227-1238.

Asai S, Mase K, Yoshioka H. 2010. Role of nitric oxide and reactive oxygen species in disease resistance to necrotrophic pathogens. *Plant Signaling & Behavior* 5: 872-874.

Auh CK, Murphy TM. 1995. Plasma membrane redox enzyme is involved in the synthesis of $O_2^{\bullet -}$ and H_2O_2 by *Phytophthora* elicitor-stimulated rose cells. *Plant Physiology* 107: 1241–1247.

Bandara YMAY, Weerasooriya DK, Tesso TT, Prasad PVV, Little CR. 2017a. Stalk rot fungi affect grain sorghum yield components in an inoculation stage-specific manner. *Crop protection* 94: 97-105.

Bandara YMAY, Weerasooriya DK, Tesso TT, Little CR. 2017b. Stalk rot diseases impact sweet sorghum biofuel traits. *BioEnergy Research* 10: 26-35.

Bandara YMAY, Weerasooriya DK, Tesso TT, Little CR. 2016. Stalk rot fungi affect leaf greenness (SPAD) of grain sorghum in a genotype-and growth-stage-specific Manner. *Plant Disease* 100: 2062-2068.

Bonfoco E, Krainc D, Ankarcrona M, Nicotera P, Lipton SA. 1995. Apoptosis and necrosis: two distinct events induced, respectively, by mild and intense insults with Nmethyl-D-aspartate or

nitric oxide/superoxide in cortical cell cultures. *Proceedings of the National Academy of Sciences USA* 92: 7162-7166.

Choquer M, Fournier E, Kunz C, Levis C, Pradier JM, Simon A, Viaud M. 2007. *Botrytis cinerea* virulence factors: new insights into a necrotrophic and polyphageous pathogen. *FEMS Microbiology Letters* 277: 1-10.

Cona A, Rea G, Angelini R, Federico R, Tavladoraki P. 2006. Functions of amine oxidases in plant development and defence. *Trends in Plant Science* 11: 80-88.

Corpas FJ, Barroso JB, Carreras A, Quiros M, Leon AM, Romero-Puertas MC, Gómez M. 2004. Cellular and subcellular localization of endogenous nitric oxide in young and senescent pea plants. *Plant Physiology* 136: 2722-2733.

Dangl JL, Jones JDG. 2001. Plant pathogens and integrated defence responses to infection. *Nature* 411: 826-833.

De BK, Chattopadhya SB, Arjunan G. 1992. Effect of potash on stem rot diseases of jute caused by *Macrophomina phaseolina*. *Journal of Mycopathological Research* 30: 51-55.

Delledonne M, Zeier J, Marocco A, Lamb C. 2001. Signal interactions between nitric oxide and reactive oxygen intermediates in the plant hypersensitive disease resistance response. *Proceedings of the National Academy of Sciences USA* 98: 13454-13459.

Delledonne M, Xia Y, Dixon RA, Lamb C. 1998. Nitric oxide functions as a signal in plant disease resistance. *Nature* 394: 585-588.

Doke N. 1983. Involvement of superoxide anion generation in the hypersensitive response of potato tuber tissues to infection with an incompatible race of *Phytophthora infestans* and to the hyphal wall components. *Physiological Plant Pathology* 23: 345-357.

Dugas DV, Monaco MK, Olsen A, Klein RR, Kumari S, Ware D, Klein PE. 2011. Functional annotation of the transcriptome of *Sorghum bicolor* in response to osmotic stress and abscisic acid. *BMC Genomics* 12: 514.

Durner J, Wendehenne D, Klessig DF. 1998. Defense gene induction in tobacco by nitric oxide, cyclic GMP, and cyclic ADP-ribose. *Proceedings of the National Academy of Sciences USA* 95: 10328-10333.

Edmunds L. 1964. Combined relation of plant maturity temperature soil moisture to charcoal stalk rot development in grain sorghum. *Phytopathology* 54: 513-517.

Foley RC, Kidd BN, Hane JK, Anderson JP, Singh KB. 2016. Reactive oxygen species play a role in the infection of the necrotrophic fungi, *Rhizoctonia solani* in wheat. *PloS one* 11: e0152548.

Göbel C, Feussner I, Rosahl S. 2003. Lipid peroxidation during the hypersensitive response in potato in the absence of 9-lipoxygenases. *Journal of Biological Chemistry* 278: 52834-52840.

Goodstein DM, Shu S, Howson R, Neupane R, Hayes RD, Fazo J, Rokhsar DS. 2012. Phytozome: a comparative platform for green plant genomics. *Nucleic Acids Research* 40: 1178-1186.

Govrin E, Levine A. 2000. The hypersensitive response facilitates plant infection by the necrotrophic pathogen *Botrytis cinerea*. *Current Biology* 10: 751-757.

Grant M, Brown I, Adams S, Knight M, Ainslie A, Mansfield J. 2000. The RPM1 plant disease resistance gene facilitates a rapid and sustained increase in cytosolic calcium that is necessary for the oxidative burst and hypersensitive cell death. *The Plant Journal* 23: 441-450.

Graziano M, Lamattina L. 2005. Nitric oxide and iron in plants: an emerging and converging story. *Trends in Plant Science* 10: 4-8.

Halliwell B, Gutteridge JMC. 1989. Free Radicals in Biology and Medicine (2nd ed.). Oxford, UK: Clarendon.

Hundekar A, Anahosur K. 2012. Pathogenicity of fungi associated with sorghum stalk rot. *Karnataka Journal of Agricultural Sciences* 7: 291-295.

Islam MS, Haque MS, Islam MM, Emdad EM, Halim A, Hossen QM, Alam M. 2012. Tools to kill: genome of one of the most destructive plant pathogenic fungi *Macrophomina phaseolina*. *BMC Genomics* 13: 1.

Jalloul A, Montillet JL, Assigbetsé K, Agnel JP, Delannoy E, Triantaphylides C, Nicole M. 2002. Lipid peroxidation in cotton: *Xanthomonas* interactions and the role of lipoxygenases during the hypersensitive reaction. *The Plant Journal* 32: 1-12.

Janero DR. 1990. Malondialdehyde and thiobarbituric acid-reactivity as diagnostic indices of lipid peroxidation and peroxidative tissue injury. *Free Radical Biology and Medicin*e 9: 515-540.

Jones JD, Dangl JL. 2006. The plant immune system. *Nature* 444: 323-329.

Kappus H. 1985. Lipid peroxidation: mechanisms, analysis, enzymology and biological relevance. In *Oxidative Stress* (ed. H. Sies), pp 273-310. Academic Press London, UK.

Karuppanapandian T, Moon JC, Kim C, Manoharan K, Kim W. 2011. Reactive oxygen species in plants: their generation, signal transduction, and scavenging mechanisms. *Australian Journal of Crop Science* 5: 709-725.

Kim HJ, Chen C, Kabbage M, Dickman MB. 2011. Identification and Characterization of *Sclerotinia sclerotiorum* NADPH Oxidases. *Applied and Environmental Microbiology* 77: 7721-7729.

Kimber CT, Dahlberg JA, Kresovich S. 2013. The gene pool of *Sorghum bicolor* and its improvement. In *Genomics of the Saccharinae* (Ed. A.H. Paterson), pp 23-41. Springer, New York.

Kliebenstein DJ, Rowe HC. 2008. Ecological costs of biotrophic versus necrotrophic pathogen resistance, the hypersensitive response and signal transduction. *Plant Science* 174: 551-556.

Kojima H, Urano Y, Kikuchi K, Higuchi T, Hirata Y, Nagano T. 1999. Fluorescent indicators for imaging nitric oxide production. *Angewandte Chemie International Edition* 38: 3209-3212.

Koppenol WH, Moreno JJ, Pryor WA, Ischiropoulos H, Beckman JS. 1992. Peroxynitrite, a cloaked oxidant formed by nitric oxide and superoxide. *Chemical Research in Toxicology* 5: 834-842.

Kużniak E, Skłodowska M. 2005. Fungal pathogen-induced changes in the antioxidant systems of leaf peroxisomes from infected tomato plants. *Planta* 222: 192-200.

Mayék-Pérez N, Lopéz-Castañeda C, López-Salinas E, Cumpián-Gutiérrez J, Acosta-Gallegos JA. 2001. *Macrophomina phaseolina* resistance in common bean under field conditions in Mexico. *Agrociencia* 46: 649-661.

Mittler R. 2000. Oxidative stress, antioxidants and stress tolerance. *Trends in Plant Science* 7: 405-410.

Moller IM. 2001. Plant mitochondria and oxidative stress: Electron transport, NADPH turnover, and metabolism of reactive oxygen species. *Annual Review of Plant Physiology and Plant Molecular Biology* 52: 561-591.

Murphy MP. 1999. Nitric oxide and cell death. *Biochimica et Biophysica Acta (BBA)-Bioenergetics* 1411: 401-414.

Nebert DW, Roe AL, Dieter MZ, Solis WA, Yang Y, Dalton TP. 2000. Role of the aromatic hydrocarbon receptor and [*Ah*] gene battery in the oxidative stress response, cell cycle control, and apoptosis. *Biochemical Pharmacology* 59: 65-85.

Perchepied L, Balagué C, Riou C, Claudel-Renard C, Rivière N, Grezes-Besset B, Roby D. 2010. Nitric oxide participates in the complex Interplay of defense-related signaling pathways controlling disease resistance to *Sclerotinia sclerotiorum* in *Arabidopsis thaliana*. *Molecular Plant-Microbe Interactions* 23: 846-860.

Planchet E, Kaiser WM. 2006. Nitric oxide production in plants: facts and fictions. *Plant Signaling & Behavior* 1: 46-51.

Raguchander T, Samiyappan R, Arjunan G. 1993. Biocontrol of *Macrophomina* root rot of mungbean. *Indian Phytopathology* 46: 379-382.

Rosenow D, Quisenberry J, Wendt C, Clark L. 1983. Drought tolerant sorghum and cotton germplasm. *Agricultural Water Management* 7: 207-222.

Sagi M, Fluhr R. 2006. Production of reactive oxygen species by plant NADPH oxidases. *Plant physiology* 141: 336-340.

Sagi M, Fluhr R. 2001. Superoxide production by plant homologues of the gp91phox NADPH oxidase. Modulation of activity by calcium and by tobacco mosaic virus infection. *Plant Physiology* 126: 1281-1290.

Sarkar TS, Biswas P, Ghosh SK, Ghosh S. 2014. Nitric oxide production by necrotrophic pathogen *Macrophomina phaseolina* and the host plant in charcoal rot disease of jute: Complexity of the interplay between necrotroph–host plant interactions. *PloS One* 9: e107348.

Segmueller N, Kokkelink L, Giesbert S, Odinius D, van Kan J, Tudzynski P. 2008. NADPH Oxidases are involved in differentiation and pathogenicity in *Botrytis cinerea*. *Molecular Plant-Microbe Interactions* 21: 808-819

Sharma P, Jha AB, Dubey RS, Pessarakli M. 2012. Reactive oxygen species, oxidative damage, and antioxidative defense mechanism in plants under stressful conditions. *Journal of Botany* doi:10.1155/2012/217037.

Shetty NP, Jorgensen HJL, Jensen JD, Collinge DB, Shetty HS. 2008. Roles of reactive oxygen species in interactions between plants and pathogens. *European Journal of Plant Pathology* 121: 267-280.

Stone JK. 2001. Necrotrophs. *Encyclopedia of Plant Pathology* 2: 676-677.

Su G, Suh SO, Schneider RW, Russin JS. 2001. Host specialization in the charcoal rot fungus, *Macrophomina phaseolina*. *Phytopathology* 91: 120-126.

Tarr SAJ. 1962. Root and stalk diseases: Red stalk rot, Colletotrichum rot, anthracnose, and red leaf spot. In *Diseases of Sorghum, Sudan Grass and Brown Corn*, pp. 58-73. Commonwealth Mycological Institute, Kew, Surrey, UK.

Tesso T, Perumal R, Little CR, Adeyanju A, Radwan GL, Prom LK, Magill CW. 2012. Sorghum pathology and biotechnology-a fungal disease perspective: Part II. Anthracnose, stalk rot, and downy mildew. *European Journal of Plant Science and Biotechnology* 6: 31-44.

Torres MA, Dangl JL, Jones JDG. 2002. *Arabidopsis* gp91^{phox} homologues *AtrbohD* and *AtrbohF* are required for accumulation of reactive oxygen intermediates in the plant defense response. *Proceedings of the National Academy of Sciences USA* 99: 517-522.

Troy CM, Derossi D, Prochiantz A, Greene LA, Shelanski ML. 1996. Downregulation of Cu/Zn superoxide dismutase leads to cell death via the nitric oxide-peroxynitrite pathway. *Journal of Neuroscience* 16: 253-261.

Vanacker H, Carver TL, Foyer CH. 2000. Early H_2O_2 accumulation in mesophyll cells leads to induction of glutathione during the hyper-sensitive response in the barley-powdery mildew interaction. *Plant Physiology* 123: 1289-1300.

Vandelle E, Delledonne M. 2011. Peroxynitrite formation and function in plants. *Plant Science* 181: 534-539.

van Baarlen P, Staats M, van Kan JAL. 2004. Induction of programmed cell death in lily by the fungal pathogen *Botrytis elliptica*. *Molecular Plant Pathology* 5: 559-574.

van Kan JA. 2006. Licensed to kill: the lifestyle of a necrotrophic plant pathogen. *Trends in Plant Science* 11: 247-253.

Wimalasekera R, Tebartz F, Scherer GF. 2011. Polyamines, polyamine oxidases and nitric oxide in development, abiotic and biotic stresses. *Plant Science* 181: 593-603.

Wyllie TD. 1998. Soybean Diseases of the North Central Region. In *Charcoal rot of soybean-current status* (Eds T.D. Wyllie & D.H. Scott), pp. 106-113. American Phytopathological Society, St. Paul, MN, USA.

Yang SL, Chung KR. 2012. The NADPH oxidase-mediated production of hydrogen peroxide (H_2O_2) and resistance to oxidative stress in the necrotrophic pathogen *Alternaria alternata* of citrus. *Molecular Plant Pathology* 13: 900-914.

Yoshioka H, Mase K, Yoshioka M, Kobayashi M, Asai S. 2011. Regulatory mechanisms of nitric oxide and reactive oxygen species generation and their role in plant immunity. *Nitric Oxide* 25: 216-221.

TABLES AND FIGURES

Table 3.1. Significantly ($q < 0.05$) differentially expressed genes (related to host oxidative stress) between SC599 (charcoal-rot-resistant) and Tx7000 (charcoal-rot-susceptible) sorghum genotypes in response to *Macrophomina phaseolina* inoculation at 7 days post-inoculation.

Gene annotation	Metabolic pathway	Gene ID	Geno × Trt* q-value	SC599 (MP-CON)†		Tx7000 (MP-CON)	
				log2 DE‡	q-value	log2 DE	q-value
Cytochrome P450	Unknown	*Sb03g032210*	9.3E-12	1.29	0.1893	-6.03	5.4E-06
		Sb09g025490	4.1E-03	0.48	0.9194	-5.87	1.2E-06
		Sb06g015320	1.7E-04	1.70	0.2952	-5.17	3.0E-04
		Sb07g000550	7.1E-03	-	-	-4.82	1.6E-04
		Sb05g022010	3.8E-03	-	-	-4.58	2.6E-03
		Sb02g030640	2.1E-02	0.88	0.7566	-3.63	3.2E-02
		Sb03g003590	1.1E-03	0.65	0.7830	-3.42	9.5E-05
		Sb01g032440	5.6E-04	2.22	0.0601	-3.18	6.8E-02
		Sb04g000730	1.4E-04	0.42	0.8226	-2.91	7.9E-04
		Sb01g036360	2.1E-04	0.00	0.9992	-2.79	5.4E-10
		Sb2967s002010	9.2E-04	0.97	0.4544	-2.58	4.3E-05
		Sb06g025990	3.4E-06	0.64	0.3355	-2.39	3.6E-07
		Sb01g035170	1.8E-09	2.84	0.0001	-2.08	6.9E-09
		Sb06g030010	2.7E-06	0.91	0.1931	-1.58	1.8E-04
		Sb03g037380	1.9E-03	0.69	0.5468	-1.21	4.4E-05
		Sb09g021890	4.9E-02	1.06	0.2254	-0.22	5.9E-01
		Sb08g019430	3.0E-02	-0.44	0.8043	1.01	1.7E-02
		Sb01g007400	1.1E-02	-	-	1.74	4.6E-03
		Sb02g022600	2.1E-03	-0.80	0.5789	1.94	1.7E-04
		Sb03g042660	2.5E-05	-1.10	0.4289	1.98	4.2E-07
		Sb08g019480	1.1E-02	-0.22	0.9559	2.34	8.3E-05
		Sb03g002060	1.9E-02	0.49	0.7760	2.41	2.1E-07
		Sb01g031080	2.8E-05	-1.41	0.2741	2.65	2.8E-09
		Sb08g019470	4.6E-02	-	-	2.83	1.7E-02
		Sb03g040280	1.2E-02	-0.35	0.9368	2.94	7.9E-06
		Sb07g000520	3.4E-04	0.57	0.7335	3.53	3.9E-16

		Sb10g004820	3.8E-03	-	-	3.65	6.4E-05
		Sb02g043130	1.6E-04	0.12	0.9833	4.74	5.2E-15
		Sb01g007420	7.1E-09	-1.16	0.2596	4.96	5.6E-15
		Sb05g010360	7.6E-10	-1.45	0.2546	5.00	1.7E-30
		Sb05g010360	7.6E-10	-1.45	0.2546	5.00	1.7E-30
		Sb07g000510	1.1E-04	0.89	0.3230	5.46	2.2E-06
		Sb01g017160	6.1E-20	-2.51	0.0011	5.90	1.1E-32
		Sb10g024663	5.8E-16	-0.79	0.4097	6.43	5.0E-10
		Sb01g048030	4.9E-02	-	-	6.75	8.3E-08
		Sb07g008860	2.2E-05	-	-	7.15	2.2E-09
		Sb02g000220	2.1E-06	-2.03	0.1498	7.87	2.9E-64
		Sb07g008870	1.3E-03	-	-	8.27	2.2E-12
NADPH oxidase	Apoplastic superoxide generation	*Sb0621s002010*	6.4E-05	0.61	0.7974	-3.20	8.4E-29
NADH dehydrogenase 1 alpha subcomplex	Respiratory chain complex I	*Sb03g033415*	1.1E-04	-0.47	0.7917	2.14	3.6E-05
NADH dehydrogenase iron-sulfur protein 4		*Sb02g037780*	9.4E-03	-0.01	0.9979	0.97	1.8E-05
Amine oxidase	Unknown	*Sb01g044230*	1.4E-02	0.68	0.8358	-4.96	1.8E-03
		Sb06g032450	3.3E-03	-0.68	0.4749	0.92	1.2E-03
		Sb06g032460	1.3E-15	-1.58	0.0617	4.10	1.5E-58
		Sb07g005780	8.0E-04	-	-	-2.04	1.3E-03
Amine oxidase-related		*Sb01g006160*	1.1E-03	1.04	0.2741	-1.39	2.9E-03
Copper methylamine oxidase precursor		*Sb02g036990*	9.3E-12	2.52	0.0001	-3.71	1.1E-03
		Sb04g028410	2.8E-06	0.61	0.6758	-2.84	1.4E-12
		Sb06g020020	1.7E-20	-1.02	0.1013	3.33	6.1E-48
Nitric oxide synthase (NOS) (EC 1.14.13.39)	Citrulline-nitric oxide cycle	*Sb04g000530*	1.4E-02	0.42	0.7458	-0.82	1.1E-02
		Sb01g039180	1.0E-03	0.78	0.7386	-2.84	6.5E-04
		Sb05g000240	1.1E-02	-	-	-3.11	7.4E-02
		Sb07g024150	4.2E-02	-	-	-2.41	1.3E-01
		Sb10g002510	1.7E-04	0.67	0.3981	-1.01	1.4E-04
		Sb09g002030	3.7E-02	1.02	0.6437	-1.87	1.4E-02
Nitrite reductase (NO-forming) (EC 1.7.2.1)	Nitrate reduction I	*Sb08g011530*	2.1E-11	-1.37	0.4544	9.34	2.9E-76
		Sb04g027860	1.3E-02	-0.42	0.9108	7.48	2.1E-31
		Sb05g000680	3.0E-03	-	-	4.00	7.0E-05
		Sb03g039960	7.7E-05	-	-	5.66	1.0E-11
		Sb04g025630	4.3E-02	-0.49	0.4999	0.27	2.9E-01
NADH-cytochrome b5 reductase (EC 1.7.1.1)	Nitrate reduction II (assimilatory)	*Sb09g023850*	2.4E-03	-0.38	0.7270	1.04	7.2E-04
		Sb07g022750	2.9E-05	0.80	0.6184	-2.71	3.6E-27
		Sb07g026290	1.1E-02	0.64	0.4211	-0.75	4.2E-02

		Sb04g007060	1.4E-06	1.58	0.3029	-5.19	5.1E-18

* Geno × Trt = genotype by treatment interaction where treatment consists of *M. phaseolina* and control inoculations. †MP = *M. phaseolina,* CON = control. ‡ log2 DE = log2-fold differential expression.

Table 3.2. *P*-values of F-statistic from analysis of variance (ANOVA) for in vitro reactive oxygen/nitrogen species (ROS/RNS) and thiobarbituric acid reactive substances (TBARS) assays performed at 4, 7, and 10 days post-inoculation (DPI). Both assays were based on cell extracts isolated from charcoal-rot-resistant (SC599, SC35) and susceptible (Tx7000, BTx3042) sorghum genotypes after inoculation with *Macrophomina phaseolina* and phosphate-buffered saline (mock-inoculated control) ($\alpha = 0.05$).

DPI	Effect	Pr > F	
		ROS/RNS	TBARS
4	Genotype	0.0279	0.0024
	Treatment	0.0081	0.0436
	Genotype*Treatment	0.0044	0.0212
7	Genotype	< 0.0001	< 0.0001
	Treatment	0.0538	0.0197
	Genotype*Treatment	0.0145	0.0226
10	Genotype	< 0.0001	0.0007
	Treatment	0.0026	< 0.0001
	Genotype*Treatment	0.0009	0.0068

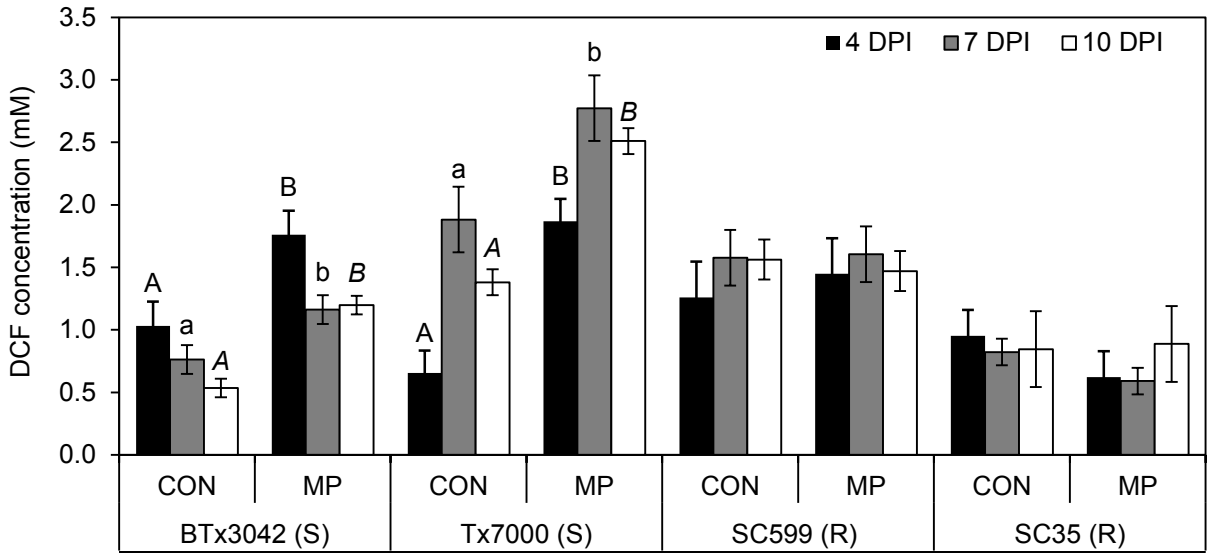

Figure 3.1. Comparison of the mean total free radical content (sum of the reactive oxygen and nitrogen species as measured by dichlorodihydrofluorescein (DCF) concentration) among two treatments (CON, MP) in charcoal-rot-susceptible (BTx3042, Tx7000) and resistant (SC599, SC35) genotypes at three post-inoculation stages (4, 7, and 10 days post-inoculation (DPI)). Treatment means followed by different letters within each genotype at a given DPI are significantly different. Treatment means without letter designations are not significantly different within each genotype at a given DPI at $\alpha = 0.05$. Error bars represent standard errors. CON = phosphate-buffered saline mock-inoculated control, MP = *Macrophomina phaseolina*-inoculated.

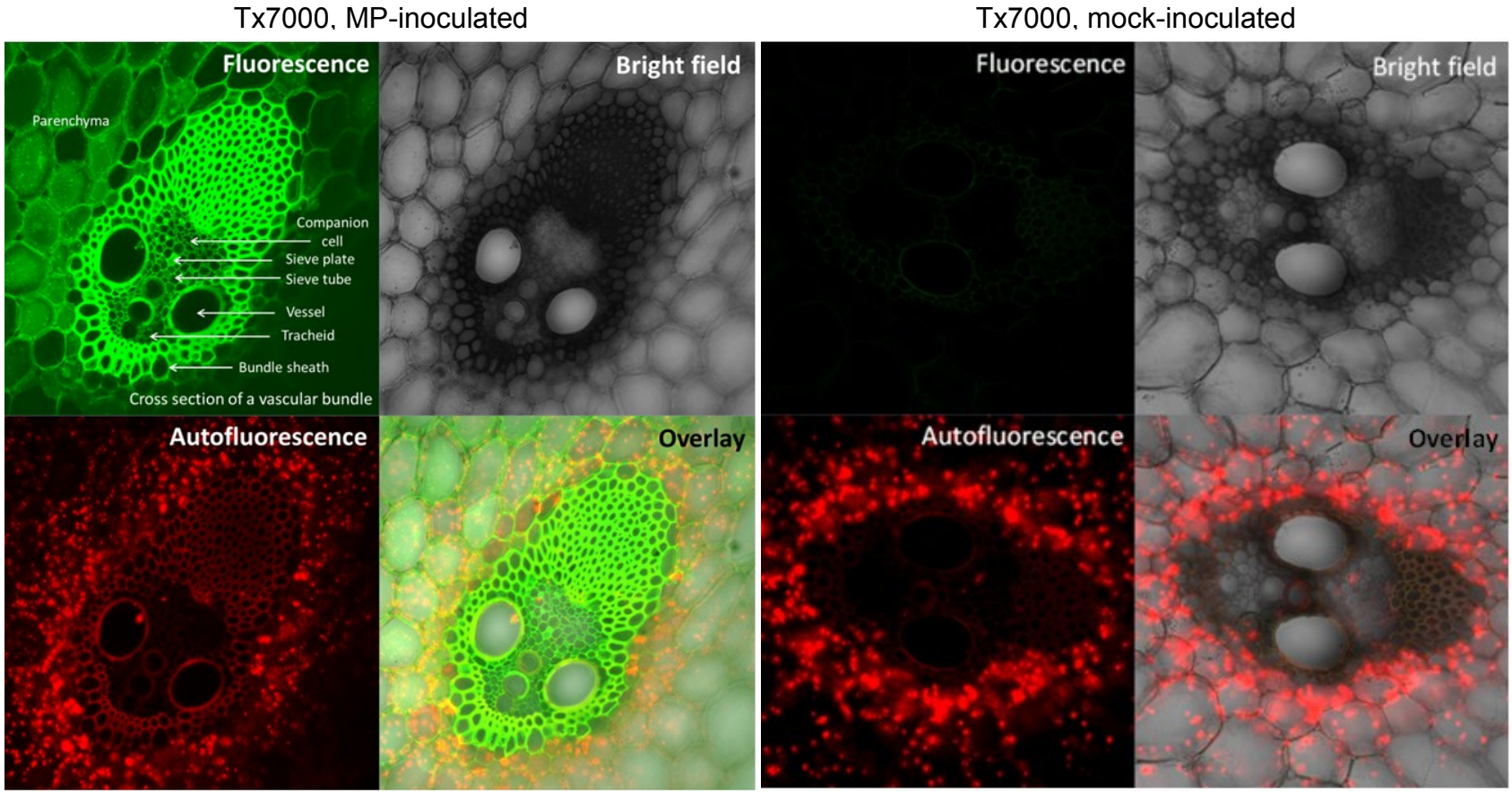

Figure 3.2. Detection of nitric oxide (NO) in sorghum stem tissues after staining with 4-amino-5-methylamino-2',7'-difluorofluorescein diacetate (DAF FM-DA) by confocal microscopy. Cross-section of a single vascular bundle of the charcoal rot-susceptible sorghum genotype, Tx7000, after receiving the *Macrophomina phaseolina* (left panel) and mock-inoculated control treatments (right panel) at 7 days post-inoculation. Stem cross-sections showing bright green fluorescence correspond to the detection of NO. Red color corresponds to chlorophyll autofluorescence (Magnification = 200X).

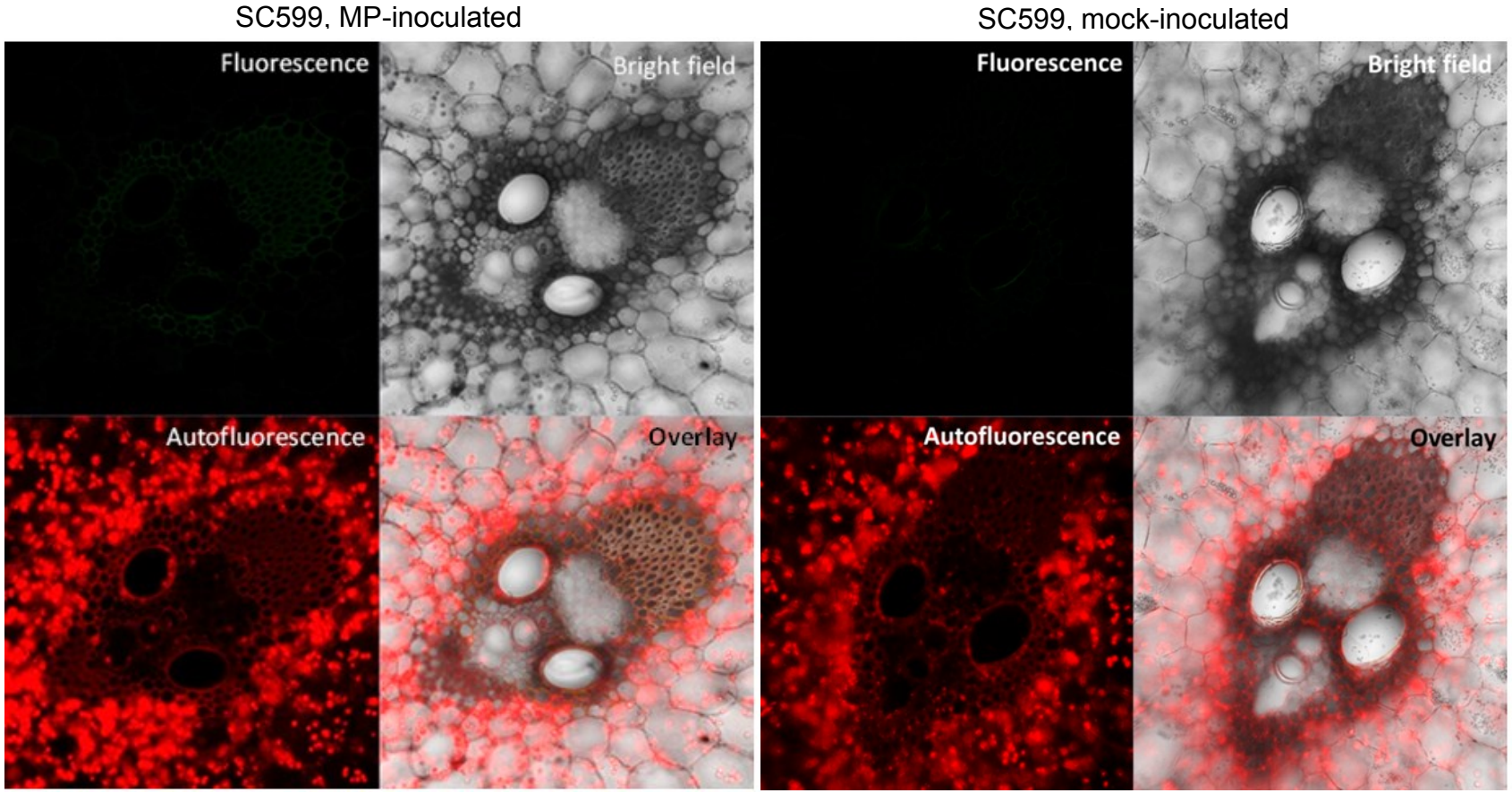

Figure 3.3. Detection of nitric oxide (NO) in sorghum stem tissues after staining with 4-amino-5-methylamino-2',7-difluorofluorescein diacetate (DAF FM-DA) by confocal microscopy. Cross-section of a single vascular bundle of the charcoal rot-resistant sorghum genotype, SC599, after receiving the *Macrophomina phaseolina* (left panel) and mock-inoculated control treatments (right panel) at 7 days post-inoculation. Lack of bright green in "fluorescence" and "overlay" micrographs indicates the absence of NO after both treatments. Red color corresponds to chlorophyll autofluorescence (Magnification = 200X).

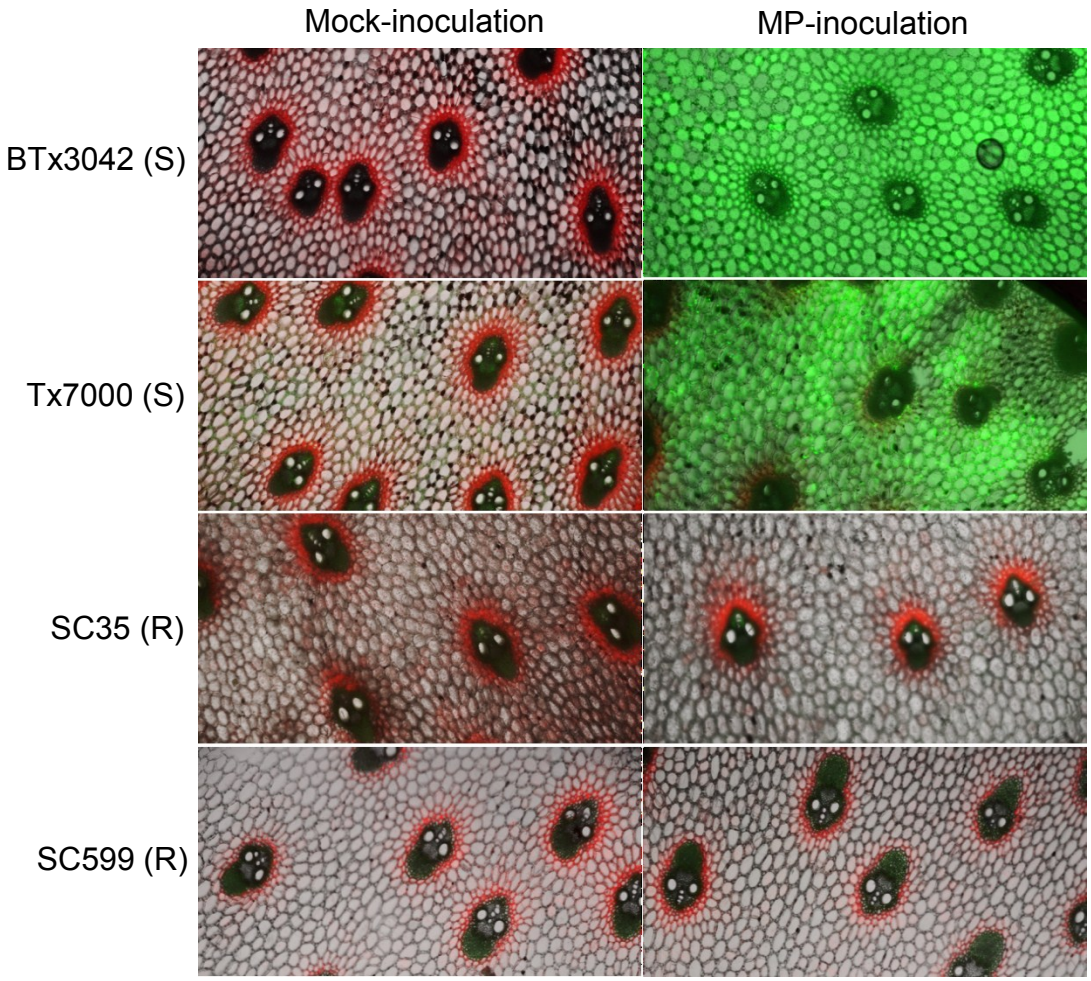

Figure 3.4. Detection of nitric oxide (NO) in sorghum stem tissues after staining with 4-amino-5-methylamino-2′,7′-difluorofluorescein diacetate (DAF FM-DA) by confocal microscopy. Cross-sections showing the vascular bundles and surrounding parenchyma (pith) cells of charcoal rot-susceptible (BTx3042, Tx7000) and -resistant (SC35, SC599) sorghum genotypes after receiving the *Macrophomina phaseolina* and mock-inoculated control treatments at 7 days post-inoculation. Stem cross-sections showing bright green fluorescence correspond to the detection of NO. Red color corresponds to chlorophyll autofluorescence (Magnification = 25X).

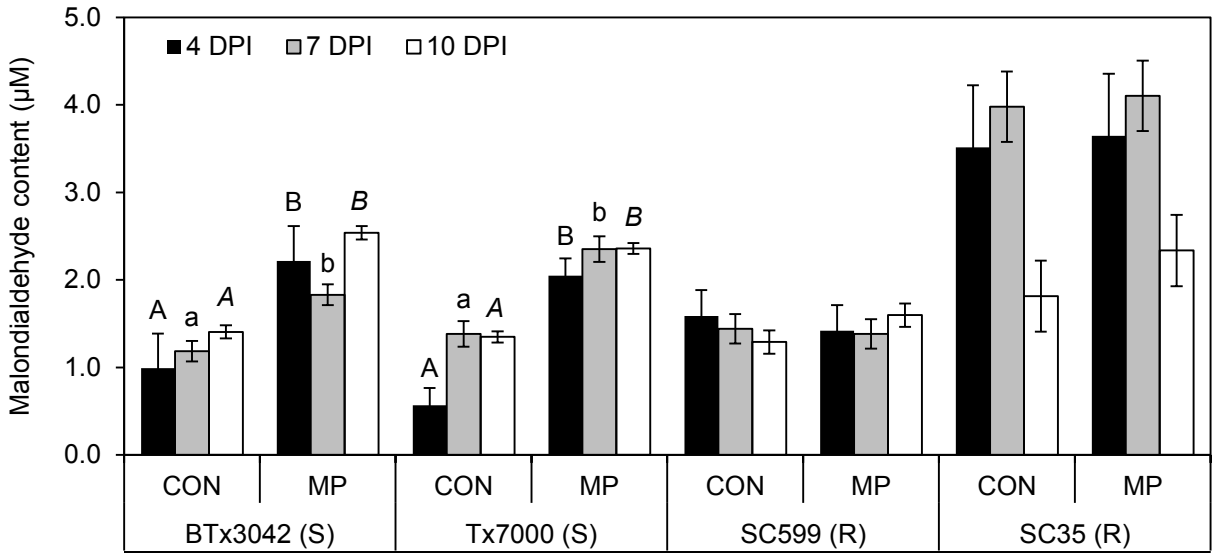

Figure 3.5. Comparison of the mean malondialdehyde content among two treatments (CON, MP) in charcoal rot-susceptible (BTx3042, Tx7000) and -resistant (SC599, SC35) genotypes at three post inoculation stages (4, 7, and 10 DPI). Treatment means followed by different letters within each genotype at a given DPI are significantly different. Treatments without letter designations are not significantly different within each genotype at a given DPI at $\alpha = 0.05$. Error bars represent standard errors. CON = phosphate-buffered saline mock-inoculated control, MP = *Macrophomina phaseolina*-inoculated.

Chapter 4 - Dynamics of the host antioxidant system in the *Sorghum-Macrophomina* interaction

ABSTRACT

The plant antioxidant system plays a crucial role in cellular detoxification processes and redox buffering. Genome wide transcriptome profiling was conducted through RNA sequencing to investigate the dynamics of the *Sorghum bicolor* (L.) Moench antioxidant system in response to *Macrophomina phaseolina* (MP) infection at 2, 7, and 30 days post-inoculation (DPI). The highest number of genes were found to be differentially expressed at 7 DPI. Compared to the mock-inoculated control treatment, MP significantly up-regulated the glutathione synthetase, glutamate cysteine ligase (involved in glutathione biosynthesis), glutathione s-transferase (GST), glutathione peroxidase (GPX), and glutathione reductase (GR) genes in a charcoal-rot-susceptible sorghum genotype (Tx7000), but not in a resistant genotype (SC599) at 7 DPI. Thirty genes with peroxidase activity were differentially expressed between SC599 and Tx7000 after *M. phaseolina* inoculation. Eleven of these were significantly down-regulated in Tx7000 while 14 were significantly up-regulated. To compliment the gene expression data, cell extracts were acquired from MP- and mock-inoculated resistant (SC599, SC35) and susceptible (Tx7000, BTx3042) sorghum stalks and their reduced (GSH) and oxidized glutathione (GSSG), and GST, GPX, GR, peroxidase activities were measured using standard protocols. A significantly reduced GSH/GSSG ratio was observed in Tx7000 and BTx3042 indicating the strong oxidative stress induced in charcoal-rot-susceptible genotypes under MP infection. MP significantly increased GST, GPX, GR, and peroxidase activities of Tx7000 and BTx3042. The importance of GSH in controlling the MP infection-associated oxidative stress was bolstered by the significantly reduced disease severity observed in Tx7000 and BTx3042 upon exogenous GSH application.

Keywords: sorghum, *Macrophomina phaseolina*, necrotrophic fungi, oxidative stress, antioxidant system, glutathione, glutathione s-transferase, glutathione peroxidase, glutathione reductase, catalase, superoxide dismutase, peroxidase

INTRODUCTION

Glutathione, the tripeptide γ-glutamyl-cysteinyl-glycine, plays a key role in detoxification and redox buffering processes in the cell (Noctor and Foyer, 1998). It is the most abundant form of organic sulphur in plants (Dixon et al., 1998). Reduced glutathione (GSH) is the most vital intracellular non-protein thiol compound and plays a major role in the protection of cell and tissue structures from oxidative injury (Foyer and Noctor 2005; Foyer and Noctor 2009; Foyer and Noctor 2011). Among others, such as vitamin C, vitamin E, plant polyphenols, and carotenoids, GSH is a key non-enzymatic antioxidant (Shahidi and Zhong, 2010). These non-enzymatic antioxidants neutralize reactive oxygen species (ROS) through a process known as radical scavenging (Nimse and Pal, 2015). Within cells, free glutathione is mainly present in its reduced form (GSH), which could be rapidly oxidized to glutathione disulfide (GSSG) under oxidative stress. Therefore, the GSH to GSSG ratio is an informative indicator of oxidative stress (Marí et al., 2009). Plants respond to pathogen attacks by varying the levels of GSH. For instance, an increase in GSH content has been reported in leaves attacked by avirulent biotrophic pathogens (Edwards et al., 1991; El-Zahaby et al., 1995; Vanacker et al., 1998) while a decrease has been reported in leaves attacked by some necrotrophic fungi (Gonnen and Schlösser, 1993; Kuzniak and Sklodowska, 1999). GSH is synthesized from amino acids by the sequential action of *g-glutamylcysteine synthetase* (*glutamate cysteine ligase*) and *glutathione synthetase* (Alscher and Hess, 1993). The de-novo synthesis of glutathione from its amino acid constituents is required for the elevation of glutathione as an adaptive response to oxidative stress (Nimse and Pal, 2015).

Glutathione S-transferase (GST) is an important antioxidant enzyme which catalyzes the conjugation of GSH to an electrophilic substrate (Edwards et al., 2000). Many secondary metabolites produced by plants are phytotoxic even to the cells that produce them, and therefore the appropriate cellular localization (usually the vacuole) is important (Matern et al., 1986; Sandermann, 1992; Sandermann, 1994) and the GSH/GST system plays a key role in phytotoxin compartmentalization. For example, anthocyanin pigments require GSH conjugation by GST for transport into the vacuole as inappropriate cytoplasmic retention of anthocyanins leads to cytotoxicity (Marrs et al., 1995). Moreover, the endogenous products of oxidative damage initiated by reactive oxygen species such as lipid peroxides (e.d. 4-hydroxyalkenals) and

oxidative DNA degradation products (e.g. base propanols) are cytotoxic. Plant and animal GSTs play a key role in conjugating GSH with such endogenously produced electrophiles, which results in their detoxification (Bartling et al., 1993; Berhane et al., 1994; Danielsonn et al., 1987). Previous findings showed that the transcription of plant GST genes is regulated by various abiotic (Edwards et al., 2000; Seppanen et al., 2000; Moons, 2003; Kiyosue et al., 1993; Bianchi et al., 2002) and biotic stresses such as pathogen attack (Mauch and Dudler, 1993; Liao et al, 2014).

Glutathione peroxidase is another major ROS scavenging enzyme in plants (Mittler et al., 2004). Expression of glutathione peroxidase has been found to be highly up-regulated in response to pathogen infection (Agrawal et al., 2002; Levine et al., 1994). Using reduced glutathione (GSH) as an electron donor, it catalyzes the reduction of H_2O_2 or organic hydroperoxides to water or corresponding alcohols while GSH is oxidized into glutathione disulfide (GSSG) (Margis et al., 2008). GSSG is reduced back to GSH by glutathione reductase in an NADPH-dependent manner (Meloni et al., 2003; Huber et al., 2008). Glutathione reductase secreted by *Magnaporthe oryzae* has been shown to be required for neutralizing plant generated ROS during the rice blast disease (Fernandez and Wilson, 2014).

Activation of peroxidase (PX), catalase (CAT), and superoxide dismutase (SOD) in response to various pathogens and its contribution to enhanced disease resistance is well documented (Malencic et al., 2010; Kiprovski et al., 2012; Debona et al., 2012; Fortunato et al., 2015). PX and CAT are important antioxidant enzymes involved in decomposing hydrogen peroxide to water (Hammond-Kosack & Jones, 1996). CAT is an important H_2O_2-scavenging enzyme in plants (Willekens et al., 1997) and has one of the highest turnover rates of all enzymes. One molecule of catalase can convert six million molecules of H_2O_2 to H_2O and O_2 per minute (Gill & Tuteja, 2010). SOD is involved in regulating the superoxide anions. It converts superoxide anions to hydrogen peroxide, which can be subsequently detoxified into water through PX and CAT activity (Hammond-Kosack & Jones, 1996).

The soilborne necrotrophic fungus, *Macrophomina phaseolina* is an important phytopathogen which causes diseases in over 500 different plant species (Islam et al., 2012). It causes charcoal

rot disease in many economically important crops such as sorghum, soybean, maize, alfalfa and jute (Islam et al., 2012). Charcoal rot is a major fungal disease in sorghum [*Sorghum bicolor* (L.) Moench], causing tremendous crop losses whereever sorghum is grown (Tarr, 1962, Tesso *et al*., 2012). In Chapter 3, the ability of *M. phaseolina* to induce charcoal rot disease susceptibility in sorghum through invoked host oxidative stress was examined. In this context, the potential role of host glutathione and its related enzymes are worthy of study to uncover the relationship between enhanced host oxidative stress and glutathione dynamics. Therefore, the objectives of the current study were (i) to make use of the RNA-Seq data (outlined in Chapter 2) to investigate differentially expressed glutathione related genes and other antioxidant encoding genes between charcoal-rot-resistant and susceptible sorghum genotypes in response to *M. phaseolina* inoculation and (ii) to uncover the potential links between glutathione (and related enzymes) and the charcoal rot disease reaction at the transcriptional and biochemical levels.

MATERIALS AND METHODS

Plant materials

A different set of plants with the same treatment and design structure (mentioned in the Chapter 3) were used to obtain stalk tissues for the functional investigations outlined in the current Chapter.

Preparation of tissue lysates for functional assays and absorbance/fluorescence measurement

Stalk tissues were retrieved from -80°C storage and approximately 1 g of stalk tissues (1 cm away from the symptomatic region) was quickly chopped in to liquid nitrogen (in a mortar) using a sterile scalpel. The stalk pieces were ground into a powder using a pestle. Approximately 200 mg of this tissue powder was transferred into microcentrifuge tubes filled with 1 ml of potassium phosphate buffer (50 mM potassium phosphate (pH 6.8), 0.1 mM ethylenediaminetetraacetic (EDTA), 1 mM phenylmethylsulfonyl fluoride, and 2% (wt/vol) polyvinylpolypyrrolidone (PVPP); used for all glutathione related assays), 1 ml of 1X PBS with 1mM EDTA (for catalase and peroxidase assays), and 1 ml of 1X Lysis buffer (10 mM Tris, pH 7.5, 150 mM NaCl, 0.1

mM EDTA; for superoxide dismutase assay). Buffer selections were based on the instructions by assay kit manufacturers. Samples were centrifuged at 10000 g for 10 min at 4°C. Supernatants were transferred into new microcentrifuge tubes and immediately stored at -80°C until used in assays. All absorption/fluorescence measurements were performed using a 96-well plate reader (Synergy H1 Hybrid Reader, BioTek, Winooski, VT, USA) at specified wavelengths (see below). Path length correction was performed using an option available in the plate reader during the measurements. All functional experiments were repeated twice.

Quantification of total, oxidized, and reduced glutathione

The EnzyChrom™ GSH/GSSG Assay Kit (BioAssay Systems, Hayward, CA, USA) was used to quantify the total, oxidized, and reduced glutathione concentrations of the samples. The assay is based on an enzymatic method that utilizes Ellman's Reagent (DTNB) and glutathione reductase (GR). DTNB reacts with glutathione to form a yellow product. The rate of change in the optical density, measured at 412 nm, is directly proportional to glutathione concentration in the sample. In the current study, the total glutathione concentration (reduced + oxidized) was determined following the protocol described by the manufacturer with some modifications. Briefly, 10µL of each sample was diluted in 90 µL 1X Assay Buffer and transferred to a Nunc™ 96-Well Polypropylene MicroWell™ Plate (Thermo Scientific Nunc, Roskilde, Denmark). The standards were prepared according to the manufacturer's instructions. A master mix of the working reagent (WR), sufficient for all samples and standards, was prepared (105 µL 1X assay buffer, 1 µL GR enzyme, 0.25 µL NADPH and 0.5 µL DTNB per reaction). Fifty µL of WR was immediately added to each standard and sample and was well mixed. The optical density (OD) was read at 412 nm at 0 min and again at 10 min. OD_{0min} was subtracted from OD_{10min} for each standard and sample. Then, the ΔOD_{BLANK} (1X assay buffer) was subtracted from ΔOD values of all standards and the ΔΔOD's were plotted against standard concentrations. The slope was determined using linear regression fitting and the total glutathione (GSH_{TOTAL}) concentrations of the samples were calculated using the following equation:

$$GSH_{TOTAL}\ (\mu M) = \frac{(\Delta OD_{SAMPLE} - \Delta OD_{BLANK})}{Slope} \times n$$

Where n = dilution factor

The same procedure explained above was used to determine the oxidized glutathione (GSSG) concentration. However, at the beginning, 45 µL from each sample was mixed with 5 µL of 1-methyl-2-vinylpyridinium triflate to scavenge GSH in the solution. From this solution, 10 µL was drawn and diluted in 90 µL 1X assay buffer to proceed further as described above. The GSSG concentrations of the samples were calculated using the following equation:

$$GSSG(\mu M) = 0.5 \times \frac{(\Delta OD_{S(GSSG)} - \Delta OD_{BLANK})}{Slope} \times n$$

Where, $\Delta OD_{S(GSSG)}$ = sample treated with scavenger, and n = dilution factor

The reduced glutathione (GSH) concentrations of the samples were determined using the following equation:

$$GSH(\mu M) = [GSH_{TOTAL}] - 2 \times [GSSG]$$

Quantification of glutathione S-transferase (GST) activity

Glutathione S-Transferase (GST) Assay Kit (SIGMA, Saint Louis, MO, USA) was used to quantify the GST activity of samples. This assay kit utilizes 1-chloro-2,4-dinitrobenzene (CDNB) as the GSH conjugant. Upon GST-mediated conjugation of CDNB with the thiol group of GSH, there is an increase in the absorbance at 340 nm. Therefore, absorbance is directly proportional to GST-specific activity. In the current study, following the manufacturer's instructions, a master mix containing Dulbecco's phosphate buffered saline (19.6 mL), 200 mM L-glutathione reduced (0.2 mL), and 100 mM CDNB (0.2 mL) (sufficient for all samples) was prepared. Twenty µL of each sample was transferred to a Nunc™ 96-Well Polypropylene MicroWell™ Plate (Thermo Scientific Nunc, Roskilde, Denmark) and mixed with 180 µL of master mix. Two-hundred µL of the master mix was used as the blank. Optical density (OD) was read at 340 nm at 0 min and again at 10 min. The change in optical density (ΔOD_{340})/minute was

calculated in the linear range of the plot for each sample and for the blank using the following equation:

$$(\Delta OD340)/\min = \frac{OD340(10\,\min - 0\min)}{10\,\min}$$

The (ΔOD_{340})/minute of the blank was subtracted from the (ΔOD_{340})/minute of the sample. This rate was used to calculate the GST-specific activity using the following equation.

$$\text{GST specific activity } (\mu mol/ml/min) = \frac{(\Delta OD_{340})/min \times V\,(ml) \times n}{\varepsilon mM \times V_{enz}\,(ml)}$$

Where, n = dilution factor, εmM = extinction coefficient for CDNB conjugate at 340 nm (5.3 mM^{-1} cm^{-1}), V = reaction volume (200 µL), V_{enz} = the volume of the enzyme sample tested (20 µL).

Quantification of glutathione peroxidase (GPx) activity

The EnzyChrom™ Glutathione Peroxidase Assay Kit (EGPX-100) (BioAssay Systems, Hayward, CA, USA) was used to quantify the glutathione peroxidase activity of the samples. This assay directly measures NADPH consumption in the enzyme coupled reactions. The reduction in optical density at 340 nm is directly proportional to the enzyme activity in the sample. In the current study, following the manufacturer's instructions, 10 µL of each standards or samples was transferred into wells of a Nunc™ 96-Well Polypropylene MicroWell™ Plate (Thermo Scientific Nunc, Roskilde, Denmark). 190 µL assay buffer was added to all standard wells. 90 µL working reagent (containing 90 µL assay buffer, 5 µL glutathione, 3 µL 35 mM NADPH and 2 µL GR enzyme per well) was quickly added to the sample/control wells and mixed briefly yet thoroughly. 100 µL of 1× substrate solution was added to all sample and control wells. Tap contents were thoroughly mixed and the optical density was immediately read at 340 nm at 0 min (OD0) and again at 4 min (OD4). OD values at 4 min were used for NADPH standards. The blank value was subtracted from the standard values and resulting ΔODs were plotted against standard concentrations to determine the slope of the standard curve. The ΔOD_S = (OD0 – OD4) for the samples and ΔOD_B = (OD0 – OD4) for the background control were

determined. Finally, the GPx activity of each sample was computed using the following equation. A unit is defined as the amount of GPx that produces 1 mmole of GS-SG per min at pH 7.6 and room temperature.

$$\text{GPx activity(U/L)} = \frac{\Delta OD_S - \Delta OD_B}{\text{slope}(mM^{-1}) \times 4(\text{min})} \times n$$

Where, n is the sample dilution factor.

Quantification of glutathione reductase (GR) activity

The EnzyChrom™ Glutathione Reductase Kit (ECGR-100) (BioAssay Systems, Hayward, CA, USA) was used to quantify the glutathione reductase activity of the samples. This assay utilizes Ellman's method in which DTNB reacts with the GSH generated from the reduction of GSSG by the GR in a sample to form a yellow product (TNB^{2-}). The rate of change in optical density, measured at 412 nm, is directly proportional to GR activity in the sample. In the current study, following manufacturer's instruction, 20 µL from each sample, 100 µL of calibrator and 100 µL assay buffer were transferred to separate wells in a Nunc™ 96-well polypropylene MicroWell™ plate (Thermo Scientific Nunc, Roskilde, Denmark). Eighty µL of working reagent (containing 8 µL substrate, 8 µL co-substrate, 1 µL GDH, 0.5 µL DTNB and 70 µL assay buffer per well) was added to each sample well and mixed. The plate was incubated at 25°C for 10 min and the optical density was read at 412 nm at 10 min and again at 30 min. OD10 was subtracted from OD30 for each sample to compute the ΔOD_S. GR activity was calculated using the equation below. A Unit (U) of GR is the defined as the amount of GR that will catalyze the conversion of 1 µmole of GSSG to 2 µmole GSH per min at pH 7.6.

$$\text{GR activity (U/L)} = \frac{440}{\text{t (min)}} \times \frac{\Delta ODs}{(OD_{CAL} - OD_{Buffer})} \times n$$

Where, OD_{CAL} and OD_{Buffer} are OD412 nm (OD0) values of the calibrator and assay buffer; and t is the reaction time (20 min), and n is the dilution factor.

Quantification of peroxidase (PX) activity

The Amplex Red Hydrogen Peroxide/Peroxidase Assay Kit (Molecular Probes, Eugene, OR, USA) was used for peroxidase activity determination. In the presence of peroxidase, the Amplex Red reagent reacts with H_2O_2 in a 1:1 stoichiometry to produce the red-fluorescent oxidation product, resorufin. In the current study, 50 µL of the sample was diluted in a microcentrifuge tube by adding 200 µL of 1X reaction buffer. Fifty µL from each diluted sample was transferred to a black 96-well microplate. Then 50 µL of the Amplex Red reagent/H_2O_2 working solution (100 µM Amplex Red reagent containing 2 mM H_2O_2) was added. The microplate was covered with aluminum foil to protect from light and was incubated at room temperature for 30 minutes. Fluorescence was read at 545 nm excitation and 590 nm detection. Blanks included every component mentioned above except peroxidase sample (instead peroxidase, 50 µL 1X reaction Buffer was added). For each point, the value derived from the control was subtracted. A horseradish peroxidase (HRP) standard curve was prepared by following the protocol described by assay kit manufacturer. The peroxidase activity of samples was determined using the HRP standard curve and expressed as mili-units of peroxidase per mL per 200 mg of fresh stalk tissue where 1 unit (U) is defined as the amount of enzyme that will form 1.0 mg purpurogallin from pyrogallol in 20 seconds at pH 6.0 and 20°C.

Quantification of catalase (CAT) activity

CAT activity was determined using the OxiSelect Catalase Activity Assay Kit (Cell Biolabs, San Diego, CA, USA). This assay involves two reactions. The first reaction is the catalase induced decomposition of externally introduced H_2O_2 (with known concentration) into water and oxygen. The rate of this decomposition is proportional to the catalase concentration in the sample. In the presence of horseradish peroxidase (HRP) catalyst, the remaining hydrogen peroxide in the reaction mixture facilitates the coupling reaction of the two chromagens used in the assay, forming quinoneimine dye. Absorption of this dye is measured at 520 nm. The absorption is proportional to the amount of hydrogen peroxide remaining in the reaction mixture, which is indicative of the original catalase activity of the sample. In the current study, 20 µL of the sample was transferred to a clear 96-well microtiter plate. Fifty µL of hydrogen peroxide working solution (12 mM) was added to each well, thoroughly mixed and incubated for 1 minute. The

reaction was stopped by adding 50 µL of the catalase quencher into each well and mixed. Five µL of each reaction well was transferred to a new 96-well microtiter plate. Two hundred-fifty µL of chromogenic working solution was added to each well. The plate was incubated for 1 hour with vigorous mixing on a shaker (140 rotations per min). Absorbance was measured at 520 nm. A catalase standard curve was prepared by following the protocol described by assay kit manufacturer. The catalase activity of the samples was determined using the standard curve and expressed as units of catalase per mL per 200 mg of fresh stalk tissue where 1 unit (U) is defined as the amount of enzyme that will decompose 1.0 µmole of H_2O_2 per minute at pH 7.0 and 25°C.

Quantification of superoxide dismutase (SOD) activity

The OxiSelect Superoxide Dismutase Activity Assay kit (Cell Biolabs, San Diego, CA, USA) was used to quantify SOD activity. This assay uses a xanthine/xanthine oxidase (XOD) system to generate superoxide anions. The chromagen included in this assay produces a water-soluble formazan dye upon reduction by superoxide anions and the activity of SOD is computed as the inhibition of chromagen reduction. Therefore, in the presence of SOD, superoxide anion concentrations are reduced, resulting a weak colorimetric signal. In the current study, 20 µL from each sample was transferred to a 96-well microtiter plate. Five µL xanthine solution (1X), 5 µL chromagen solution, 10 µL SOD assay buffer (10X), and 50 µL distilled water were added to each well. Finally, 10 µL of xanthine oxidase solution (1X) was added to each well and mixed well. Blank tests included every components mentioned above except 20 µL of 1X lysis buffer instead SOD sample. After a 1 hour of incubation at 37ºC, absorbance was read at 490 nm. SOD activity was computed using formula below:

$$\text{SOD activity (\% inhibition)} = [(OD_{blank} - OD_{sample}) \div OD_{blank}] \times 100$$

Assessment of the impact of exogenous glutathione application on charcoal rot disease severity

Establishment and maintenance of plants

A greenhouse experiment was conducted with two charcoal-rot-resistant (SC599, SC35) and two susceptible (Tx7000, BTx3042) sorghum lines. The experiment was arranged in randomized

complete block design (RCBD) with three blocks. The seeds treated with captan (N-trychloromethyl thio-4-cyclohexane-1,2 dicarboxamide) were planted in 19 L Poly Tainer pots filled with Metro-Mix 360 growing medium (Sun Gro Bellevue, WA, U.S.A) and kept in a greenhouse at 25-32°C with a 16-h light/8-h dark photoperiod. Two weeks after seedling emergence, each pot was thinned to three seedlings. There were three pots per genotype per block and pots were randomly assigned for three inoculation treatments (pathogen, pathogen + glutathione, and mock-inoculated control), respectively. The treatment structure was a 4 × 3 factorial where factors consisted of four sorghum genotypes and three inoculation treatments. The three plants in each pot were considered as sub sample units and their averages were used for final data analysis. The experiment was repeated twice.

Inoculum preparation, inoculation, glutathione application, and measurement of disease severity

Inoculum preparation and inoculation were performed as described under RNASeq experiment (see Chapter 2). A 10 mM L-GSH (reduced glutathione) (SIGMA, Saint Louis, MO, USA) solution was prepared by dissolving glutathione in sterile distilled water. At 5 and 10 days post inoculation (DPI), 0.1 mL of glutathione solution was injected into 3 plants in each pot assigned for pathogen + glutathione treatment using the same point as for inoculations. Plants in pots that were assigned for pathogen and mock inoculation treatments were injected with 0.1 mL of sterile distilled water at same days (5 and 10 DPI). All plants were harvested at 35 d after initial inoculation. Stems were split longitudinally to measure the disease severity, lesion length (cm).

Statistical analysis of functional and disease severity data

Data were analyzed for variance (ANOVA) using the PROC GLIMMIX procedure of SAS software version 9.2 (SAS Institute, 2008). Variance components for fixed factors were estimated using restricted maximum likelihood (REML) method. The genotype and inoculation treatment were considered fixed while repeated experiments and block were treated as random. Studentized residual plots and Q-Q plots were used to test the assumptions of identical and independent distribution of residuals and their normality, respectively. Whenever heteroskedasticity was observed, appropriate heterogeneous variance models were fitted to meet the model assumptions by specifying a random/group statement (group = genotype or

inoculation treatment) following the model statement. Bayesian information criterion (BIC) was used to determine the most parsimonious model. Means separations were carried out using the PROC GLMMIX procedure of SAS. Main effects of factors were determined with adjustments for multiple comparisons using the Tukey-Kramer test. Whenever the genotype × treatment interaction was statistically significant, the simple effects of inoculation treatment were determined at each genotype level.

RESULTS

Differential expression of genes related to the sorghum antioxidant system in response to *M. phaseolina* infection

Table 4.1 provides a summary of the differentially expressed genes between two sorghum genotypes after *M. phaseolina* inoculation that are related to metabolism of host glutathione and its related enzymes. Differential gene expression analysis revealed eleven and 53 glutathione-related genes that are differentially expressed between SC599 and Tx7000 in response to pathogen inoculation at 2 and 7 DPI, respectively. None of the glutathione-related genes were differentially expressed at 30 DPI. Out of eleven differentially expressed genes at 2 DPI, eight encoded GST, two encoded glutaredoxin while the remaining gene encoded GPx. There was a net GST up-regulation (log2 fold = 4.16) in Tx7000 after pathogen inoculation. Both glutaredoxin genes were significantly down-regulated in SC599 (net log2 fold = -2.18) while one of them was significantly up-regulated in Tx7000 (net log2 fold = 1.27). The GPx gene was significantly upregulated in SC599 while that of Tx7000 did not change. Out of 53 glutathione-related differentially expressed genes at 7 DPI, 42 encoded GST, six GPx, one each for glutathione synthetase and glutamate cysteine ligase, and two each for GR and glutaredoxin. Out of the 42 GST genes, 32 were significantly up-regulated in pathogen-inoculated Tx7000 while six were significantly down-regulated. The majority (except three genes) of these genes in SC599 were not significantly differentially expressed. The net log2 fold up-regulation of GST genes in pathogen-inoculated Tx7000 was 120 while the net log2 fold down-regulation of GST genes in pathogen-inoculated SC599 was 11.6. Out of five GPx genes, four were significantly up-regulated in pathogen-inoculated Tx7000 while one was significantly down-regulated. The

net log_2 fold up-regulation was 9. None of these genes were significantly differentially expressed in SC599. Both glutathione synthetase and glutamate cysteine ligase genes were significantly up-regulated in pathogen-inoculated Tx7000 while those of SC599 were non-significantly down-regulated. The two GR genes were significantly up-regulated in pathogen-inoculated Tx7000 (net log2 fold = 4.5) while the two glutaredoxin genes were significantly down-regulated (net log2 fold = 4.6). None of these four genes were significantly differentially expressed in SC599 after pathogen inoculation.

Eleven and 30 genes with peroxidase activity were significantly differentially expressed between SC599 and Tx7000 in response to *M. phaseolina* inoculation at 2 and 7 DPI, respectively, while none of the peroxidase-encoding genes was differentially expressed at 30 DPI. Out of eleven differentially expressed genes at 2 DPI, four were significantly down-regulated (compared to control) in SC599 while one was significantly up-regulated, resulting in a 5.5 net log2 fold down-regulation. On the other hand, out of those eleven genes in Tx7000, two were significantly down-regulated while five were up-regulated, resulting a 7.5 net log2 fold up-regulation. Out of 30 differentially expressed genes at 7 DPI, eleven were significantly down-regulated in Tx7000 while fourteen were significantly up-regulated, resulting in a 13.3 net log2 fold up-regulation. None of those 30 genes were significantly differentially expressed in SC599. At 7 DPI, a gene encodes for catalase (*Sb01g048280*) was significantly down regulated (log2 fold = -3.23) in Tx7000 while another gene (*Sb07g023950*) responsible for superoxide dismutase was differentially expressed between genotypes due to pathogen infection. None of the catalase or superoxide dismutase encoding genes were differentially expressed at 2 or 30 DPI.

Analysis of variance (ANOVA) for functional assays and disease severity experiment

Table 4.2 provides the F-statistic *P*-values from the analysis of variance (ANOVA) for the functional assays conducted in the current study. Although the treatment (*M. phaseolina*- and mock-inoculated control) had a significant main effect on total, oxidized, and reduced glutathione concentration and GPx activity at 4 DPI, treatment effect was genotype-specific for said response variables at 7 and 10 DPI. Treatment did not have a significant main or simple effect on the reduced to oxidized glutathione ratio and GR activity at 4 DPI. However, the genotype by treatment interaction was significant on reduced to oxidized glutathione ratio and

GR activity at 7 and 10 DPI. The genotype-by-treatment interaction was significant on GST activity at all post inoculation stages. The genotype-by-treatment interaction was also significant for lesion length (P = 0.0089). The two-way interaction between genotype and inoculation treatment was significant for PX and CAT assays at all three post-inoculation stages (4, 7, and 10 DPI). SOD activity was an exception where genotype had a significant main effect at 4 DPI while both genotype and inoculation treatment had significant main effects at 7 and 10 DPI.

Sorghum glutathione dynamics after *M. phaseolina* inoculation

Compared to control, *M. phaseolina* significantly increased the total (49%, P = 0.0011), oxidized (50%, P = 0.0002), and reduced (48%, P = 0.0424) glutathione concentrations across genotypes at 4 DPI (Figure 4.1.A, C, and E). Although pathogen inoculation significantly reduced the total, oxidized, and reduced glutathione concentration of Tx7000 (40%, P < 0.0001; 27.7%, P < 0.0001; 58.1%, P < 0.0001, respectively) and BTx3042 (43%, P < 0.0001; 12.7%, P = 0.0471; 81.6%, P < 0.0001, respectively) at 7 DPI, inoculation did not significantly affect those in two resistant genotypes, SC599 and SC35 (Figure 4.1.B, D, and F). Interestingly, compared to control, pathogen inoculation significantly increased the total and oxidized glutathione concentration of Tx7000 (161%, P < 0.0001; 234%, P < 0.0001, respectively) and BTx3042 (192%, P < 0.0001; 294%, P < 0.0001, respectively) at 10 DPI, although inoculation did not significantly affect the total and oxidized glutathione concentration in SC599 and SC35 (Figure 4.1.B). Pathogen inoculation significantly decreased reduced glutathione concentration of Tx7000 (36.4%, P < 0.0001) while significantly increasing it in BTx3042 (44.6%, P < 0.0001) at 10 DPI (Figure 4.1.F). Inoculation did not significantly affect the reduced glutathione concentration of two resistant genotypes (Figure 4.1.F). Although pathogen inoculation significantly decreased the reduced to oxidized glutathione ratio of Tx7000 (7 DPI: 41.4%, P < 0.0001; 10 DPI: 57.9%, P < 0.0001) and BTx3042 (7 DPI: 79.2%, P < 0.0001; 10 DPI: 64.6%, P < 0.0001) at 7 and 10 DPI, inoculation did not significantly affect the reduced to oxidized glutathione ratio in SC599 and SC35 (Figure 4.2).

Behavior of sorghum GST, GPx, and GR enzymes after *M. phaseolina* inoculation

Compared to control, at all post inoculation stages, *M. phaseolina* significantly increased the GST specific-activity (µmol/mL/min) of Tx7000 (4 DPI: 376.8%, P = 0.0002; 7 DPI: 233.8%, P

= 0.0008; 10 DPI: 223.3%, P = 0.0354) and BTx3042 (4 DPI: 55.3%, P = 0.0325; 7 DPI: 111.5%, P = 0.0469; 10 DPI: 164.2%, P = 0.0043) (Figure 4.3.A). However, pathogen inoculation did not significantly affect the GST-specific activity of two resistant genotypes at any post-inoculation stage. Compared to control, pathogen inoculation significantly increased GPx activity (U/L) across genotypes (66.2%, $P < 0.0001$) at 4 DPI (Figure 4.3.B). Although *M. phaseolina* significantly increased the GPx activity of Tx7000 (7 DPI: 42.5%, $P < 0.0001$; 10 DPI: 35.5%, $P = 0.011$) and BTx3042 (7 DPI: 65.3%, $P < 0.0001$; 10 DPI: 30.8%, $P = 0.0106$) at 7 and 10 DPI, pathogen inoculation did not significantly affect the GPx activity in two resistant genotypes (Figure 4.3.C). *M. phaseolina* inoculation did not significantly affect the GR activity of tested genotypes at 4 DPI (Figure 4.3.D). At 7 DPI, pathogen inoculation significantly increased the GR activity of Tx7000 (74.5%, P = 0.0363) and BTx3042 (43.2%, $P < 0.0001$). Interestingly, pathogen inoculation significantly reduced the GR activity of Tx7000 (45.4%, $P < 0.0001$) and BTx3042 (29.1%, $P < 0.0001$) at 10 DPI (Figure 4.3.E). Pathogen did not significantly affect the GR activity of two resistant genotypes at 7 and 10 DPI.

Behavior of sorghum PX, CAT, and SOD enzymes after *M. phaseolina* inoculation

M. phaseolina inoculation significantly increased PX activity (mU/mL) in both susceptible genotypes at all post-inoculation stages (Figure 4.4). PX activity was increased in BTx3042 by 36.9, 41.6, and 37.6% at 4, 7, and 10 DPI, respectively, while the same for Tx7000 were 89.0, 37.0, and 25.9%. *M. phaseolina* inoculation did not significantly affect the PX activity of the two resistant genotypes, SC599 and SC35. Although not significant, SC599 and SC35 had reduced PX activity in comparison to respective controls at three post-inoculation stages.

Compared to the respective controls, the CAT activity (U/mL) of the two resistant genotypes was significantly increased after *M. phaseolina* inoculation at three post-inoculation stages (Figure 4.5). The percent activity increment for SC599 was 50.8, 33.8, and 29.5 at 4, 7, and 10 DPI, respectively while the same for SC35 was 104.4, 55.5, and 97.8. SC599 exhibited a general trend of declining activity over time against both control and pathogen inoculations. Activity of SC35 followed an increasing and then decreasing trend over time for both inoculation treatments. Interestingly, *M. phaseolina* inoculation significantly decreased the CAT activity of BTx3042 (-

38.1%) and Tx7000 (-39.3%) at 7 DPI, although no significant impact was observed at 4 and 10 DPI.

In the current study, we did not find SOD activity to be sorghum genotype-specific. Although *M. phaseolina* inoculation did not significantly affect SOD activity at 4 DPI, it significantly decreased activity at 7 and 10 DPI across four genotypes (Figure 4.6.A). The percent reduction in SOD activity was 14.7 and 15.6 at 7 and 10 DPI, respectively. The SOD activity of the four genotypes was not significantly different among each other at 4 DPI across inoculation treatments (Figure 4.6.B). However, SOD activity in SC35 reduced over time and became significantly lower than BTx3042 and Tx7000 at 7 DPI. At 10 DPI, it had a significantly decreased activity than all other genotypes.

Exogenous GSH application reduce charcoal rot disease severity

Compared to the *M. phaseolina* treatment, the *M. phaseolina* + glutathione treatment significantly reduced the lesion length of both charcoal-rot-susceptible genotypes ($P < 0.016$) while glutathione application did not significantly affect the lesion length of the two resistant genotypes (Figure 4.7).

DISCUSSION

Glutathione plays a crucial role in protecting plants from numerous environmental stresses, including oxidative stress due to the generation of active oxygen species, xenobiotics, and some heavy metals (Xiang and Oliver, 1998). In the current study, most of the glutathione-related gene differential expression occurred at 7 DPI revealing the importance of pathogen mediated expression differences of said genes at 7 DPI. Gene expression data at 7 DPI revealed enhanced glutathione biosynthetic capacity; enhanced GST, GPx, and GR activity; and impeded glutaredoxin activity in the charcoal-rot-susceptible sorghum genotype, Tx7000, after *M. phaseolina* inoculation. An increase in the expression of GST and GPx has been identified in soybean cells adjacent to those undergoing the hypersensitive cell death induced by an avirulent phytopathogen (Levine et al., 1994).

In Chapter 3, evidence for enhanced reactive oxygen/nitrogen species biosynthesis in *M. phaseolina* inoculated charcoal-rot-susceptible sorghum genotypes such as Tx7000 and BTx3042 was shown. Glutathione is involved in quenching reactive oxygen (Foyer et al., 1994) and nitrogen (Airak et al., 2011) species. Therefore, enhanced glutathione expression helps to reduce the strong oxidative stress encountered by Tx7000 after pathogen inoculation. Figure 4.8 depicts the proposed cellular antioxidative mechanism of charcoal-rot-susceptible sorghum genotype, Tx7000 after *M. phaseolina* infection.

To understand the translational aspects of gene expression data in detail, we conducted all functional experiments at three post-inoculation stages (4, 7, and 10 DPI). Functional assays revealed significantly decreased total glutathione, GSSG, and GSH concentrations of two susceptible genotypes at 7 DPI upon pathogen inoculation. Reduced GSH content has previously been observed in tomato leaves infected with the necrotrophic fungus *Botrytis cinerea* (Kuzniak and Sklodowska, 1999) and in *Avena sativa* leaves inoculated with *Drechslera avenae* and *D. siccans* (Gonnen and Schlösser, 1993). Decrease in GSH impedes the host antioxidant capacity and can in turn promote host cell death that facilitates the spread of necrotrophic phytopathogens. GSH is synthesized (*de novo*) from amino acids by the sequential action of *g-glutamylcysteine synthetase* (*glutamate cysteine ligase*) and *glutathione synthetase* (Alscher and Hess, 1993) and the *de-novo* GSH synthesis is required for the elevation of GSH levels as an adaptive response to oxidative stress (Nimse and Pal, 2015). The transcriptional data of the current study suggested the enhanced *de novo* GSH biosynthetic capacity in Tx7000 due to up-regulation of *glutathione synthetase* and *glutamate cysteine ligase*. However, confirming the up-regulated GST and GPx gene expression in pathogen-inoculated Tx7000 at 7 DPI, the functional assays provided evidence for enhanced GST-specific activity and GPx activity in both susceptible genotypes (Tx7000, BTx3042), leading to a net decline in GSH. Despite the enhanced GPx activity, GSSG concentration of pathogen-inoculated susceptible genotypes at 7 DPI remained significantly lower mainly due to enhanced GR activity, which rapidly converts GSSG in to GSH. Therefore, the primary cause behind the decreased amounts of reduced GSH in the pathogen-inoculated susceptible genotypes appeared to be the enhanced GST-specific activity.

In plants, glutathione S-conjugates are either sequestered in the vacuole (Coleman et al., 1997; Wolf et al., 1996) or transferred to the apoplast, a process termed "storage excretion" (Sandermann, 1992; Martinoia et al., 1993; Sandermann, 1994). Therefore, GST activity results in irreversible GSH depletion leading to decreased levels of GSH if not to *de novo* GSH biosynthesis. Moreover, jasmonic acid is a potent expression stimulator for genes involved in GSH biosynthesis and recycling, which could possibly lead to boosted GSH levels (Xiang and Oliver, 1998). In Chapter 2, it was shown that some key genes involved in jasmonic acid biosynthetic pathway were strongly down-regulated in *M. phaseolina*-inoculated Tx7000 at 7 DPI. Therefore, it seems plausible that down-regulated jasmonic acid biosynthesis in charcoal-rot-susceptible sorghum genotypes after *M. phaseolina* inoculation contributes to decreased GSH recycling, which may limit the availability of GSH.

Interestingly, the pathogen-inoculated susceptible genotypes had significantly increased total glutathione and GSSG concentrations at 10 DPI. Enhanced GPx activity along with reduced GR activity contributes to increased GSSG concentration of pathogen-inoculated susceptible genotypes. Moreover, some GSTs can also function as GPx (Bartling et al., 1993; Cummins et al., 1999) which contributes to increased GSSG concentration. As the GST-specific activity of susceptible genotypes were significantly higher after pathogen inoculation, the observed increase in total glutathione of these genotypes becomes possible only when there is strongly enhanced *de-novo* glutathione biosynthesis. This could contribute to the significantly higher GSH concentration of BTx3042. However, the significantly decreased GSH concentration observed in pathogen-inoculated Tx7000 at 10 DPI is possibly due to its greater rate of GSH utilization (demonstrated by increased GST and GPx activities) than the *de novo* glutathione synthesis and recycling.

It has been suggested that the GSH/GSSG ratio is indicative of the cellular oxidative status and redox balance (Droge, 2002; Foyer and Noctor, 2003). Under strong oxidative stress, GSH is rapidly converted into GSSG, which results in a lower GSH/GSSG ratio. The lower GSH/GSSG ratios observed in susceptible genotypes after *M. phaseolina* inoculation at 7 and 10 DPI further confirmed the strong oxidative stress experienced by these genotypes under *M. phaseolina* inoculation.

In maize, inappropriate accumulation of anthocyanins in cytoplasm causes localized necrosis, poor vigor, or even death of plants. Certain GSTs like BZ-2 has been identified to catalyze the formation of anthocyanin-GSH conjugates, which allows transport into vacuoles thus reducing the cytotoxic effects of higher anthocyanin concentrations (Marrs et al., 1995). The charcoal-rot-susceptible sorghum genotypes tested in this study accumulated comparatively greater amounts of anthocyanins than resistant genotypes, which is manifested as longer pigmented lesions within split stems. In fact, the length of this lesion is used as a measure of charcoal rot resistance. Moreover, ROS are claimed to play a critical role as signaling molecules for anthocyanin production (Hatier and Gould, 2008). In Chapter 3, enhanced ROS biosynthesis in *M. phaseolina*-inoculated charcoal-rot-susceptible genotypes, Tx7000 and BTx3042 was reported. Therefore, the overaccumulation of anthocyanins in these genotypes after *M. phaseolina* infection is plausible where their GSH/GST system might play a pivotal role in decreasing the cytotoxic effects of anthocyanin overaccumulation. This, in turn could reduce susceptibility to *M. phaseolina*. Therefore, among many possible substrates for GSH/GST system, anthocyanin could to be a major candidate in compatible charcoal rot reactions.

Elevated GSH biosynthetic capacity has been shown to ironically cause increased oxidative stress in transgenic tobacco plants (Creissen et al., 1999). If this is the case with sorghum after *M. phaseolina* infection, enhanced GSH could escalate charcoal rot susceptibility. Necrotrophic pathogens such as *M. phaseolina* benefited from oxidative stress-mediated host cell death. However, the reduced disease severity observed in two susceptible genotypes after exogenous GSH application shows that GSH does not enhance disease susceptibility, but reduces disease severity. In fact, exogenous GSH can mimic fungal elicitors in activating the expression of defence-related genes (Dron et al. 1988) including PATHOGENESIS-RELATED PROTEIN 1 (Gomez et al. 2004), which contributes to reduced disease susceptibility.

The fungal necrotroph *Botrytis cinerea* triggers a progressive inhibition of SOD, CAT, and PX parallel to disease symptom development in tomato and leads to a collapse of the peroxisomal antioxidant system at advanced stages of infection (Kuzniak and Sklodowska, 2005). However, infection by the necrotrophic fungus, *Corynespora cassiicola* enhanced PX activity in soybean leaves (Fortunato et al., 2015). Gene expression (7 DPI) and the peroxidase functional

experiment (4, 7, 10, and DPI) conducted in the current study revealed a significant up-regulation of PX activity in charcoal-rot-susceptible genotypes after *M. phaseolina* inoculation. This suggested the enhanced accumulation of H_2O_2 under infection. PXs are important antioxidant enzymes that convert toxic H_2O_2 in to H_2O and O_2 (Hammond-& Jones, 1996). It is hypothesized that increased peroxidase activity in Tx7000 and BTx3042 helps to lower H_2O_2 concentrations and thus reduce oxidative stress under pathogen infection.

In tobacco, the reduction of catalase activity results in hyper-responsiveness to biotrophic pathogens (Mittler et al., 1999), while the catalase overexpression leads to enhanced disease sensitivity (Polidoros et al., 2001). Previous reports revealed that catalase activity is suppressed during the interaction of plants with invading pathogens and in turn contributes to the escalation of pathogen-induced programmed cell death (PCD) (Draper, 1997; Chamnongpol et al., 1996; Chen et al., 1993; Takahashi et al., 1997). Suppressed catalase activity-associated ROS production augmentation, is therefore crucial for conferring resistance against biotrophic and hemi-biotrophic plant pathogens while conducive for necrotrophic infection. In the current study, we found that *M. phaseolina* inoculation leads to reduced catalase activity in two charcoal-rot-susceptible sorghum genotypes at 7 DPI. One potential reason for this observation is the reaction between NO and catalase. NO and ONOO- can directly bind with heme-containing antioxidant enzymes such as catalase and inhibits its activity (Kerwin et al., 1995; Pacher et al., 2007). In Chapter 3, it was shown that NO is produced in pathogen-inoculated Tx7000 and BTx3042 at 7 DPI and could in turn, inhibit catalase activity. Enhanced catalase activity in the two resistant genotypes after *M. phaseolina* inoculation at all post-inoculation could contribute to active scavenging of H_2O_2 and ease oxidative stress. This in turn could subvert *M. phaseolina* colonization in SC599 and SC35, which contributes to resistance.

A significant reduction in superoxide dismutase activity was observed at 7 and 10 DPI by *M. phaseolina* (compared to control treatment) across the four genotypes tested in the current study. *M. phaseolina*'s ability to increase the $O_2^{\cdot -}$ generation potential of Tx7000 was suggested by transcriptional data. This, arguably, increases the Tx7000's necessity for more SOD as it is the only plant enzyme capable of scavenging $O_2^{\cdot -}$. However, in Chapter 3 we showed evidence for enhanced $ONOO^-$ synthesis in susceptible genotypes under pathogen inoculation. Formation of

$ONOO^-$ leads to decreased endogenous $O_2^{\cdot -}$ levels. Therefore, it may be possible that $O_2^{\cdot -}$ reduces to a level where additional SOD is not required by the susceptible genotypes tested. This ultimately manifested as reduced SOD activity after *M. phaseolina* inoculation.

CONCLUSIONS

Owing to its broad host range, wide geographic distribution, and ability to cause a variety of economically significant diseases, *M. phaseolina* is known to be a globally important necrotrophic fungus. However, compared to other necrotrophic pathosystems, less is known about *M. phaseolina*. Classically, necrotrophs are thought to kill the host using various phytotoxins, cell wall degrading enzymes, and reactive oxygen species that are secreted into the host tissues. Our recent findings showed that *M. phaseolina* can manipulate sorghum metabolic pathways that lead to enhanced oxidative stress that contribute to charcoal rot disease susceptibility in certain sorghum genotypes. Enzymes such as GST, GR, and GPx, PX, CAT, and SOD are integral components of the antioxidant system of many organisms including plants and play a pivotal role in maintaining cellular redox balance. As our current transcriptional and functional investigations suggested, the dynamics of these enzymes in charcoal-rot-susceptible sorghum genotypes (Tx7000 and BTx3042) should be viewed as mechanisms leading to reduced oxidative stress and charcoal rot susceptibility after *M. phaseolina* infection rather than those resulting in enhanced disease resistance.

REFERENCES

Agrawal GK, Rakwal R, Jwa NS, Agrawal, V.P. 2002. Effects of signaling molecules, protein phosphatase inhibitors and blast pathogen (*Magnaporthe grisea*) on the mRNA level of a rice (*Oryza sativa* L.) phospholipid hydroperoxide glutathione peroxidase (OsPHGPX) gene in seedling leaves. *Gene* 283: 227-236.

Airaki M, Sánchez-Moreno L, Leterrier M, Barroso JB, Palma JM, Corpas FJ. 2011. Detection and quantification of S-nitrosoglutathione (GSNO) in pepper (*Capsicum annuum* L.) plant organs by LC-ES/MS. *Plant and Cell Physiology* 52: 2006-2015.

Alscher RG, Hess JL. 1993. Antioxidants in Higher Plants. CRC press, Boca Raton, FL.

Bartling D, Radzio R, Steiner U, Weiler EW. 1993. A glutathione S-transferase with glutathione peroxidase activity from *Arabidopsis thaliana*: molecular cloning and functional characterization. *European Journal of Biochemistry* 216: 579-586.

Berhane K, Widersten M, Engstrom A, Kozarich J, Mannervik B. 1994. Detoxication of base propenals and other alpha, beta-unsaturated aldehyde products of radical reactions and lipid peroxidation by human glutathione S-transferases. *Proceedings of the National Academy of Sciences USA* 91: 1480-1484.

Bianchi MW, Roux C, Vartanian N. 2002. Drought regulation of GST8, encoding the Arabidopsis homologue of ParC/Nt107 glutathione transferase/peroxidase. *Physiologia Plantarum* 116: 96-105.

Chamnongpol S, Willekens H, Langebartels C, Van Montagu M, Inze D, Van Camp W. 1996. Transgenic tobacco with a reduced catalase activity develops necrotic lesions and induces pathogenesis-related expression under high light. *The Plant Journal* 10: 491-503.

Chen Z, Silva H, Klessig, DF. 1993. Active oxygen species in the induction of plant systemic acquired resistance by salicylic acid. *Science* 262: 1883-1886.

Coleman JOD, Blake-Kalff MMA, Davies TGE. 1997. Detoxification of xenobiotics by plants: chemical modification and vacuolar compartmentation. *Trends in Plant Science* 2: 144-151.

Creissen G, Firmin J, Fryer M, Kular B, Leyland N, Reynolds H, Pastori G, Wellburn F, Baker N, Wellburn A. Mullineaux P. 1999. Elevated glutathione biosynthetic capacity in the chloroplasts of transgenic tobacco plants paradoxically causes increased oxidative stress. *Plant Cell* 11: 1277-1291.

Cummins I, Cole DJ, Edwards R. 1999. A role for glutathione transferases functioning as glutathione peroxidases in resistance to multiple herbicides in black-grass. *The Plant Journal* 18: 285-292.

Danielson UH, Esterbauer H, Mannervik B. 1987. Structure-activity relationships of 4-hydroxyalkenals in the conjugation catalyzed by mammalian glutathione S-transferases. *Biochemical Journal* 247: 707-712.

Debona D, Rodrigues FÁ, Rios JA, Nascimento KJT. 2012. Biochemical changes in the leaves of wheat plants infected by *Pyricularia oryzae*. *Phytopathology* 102: 1121-1129.

Dixon DP, Cummins I, Cole DJ, Edwards R. 1998. Glutathione-mediated detoxification systems in plants. *Current Opinion in Plant Biology* 1: 258-266.

Draper J. 1997. Salicylate, superoxide synthesis and cell suicide in plant defense. *Trends in Plant Science* 2: 162-165.

Droge W. 2002. Free radicals in the physiological control of cell function. *Physiological Reviews* 82: 47-95.

Dron M, Clouse SD, Dixon RA, Lawton MA, Lamb CJ. 1988. Glutathione and fungal elicitor regulation of a plant defense gene promoter in electroporated protoplasts. *Proceedings of the National Academy of Sciences USA* 85: 6738-6742.

Edwards R, Blount JW, Dixon RA. 1991. Glutathione and elicitation of the phytoalexin response in legume cell cultures. *Planta* 184: 403-409.

Edwards R, Dixon DP, Walbot V. 2000. Plant glutathione S-transferases: enzymes with multiple functions in sickness and in health. *Trends in Plant Science* 5: 193-198.

El-Zahaby HM, Gullner G, Kiraly Z. 1995. Effects of powdery mildew infection of barley on the ascorbate–glutathione cycle and other antioxidant in different host–pathogen interactions. *Phytopathology* 85: 1225-1230.

Fernandez J, Wilson RA. 2014. Characterizing roles for the glutathione reductase, thioredoxin reductase and thioredoxin peroxidase-encoding genes of *Magnaporthe oryzae* during rice blast disease. *PLoS One* 9: e87300.

Fortunato AA, Debona D, Bernardeli AMA, Rodrigues FÁ. 2015. Changes in the antioxidant system in soybean leaves infected by *Corynespora cassiicola*. *Phytopathology* 105: 1050-1058.

Foyer CH, Lelandais M, Kunert, KJ. 1994. Photooxidative stress in plants. *Physiologia Plantarum* 92: 696–717.

Foyer CH, Noctor G. 2003. Redox sensing and signalling associated with reactive oxygen in chloroplasts, peroxisomes and mitochondria. *Physiologia Plantarum* 119: 355–364.

Foyer CH, Noctor G. 2005. Redox homeostasis and antioxidant signaling: a metabolic interface between stress perception and physiological responses. *Plant Cell* 17: 1866-1875.

Foyer CH, Noctor G. 2009. Redox regulation in photosynthetic organisms: signaling, acclimation, and practical implications. *Antioxidants & Redox Signaling* 11: 861-905.

Foyer CH, Noctor G. 2011. Ascorbate and glutathione: the heart of the redox hub. *Plant Physiology* 155: 2-18.

Gill SS, Tuteja N. 2010. Reactive oxygen species and antioxidant machinery in abiotic stress tolerance in crop plants. *Plant physiology and biochemistry* 48: 909-930.

Gomez LD, Noctor G, Knight M, Foyer CH. 2004. Regulation of calcium signaling and gene expression by glutathione. *Journal of Experimental Botany* 55: 1851-1859.

Gonnen MV, Schlösser E. 1993. Oxidative stress in interaction between *Avena sativa* L. and *Drechlera* spp.. *Physiological and Molecular Plant Pathology* 42: 221–234.

Goodstein DM, Shu S, Howson R, Neupane R, Hayes RD, Fazo J, Rokhsar DS. 2012. Phytozome: a comparative platform for green plant genomics. *Nucleic Acids Research* 40: 1178-1186.

Hammond-Kosack KE, Jones JD. 1996. Resistance gene-dependent plant defense responses. *Plant Cell* 8: 1773-1791.

Hatier JHB, Gould KS. 2008. Foliar anthocyanins as modulators of stress signals. *Journal of Theoretical Biology* 253: 625-627.

Huber PC, Almeida WP, Fátima ÂD. 2008. Glutathione and related enzymes: biological roles and importance in pathological processes. *Química Nova* 31: 1170-1179.

Islam MS, Haque MS, Islam MM, Emdad EM, Halim A, Hossen QMM, Hossain MZ, Ahmed B, Rahim S, Rahman MS, Alam MM. 2012. Tools to kill: genome of one of the most destructive plant pathogenic fungi *Macrophomina phaseolina*. *BMC Genomics* 13: 1.

Kerwin JF, Lancaster JR, Feldman P.L. 1995. Nitric oxide: a new paradigm for second messengers. *Journal of Medicinal Chemistry* 38: 4343-4362.

Kiprovski B, Malencic D, Popovic M, Budakov D, Stojšin V, Baleševic-Tubic S. 2012. Antioxidant systems in soybean and maize seedlings infected with Rhizoctonia solani. *Journal of Plant Pathology* 94: 313-324.

Kiyosue T, Yamaguchi-Shinozaki K, Shinozaki K. 1993. Characterization of two cDNAs (ERD11 and ERD13) for dehydration-inducible genes that encode putative glutathione S-transferases in *Arabidopsis thaliana*. *FEBS Letters* 335: 189-192.

Kuzniak E, Sklodowska M. 1999. The effect of *Botrytis cinerea* infection on ascorbate glutathione cycle in tomato leaves. *Plant Science* 148: 69-76.

Kużniak E, Skłodowska M. 2005. Fungal pathogen-induced changes in the antioxidant systems of leaf peroxisomes from infected tomato plants. *Planta* 222: 192-200.

Levine A, Tenhaken R, Dixon R, Lamb C. 1994. H_2O_2 from the oxidative burst orchestrates the plant hypersensitive disease resistance response. *Cell* 79: 583-593.

Liao W, Ji L, Wang J, Chen Z, Ye M, Ma H, An X. 2014. Identification of glutathione S-transferase genes responding to pathogen infestation in *Populus tomentosa*. *Functional & Integrative Genomics* 14: 517-529.

Malenčić D, Kiprovski B, Popović M, Prvulović D, Miladinović J, Djordjević V. 2010. Changes in antioxidant systems in soybean as affected by *Sclerotinia sclerotiorum* (Lib.) de Bary. *Plant physiology and biochemistry* 48: 903-908.

Margis R, Dunand C, Teixeira FK, Margis-Pinheiro M. 2008. Glutathione peroxidase family–an evolutionary overview. *FEBS journal* 275: 3959-3970.

Marí M, Morales A, Colell A, García-Ruiz C, Fernández-Checa JC. 2009. Mitochondrial glutathione, a key survival antioxidant. *Antioxidants & Redox Signaling* 11: 2685-2700.

Marrs KA, Alfenito MR, Lloyd AM, Walbot V. 1995. A glutathione S-transferase involved in vacuolar transfer encoded by the maize gene Bronze-2. *Nature* 375: 397-400.

Martinoia E, Grill E, Tommasini R, Kreuz K, Amrhein N. 1993. ATP-dependent glutathione S-conjugate 'export' pump in the vacuolar membrane of plants. *Nature* 364: 247-249.

Matern U, Reichenbach C, Heller W. 1986. Efficient uptake of flavonoids into parsley (*Petroselinum hortense*) vacuoles requires acylated glycosides. *Planta* 167: 183-189.

Mauch F, Dudler R. 1993. Differential induction of distinct glutathione-S-transferases of wheat by xenobiotics and by pathogen attack. *Plant Physiology* 102: 1193-201.

Meloni DA, Oliva MA, Martinez CA, Cambraia J. 2003. Photosynthesis and activity of superoxide dismutase, peroxidase and glutathione reductase in cotton under salt stress. *Environmental and Experimental Botany* 49: 69-76.

Mittler R, Herr EH, Orvar BL, van Camp W, Wilikens H, Inzé D, Ellis BE. 1999. Transgenic tobacco plants with reduced capability to detoxify reactive oxygen intermediates are hyperresponsive to pathogen infection. *Proceedings of the National Academy of Sciences USA* 96: 14165-14170.

Mittler R, Vanderauwera S, Gollery M, Van Breusegem F. 2004. Reactive oxygen gene network of plants. *Trends in Plant Science* 9: 490-498.

Moons A. 2003. Osgstu3 and osgtu4, encoding tau class glutathione S-transferases, are heavy metal- and hypoxic stress-induced and differentially salt stress responsive in rice roots, *FEBS Letters* 553: 427-432.

Nimse SB, Pal D. 2015. Free radicals, natural antioxidants, and their reaction mechanisms. *RSC Advances* 5: 7986-8006.

Noctor G, Foyer CH. 1998. Ascorbate and glutathione: keeping active oxygen under control. *Annual Review of Plant Biology* 49: 249-279.

Pacher P, Beckman JS, Liaudet L. 2007. Nitric oxide and peroxynitrite in health and disease. *Physiological Reviews* 87: 315-424.

Polidoros AN, Mylona PV, Scandalios JP. 2001. Transgenic tobacco plants expressing the maize *Cat2* gene have altered catalase levels that affect plant-pathogen interactions and resistance to oxidative stress. *Transgenic Research* 10: 555-569.

Sandermann H. 1992. Plant metabolism of xenobiotics. *Trends in Biochemical Sciences* 17: 82-84.

Sandermann H. 1994. Higher plant metabolism of xenobiotics: the "green liver" concept. *Pharmacogenetics* 4: 225-241.

Seppanen MM, Cardi T, Hyokki MB, Pehu E. 2000. Characterisation and expression of cold induced glutathione S-transferase in freezing tolerant *Solanum commersonii*, sensitive *S. tuberosum* and their interspecific somatic hybrids. *Plant Science* 153: 125-133.

Shahidi F, Zhong Y. 2010. Novel antioxidants in food quality preservation and health promotion. *European Journal of Lipid Science and Technology* 112: 930-940.

Takahashi H, Chen Z, Du H, Liu Y, Klessig DF. 1997. Development of necrosis and activation of disease resistance in transgenic tobacco plants with severely reduced catalase levels. *The Plant Journal* 11: 993-1005.

Tarr SAJ. 1962. Root and stalk diseases: Red stalk rot, Colletotrichum rot, anthracnose, and red leaf spot, in: Diseases of Sorghum, Sudan Grass and Brown Corn. Commonwealth Mycological Institute, Kew, Surrey, UK, pp. 58-73.

Tesso T, Perumal R, Little CR, Adeyanju A, Radwan GL, Prom LK, Magill CW. 2012. Sorghum pathology and biotechnology-a fungal disease perspective: Part II. Anthracnose, stalk rot, and downy mildew. *European Journal of Plant Pathology* 6: 31-44.

Vanacker H, Carver TLW, Foyer CH. 1998. Pathogen-induced changes in the antioxidant status of the apoplast in barley leaves. *Plant Physiology* 117: 1103-1114.

Willekens H, Chamnongpol S, Davey M, Schraudner M, Langebartels C, van Montagu M, van Camp W. 1997. Catalase is a sink for H_2O_2 and is indispensable for stress defence in C3 plants. *The EMBO Journal* 16: 4806-4816.

Wolf AE, Dietz KJ, Schroder P. 1996. A carboxypeptidase degrades glutathione conjugates in the vacuoles of higher plants. *FEBS Letters* 384: 31-34.

Xiang C, Oliver DJ. 1998. Glutathione metabolic genes coordinately respond to heavy metals and jasmonic acid in Arabidopsis. *Plant Cell* 10: 1539-1550.

TABLES AND FIGURES

Table 4.1. Significantly ($q < 0.05$) differentially expressed genes related to the host antioxidant system between SC599 (charcoal-rot-resistant) and Tx7000 (charcoal-rot-susceptible) sorghum genotypes in response to *Macrophomina phaseolina* inoculation at 2 and 7 days post-inoculation.

Gene name	Gene annotation	Geno × Trt*	S599 (MP-CON)†		Tx7000 (MP-CON)	
		q-value	log2 DE‡	q-value	log2 DE	q-value
2 days post-inoculation						
Sb01g001130	Glutathione S-transferase	1.1E-02	0.03	9.7E-01	-1.90	4.9E-03
Sb08g006680		2.4E-02	0.04	9.5E-01	-1.13	2.9E-02
Sb01g030800		7.0E-04	0.99	2.0E-02	-0.90	4.1E-02
Sb03g044980		1.4E-02	1.61	1.9E-06	0.35	2.7E-01
Sb01g031000		5.3E-03	-1.17	1.6E-01	1.51	6.5E-02
Sb02g027080		3.3E-02	0.51	2.4E-01	1.88	9.8E-02
Sb03g045840		4.3E-02	0.07	9.6E-01	2.18	2.2E-04
Sb03g045830		1.2E-03	-0.28	7.8E-01	2.18	3.2E-05
Sb04g032520	Glutathione peroxidase	3.9E-07	0.99	8.1E-05	-0.46	1.5E-01
Sb03g000550	Glutaredoxin	1.8E-04	-1.47	3.0E-07	0.43	3.6E-01
Sb02g041880		6.4E-05	-0.71	9.0E-03	0.84	2.5E-02
Sb10g028480	Peroxidase	2.2E-02	0.07	9.4E-01	-2.72	8.5E-03
Sb07g027300		3.7E-02	0.53	4.1E-01	-1.47	3.8E-02
Sb06g017080		2.2E-02	0.73	1.0E-01	-0.96	6.8E-02
Sb03g004380		5.8E-03	-2.58	1.1E-05	-0.06	9.5E-01
Sb02g044060		3.1E-02	-0.65	1.2E-03	-0.01	9.8E-01
Sb02g001140		3.8E-04	-1.48	1.3E-03	1.56	1.2E-02
Sb09g018150		2.0E-02	-1.54	2.4E-02	1.64	1.3E-01
Sb03g046760		1.5E-03	0.04	9.8E-01	1.93	7.5E-09
Sb05g001030		2.3E-02	-0.50	3.6E-01	2.01	1.3E-02
Sb09g029440		2.8E-18	0.75	2.2E-03	2.66	5.5E-45
Sb01g041760		4.6E-02	0.48	7.8E-01	3.53	5.9E-06
7 days post-inoculation						
Sb03g025210	Glutathione S-transferase	3.7E-05	0.63	8.3E-01	-5.18	4.7E-11
Sb01g030800		3.0E-11	1.55	2.1E-02	-2.41	6.4E-11
Sb01g030810		6.9E-03	0.91	6.2E-01	-2.06	6.0E-05
Sb08g007310		3.5E-02	-0.85	9.6E-01	-1.32	3.0E-03
Sb06g017640		1.8E-02	-0.17	9.3E-01	-1.17	1.4E-04
Sb09g001690		8.5E-03	1.00	3.1E-01	-0.94	2.5E-01
Sb10g008310		1.9E-04	0.49	4.4E-01	-0.69	1.8E-02
Sb09g003700		4.2E-02	-1.42	1.7E-01	0.29	6.8E-01
Sb06g017110		8.9E-03	-0.50	4.9E-01	0.52	1.4E-01
Sb09g003750		5.0E-04	-	-	0.69	2.1E-04
Sb03g015070		4.3E-02	-	-	0.81	6.7E-01
Sb04g023210		2.8E-02	-0.25	9.0E-01	0.93	1.5E-03
Sb05g007005		2.4E-04	-0.64	3.3E-01	1.03	2.2E-03
Sb09g003690		1.2E-06	-1.22	4.1E-02	1.05	4.2E-05
Sb01g005990		3.1E-02	-0.25	9.4E-01	1.40	1.4E-06
Sb01g001130		2.0E-02	-0.35	8.8E-01	1.46	3.2E-03
Sb01g006010		7.5E-03	-0.16	9.7E-01	2.07	8.4E-07
Sb03g045840		8.9E-04	-1.24	4.3E-01	2.16	5.3E-05
Sb08g006690		1.2E-05	-1.07	2.7E-01	2.17	5.7E-07
Sb05g001525		3.6E-02	-0.90	7.3E-01	2.24	8.0E-03
Sb01g031030		7.8E-05	-1.03	4.2E-01	2.44	7.4E-09
Sb08g007300		1.1E-04	-	4.2E-01	2.61	4.2E-07
Sb01g030930		4.8E-05	-0.04	-	3.23	3.6E-16
Sb01g006000		6.2E-08	-0.11	9.8E-01	3.35	5.3E-17
Sb02g027080		3.7E-09	-0.32	8.6E-01	3.79	1.6E-09
Sb01g030870		6.2E-04	-0.06	9.9E-01	3.83	3.0E-10
Sb01g030790		1.3E-02	0.09	9.9E-01	3.90	2.8E-07

Sb03g031780		6.5E-04	-0.28	9.5E-01	4.04	2.9E-11
Sb01g030880		5.2E-05	-1.51	3.6E-01	4.14	9.4E-12
Sb03g045830		4.3E-09	-0.97	4.4E-01	4.18	1.3E-13
Sb09g003750		5.0E-04	-	-	4.46	2.1E-04
Sb04g022250		1.6E-04	-0.01	1.0E+00	4.59	6.0E-26
Sb01g030980		2.1E-20	-0.04	9.9E-01	5.58	7.1E-89
Sb01g030830		5.5E-03	0.70	8.4E-01	5.99	6.7E-06
Sb01g031040		2.4E-07	-	-	6.58	2.3E-15
Sb01g030990		5.2E-17	-0.04	-	6.83	4.5E-08
Sb01g031020		3.1E-03	-	-	7.17	9.4E-09
Sb01g031000		2.5E-35	-2.42	1.1E-03	7.24	2.8E-40
Sb01g031010		5.8E-14	0.07	-	7.48	3.9E-10
Sb02g003090		2.3E-20	-0.94	6.2E-01	7.88	2.1E-89
Sb01g031050		4.0E-06	-	-	8.00	1.3E-11
Sb02g038130		2.3E-34	-0.20	-	9.54	1.0E-35
Sb08g016750	Glutathione synthetase	2.4E-06	-0.92	6.2E-02	1.92	1.2E-05
Sb09g002470	Glutamate cysteine ligase	1.5E-03	-0.88	2.5E-01	0.85	6.5E-03
Sb10g005820	Glutathione peroxidase	1.6E-04	0.83	3.8E-01	-2.04	1.8E-05
Sb06g024920		8.5E-04	-0.24	8.8E-01	0.99	1.3E-07
Sb01g034870		5.9E-07	-0.83	1.0E-01	1.28	1.5E-05
Sb04g032520		5.1E-03	0.19	9.6E-01	2.13	1.1E-10
Sb01g035940		1.6E-03	-	-	6.64	1.5E-07
Sb04g036870	Glutathione reductase	1.5E-03	-0.26	9.0E-01	1.52	1.4E-07
Sb01g021980		6.1E-05	-0.33	9.2E-01	2.95	7.6E-10
Sb03g000550	Glutaredoxin	1.8E-05	1.28	3.4E-01	-3.54	4.8E-11
Sb06g014830		1.2E-02	0.28	8.8E-01	-1.03	8.4E-03
Sb03g004380	Peroxidase	1.1E-03	-	-	-6.32	3.9E-27
Sb10g010040		2.2E-02	-0.06	1.0E+00	-4.85	9.3E-04
Sb09g024590		2.0E-06	0.22	9.6E-01	-4.31	2.2E-08
Sb10g021610		4.0E-05	0.10	9.8E-01	-4.14	6.1E-16
Sb01g031740		2.2E-02	-	-	-4.08	1.0E-02
Sb08g016840		3.3E-03	-	-	-3.58	3.3E-05
Sb05g009400		1.7E-02	-	-	-3.33	5.4E-02
Sb04g008590		2.7E-02	-	-	-2.89	1.0E-01
Sb10g027490		3.5E-02	0.34	9.4E-01	-2.66	2.8E-03
Sb06g027520		5.0E-04	0.93	2.2E-01	-2.08	1.3E-03
Sb06g027520		5.0E-04	0.93	2.2E-01	-2.08	1.3E-03
Sb02g037840		4.9E-03	1.55	2.4E-01	-1.96	8.4E-02
Sb04g003240		3.3E-02	0.31	9.3E-01	-1.70	1.1E-07
Sb04g030170		1.9E-03	0.07	9.7E-01	-0.97	1.4E-03
Sb03g010250		7.6E-03	1.58	1.4E-01	-0.80	2.9E-01
Sb08g004880		3.0E-02	-0.28	8.6E-01	0.73	1.7E-02
Sb08g016820		8.7E-03	-1.08	2.8E-01	1.01	2.6E-02
Sb05g001030		3.4E-02	-0.39	8.3E-01	1.08	2.2E-02
Sb09g004650		3.3E-03	-1.06	4.2E-01	1.57	9.0E-05
Sb09g004660		3.5E-02	-	-	1.72	3.1E-01
Sb10g028500		4.8E-02	0.36	9.0E-01	2.29	3.2E-07
Sb03g036760		1.8E-07	-1.33	1.9E-01	2.92	2.8E-05
Sb09g020960		3.8E-02	-	-	3.35	2.2E-02
Sb03g046760		1.4E-06	-0.60	8.3E-01	3.94	1.5E-64
Sb06g030940		1.2E-04	-	-	5.27	1.9E-04
Sb05g001000		2.6E-10	-	-	6.07	1.4E-08
Sb09g021000		5.3E-04	-	-	6.13	4.5E-06

Sb01g020830		2.9E-08	-0.56	8.1E-01	6.17	1.1E-21
Sb03g013200		4.2E-04	-	-	7.65	1.0E-10
Sb01g041760		3.4E-04	-	-	9.28	8.2E-27
Sb01g048280	Catalase	1.5E-04	1.10	3.8E-01	-3.23	1.2E-06
Sb07g023950	Superoxide dismutase	2.1E-02	1.07	1.8E-01	-0.27	4.4E-01

* Geno × Trt = genotype by treatment interaction where treatment consists of *M. phaseolina* and control inoculations. †MP = *M. phaseolina,* CON =control. ‡ log2 DE = log2 fold differential expression.

Table 4.2. *P*-values of F-statistics from analysis of variance (ANOVA) for functional assays including total glutathione (GSH_{total}), oxidized glutathione (GSSG), reduced glutathione (GSH), reduced to oxidized glutathione ratio (GSH/GSSG), glutathione-s-transferase activity (GST), glutathione peroxidase activity (GPx), glutathione reductase activity (GR), peroxidase activity (PX), catalase activity (CAT), and superoxide dismutase activity (SOD) measured with four sorghum genotypes (Tx7000, BTx3042, SC599, SC35) after inoculation with *M. phaseolina* at three post-inoculation stages (4, 7, and 10 days post-inoculation, DPI) ($\alpha = 0.05$).

DPI	Effect	Pr > F									
		GSH_{total}	GSSG	GSH	GSH/GSSG	GST	GPx	GR	PX	CAT	SOD
4	Genotype (G)	0.0113	0.0010	0.3611	0.2394	0.0002	<0.0001	0.0158	<0.0001	0.0002	0.0151
	Treatment (T)	0.0011	0.0003	0.0424	0.7391	0.1287	<0.0001	0.2184	<0.0001	0.0003	0.9888
	G × T	0.6190	0.0602	0.0918	0.1206	0.0370	0.1323	0.9938	0.0074	0.0103	0.3789
7	Genotype (G)	<0.0001	<0.0001	0.0285	0.0138	<0.0001	<0.0001	<0.0001	<0.0001	<0.0001	0.0067
	Treatment (T)	<0.0001	0.0060	0.0009	0.0287	0.0274	<0.0001	0.0005	0.0001	0.0006	0.0193
	G × T	<0.0001	0.0144	<0.0001	<0.0001	0.0089	0.0017	0.0026	0.0183	<0.0001	0.9799
10	Genotype (G)	<0.0001	<0.0001	<0.0001	0.0002	0.0176	0.0019	0.0098	<0.0001	<0.0001	<0.0001
	Treatment (T)	<0.0001	<0.0001	0.5276	0.0003	0.1216	0.1306	0.0003	0.0013	<0.0001	0.0416
	G × T	<0.0001	<0.0001	<0.0001	0.0010	0.0351	0.0019	<0.0001	0.0171	<0.0001	0.5281

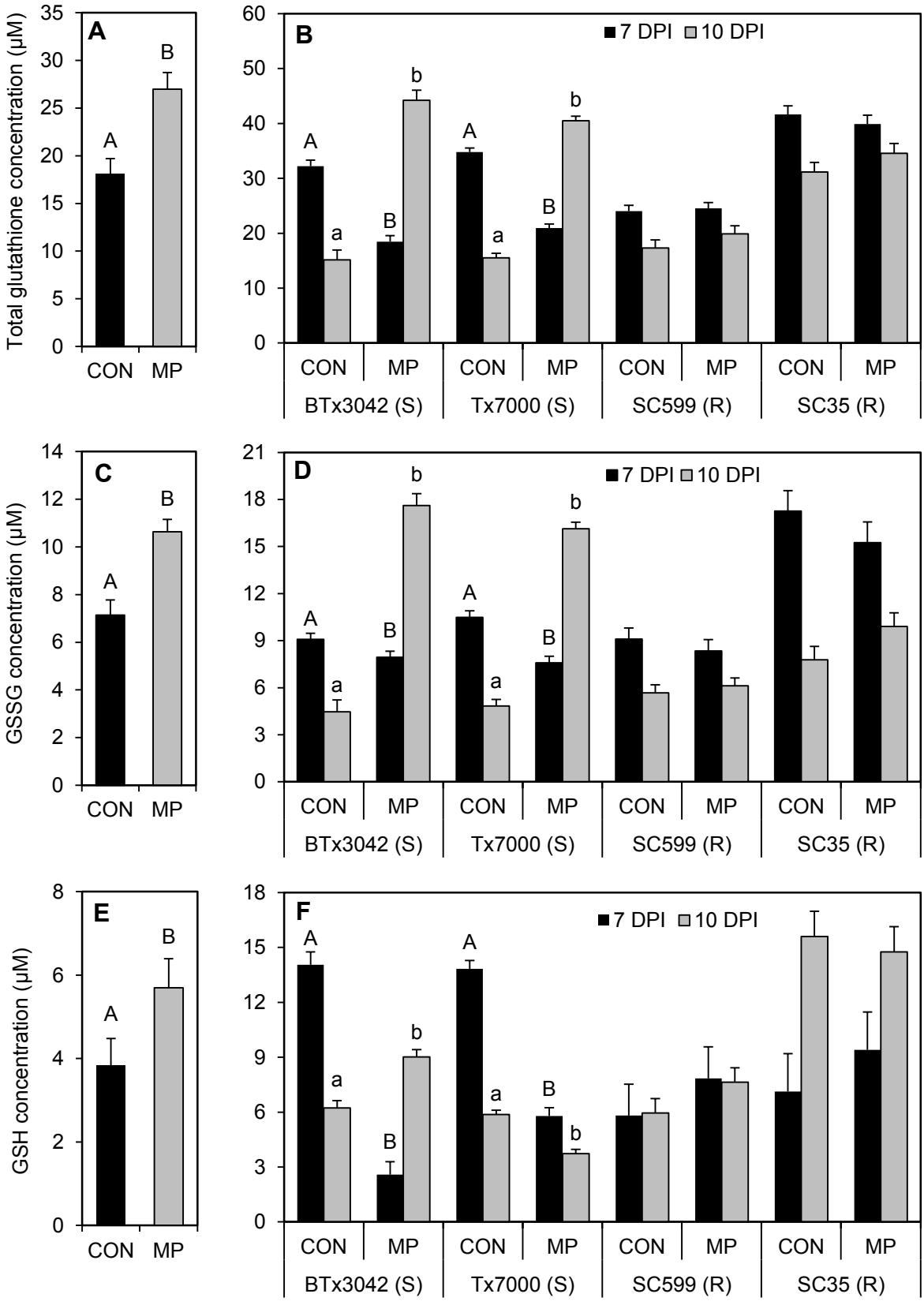
A
B
C
D
E
F
Total glutathione concentration (µM)
GSSG concentration (µM)
GSH concentration (µM)
7 DPI
10 DPI
CON
MP
BTx3042 (S)
Tx7000 (S)
SC599 (R)
SC35 (R)

Figure 4.1. Comparison of the mean total glutathione content between two treatments (A) across four genotypes at 4 days post-inoculation (DPI), (B) among four genotypes at 7 and 10 DPI; oxidized glutathione (GSSG) content between two treatments (C) across four genotypes at 4 DPI, (D) among four genotypes at 7 and 10 DPI; and the reduced glutathione (GHS) content between two treatments (E) across four genotypes at 4 DPI, (F) among four genotypes at 7 and 10 DPI. In panels A, C, and E, treatment means followed by different letters are significantly different. In panels B, D, and F, treatment means followed by different letters within each genotype at a given DPI are significantly different. Treatment means without letter designations within each genotype at a given DPI are not significantly different ($\alpha = 0.05$). Error bars represent standard errors. CON = phosphate-buffered saline mock-inoculated control, MP = *Macrophomina phaseolina*.

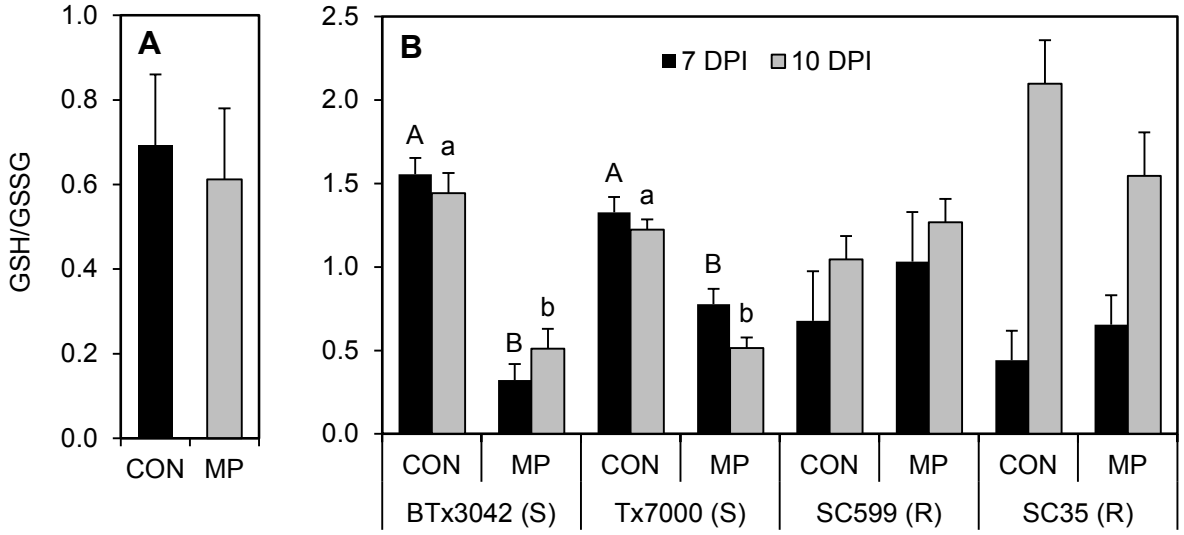

Figure 4.2. Comparison of the mean GSH/GSSG ratio between two treatments (A) across four genotypes at 4 days post-inoculation (DPI), and (B) among four genotypes at 7 and 10 DPI. Treatment means without letter designations are not significantly different. In panel B, treatment means followed by different letters within each genotype at a given DPI are significantly different while the treatment means without letter designations within each genotype at a given DPI are not significantly different ($\alpha = 0.05$). Error bars represent standard errors. CON = phosphate-buffered saline mock-inoculated control, MP = *Macrophomina phaseolina*.

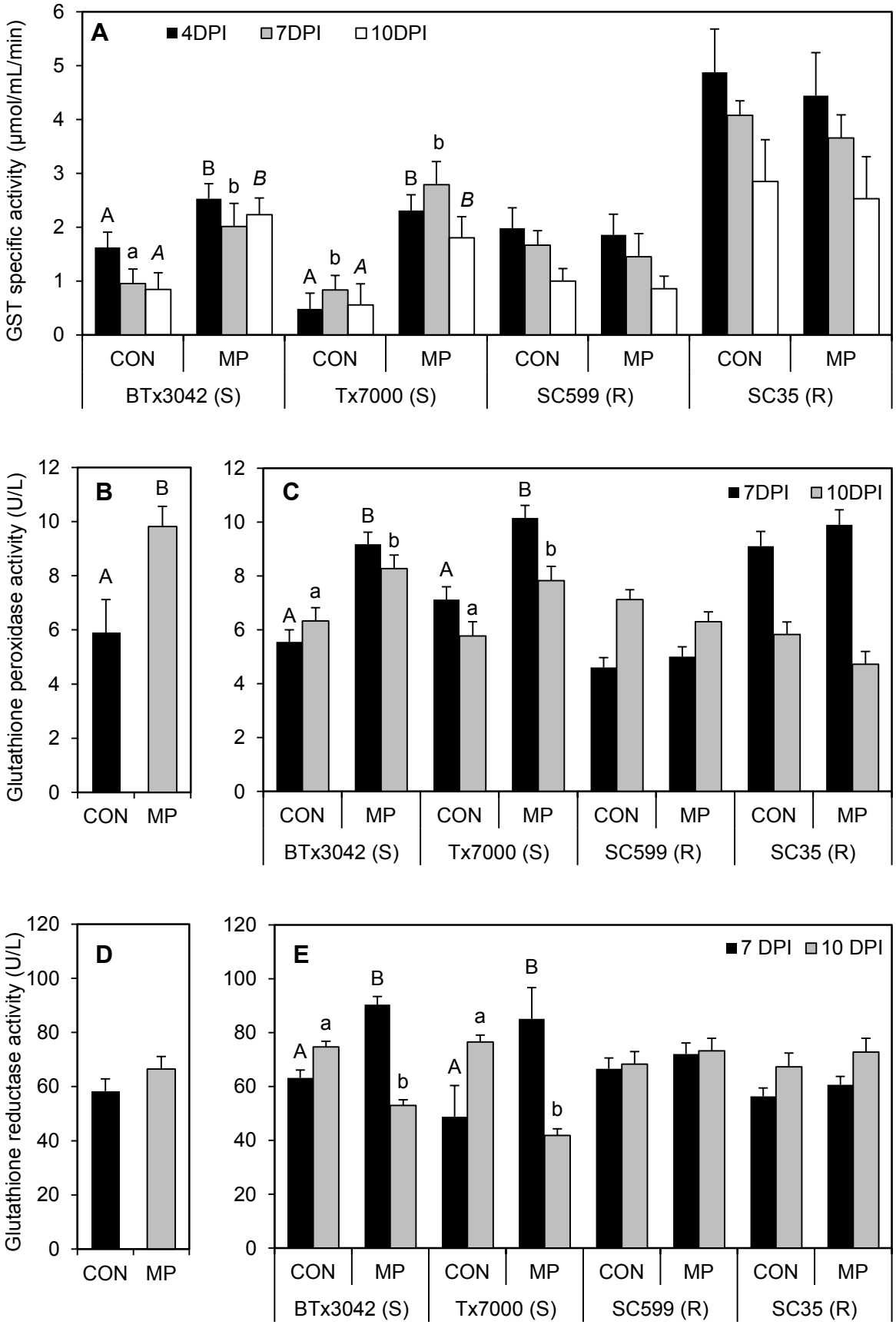
A
4DPI
7DPI
10DPI
GST specific activity (µmol/mL/min)
CON
MP
BTx3042 (S)
Tx7000 (S)
SC599 (R)
SC35 (R)
B
Glutathione peroxidase activity (U/L)
C
D
Glutathione reductase activity (U/L)
E
7 DPI
10 DPI

Figure 4.3. Comparison of the mean (A) glutathione-s-transferase specific activity between two treatments among four genotypes at 4, 7, and 10 days post-inoculation (DPI); glutathione peroxidase activity between two treatments (B) across four genotypes at 4 DPI, (C) among four genotypes at 7 and 10 DPI; and the glutathione reductase activity between two treatments (D) across four genotypes at 4 DPI, (E) among four genotypes at 7 and 10 DPI. In panels B and D, treatment means followed by different letters are significantly different. In panels A, C, and E, treatment means followed by different letters within each genotype at a given DPI are significantly different. Treatment means without letter designations within each genotype at a given DPI are not significantly different ($\alpha = 0.05$). Error bars represent standard errors. CON = phosphate-buffered saline mock-inoculated control, MP = *Macrophomina phaseolina*.

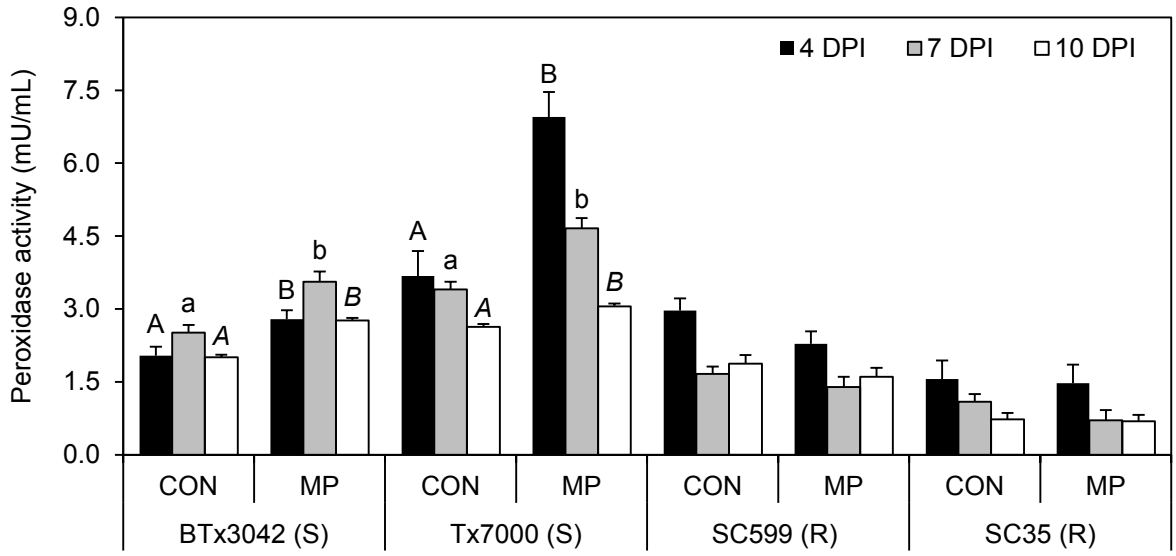

Figure 4.4. Comparison of the mean peroxidase activity among two treatments (CON, MP) in charcoal-rot-susceptible (BTx3042, Tx7000) and resistant (SC599, SC35) genotypes at three post-inoculation stages (4, 7, and 10 DPI). Treatment means followed by different letters within each genotype at a given DPI are significantly different while the treatment means without letter designations within each genotype at a given DPI are not significantly different at $\alpha = 0.05$. Error bars represent standard errors. CON = phosphate-buffered saline mock-inoculated control, MP = *Macrophomina phaseolina*.

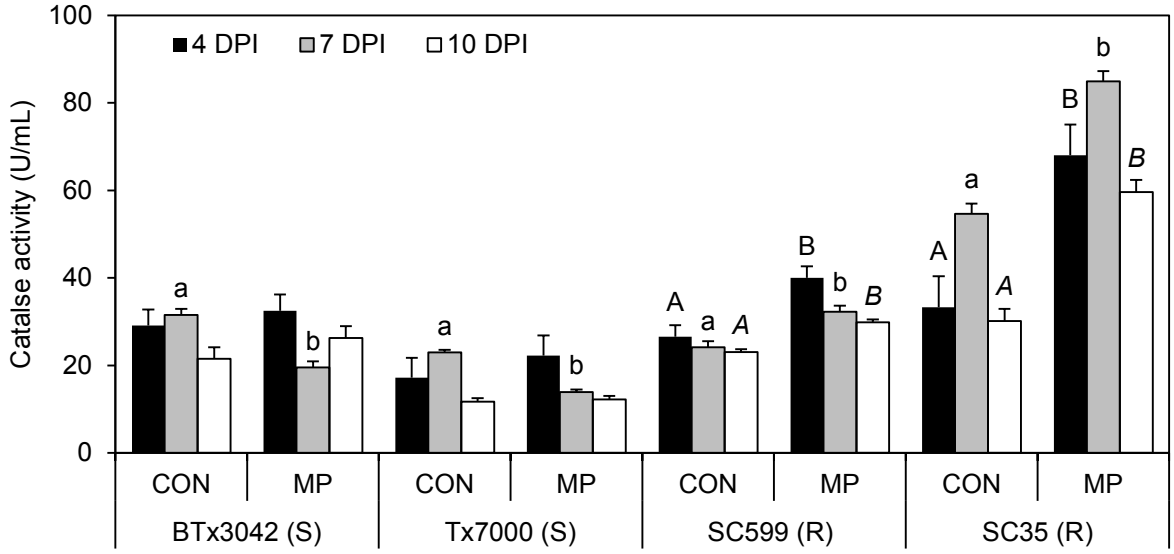

Figure 4.5. Comparison of the mean catalase activity among two treatments (CON, MP) in charcoal-rot-susceptible (BTx3042, Tx7000) and resistant (SC599, SC35) genotypes at three post-inoculation stages (4, 7, 10 DPI). Treatment means followed by different letters within each genotype at a given DPI are significantly different while the treatment means without letter designations within each genotype at a given DPI are not significantly different at $\alpha = 0.05$. Error bars represent standard errors. CON = phosphate-buffered saline mock-inoculated control, MP = *Macrophomina phaseolina*.

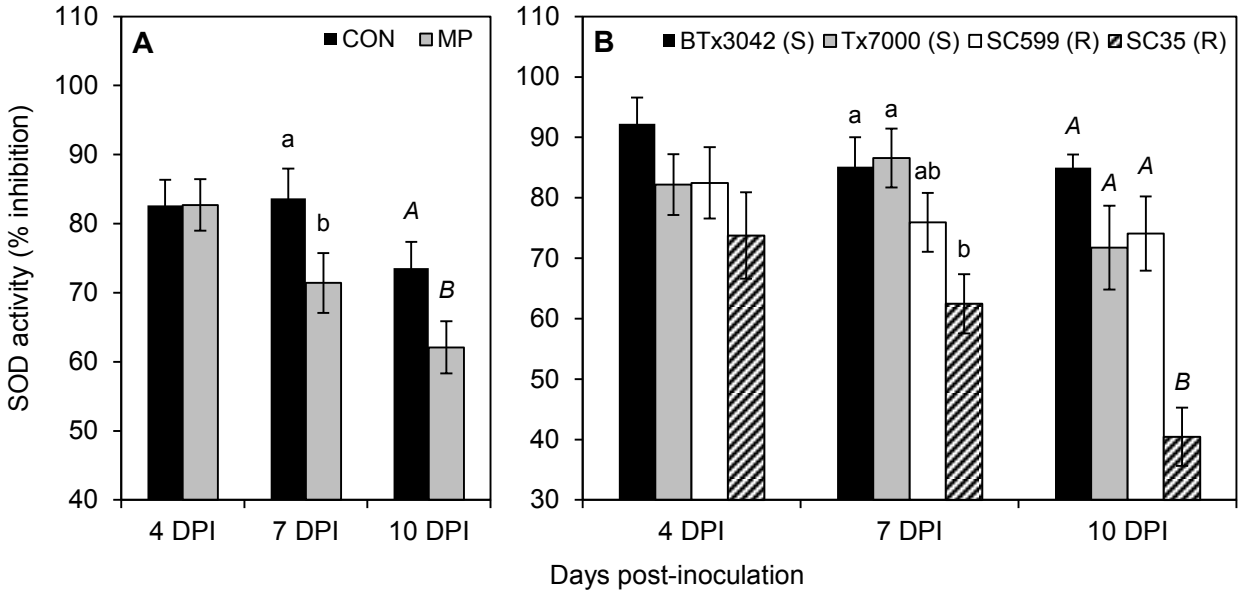

Figure 4.6. Comparison of the mean superoxide dismutase activity (A) among two treatments (CON, MP) across four sorghum genotypes (BTx3042, Tx7000, SC599, SC35) at three post-inoculation stages (4, 7, and 10 DPI) and (B) among four sorghum genotypes across two treatments at three post inoculation stages. Treatment means followed by different letters within a given DPI are significantly different while the treatment means without letter designations are not significantly different at $\alpha = 0.05$. Genotype means followed by different letters within a given DPI are significantly different based on the adjusted *P*-value for multiple comparisons using Tukey-Kramer's test at $\alpha = 0.05$ while the genotype means without letter designations within a given DPI are not significantly different. Error bars represent standard errors. CON = phosphate-buffered saline mock-inoculated control, MP = *Macrophomina phaseolina*.

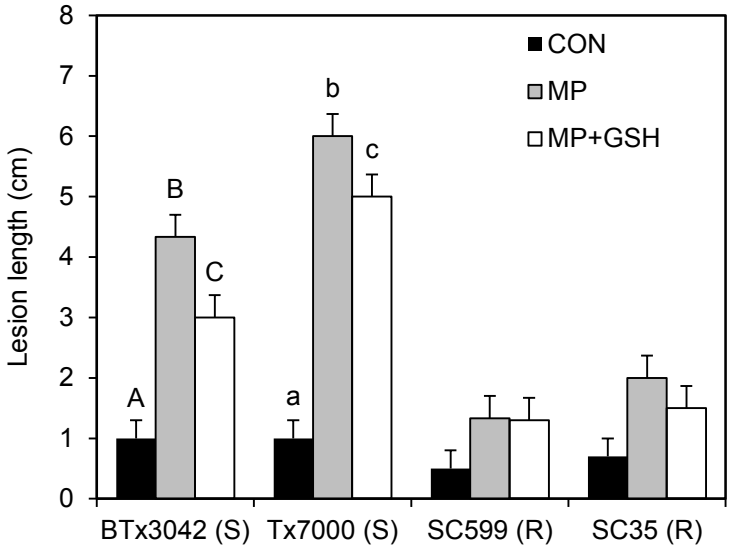

Figure 4.7. Comparison of mean lesion length between three treatments (CON, MP, MP + GSH) among tested sorghum genotypes at 35 d after inoculation. Treatment means followed by different letters within each genotype are significantly different based on the adjusted *P*-value for multiple comparisons using Tukey-Kramer's test at comparisonwise error rate (α_{CER}) = 0.016. The means without letter designations within each genotype are not significantly different. Error bars represent standard errors. CON = phosphate-buffered saline mock-inoculated control, MP = *Macrophomina phaseolina*, GSH = reduced glutathione.

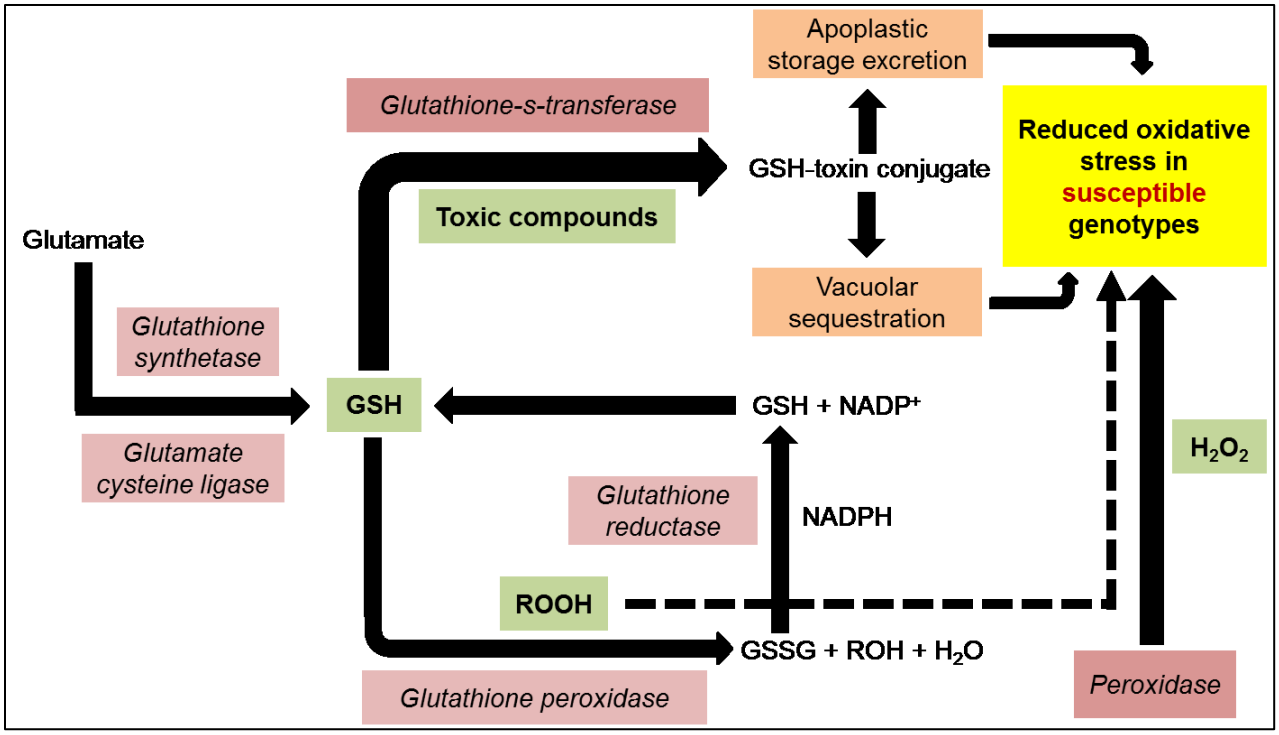

Figure 4.8. Proposed cellular antioxidative mechanism of charcoal-rot-susceptible sorghum genotype, Tx7000 after *M. phaseolina* infection. GSH = reduced glutathione, GSSG = oxidized glutathione, ROOH = hydroperoxide, ROH = alcohol. *Pink box* = up-regulation/increased activity, *green box* = reduced quantity. Transcriptional and functional data suggested a general enhancement of Tx7000 antioxidative machinery to impede the strong oxidative stress after *M. phaseolina* infection.

Chapter 5 - *Macrophomina phaseolina* promotes stalk tissue degradation in charcoal-rot-susceptible sorghum genotypes through induced host cell wall degrading enzymes

ABSTRACT

Macrophomina phaseolina (MP) is an important necrotrophic fungus that causes charcoal rot disease in *Sorghum bicolor* (L.) Moench. An RNA-Seq experiment revealed MP's ability to significantly up-regulate host cell wall degrading enzyme (CWDE) genes (pectinesterase, polygalacturonase, cellulase, endoglucanase, and glycosyl hydrolases) in a charcoal-rot-susceptible sorghum genotype (Tx7000), but not in a resistant genotype (SC599). Crude enzyme mixtures were extracted from MP- and mock-inoculated susceptible (Tx7000, BTx3042) and resistant (SC599, SC35) sorghum genotypes for functional validations. A gel diffusion assay (pectin substrate) revealed significantly increased pectinesterase activity in MP-inoculated Tx7000 and BTx3042. Polygalacturonase activity was determined using ruthenium red absorbance assay (535 nm). A significantly increased polygalacturonase activity was observed in two susceptible genotypes after MP inoculation. The activity of cellulose degrading enzymes was determined using 2-cynoacetamide fluorimetric assay (excitation and emission maxima at 331 and 383 nm, respectively). Assay revealed significantly increased cellulose degrading enzyme activity in MP-inoculated Tx7000 and BTx3042. Although necrotrophs such as MP can produce their own CWDEs to facilitate the infection process and are known as virulence factors, findings of the current study revealed the MP's ability to promote charcoal rot susceptibility in grain sorghum through induced host CWDEs.

Keywords: Sorghum, *Macrophomina phaseolina*, charcoal rot, cell wall degrading enzymes, cellulase, endoglucanase, glycosyl hydrolase, polygalacturonase, pectinesterase.

INTRODUCTION

The plant cell wall can be considered as an exoskeleton that protects the cell protoplast. It is made up of a highly integrated and structurally complex network of polysaccharides, including cellulose, hemicelluloses, and pectin (Cosgrove, 2005). The cellulose microfibrils are embedded in a matrix of pectin, hemicellulose, lignin, and structural proteins (Cosgrove, 2005; Rose et al., 2004). The cell wall is a dynamic structure that is regularly modified in response to various environmental cues. For example, upon pathogen attack, plants often deposit callose rich cell wall appositions (i.e. papillae) at penetration sites, accumulate phenolic compounds and various toxins in the wall, and synthesize lignin-like polymers to reinforce the wall (Huckelhoven, 2007). Therefore, the plant cell wall is a significant defensive barrier that pathogens encounter before facing intracellular plant defense machinery (Lipka et al., 2005; Underwood & Somerville, 2008; Hematy et al., 2009; Underwood, 2012).

Although the cell wall poses a significant barrier for pathogen entrance, plant pathogens (esp. necrotrophs) have mechanisms to overcome this barrier. To breach the cell wall and use plant cell walls nutritionally, pathogens secrete a diverse array of degradative enzymes, including laccases, proteases, exo- and endopolygalacturonases, pectin methylesterases, pectin lyases and pectate lyases, acetyl esterases, xylanases, and a variety of endoglucanases that cleave cellulose, xyloglucan, and other glucans (Esquerre-Tugaye et al., 2000; Kars et al., 2005; Di Matteo et al., 2006; Lebeda et al., 2001). Studies have revealed a positive correlation between certain CWDEs and virulence of the necrotroph pathogen *B. cinerea*, the wilt pathogen *V. dahliae*, and the blotch fungus *Mycosphaerella graminicola*, among others (Brito et al., 2006; Espino et al., 2005; Fernandez-Acero et al., 2010; Kema et al., 2008). When the *Arabidopsis thaliana* is infected with *Ustilago maydis*, pathogen genes responsible for the degradation of cellulose, including an endoglucanase, and for the degradation of hemicellulose, including an arabinofuranosidase and a xylanase, are up-regulated (Martinez-Soto et al., 2013). An endopolygalacturonase gene, Bcpg1 is required by *Botrytis cinerea* for full virulence of on different hosts (Have et al., 1998) and *Alternaria citri* for citrus fruit (Isshiki et al., 2001). A *Claviceps purpurea* strain with two deleted polygalacturonase genes (cppg1 and cppg2) is nonpathogenic on rye (Oeser et al., 2002). In the rice blast fungus *Magnaporthe oryzae*, transcript levels of genes encoding cellulases,

hemicellulases, and pectate lyases increase during infection, relative to a minimal media control (Mathioni et al., 2011).

As a countermeasure, plants produce proteins which can inhibit microbial CWDEs thus protect their cell walls from hydrolytic attacks. A large number of plant proteins have been isolated that can inhibit the activity of a variety of CWDEs including polygalacturonase inhibitors (PGIPs), pectin methylesterases inhibitors (PMEI), pectin lyase inhibitor protein (PNLIP), *Triticum aestivum* xylanase inhibitor (TAXI), xylanase inhibitor protein (XIP), and xyloglucan endoglucanase inhibiting protein (XEGIP) (Juge N, 2006; De Lorenzo et al., 2001). The pectin degrading enzyme inhibitors are common in dicots and noncommelinoid monocots while the xylan degrading enzyme inhibitors are common in grasses (Sarkar et al., 2009). While inhibitors like PGIPs do not hinder the plants' own polygalacturonases (Cervone et al., 1990), some inhibitors can only inhibit the enzymes of plant origin. For instance, PMEIs inhibit pectin methylesterases of plant origin but typically do not inhibit pectin methylesterases produced by plant pathogens (D'Avino et al., 2003; Giovane et al., 2004; Di Matteo et al., 2005). However, the inhibition of plant CWDEs can still contribute to reduced susceptibility to necrotrophs. For example, the overexpression of PMEIs in *Arabidopsis* limits fungal infection by *Botrytis cinerea* by decreasing plant PME activity and altering the level of pectin methylesterification of the cell wall (Lionetti et al., 2007). Other than deactivating fungal CWDEs, inhibitors can also play an important role in eliciting plant defense reposes. For example, impaired fungal polygalacturonase activity by PGIPs results in accumulation of long-chain oligogalacturonides, which are capable of eliciting defense responses in plants (Cervone et al., 1989; Ridley et al., 2001).

Macrophomina phaseolina (Tassi) Goid is a globally important, soil borne, necrotrophic fungal pathogen that causes numerous diseases in over 500 different plant species (Islam et al., 2012), including major food crops (Su et al., 2001), pulse crops (Mayek-Pe´rez et al., 2001), fiber crops [jute (De et al., 1992), cotton (Aly et al., 2007)] and oil crops (Wyllie, 1998). Charcoal rot disease caused by *M. phaseolina* is an economically important disease in many crops including sorghum, soybean, maize, alfalfa, and jute (Islam et al., 2012). Charcoal rot in sorghum is characterized by degradation of pith tissue at or near the base of the stalk causing death of stalk pith cells (Edmunds, 1964). Infected plants often have damaged vascular and cortical tissues in

both the root and stalk systems that may reduce nutrient and water absorption and translocation (Hundekar and Anahosur, 2012). Recent studies revealed the negative impacts of charcoal rot disease on grain (Bandara et al., 2017a; Bandara et al., 2016) and sweet (Bandara et al., 2017b) sorghum production. Through genome analysis, Islam et al. (2012) showed that the *M. phaseolina* genome contains genes that can encode for 219 glycoside hydrolase related proteins and 16 polysaccharide lyase proteins. Some studies have shown the *M. phaseolina*'s ability to produce CWDEs under in vitro conditions (Ramos et al., 2016).

Although necrotrophs such as *M. phaseolina* use their own CWDEs as virulence factors during the infection and colonization, potential of necrotroph-infection associated up-regulation of host CWDEs and their contribution to enhanced disease susceptibility are poorly described. Here, we make use of the RNA-Seq data outlined in the Chapter 2 to further investigate the differentially expressed genes that are associated with host CWDEs and their inhibitors. As RNA-Seq data provided evidence on enhanced CWDEs transcript up-regulation in charcoal-rot-susceptible sorghum genotype (Tx7000) after *M. phaseolina* inoculation, the major objective of the current study was to confirm the transcriptional inferences using follow up functional/biochemical studies in relation to cellulase, polygalacturonase, and pectin methylesterase activities of known resistant (SC599, SC35) and susceptible (Tx7000, BTx3042) sorghum genotypes in response to *M. phaseolina* inoculation.

MATERIALS AND METHODS

Plant materials

A different set of plants with the same treatment and design structure (mentioned in the Chapter 3) were used to obtain stalk tissues for the functional investigations outlined in the current Chapter. Tissue collection and storage were also performed according to the methods described in the Chapter 3.

Preparation of tissue lysates for functional assays, and absorbance/fluorescence measurement

In a mortar, 1 g of stalk tissues (1 cm away from the symptomatic region) was chopped in to liquid nitrogen using a sterile scalpel. The stalk pieces were ground into a powder using a pestle. Approximately 200 mg of this tissue powder was transferred into microcentrifuge tubes filled with 1 ml of 1 X lysis buffer (10 mM Tris, pH 7.5, 150 mM NaCl, 0.1 mM EDTA). Samples were centrifuged at 10,000 g for 10 min at 4°C. Supernatants were transferred into new microcentrifuge tubes and stored at -80°C until used in assays. All absorption/fluorescence measurements were performed using a 96-well plate reader (Synergy H1 Hybrid Reader; BioTek, Winooski, VT, USA) at specified wavelengths (see below). All enzyme activities were expressed per g of stalk tissues. All enzyme assays were repeated once.

Measuring the cumulative activity of cellulose degrading enzymes

A 2-cyanoacetamide-based protocol, described by Honda et al. (1980), was used with modifications to measure the cumulative activity of cellulose degrading enzymes in cell extracts. 2-cyanoacetamide reacts with reducing carbohydrates such as glucose in borate buffer to give strong fluorescence. Its excitation and emission maxima are at 331 and 383 nm, respectively. The borate-phosphate buffer (BP; pH 8.0, 5 mL) was prepared from 0.3 M sodium tetraborate and 0.3 M potassium dihydrogen phosphate. Determination of the cellulase enzyme activity of cell extracts (samples) was carried out using carboxymethyl cellulose (CMC) as the substrate. CMC is degraded by enzymes such as cellulases, endoglucanases, glucan endo-1,3-beta-glucosidases, and glycosyl hydrolases into glucose. Glucose reacts with 2-cyanoacetamide and fluoresces. The glucose naturally present in each sample was determined first without adding CMC. These baseline values (0.5 × value) were subtracted from respective samples with added CMC to determine the glucose coming from CMC only. This glucose concentration is proportional to the cellulase activity of the sample. To develop a calibration curve, glucose (Sigma, USA) was dissolved in borate-phosphate buffer to obtain 0, 200, 400, 600, and 800 mg L^{-1} standard solutions. Reaction components were mixed in microcentrifuge tubes according to the following table (in µl).

Glucose standard	Sample	CMC	2-cyanoacetamide	BP	1X lysis buffer
For calibration curve					
5	0	0	50	200	0
Assessment of the original glucose content of the sample					
0	5	0	50	200	0
Assessment of the glucose coming from CMC due to enzyme activity					
0	2.5	2.5	50	200	0
Blank					
0	0	2.5	50	200	2.5

Tubes were incubated in a boiling water bath for 30 min. After cooling the tubes to room temperature, 200 µl of reaction mixture from each tube was transferred to clear flat-bottom 96-well microplate and fluorescence was measured. Using the calibration curve, the cellulose degrading enzyme activity of samples were determined and expressed as relative units (RU). One RU was defined as the amount of glucose (mg/mL) generated by the crude enzyme mixture extracted from 1 g of stalk tissue through CMC hydrolysis.

Measuring polygalacturonase (PG) activity

PG activity of cell extracts was quantified according to the protocol described by Ortiz et al. (2014) with some modifications. This assay is based on the reaction between polygalacturonic acid and ruthenium red. Upon precipitation of high molecular weight polygalacturonic acid by ruthenium red, the optical density (OD) of the remaining ruthenium red is determined. The reduction in OD between blank and sample is used as a measure of PG activity, i.e. the higher the PG activity, the higher the polygalacturonic acid hydrolysis, thus less polygalacturonic acid is available to precipitate with ruthenium red. Therefore, the OD reduction is less. In the current assay, a 0.2% polygalacturonic acid-sodium salt stock solution was prepared in citrate phosphate buffer (50 mM, pH 5.0). This solution was obtained by dissolving 0.2 g of polygalacturonic acid-sodium salt (Sigma–Aldrich, Germany) in citric acid solution and then adjusting the pH to 5.0 with dibasic sodium phosphate. Polygalacturonic acid-sodium salt, citrate phosphate buffer, 1X lysis buffer (see B (i) section above) and crude enzyme samples were mixed in microcentrifuge tubes according to the following table (in µl) and kept on ice.

0.2% PGA	BCP	1X lysis buffer	Sample
For calibration curve			
10	0	10	0
8	2	10	0
6	4	10	0
4	6	10	0
2	8	10	0
0	10	10	0
Samples			
10	0	0	10
Blank			
0	10	10	0

The reaction tubes were then incubated for 20 min at 40°C in a waterbath. After incubation, the tubes were placed on ice, 40 µl of 1.125 mg/ml ruthenium red aqueous solution was added to each tube, and mixed for 30 s. The mixture was diluted by adding 100 µl of 8 mM NaOH solution, mixed for 30 s, and centrifuged at 4°C and 3200 g for 10 min. For OD quantification, a 25 µl aliquot of the supernatant was transferred to clear flat-bottom 96-well microplate containing 175 µl of water, and absorbance was read at 535 nm. Using the calibration curve, the PG activity of samples were determined and expressed as relative units (RU). One RU was defined as the amount of polygalacturonic acid (µg) hydrolyzed per minute with crude enzyme mixture extracted from 1g of stalk tissue.

Measuring pectin methylesterase activity

Pectin methylesterase activity was quantified by the gel diffusion assay as described by Downie et al. (1998) with some modifications. The medium contained 1% agar, 0.05% citrus pectin (Sigma, USA), 10 mM phosphate buffered saline (pH 7.2), and 10 mM EDTA. Each petri plate (90 mm diameter) contained 15 ml of medium. Wells with a diameter of 4 mm were made in center of the agar plates using a sterile cork borer, and the protein samples were loaded in each well. Plates were incubated at 30˚C for 16 h. The gels were stained with 0.05% (w/v) ruthenium red for 45 min and destained with water. The pectin methylesterase activity appeared as dark red areas against a light red background. The diameter of the red stained areas resulting from the hydrolysis of esterified pectin in the gel was measured. Pectin methylesterase activity was

expressed in relative units (RU; 1 RU = 10 mm of dark red areas). The radius of the red-stained zone increased with increasing quantities of pectin methylesterase.

RESULTS

Differential expression of genes related to host CWDEs in response to *M. phaseolina* infection

Table 5.1 provides a summary of the differentially expressed host CWDE genes between two sorghum genotypes after *M. phaseolina* inoculation. Differential gene expression analysis revealed fifteen and 34 CWDE genes (involved in cellulose and homogalacturonan degradation) that were differentially expressed between SC599 and Tx7000 in response to pathogen inoculation at 2 and 7 DPI, respectively. Moreover, three and thirteen genes that are related to cellulose biosynthesis were differentially expressed between two genotypes after pathogen inoculation at 2 and 7 DPI, respectively. None of the CWDEs or cellulose biosynthetic genes was differentially expressed at 30 DPI.

Of the fifteen differentially expressed CWDEs genes at 2 DPI, twelve are involved in cellulose degradation. These included cellulase (1), endoglucanase (3), glucan endo-1,3-β-glucosidase precursor (2), and glycosyl hydrolase family 17 (6). The net log2 fold up-regulation of these 12 genes in Tx7000 was 11.5 whereas the net down-regulation in SC599 was 3.9. The remaining three genes were related to homogalacturonan degradation. These included two polygalacturonase (PG) genes and an invertase/pectin methylesterase (PME) inhibitor family protein. The net up- and down- regulation of the two PG genes in Tx7000 and SC599 were 2.4 and 3.8, respectively. The PME inhibitor family protein gene was significantly up-regulated in SC599 while that of Tx7000 was not significantly differentially expressed. In addition, three cellulose biosynthesis related genes were differentially expressed at 2 DPI. These included CESA2-cellulose synthase, CSLA4-cellulose synthase-like family A, and CSLE6-cellulose synthase-like family E. The net up- and down- regulation of these three genes in Tx7000 and SC599 were 3.7 and 1.7, respectively.

Thirty-four CWDE genes were differentially expressed at 7 DPI. These included twelve cellulose degradation related genes including cellulase (1), endoglucanase (1), glucan endo-1,3-β-glucosidase precursor (2), and glycosyl hydrolases family 17 (8). The net log2 fold up-regulation of these twelve genes in Tx7000 was 33.2 while the net down-regulation in SC599 was 5.5. The remaining 22 genes were related to homogalacturonan degradation. These genes included PME (6), PG (9), PME/invertase inhibitor family protein (6), and a PME inhibitor domain containing protein. The net up- and down-regulation of the six PME genes in Tx7000 and SC599 were 14.3 and 3.1, respectively. The nine PG genes showed a 3.2 net log2 fold up-regulation in Tx7000 while none were significantly differentially expressed in SC599. The net up- and down-regulation of the six PME inhibitor family protein genes in Tx7000 and SC599 were 9.8 and 2.5, respectively. The PME inhibitor domain containing protein gene was also significantly up-regulated in Tx7000 while that of SC599 was not significantly differentially express. The 13 cellulose biosynthesis related genes included five cellulose synthase genes (CESA2, CESA3, CESA4, CESA7, CESA9,) and eight cellulose synthase-like genes (CSLA4, CSLA7, CSLC1, CSLC7, CSLE2, CSLF2, CSLF6, and CSLH1). The net down- and up- regulation of the five cellulose synthase genes in Tx7000 and SC599 were 15.4 and 2.2, respectively while the same for eight cellulose synthase-like genes were 4.0 and 1.1, respectively.

Analysis of variance for enzyme assays

Table 5.2 provides the F and *P*-values from analysis of variance (ANOVA) for the enzyme assays conducted in this study. The genotype by treatment interaction effect was found to be significant for all enzymes investigated (cellulase, PG, and PME) at 4, 7, and 10 DPI ($\alpha = 0.05$).

Dynamics of sorghum CWDEs under *M. phaseolina* inoculation

Compared to the control treatment, *M. phaseolina* inoculation significantly increased the activity of the cellulose degradation enzymes in two charcoal-rot-susceptible genotypes at 4 (Tx7000: 77%, $P < 0.0001$; BTx3042: 102%, $P = 0.0006$), 7 (Tx7000: 70%, $P = 0.0098$; BTx3042: 48%, $P = 0.0011$), and 10 (Tx7000: 39%, $P = 0.0196$; BTx3042: 75%, $P = 0.0005$) DPI (Figure 5.1). However, pathogen inoculation did not significantly affect the activity of cellulose degrading enzymes in SC599 and SC35 at any post inoculation stage.

Compared to the control treatment, *M. phaseolina* inoculation significantly increased the PG activity in both charcoal-rot-susceptible genotypes at 4 (Tx7000: 149%, $P = 0.0007$; BTx3042: 196%, $P = 0.0218$), 7 (Tx7000: 209%, $P = 0.0057$; BTx3042: 102%, $P < 0.0001$), and 10 (Tx7000: 127%, $P = 0.0030$; BTx3042: 139%, $P < 0.0001$) DPI (Figure 5.2). Although pathogen inoculation did not significantly affect the PG activity of SC599 at 4 DPI, inoculation significantly decreased PG activity at 7 (-53%, $P = 0.0460$) and 10 (-51%, $P = 0.0147$) DPI. Although pathogen inoculation did not significantly affect the PG activity of SC35 at 4 and 7 DPI, inoculation significantly decreased PG activity at 10 DPI (-56%, < 0.0001).

Compared to the control treatment, *M. phaseolina* inoculation significantly increased the PME activity of two charcoal-rot-susceptible genotypes at 4 (Tx7000: 29%, $P = 0.0046$; BTx3042: 62%, $P = 0.0005$), 7 (Tx7000: 26%, $P = 0.0113$; BTx3042: 24%, $P = 0.0136$), and 10 (Tx7000: 58%, $P = 0.0067$; BTx3042: 33%, $P = 0.0202$) DPI (Figure 5.3). Pathogen inoculation did not significantly affect the PME activity of SC599 and SC35 at any post-inoculation stage, except for the significantly decreased PME activity of SC599 (-22%, $P = 0.0081$) at 4 DPI.

DISCUSSION

Host tissue penetration is a prerequisite for infection and pathogens use physical (appressoria) and chemical (CWDEs) means to facilitate penetration. The enormous turgor pressure generated through appressorium results in a strong physical force on the phylloplane which enables the fungus to breach the cuticle and cell wall (Choi et al., 2011; Park et al., 2009). CWDEs usually play a supplementary role in the penetration of pathogens that can produce highly melanized appressoria (Linsel et al., 2011; Yi et al., 2008). For example, as *Botrytis cinerea* do not possess thick melanin layer in its appressoria, the penetration is accomplished by the release of CWDEs that digest the host cell wall rather than by physical force (Choquer et al., 2007). In fact, many plant pathogenic fungi, especially necrotrophs, rely on the manufacture of CWDEs to enter plant tissue (Łaźniewska et al., 2012). Although the appressoria production by *M. phaseolina* is reported (Ammon et al., 1975), penetration of interior cell walls has been shown to be a result of both mechanical pressure (appressoria) and chemical softening (by CWDEs) (Ammon et al., 1974). In fact, Islam et al. (2012) have recently shown that *M. phaseolina* genome contains genes that can encode for 219 glycoside hydrolase related proteins and 16 polysaccharide lyase

proteins. Ramos et al. (2016) have shown the *M. phaseolina*'s ability to produce CWDEs under in vitro conditions. Therefore, CWDEs appeared to be virulence factors for *M. phaseolina*. In the current study, we provide gene expression and functional evidences on the ability of *M. phaseolina* to induce CWDEs in charcoal-rot-susceptible sorghum genotypes.

Cellulose is an integral component of plant cell walls and the conversion of cellulose polymers into simple sugars such as glucose requires the use of cellulases. Cellulase is comprised of three distinct classes of enzymes (endoglucanases, cellobiohydrolases, and β-glucosidases) that act synergistically to break down the cellulose polymer (Yennamalli et al., 2013). These cellulases are also categorized under a broader enzyme group called glycosyl hydrolases (Yennamalli et al., 2013). In the current study, compared to mock inoculated controls, the cellulose degradation capacity (including cellulase, endoglucanase, glucan endo-1,3-β-glucosidase precursor, and glycosyl hydrolase family 17) was found to be significantly greater in charcoal-rot-susceptible genotypes (Tx7000, BTx3042) after *M. phaseolina* inoculation while the same was significantly lower in the two resistant genotypes (SC599, SC35). Therefore, pathogen inoculation-associated host CWDEs transcripts and augmented activity appeared to contribute to enhanced charcoal rot susceptibility in grain sorghum.

Cellulose deficiency in the primary cell wall elicits jasmonic acid signalling and enhances resistance to some bacteria, fungi and aphids (Ellis et al., 2002a; Ellis et al., 2002b). Further, mutations of certain *cellulose synthase* genes result in activation of jasmonic acid signaling (Ellis and Turner, 2001; Ellis et al., 2002a; Ellis et al., 2002b). Moreover, the oligosaccharides generated by cell wall degrading enzymes can act as elicitors to trigger jasmonic acid pathways (Aziz et al., 2007; Aziz et al., 2004; Moscatiello et al., 2006). In the current study, although cellulose synthase and cellulose synthase-like genes showed net up-regulation in *M. phaseolina*-inoculated Tx7000 at 2 DPI, a net down-regulation was observed at 7 DPI. This revealed the potential cellulose deficiency faced by Tx7000 after pathogen inoculation at 7 DPI. Although not tested, this deficiency should contribute to enhanced jasmonic acid biosynthetic capacity of Tx7000. However, in Chapter 6, we demonstrated that the jasmonic acid biosynthetic capacity of the charcoal-rot-susceptible genotype, Tx7000 decreases after *M. phaseolina* inoculation, despite the impeded cellulose biosynthesis.

In addition to enhanced cellulose degradation, the current study provided gene expression and functional evidence for enhanced homogalacturonan degradation (though up-regulated PME and PGU activity) in charcoal-rot-susceptible sorghum genotypes after *M. phaseolina* inoculation. PMEs catalyze the demethylesterification of homogalacturonan. If this occurs on non-contiguous sugars (i.e. random demethylesterification), the molecule becomes a substrate for pectin degrading enzymes, leading to cell wall disintegration (Micheli, 2001; Pelloux et al., 2007). In addition, the action of PMEs makes homogalacturonan vulnerable to degradation by hydrolases such as PGUs, contributing to the softening of the cell wall (Brummell and Harpster, 2001; Wakabayashi et al., 2003). Therefore, the increased PME activity observed in pathogen inoculated Tx7000 and BTx3042 may contribute to enhanced charcoal rot disease susceptibility. However, it is important to note that if the PME mediated demethylesterification occurs on contiguous sugar residues (i.e. blockwise demethylesterification), Ca^{2+} bonds can form between pectin molecules, which results in rigid cell walls (Micheli, 2001; Pelloux et al., 2007). If this is the case with Tx7000 and BTx3042, their enhanced PME activity upon *M. phaseolina* inoculation should be viewed as a mechanism of cell wall reinforcement which in turn impedes the ability of the pathogen to penetrate and should be contributed to reduced disease susceptibility. Therefore, more specific experiments are needed to determine the role of PMEs in the sorghum-*Macrophomina* interaction. However, the net up-regulation of PME inhibitors (PMEIs) in Tx7000 after pathogen inoculation, particularly at 7 DPI, indirectly suggests that host-derived PME results in cell wall disintegration rather than reinforcement. Therefore, PME may contribute to enhanced charcoal rot disease susceptibility whereas PMEIs contribute to reduced disease susceptibility. The PMEIs can play a major role in pathogenesis by influencing the susceptibility of the wall to cell wall degrading enzymes (Cole et al., 1998; De Lorenzo et al., 2001; D'Ovidio et al., 2004).

Some CWDE inhibitors may play other roles in defense responses. For example, pepper pectin methylesterase inhibitor protein (CaPMEI1) shows antifungal properties against necrotrophic fungi such as *F. oxysporum* f.sp. *matthiole*, *A. brassicicola*, and *B. cinerea* by delaying their spore germination and hyphal development (An et al., 2008). If this occures with the sorghum-*Macrophomina* pathosystem, it may be possible that Tx7000 attempts to reduce its susceptibility to disease by overexpressing PMEIs and restricting *M. phaseolina* spread.

The oligosaccharides generated by cell wall degrading enzymes can act as elicitors that trigger plant defences (Aziz et al., 2007). Treatment of plants with these oligosaccharides can trigger the production of reactive oxygen species (ROS) (Aziz et al., 2004; Moscatiello et al., 2006). Moreover, the degradation of homogalacturonan (the main component of pectin) by polygalacturonases results in oligogalacturonide release in *Arabidopsis* under *B. cinerea* infection and induces a robust NADPH oxidase (AtrbohD)-dependent oxidative burst (Galletti et al., 2008). In the current study, we observed significantly higher CWDE activity in *M. phaseolina*-inoculated charcoal-rot-susceptible sorghum genotypes. It is possible that these genotypes accumulate more oligosaccharides and oligogalacturonides, which results in enhanced ROS production. ROS can in turn trigger cell death and contribute to increased susceptibility to any necrotrophic pathogen such as *M. phaseolina*. In Chapter 3, we showed that charcoal-rot-susceptible sorghum genotypes tend to over-accumulate ROS upon *M. phaseolina* inoculation.

CONCLUSIONS

CWDEs are involved in plant growth and development. Plant pathogens, particularly the necrotrophs, also produce and secrete plant CWDEs to facilitate the host penetration and subsequent infection. Our current findings showed the ability of *M. phaseolina* to manipulate host CWDEs which may result in induced stalk cell wall degradation of charcoal-rot-susceptible sorghum genotypes. Although *M. phaseolina* has the capacity to produce its own CWDEs, its ability to induce host derived CWDEs could be an evolutionary stable virulence strategy. As sorghum (all plants in general) cannot avoid producing CWDEs due to associated fitness cost, *M. phaseolina* appears to take advantage of deploying the plant's own CWDEs to promote charcoal rot disease susceptibility in grain sorghum.

REFERENCES

Aly AA, Abdel-Sattar MA, Omar MR, Abd-Elsalam KA. 2007. Differential antagonism of *Trichoderma* sp. against *Macrophomina phaseolina*. *Journal of Plant Protection Research* 47: 91-102.

Ammon V, Wyllie TD, Brown MF. 1975. Investigation of the infection process of *Macrophomina phaseolina* on the surface of soybean roots using scanning electron microscopy. *Mycopathologia* 55: 77-81.

Ammon V, Wyllie TD, Brown MF. 1974. An ultrastructural investigation of pathological alterations induced by *Macrophomina phaseolina* (Tassi) Goid in seedlings of soybean, *Glycine max* (L.) Merrill. *Physiological Plant Pathology* 4: 1-2.

An SH, Sohn KH, Choi HW, Hwang IS, Lee SC, Hwang BK. 2008. Pepper pectin methylesterase inhibitor protein CaPMEI1 is required for antifungal activity, basal disease resistance and abiotic stress tolerance. *Planta* 228: 61-78.

Aziz A, Gauthier A, Bezier A, Poinssot B, Joubert JM, Pugin A, Heyraud A, Baillieul F. 2007. Elicitor and resistance-inducing activities of β-1,4 cellodextrins in grapevine, comparison with β-1,3 glucans and α-1,4 oligogalacturonides. *Journal of Experimental Botany* 58: 1463-1472.

Aziz A, Heyraud A, Lambert B. 2004. Oligogalacturonide signal transduction, induction of defense-related responses and protection of grapevine against *Botrytis cinerea*. *Planta* 218: 767-774.

Bandara YMAY, Weerasooriya DK, Tesso TT, Prasad PVV, Little CR. 2017a. Stalk rot fungi affect grain sorghum yield components in an inoculation stage-specific manner. *Crop Protection* 94: 97-105.

Bandara YMAY, Weerasooriya DK, Tesso TT, Little CR. 2017b. Stalk rot diseases impact sweet sorghum biofuel traits. *BioEnergy Research* 10: 26-35.

Bandara YMAY, Weerasooriya DK, Tesso TT, Little CR. 2016. Stalk rot fungi affect leaf greenness (SPAD) of grain sorghum in a genotype-and growth-stage-specific manner. *Plant Disease* 100: 2062-2068.

Bandara YMAY, Perumal R, Little CR. 2015. Integrating resistance and tolerance for improved evaluation of sorghum lines against Fusarium stalk rot and charcoal rot. *Phytoparasitica* 43: 485-499.

Benjamini Y, Hochberg Y. 1995. Controlling the false discovery rate: a practical and powerful approach to multiple testing. *Journal of the Royal Statistical Society: Series B (Methodological)* 57: 289-300.

Brito N, Espino JJ, Gonzalez C. 2006. The endo-β-1,4-xylanase xyn11A is required for virulence in *Botrytis cinerea*. *Molecular Plant-Microbe Interaction* 19: 25-32.

Brummell DA, Harpster MH. 2001. Cell wall metabolism in fruit softening and quality and its manipulation in transgenic plants. *Plant Molecular Biology* 47: 311-340.

Cervone F, De Lorenzo G, Pressey R, Darvill AG, Albersheim P. 1990. Can *Phaseolus* PGIP inhibit pectic enzymes from microbes and plants? *Phytochemistry* 29: 447-449.

Cervone F, Hahn MG, De Lorenzo G, Darvill A, Albersheim P. 1989. Host-pathogen interactions: XXXIII. A plant protein converts a fungal pathogenesis factor into an elicitor of plant defense responses. *Plant Physiology* 90: 542-548.

Choi J, Kim KS, Rho HS, Lee YH. 2011. Differential roles of the phospholipase C genes in fungal development and pathogenicity of *Magnaporthe oryzae*. *Fungal Genetics and Biology* 48: 445-455.

Choquer M, Fournier E, Kunz C, Levis C, Pradier JM. 2007. *Botrytis cinerea* virulence factors: new insights into a necrotrophic and polyphageous pathogen. *FEMS Microbiology Letters* 277: 1-10.

Cole L, Dewey FM, Hawes CR. 1998. Immunocytochemical studies of the infection mechanisms of *Botrytis fabae*. *New Phytologist* 139: 611-622.

Cosgrove DJ. 2005. Growth of the plant cell wall. *Nature Reviews Molecular Cell Biology* 6: 850-861.

D'Avino R, Camardella L, Christensen TM, Giovane A, Servillo L. 2003. Tomato pectin methylesterase: modeling, fluorescence, and inhibitor interaction studies-comparison with the bacterial (*Erwinia chrysanthemi*) enzyme. *Proteins* 53: 830-839.

D'Ovidio R, Mattei B, Roberti S, Bellincampi D. 2004. Polygalacturonases, polygalacturonase-inhibiting proteins and pectic oligomers in plant-pathogen interactions. *Biochimica et Biophysica Acta* 1696: 237-244.

De BK, Chattopadhya SB, Arjunan G. 1992. Effect of potash on stem rot diseases of jute caused by *Macrophomina phaseolina*. *Journal of Mycopathological Research* 30: 51-55.

De Lorenzo G, D'Ovidio R, Cervone F. 2001. The role of polygalacturonase-inhibiting proteins (PGIPs) in defense against pathogenic fungi. *Annual Review of Phytopathology* 39: 313-335.

Di Matteo A, Bonivento D, Tsernoglou D, Federici L, Cervone F. 2006. Polygalacturonase-inhibiting protein (PGIP) in plant defence: a structural view. *Phytochemistry* 67: 528-533.

Dingle J, Reid WW, Solomons GL. 1953. The enzyme degradation of pectin and other polysaccharides. II. Application of the "cup-plate" assay to the estimation of enzymes. *Journal of the Science of Food and Agriculture* 4: 149-155.

Edmunds L. 1964. Combined relation of plant maturity temperature soil moisture to charcoal stalk rot development in grain sorghum. *Phytopathology* 54: 513-517.

Ellis C, Karafyllidis I, Turner JG. 2002. Constitutive activation of jasmonate signaling in an *Arabidopsis* mutant correlates with enhanced resistance to *Erysiphe cichoracearum*, *Pseudomonas syringae*, and *Myzus persicae*. *Molecular Plant-Microbe Interactions* 15: 1025-1030.

Ellis C, Karafyllidis I, Wasternack C, Turner JG. 2002. The *Arabidopsis* mutant cev1 links cell wall signaling to jasmonate and ethylene responses. *Plant Cell* 14: 1557-1566.

Ellis C, Turner JG. 2001. The *Arabidopsis* mutant cev1 has constitutively active jasmonate and ethylene signal pathways and enhanced resistance to pathogens. *Plant Cell* 13: 1025-1033.

Espino JJ, Brito N, Noda J, Gonzalez C. 2005. *Botrytis cinerea* endo-β-1,4-glucanase Cel5A is expressed during infection but is not required for pathogenesis. *Physiological and Molecular Plant Pathology* 66: 213-221.

Esquerre-Tugaye MT, Boudart G, Dumas B. 2000. Cell wall degrading enzymes, inhibitory proteins, and oligosaccharides participate in the molecular dialogue between plants and pathogens. *Plant Physiology and Biochemistry* 38: 157-163.

Fernandez-Acero FJ, Colby T, Harzen A, Carbu M, Wieneke U, Cantoral JM, Schmidt J. 2010. 2-DE proteomic approach to the *Botrytis cinerea* secretome induced with different carbon sources and plant-based elicitors. *Proteomics* 10: 2270-2280.

Galletti R, Denoux C, Gambetta S, Dewdney J, Ausubel FM, De Lorenzo G, Ferrari S. 2008. The AtrbohD-mediated oxidative burst elicited by oligogalacturonides in *Arabidopsis* is dispensable for the activation of defense responses effective against *Botrytis Cinerea*. *Plant Physiology* 148: 1695-1706.

Goodstein DM, Shu S, Howson R, Neupane R, Hayes RD, Fazo J, Mitros T, Dirks W, Hellsten U, Putnam N, Rokhsar DS. 2012. Phytozome: a comparative platform for green plant genomics. *Nucleic Acids Research* 40: 1178-1186.

Honda S, Matsuda Y, Takahashi M, Kakehi K, Ganno S. 1980. Fluorimetric determination of reducing carbohydrates with 2-cyanoacetamide and application to automated analysis of carbohydrates as borate complexes. *Analytical Chemistry* 52: 1079-1082.

Hematy K, Cherk C, Somerville S. 2009. Host-pathogen warfare at the plant cell wall. *Current Opinion in Plant Biology* 12: 406-413.

Huckelhoven R. 2007. Cell wall-associated mechanisms of disease resistance and susceptibility. *Annual Review of Phytopathology* 45: 101-127.

Hundekar A, Anahosur K. 2012. Pathogenicity of fungi associated with sorghum stalk rot. *Karnataka Journal of Agricultural Sciences* 7: 291-295.

Isshiki A, Akimitsu K, Yamamoto M, Yamamoto H. 2001. Endopolygalacturonase is essential for citrus black rot caused by *Alternaria citri* but not brown spot caused by *Alternaria alternata*. *Molecular Plant-Microbe Interactions* 14: 749-757.

Islam MS, Haque MS, Islam MM, Emdad EM, Halim A, Hossen QMM, Hossain MZ, Ahmed B, Rahim S, Rahman MS, Alam MM. 2012. Tools to kill: genome of one of the most destructive plant pathogenic fungi Macrophomina phaseolina. *BMC Genomics* 13: 493.

Juge N. 2006. Plant protein inhibitors of cell wall degrading enzymes. *Trends in Plant Science* 11: 359-367.

Kema GH, van der Lee TA, Mendes O, Verstappen EC, Lankhorst RK, Sandbrink H, van der Burgt A, Zwiers LH, Csukai M, Waalwijk C. 2008. Large-scale gene discovery in the *Septoria*

tritici blotch fungus *Mycosphaerella graminicola* with a focus on in planta expression. *Molecular Plant-Microbe Interactions* 21: 1249-1260.

Łaźniewska J, Macioszek VK, Kononowicz AK. 2012. Plant-fungus interface: the role of surface structures in plant resistance and susceptibility to pathogenic fungi. *Physiological and Molecular Plant Pathology* 78: 24-30.

Lebeda A, Luhová L, Sedlářová M, Jančová D. 2001. The role of enzymes in plant–fungal pathogens interactions. *Journal of Plant Diseases and Protection* 108: 89-111.

Linsel KJ, Keiper FJ, Forgan A, Oldach KH. 2011. New insights into the infection process of *Rhynchosporium secalis* in barley using GFP. *Fungal Genetics and Biology* 48: 124-131.

Lionetti V, Raiola A, Camardella L, Giovane A, Obel N, Pauly M, Favaron F, Cervone F, Bellincampi D. 2007. Overexpression of pectin methylesterase inhibitors in *Arabidopsis* restricts fungal infection by *Botrytis cinerea*. *Plant Physiology* 143: 1871-1880.

Lipka V, Dittgen J, Bednarek P, Bhat R, Wiermer M, Stein M, Landtag J, Brandt W, Rosahl S, Scheel D, Llorente F. 2005. Pre- and postinvasion defenses both contribute to nonhost resistance in *Arabidopsis*. *Science* 310: 1180-1183.

Martin M. 2011. Cutadapt removes adapter sequences from high-throughput sequencing reads. *EMBnet Journal* 17: 10-12.

Martinez-Soto D, Robledo-Briones AM, Estrada-Luna AA, Ruiz-Herrera J. 2013. Transcriptomic analysis of *Ustilago maydis* infecting *Arabidopsis* reveals important aspects of the fungus pathogenic mechanisms. *Plant Signaling & Behavior* 8: 8, e25059.

Mathioni SM, Belo A, Rizzo CJ, Dean RA, Donofrio NM. 2011. Transcriptome profiling of the rice blast fungus during invasive plant infection and in vitro stresses. *BMC Genomics* 12: 49.

Mayek-Perez N, Lopez-Castaneda C, Lopez-Salinas E, Cumpian-Gutierrez J, Acosta-Gallegos JA. 2001. *Macrophomina phaseolina* resistance in common bean under field conditions in Mexico. *Agrociencia* 46: 649-661.

Micheli F. 2001. Pectin methylesterases: cell wall enzymes with important roles in plant physiology. *Trends in Plant Science* 6: 414-419.

Moscatiello R, Mariani P, Sanders D, Maathuis FJ. 2006. Transcriptional analysis of calcium-dependent and calcium-independent signalling pathways induced by oligogalacturonides. *Journal of Experimental Botany* 57: 2847-2865.

Oeser B, Heidrich PM, Muller U, Tudzynski P, Tenberge, K.B. 2002. Polygalacturonase is a pathogenicity factor in the *Claviceps purpurea*/rye interaction. *Fungal Genetics and Biology* 36: 176-86.

Ortiz GE, Guitart ME, Albertó E, Lahore HMF, Blasco M. 2014. Microplate assay for endo-polygalacturonase activity determination based on ruthenium red method. *Analytical Biochemistry* 454: 33-35.

Park JY, Jin J, Lee YW, Kang S, Lee YH. 2009. Rice blast fungus (*Magnaporthe oryzae*) infects *Arabidopsis* via a mechanism distinct from that required for the infection of rice. *Plant Physiology* 149: 474-486.

Paterson AH, Bowers JE, Bruggmann R, Dubchak I, Grimwood J, Gundlach H, Haberer G, Hellsten U, Mitros T, Poliakov A, Schmutz J. 2009. The *Sorghum bicolor* genome and the diversification of grasses. *Nature* 457: 551-556.

Pelloux J, Rusterucci C, Mellerowicz EJ. 2007. New insights into pectin methylesterase structure and function. *Trends in Plant Science* 12: 267-277.

Ramos AM, Gally M, Szapiro G, Itzcovich T, Carabajal M, Levin L. 2016. In vitro growth and cell wall degrading enzyme production by Argentinean isolates of *Macrophomina phaseolina*, the causative agent of charcoal rot in corn. *Revista Argentina de Microbiología* 48: 267-273.

Ridley BL, O'Neill MA, Mohnen D. 2001. Pectins: structure, biosynthesis, and oligogalacturonide related signaling. *Phytochemistry* 57: 929-967.

Rose JK, Saladie M, Catala C. 2004. The plot thickens: new perspectives of primary cell wall modification. *Current Opinion in Plant Biology* 7: 296-301.

Sarkar P, Bosneaga E, Auer M. 2009. Plant cell walls throughout evolution: towards a molecular understanding of their design principles. *Journal of Experimental Botany* 60: 3615-3635.

Su G, Suh SO, Schneider, R. W., and Russin J.S. 2001. Host specialization in the charcoal rot fungus, *Macrophomina phaseolina*. *Phytopathology* 91: 120-126.

Have AT, Mulder W, Visser J, van Kan JA. 1998. The endopolygalacturonase gene *Bcpg1* is required for full virulence of *Botrytis cinerea*. *Molecular Plant-Microbe Interactions* 11: 1009-1016.

Underwood W. 2012. The plant cell wall: a dynamic barrier against pathogen invasion. *Frontiers in Plant Science* 3: 85.

Underwood W, Somerville SC. 2008. Focal accumulation of defences at sites of fungal pathogen attack. *Journal of Experimental Botany* 59: 3501-3508.

Wakabayashi K, Hoson T, Huber DJ. 2003. Methyl de-esterification as a major factor regulating the extent of pectin depolymerization during fruit ripening: a comparison of the action of avocado (*Persea americana*) and tomato (*Lycopersicon esculentum*) polygalacturonases. *Journal of Plant Physiology* 160: 667-673.

Wyllie TD. 1998. Soybean Diseases of the North Central Region. Pages 106-113 in: Charcoal rot of soybean-current status. T. D. Wyllie and D. H. Scott, eds. American Phytopathological Society, St. Paul, MN, USA.

Yennamalli RM, Rader AJ, Kenny AJ, Wolt JD, Sen TZ. 2013. Endoglucanases: insights into thermostability for biofuel applications. *Biotechnology for Biofuels* 6: 136.

Yi M, Park JH, Ahn JH, Lee YH. 2008. MoSNF1 regulates sporulation and pathogenicity in the rice blast fungus *Magnaporthe oryzae*. *Fungal Genetics and Biology* 45: 1172-1181.

TABLES AND FIGURES

Table 5.1. Significantly ($q < 0.05$) differentially expressed genes (related to cell wall degradation) between SC599 (charcoal-rot-resistant) and Tx7000 (charcoal-rot-susceptible) sorghum genotypes in response to *Macrophomina phaseolina* inoculation at 2 and 7 days post-inoculation.

Metabolic pathway	Gene annotation	Gene	Geno × Trt*	SC599 (MP-CON)†		Tx7000 (MP-CON)	
			q-value	log2 DE‡	q-value	log2 DE	q-value
2 days post-inoculation							
Cellulose degradation	Cellulase	*Sb01g024390*	1.0E-03	-0.559	3.9E-01	2.869	6.5E-03
	Endoglucanase	*Sb06g017600*	1.0E-03	-1.905	1.1E-01	-	-
		Sb02g024050	4.1E-02	2.370	1.1E-08	0.276	7.8E-01
		Sb02g030990	4.6E-06	1.338	1.0E-04	-0.646	2.0E-02
	Glucan endo-1,3-beta-glucosidase precursor	*Sb01g012380*	3.8E-02	-0.172	8.0E-01	1.456	1.2E-02
		Sb02g035460	8.5E-03	-2.994	3.6E-05	0.788	4.7E-01
	Glycosyl hydrolases family 17	*Sb09g018730*	4.9E-02	0.842	9.2E-02	2.445	2.5E-08
		Sb10g020900	1.8E-05	-1.810	2.5E-03	1.727	3.5E-03
		Sb01g009770	1.8E-02	-0.172	8.0E-01	1.404	3.0E-03
		Sb01g041880	2.8E-03	-1.669	6.4E-03	0.876	1.9E-01
		Sb03g045630	3.0E-02	2.594	7.5E-08	0.328	7.4E-01
		Sb04g021700	4.3E-02	-1.740	3.8E-02	-0.020	9.8E-01
Cellulose biosynthesis	CESA2 - cellulose synthase	*Sb03g047220*	1.9E-02	0.354	6.8E-01	2.646	1.4E-04
	CSLA4 - cellulose synthase-like family A	*Sb01g022320*	1.9E-03	-0.200	6.7E-01	0.758	4.5E-03
	CSLE6 - cellulose synthase-like family E	*Sb02g027570*	8.8E-04	-1.858	9.7E-06	0.262	5.6E-01
Homogalacturonan degradation	Polygalacturonase	*Sb09g027150*	1.6E-04	-0.311	5.9E-01	2.325	3.6E-06
	Polygalacturonase	*Sb10g000660*	3.3E-07	-2.099	9.2E-14	1.450	1.2E-02
	Invertase/PME inhibitor family protein	*Sb07g000870*	5.3E-03	1.986	1.5E-09	0.511	3.7E-01
7 days post-inoculation							

Cellulose degradation	Cellulase	*Sb01g024390*	2.0E-06	-1.406	3.9E-01	4.382	4.6E-44
	Endoglucanase	*Sb04g028520*	1.5E-03	0.057	9.9E-01	3.062	5.7E-08
	Glucan endo-1,3-beta-glucosidase precursor	*Sb02g035490*	2.8E-19	-1.529	8.7E-02	5.818	6.4E-33
		Sb05g027690	7.3E-09	-0.326	8.5E-01	3.328	3.5E-17
	Glycosyl hydrolases family 17	*Sb03g045460*	3.3E-03	-0.722	8.2E-01	6.477	6.3E-08
		Sb03g045630	4.4E-02	0.611	8.6E-01	4.007	1.9E-14
		Sb03g045480	5.6E-05	-	-	2.888	2.0E-03
		Sb09g021800	1.1E-04	-1.555	2.1E-01	2.423	1.2E-08
		Sb09g024320	1.6E-02	0.099	9.8E-01	2.148	2.5E-08
		Sb03g040630	1.0E-08	-0.929	1.9E-01	1.959	8.7E-12
		Sb01g009770	3.3E-04	0.560	5.4E-01	-1.623	1.7E-04
		Sb10g023710	3.3E-03	-0.403	6.5E-01	-1.644	1.5E-09
Cellulose biosynthesis	CESA2 - cellulose synthase	*Sb03g047220*	1.4E-26	-1.602	2.6E-02	5.231	1.1E-64
	CESA3 - cellulose synthase	*Sb02g010110*	3.0E-03	1.602	2.1E-01	-1.712	4.5E-04
	CESA9 - cellulose synthase	*Sb02g025020*	6.2E-03	0.842	7.8E-01	-6.022	3.7E-06
	CESA4 - cellulose synthase	*Sb03g034680*	1.3E-02	0.520	9.1E-01	-6.215	1.4E-06
	CESA7 - cellulose synthase	*Sb01g019720*	1.3E-02	0.830	7.8E-01	-6.707	1.2E-09
	CSLF2 - cellulose synthase-like family F	*Sb02g035980*	5.9E-03	-0.649	8.5E-01	3.463	2.7E-05
	CSLE2 - cellulose synthase-like family E	*Sb04g029420*	4.2E-07	-1.262	6.7E-02	2.343	1.0E-06
	CSLA4 - cellulose synthase-like family A	*Sb01g045850*	7.3E-03	0.111	9.6E-01	1.763	4.4E-04
	CSLC7 - cellulose synthase-like family C	*Sb09g025260*	2.5E-02	0.436	7.9E-01	-1.088	1.4E-02
	CSLA7 - cellulose synthase-like family A	*Sb02g040200*	4.6E-02	0.007	1.0E+00	-1.466	4.0E-05
	CSLC1 - cellulose synthase-like family C	*Sb03g035660*	5.0E-02	1.044	6.6E-01	-2.197	7.3E-02
	CSLF6 - cellulose synthase-like family F	*Sb07g004110*	1.1E-03	1.738	1.4E-02	-2.313	8.4E-03
	CSLH1 - cellulose synthase-like family H	*Sb06g016750*	8.6E-05	-0.337	9.3E-01	-4.503	3.0E-14
Homogalacturonan degradation	PME/invertase inhibitor family protein	*Sb07g000860*	4.3E-06	-	-	6.286	1.8E-06
		Sb06g000550	2.2E-09	-1.200	2.2E-01	4.514	8.3E-13
		Sb07g000870	1.3E-08	-1.279	1.7E-01	4.164	1.6E-09
		Sb07g000850	1.9E-03	-	-	2.794	7.4E-07
		Sb01g017520	8.1E-06	-	-	-5.465	7.6E-05
		Sb06g017880	1.2E-09	-	-	-2.498	1.9E-04

PME inhibitor domain containing protein	*Sb04g021920*	9.5E-08	0.572	6.9E-01	4.225	1.8E-29
PME (Pectin methylesterase)	*Sb03g012820*	1.3E-08	-	-	6.741	1.9E-07
	Sb09g017920	4.5E-04	-0.168	9.8E-01	4.741	5.8E-21
	Sb02g012560	5.8E-08	-0.774	6.6E-01	3.293	1.2E-15
	Sb01g022290	5.9E-08	-0.789	3.4E-01	1.870	2.8E-13
	Sb03g036790	9.6E-05	-1.371	2.2E-01	1.727	1.6E-03
	Sb07g022090	4.1E-03	-	-	-4.046	1.2E-02
Polygalacturonase	*Sb03g042350*	1.1E-09	-	-	6.262	3.6E-09
	Sb07g000740	1.8E-07	-0.756	5.2E-01	2.920	1.6E-13
	Sb09g027150	9.2E-04	0.531	6.8E-01	2.915	2.7E-12
	Sb02g028280	4.8E-15	-0.427	6.2E-01	2.731	1.8E-22
	Sb02g025730	2.0E-02	-0.006	1.0E+00	0.935	2.8E-04
	Sb04g035020	1.3E-02	0.581	5.7E-01	-0.881	6.6E-02
	Sb01g002550	7.7E-14	0.348	5.7E-01	-2.002	1.2E-12
	Sb03g013310	1.1E-02	-	-	-3.766	2.1E-02
	Sb01g004220	3.5E-04	1.252	5.4E-01	-5.882	1.4E-10

***** Geno × Trt = genotype by treatment interaction where treatment consists of *M. phaseolina* and control inoculations. †MP = *M. phaseolina,* CON = control. ‡ log2 DE = log2 fold differential expression.

Table 5.2. F-statistic and *P*-values from analysis of variance (ANOVA) for functional assays including cellulase, pectin methylesterase (PME), and polygalacturonase (PG) activity measured with four sorghum genotypes after inoculation with *M. phaseolina* at three post-inoculation stages ($\alpha = 0.05$).

DPI	Effect	Cellulase		PGU		PME	
		F value	Pr > F	F value	Pr > F	F value	Pr > F
4	Genotype	16.3	<0.0001	2.4	0.0940	8.4	0.0006
	Treatment	20.2	0.0001	8.8	0.0067	8.6	0.0074
	Genotype*Treatment	6.4	0.0024	7.4	0.0011	10.7	0.0001
7	Genotype	17.3	<0.0001	3.3	0.0365	2.1	0.1239
	Treatment	11.8	0.0021	5.6	0.0270	1.9	0.1803
	Genotype*Treatment	3.0	0.0489	9.2	0.0003	0.7	0.0037
10	Genotype	39.7	<0.0001	17.1	<0.0001	2.3	0.1082
	Treatment	20.8	0.0001	7.8	0.0100	5.4	0.0292
	Genotype*Treatment	4.1	0.0175	28.9	<0.0001	5.6	0.0049

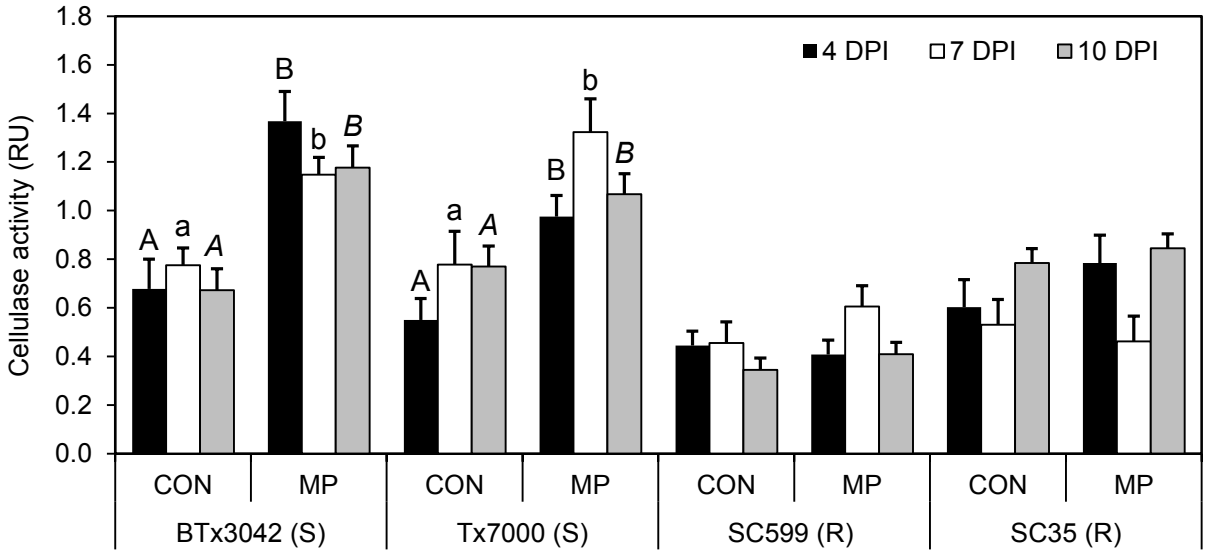

Figure 5.1. Comparison of the mean cellulose degrading enzyme activity (relative units) among two treatments (CON, MP) in charcoal-rot-susceptible (BTx3042, Tx7000) and resistant (SC599, SC35) genotypes at three post-inoculation stages (4, 7, and 10 DPI). Treatment means followed by different letters within each genotype at a given DPI are significantly different. Treatment means without letter designations within each genotype at a given DPI are not significantly different at $\alpha = 0.05$. Error bars represent standard errors. CON = phosphate-buffered saline mock-inoculated control, MP = *Macrophomina phaseolina*.

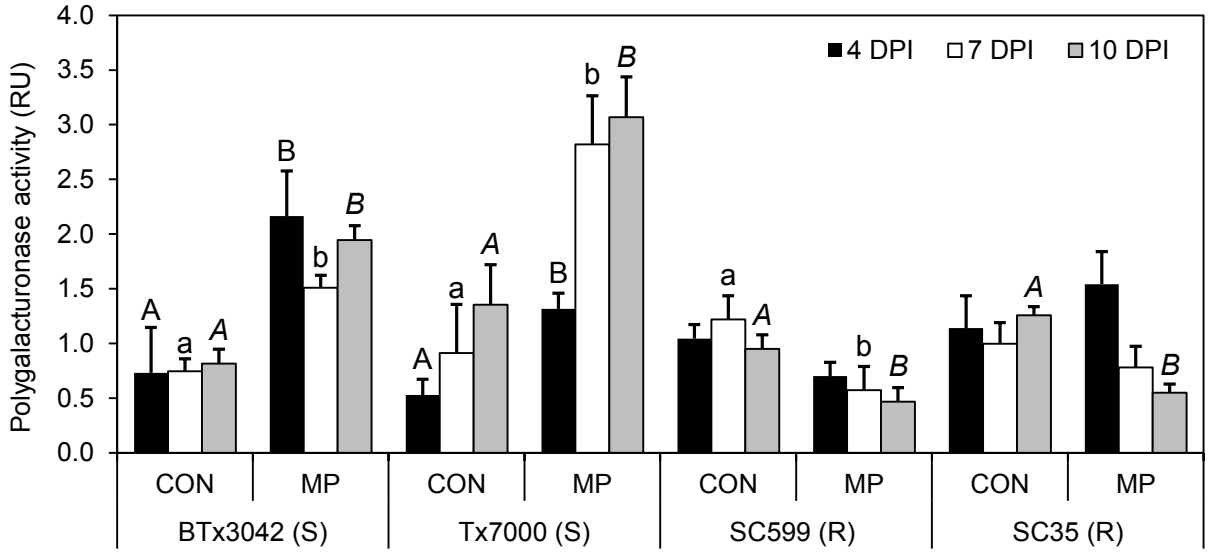

Figure 5.2. Comparison of the mean polygalacturonase activity (relative units) among two treatments (CON, MP) in charcoal-rot-susceptible (BTx3042, Tx7000) and resistant (SC599, SC35) genotypes at three post-inoculation stages (4, 7, and 10 DPI). Treatment means followed by different letters within each genotype at a given DPI are significantly different. Treatment means without letter designations within each genotype at a given DPI are not significantly different at $\alpha = 0.05$. Error bars represent standard errors. CON = phosphate-buffered saline mock-inoculated control, MP = *Macrophomina phaseolina*.

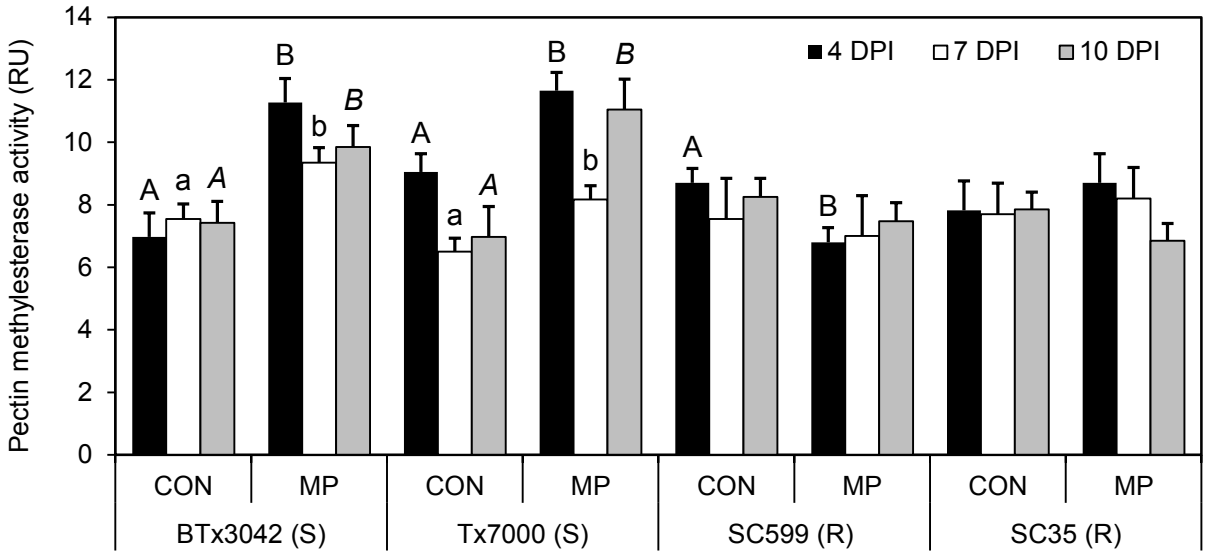

Figure 5.3. Comparison of the mean pectin methylesterase activity (relative units) among two treatments (CON, MP) in charcoal-rot-susceptible (BTx3042, Tx7000) and resistant (SC599, SC35) genotypes at three post-inoculation stages (4, 7, and 10 DPI). Treatment means followed by different letters within each genotype at a given DPI are significantly different. Treatment means without letter designations within each genotype at a given DPI are not significantly different at $\alpha = 0.05$. Error bars represent standard errors. CON = phosphate-buffered saline mock-inoculated control, MP = *Macrophomina phaseolina*.

Chapter 6 - Host lipid alterations after *Macrophomina phaseolina* infection contribute to charcoal rot susceptibility in grain sorghum.

ABSTRACT

Lipids are involved in central metabolic processes and confer basic configuration to cellular and subcellular membranes. Lipids also play a role in determining the outcome of plant-pathogen interactions. The infection-associated host lipid alterations and their role in delineating either host resistance or susceptibility against necrotrophs are poorly investigated and described. *Macrophomina phaseolina* is an important necrotrophic fungus which causes diseases in over 500 plant species including charcoal rot in sorghum. RNA sequencing and automated direct infusion electrospray ionization-triple quadrupole mass spectrometry (ESI-MS/MS) was used to quantitatively profile the transcriptomes and lipid molecular species of sorghum stalk tissues in response to *M. phaseolina* inoculation. *M. phaseolina* was capable of significantly decreasing the phosphatidylserine, phytosterol, and ox-lipid contents in a charcoal-rot-susceptible sorghum genotype (Tx7000) while significantly increasing its stigmasterol to sitosterol and monogalactosyldiacylglycerol to digalactosyldiacylglycerol ratios. The above-mentioned lipids and ratios were not significantly affected in the resistant genotype (SC599), except for significantly increased ox-lipid content. These results suggested the lethal impacts of *M. phaseolina* inoculation on plastid- and cell- membrane integrity and the lipid based signaling capacity of the charcoal-rot-susceptible sorghum genotype, Tx7000. Findings also suggested the strong oxidative stress experienced by Tx7000 under *M. phaseolina* inoculation and sheds light on the potential lipid classes involved in induced charcoal rot disease susceptibility.

Keywords: Sorghum, *Macrophomina phaseolina*, lipids, direct infusion automated electrospray ionization tandem mass spectrometry, necrotrophic fungi, RNA-Seq

INTRODUCTION

Lipids play important and indispensable roles in many physiological processes in living organisms. They are involved in central metabolism and confer basic configuration to cell and organelle membranes. Membranes are fundamental to cell structure and function. Therefore, maintenance of membrane integrity and fluidity is required for plants to survive under environmental changes (Wallis & Browse, 2002; Welti *et al*., 2007). The membrane trafficking, exo- and endocytosis, cytoskeletal rearrangements, photosynthesis, and signal transduction are some of the key functions played by lipids in eukaryotes (Wang, 2004; van Leeuwen *et al*., 2004; Funk, 2001; Shea & Del Poeta, 2006).

Lipids are significant determinants of plant-pathogen interactions. For instance, preformed structural barriers such as the cuticle contribute to first line defense against plant pathogens (Reina-Pinto & Yephremov, 2009). Cutin, a polyester of hydroxy and epoxy-hydroxy C16 and C18 fatty acids, is the major constituent of the cuticle (Kolattukudy, 2001), which provides a physical barrier between the pathogen and host cell (Jenks *et al*., 1994). The cell membrane is also a structural barrier for pathogen entrance. Phospholipids such as phosphatidylcholine (PC), phosphatidylethanolamine (PE), phosphatidylinositol (PI), phosphatidylglycerol (PG), phosphatidylserine (PS) are the important lipid constituents that make cell and mitochondria membranes (Horvath & Daum, 2013) while the galactolipids, monogalactosyldiacylglycerol (MGDG) and digalactosyldiacylglycerol (DGDG), are the major lipid constituents of chloroplast membranes (Joyard *et al*., 2010; Boudière *et al*., 2014; Fujii *et al*., 2014). Phytosterols are also constituents of plant cell membranes. Other than their structural contribution, phytosterols have also been shown to play a crucial role in plant innate immunity against phytopathogens (Wang *et al*., 2012).

Lipids and fatty acids are also important as signaling molecules in plant defense against phytopathogens (Walley *et al*., 2013; Kachroo & Kachroo, 2009; Shah, 2005; Laxalt & Munnik, 2002). Polyunsaturated fatty acids such as linoleic acid can enzymatically or non-enzymatically be oxygenated to produce oxylipins, which have diverse signaling properties in mammals, microbes, and plants (Walley *et al*., 2013; Kachroo & Kachroo, 2009; Shea & Del Poeta, 2006; Howe, 2007). Jasmonic acid is an extensively studied oxylipin in plants. Moreover, mechanical,

biotic, and low-temperature stresses increase many membrane lipids with oxidized acyl chains (i.e. ox-lipids) in *Arabidopsis thaliana* (Vu *et al*., 2012, 2014). Ox-lipids may be produced enzymatically through the action of lipoxygenase or non-enzymatically through the action of reactive oxygen species (ROS) (Zoeller *et al*., 2012). Like oxylipins, ox-lipids also function as signaling molecules that initiate stress responses in plants (Andersson *et al*., 2006). Phosphatidic acid (PA) (a phospholipid) is a potent signaling molecule in plants and animals that modulates the activities of kinases, phosphatases, phospholipases, and proteins involved in membrane trafficking, Ca2+ signaling, and the oxidative burst (Munnik, 2001; Wang, 2004). The role of PA in plant defense against pathogens is well documented (Laxalt & Munnik, 2002; Munnik, 2001; Wang, 2004). Lipids play diverse and pivotal roles in determining the outcome of plant-pathogen interactions.

Macrophomina phaseolina is a soil-borne, necrotrophic fungal pathogen that causes diseases in over 500 different plant species (Islam *et al*., 2012). Despite its broad host range, *Macrophomina* is a monotypic genus and contains only one species: *M. phaseolina* (Sutton, 1980). It can remain viable in soil and crop residue for more than four years (Short *et al*., 1980). Higher temperatures (30-35°C) and low soil moisture are conducive for the diseases caused by *M. phaseolina* including seedling blight, charcoal rot, stem rot, and root rot (Sandhu *et al*., 1999). Therefore, drought-prone regions are highly vulnerable to *M. phaseolina*-associated crop losses. Increased occurrence of the pathogen on various crop species has also been recently reported worldwide (Khangura & Aberra, 2009; Mahmoud & Budak, 2011).

M. phaseolina causes charcoal rot disease in many economically important crops such as sorghum, soybean, maize, alfalfa and jute (Islam *et al*., 2012). Charcoal rot is a high priority fungal disease in sorghum [*Sorghum bicolor* (L.) Moench], causing tremendous crop losses wherever sorghum is grown (Tarr, 1962, Tesso *et al*., 2012). Therefore, there is a pressing need to understand the molecular basis of charcoal rot resistance in sorghum to develop durable resistance strategies. The genetic control of resistance to necrotrophic pathogens in general and *M. phaseolina*, in particular, is poorly understood and large scale gene expression studies and complimentary functional studies such as lipidomics assays can provide a broader view and better understanding on the disease resistance mechanisms. In the current work, the differentially

expressed genes that are outlined in the Chapter 2 are more closely investigated with special reference to those involve in various lipid related metabolic pathways. Furthermore, we take advantage of automated direct infusion electrospray ionization-triple quadrupole mass spectrometry (ESI-MS/MS) to quantitatively profile the lipidome from sorghum stalk tissues after *M. phaseolina* infection. Plant lipidomics based on ESI-MS/MS is a useful method to study the responses of hundreds of lipid molecular species to various environmental stresses (Zheng *et al*., 2011; Welti *et al*., 2002). Therefore, the objectives of the current study were to (i) make use of the RNA-Seq data outlines in the Chapter 2 to identify differentially expressed lipid metabolism related genes, (ii) to identify the differentially expressed lipid classes and species between charcoal-rot-resistant and susceptible sorghum genotypes in response to *M. phaseolina* inoculation and (iii) to uncover the potential links between lipids and charcoal rot resistance or susceptibility at the transcriptional and functional lipidomics levels.

MATERIALS AND METHODS

Plant materials, establishment, maintenance, inoculum preparation, and inoculation

Commonly used charcoal-rot-resistant (SC599R) and susceptible (Tx7000) sorghum lines were used. Seed establishment, seedling and plant maintenance, inoculum preparation, and inoculation were conducted according to the methods described in the Chapter 2.

Lipid extraction

Stalk tissues were collected from *M. phaseolina* inoculated and mock-inoculated control plants from resistant and susceptible sorghum genotypes at 4, 7, and 10 days post-inoculation (DPI) and used for lipid extraction (five biological replicates per DPI per treatment per sorghum line = 60 plants altogether). At sampling, approximately 1 g of stalk harvested 1 cm away from the symptomatic area was chopped in to 6 mL of isopropanol with 0.01% butylated hydroxytoluene (BHT) [preheated to 75°C] in a 50 mL glass tube with a Teflon lined screw-cap (Thermo Fisher Scientific, Inc., Waltham, MA, USA). Tubes were incubated in a waterbath at 75°C for 15 min to inactivate lipid-hydrolyzing enzymes. After reaching room temperature, 3 mL of chloroform and 1.2 mL of water were added to each tube and stored at -80°C until further processing. The lipid

extraction was performed following the protocol described by Vu *et al*., (2012). Briefly, the lipid extract in isopropanol, BHT, chloroform and water was shaken on an orbital shaker at room temperature for 1 h and transferred to a new glass tube using a Pasteur pipette, leaving the stalk pieces in the original tube. Subsequently, 8 mL of chloroform: methanol (2:1) mixture was added to the stalk pieces and shaken on an orbital shaker (140 rpm) at room temperature for 1 h. The resulting solvent was transferred to the first extract. The addition, shaking and transfer steps were carried out four times including one overnight shake until the stalk pieces of every sample became white. Then the solvent was evaporated in an N-EVAP 112 nitrogen evaporator (Organomation Associates, Inc., Berlin, MA, USA), leaving the lipid extract. Lastly, the lipid extract was dissolved in 1 mL of chloroform and stored at -80 °C. The remaining stalk pieces of each sample were dried overnight in an oven at 105°C, cooled and weighed to express the lipid content on a dry weight basis. Dry weights were measured using a balance (Mettler Toledo AX, Mettler Toledo International, Inc., Columbus, OH, USA) with a detection limit of 2 µg.

Lipid profiling with electrospray ionization-triple quadrupole mass spectrometer

Automated electrospray ionization-tandem mass spectrometry approach was used for lipid profiling. Data acquisition, analysis, and acyl group identification were performed following the methods described by Xiao *et al*. (2010) with modifications and an added quality-control approach. From the lipid extracts that were dissolved in 1 mL of chloroform, an aliquot of 15 to 70 µL (corresponding to approximately 0.2 mg dry weight) was added to each of two vials (vial 1 and vial 2). Following the methods described by Welti *et al*., (2002), accurate amounts of internal standards were measured and added to vial 1 in the following quantities: 0.6 nmol phosphatidylcholine (PC) (di12:0), 0.6 nmol PC (di24:1), 0.6 nmol lysophosphatidylcholine (LPC) (13:0), 0.6 nmol LPC (19:0), 0.3 nmol phosphatidylethanolamine (PE) (di12:0), 0.3 nmol PE (di23:0), 0.3 nmol lysophosphatidylethanolamine (LPE) (14:0), 0.3 nmol LPE (18:0), 0.3 nmol phosphatidylglycerol (PG) (di14:0), 0.3 nmol PG (di20:0(phytanoyl)), 0.3 nmol lysophosphatidylglycerol (LPG) (14:0), 0.3 nmol LPG (18:0), 0.23 nmol phosphatidylinositol (PI) (16:0–18:0), 0.16 nmol PI (di18:0), 0.2 nmol phosphatidylserine (PS) (di14:0), 0.2 nmol PS (di20:0(phytanoyl)), 0.3 nmol phosphatidic acid (PA) (di14:0), 0.3 nmol PA (di20:0(phytanoyl)), 0.31 nmol TAG (tri17:1), 0.36 nmol digalactosyldiacylglycerol (DGDG) (16:0–18:0), 0.95 nmol DGDG (di18:0), 1.51 nmol monogalactosyldiacylglycerol (MGDG) (16:0–18:0) and 1.3 nmol

MGDG (di18:0). Only the last four internal standards were added to vial 2, in half the amount as vial 1. The solvents [chloroform: methanol: 300 mM ammonium acetate in water, 300:665:35 (v/v/v)] were added to the lipid extract and internal standard mixture in each vial. The final volume was 1.4 mL. Unfractionated lipid extracts were introduced by continuous infusion into the electrospray ionization (ESI) source on a triple quadrupole MS/MS (API4000, ABSciex, Framingham, MA, USA) using an autosampler (LCMini PAL, CTC Analytics AG, Zwingen, Switzerland) at 30 μL min^{-1}. Data and spectra acquisition, resolution adjustment of mass analyzers, background subtraction from each spectrum, data smoothening and peak area integration, data processing, and calculation of normalized lipid intensities were performed according to the procedures described by Vu *et al*. (2014). The lipid values are reported as normalized intensity (%) per mg stalk dry weight, where a value of one is the intensity of 1 nmol of internal standard.

Statistical analysis of lipid data

Lipid data were analyzed for variance (ANOVA) using the PROC GLIMMIX procedure of SAS software version 9.2 (SAS Institute, 2008). Analyses were conducted at lipid class level (DGDG, MGDG, SQDG, PG, phosphatidylcholine, PE, PI, PS, PA, lysoPC, lysoPE, sterol glucosides, acyl(18:2) sterol glucosides, acyl(16:0) sterol glucosides, NL297(18:2) containing TAG, NL295(18:3) containing DAG/TAG, NL273(16:0) containing DAG/TAG, HexCer, prec291(18:3-2O) or 18:4-O, prec293(18:2-2O) or 18:3-O, and ratios of MGDG:DGDG, PE:PC, galactolipids [DGDG, MGDG, SQDG]/phospholipids [PG + PC + PE + PI + PS + PA]) and individual lipid species levels. Although 227 different lipid species were detected, based on the limit of detection (>0.002 nmol) and coefficient of variation (< 0.3) criteria for pooled samples, only 132 were qualified for the final ANOVA analysis. The restricted maximum likelihood (REML) method was used to estimate variance components. Genotype (SC599, Tx7000), inoculation treatment (*M. phaseolina*, control) and time point (4, 7, and 10 DPI) were considered fixed factors. Model assumptions were tested using studentized residual plots (for identical and independent distribution of residuals) and Q-Q plots (for normality of residuals). Whenever residuals were not homogeneously distributed, appropriate heterogeneous variance models were fitted to meet the model assumptions by specifying a random/group statement (group = genotype *or* inoculation treatment *or* time point) after specifying the model statement. Bayesian

information criterion (BIC) was used to determine the most suitable model that best fit data after accounting for model assumptions. Means separations were carried out using the PROC GLMMIX procedure of SAS.

RESULTS

Differential gene expression analysis

As the highest number of genes were differentially expressed at 7 DPI, we use the expression data from 7 DPI for this paper. DESeq2 analysis for differential gene expression and follow up manual annotation for gene function revealed 68 lipid metabolism related genes with significant genotype × inoculation treatment interaction at 7 DPI. Table 6.1 shows significantly ($q < 0.05$) differentially expressed genes (DEGs) that are related to lipid associated metabolic pathways between SC599 (charcoal-rot-resistant) and Tx7000 (charcoal-rot-susceptible) sorghum genotypes in response to *Macrophomina phaseolina* inoculation at 7 DPI.

Out of 68 DEGs, 20 were involved in jasmonic acid (JA) biosynthesis. Out of these 20, seven (*Sb01g010640*, *Sb01g031910*, *Sb01g040430, Sb03g003310*, *Sb03g037150*, *Sb06g021680*, and *Sb07g028890*) encoded for phospholipase A2. Except for *Sb03g003310* and *Sb01g031910*, other genes were significantly down-regulated in Tx7000 after pathogen inoculation with a 14.1 net log2 fold down-regulation. Although many of these genes were not significantly differentially expressed in SC599, *Sb01g040430* and *Sb06g021680* were significantly up-regulated (net log2 fold change = +4.0) upon pathogen inoculation. Out of four genes that encode lipoxygenase, *Sb01g011040* and *Sb06g031350* were down-regulated while *Sb06g018040* was up-regulated in Tx7000 after pathogen inoculation (net log2 fc = -4.4). *Sb01g011050* was significantly up-regulated (log2 fc = 2.5) in pathogen-inoculated SC599 while the other three genes were not significantly differentially expressed. Two cytochrome P450 74A3 genes (*Sb01g007000* and *Sb01g042270*; net log2 fc = +4.7) and seven 12-oxophytodienoate reductase genes (*Sb06g017670*, *Sb06g017680*, *Sb09g000520*, *Sb10g007300*, *Sb10g007310*, *Sb10g007320*, *Sb10g007330*; net log2 fc = +21.7) were significantly up-regulated in Tx7000 after pathogen inoculation while none of those were significantly differentially expressed in SC599.

Out of 68 DEGs, three were involved in the trans, trans-farnesyl diphosphate biosynthesis. Trans, trans-farnesyl diphosphate is the first precursor for phytosterol biosynthesis. Genes in this pathway (*Sb01g044560*, prenyltransferase; *Sb04g038180*, para-hydroxybenzoate-polyprenyl transferase; *Sb07g005530*, polyprenyl synthetase) were significantly down-regulated in Tx7000 upon *M. phaseolina* inoculation while none of those were significantly differentially expressed in SC599.

Sixteen genes out of 68 DEGs were related to phytosterol biosynthesis (campesterol, stigmasterol, and sitosterol). Five of these sixteen represented cycloartenol synthase (*Sb06g015960*, *Sb08g019310, Sb08g019300*, *Sb08g019290*, and *Sb07g006300*) and all of them were significantly down-regulated in Tx7000 after pathogen inoculation (net log2 fc = -11.5). Another six 24-methylenesterol C-methyltransferase 2 genes (*Sb01g004280*, *Sb01g004290*, *Sb01g004295*, *Sb01g004300*, *Sb01g004310*, *Sb09g029600*) were significantly down-regulated in pathogen inoculated Tx7000 (net log2 fc = -26.9). A cycloeucalenol cycloisomerase gene (*Sb09g002170*; log2 fc = -2.2) and two cytochrome P450 51 genes (*Sb05g022370*, *Sb08g002250*; net log2 fc = -5.9) were also significantly down-regulated in pathogen inoculated Tx7000. Two genes (*Sb04g017400,* log2 fc = +1.0; *Sb03g008970,* log2 fc = +6.6) that encode for C-14 sterol reductase (sterol delta-7 reductase) and 3-beta-hydroxysteroid-delta-isomerase, respectively were significantly up-regulated in Tx7000 after *M. phaseolina* inoculation. Interestingly none of the sixteen genes involved in phytosterol biosynthesis were significantly differentially expressed in SC599 in response to pathogen inoculation.

Out of 68 DEGs, four were involved in the brassinosteroid biosynthesis. Two of those were steroid 22-alpha hydroxylase genes (*Sb03g002870* and *Sb05g002580*) and were significantly down-regulated in Tx7000 upon pathogen inoculation (net log2 fc = -5.2). The other two genes (*Sb03g040050* and *Sb02g003510*) encoded 3-oxo-5-alpha-steroid 4-dehydrogenase and were also found to be significantly down-regulated in pathogen-inoculated Tx7000 (net log2 fc = -4.3). None of these four genes were significantly differentially expressed in SC599 in response to pathogen inoculation.

Seventeen out of 68 DEGs were responsible for phosphatidic acid biosynthesis. Seven of these encoded for diacylglycerol kinase (*Sb03g036560*, *Sb04g032990*, *Sb04g035410*, *Sb05g024160*, *Sb07g020990*, *Sb07g025680,* and *Sb07g029110*). The former five were significantly up-regulated in Tx7000 upon pathogen inoculation while the latter two were significantly down-regulated. The net log2 fold diacylglycerol kinase up-regulation was 6.8. None of these eight genes were significantly differentially expressed in SC599 in response to pathogen inoculation. Another three genes encoded phospholipase C (*Sb02g044010*, *Sb06g020050*, and *Sb09g002320*) and were significantly down-regulated in *M. phaseolina*-inoculated Tx7000 (net log2 fc = -5.3) while *Sb09g002320* was significantly up-regulated (log2 fc = +1.3) in SC599 after pathogen inoculation. Six genes represented phospholipase D (*Sb01g031100*, *Sb01g033480*, *Sb02g008130*, *Sb02g024910*, *Sb03g012720*, and *Sb10g025660*). Out of these, *Sb02g008130* and *Sb02g024910* were significantly down-regulated in Tx7000 after pathogen inoculation while the latter three were significantly up-regulated (net log2 fc = -5.6). Except for *Sb10g025660* (log2 fc = -1.0), the other five phospholipase D genes were not significantly differentially expressed in SC599 after pathogen inoculation.

A phosphatidylserine synthase gene (*Sb09g027850*) was significantly up-regulated (log2 fc = +3.1) in pathogen-inoculated Tx7000 while a digalactosyldiacylglycerol synthase gene (*Sb05g003730*) responsible for monogalactosyldiacylglycerol to digalactosyldiacylglycerol conversion was significantly down-regulated (log2 fc = -1.1). None of the two genes were significantly differentially expressed in SC599 upon pathogen inoculation.

Seven genes (*Sb01g038500*, *Sb01g042150*, *Sb02g043980, Sb05g000400*, *Sb06g004770*, *Sb07g021640*, and *Sb08g000460*) out of 68 DEGs were involved in phospholipid and glycolipid desaturation and encoded for Omega-6/-3 fatty acid desaturase. The former three genes were significantly down-regulated in pathogen-inoculated Tx7000 while the rest was significantly up-regulated. The net log2 fold up-regulation was 3.0. None of the seven genes were significantly differentially expressed in SC599 after pathogen inoculation.

Lipidome analysis

A profile analysis was conducted to examine the stalk lipid composition of two sorghum genotypes (SC599 and Tx7000) under control treatment across three time points. Although relative amounts differ between genotypes, in broader terms, phospholipids (∑ PG, PC, PE, PI, PS, PA) constituted the highest quantities (%) in both genotypes followed by hexosylceramide, galactolipids (∑ DGDG, MGDG, SQDG), phytosterols (∑ sterol glucosides, acyl(18:2) sterol glucosides, acyl(16:0) sterol glucosides), di/triacylglycerol (∑ NL297(18:2) containing TAG, NL295 (18:3) containing DAG/TAG, NL273 (16:0) containing DAG/TAG), lysophospholipids (∑ LysoPC, LysoPE), and Ox-lipids (∑ prec291 (18:3-2O) or 18:4-O, prec293 (18:2-2O) or 18:3-O) respectively (Fig. 6.1).

Analysis of lipid classes

The genotype × inoculation treatment interaction effect was significant across three time points for MGD:DGDG ratio, PS, sterol glucosides (∑ campesterol-glc, stigmasterol-glc, sitosterol-glc), acyl (18:2) sterol glucosides (∑ campesterol-glc(18:2), stigmasterol-glc(18:2), sitosterol-glc(18:2)), and total ox-lipids (∑ PE(16:0/18:3-2O), MGDG(18:4-O/18:3), PC(16:0/18:3-2O), MGDG(18:3-2O/18:3), PE(18:2/18:3-O), PE(18:2/18:2-2O), and PC(16:0/18:3-O)) (Table 6.2). Compared to control treatment, pathogen inoculation significantly increased the MGDG:DGDG ratio of Tx7000 ($P = 0.0004$) but did not affect this ratio in SC599 ($P = 0.7288$) (Fig. 6.2.A). *M. phaseolina* significantly decreased the PS content of Tx7000 ($P = 0.0136$) but did not affect the PS content in SC599 ($P = 0.3882$) (Fig. 6.2.B). *M. phaseolina* also significantly reduced the sterol glucosides content of Tx7000 ($P = 0.0031$) while no significant impact was observed in SC599 ($P = 0.7141$) (Fig. 6.2.C). Although pathogen inoculation did not significantly affect acyl (18:2) sterol glucoside content in Tx7000 ($P = 0.9184$), a significant reduction was observed in SC599 ($P = 0.0012$) (Fig. 6.2.D). *M. phaseolina* inoculation significantly increased the total ox-lipid content in SC599 ($P = 0.0148$) while it significantly decreased ox-lipid in Tx7000 ($P = 0.0309$) (Fig. 6.2.E).

PA analysis revealed significantly increased PA content in SC599 after *M. phaseolina* inoculation at 4 DPI ($P < 0.0001$). MP did not significantly affect PA content in Tx7000 ($P =$

0.9166) (Fig. 6.3.A.i). The main effects of genotype and inoculation treatment on PA were evident across 7 and 10 DPI. Tx7000 had significantly greater PA content than SC599 ($P < 0.0001$) across the two inoculation treatments, and across 7 and 10 DPI (Fig. 6.3.A.ii). Compared to control, *M. phaseolina* significantly increased PA content across two genotypes, and across 7 and 10 DPI ($P = 0.0007$) (Fig. 6.3.A.iii). PG content was significantly greater in SC599 after *M. phaseolina* inoculation ($P = 0.047$) at 4 DPI while the same was significantly lower in Tx7000 after *M. phaseolina* inoculation ($P = 0.0173$) (Fig. 6.3.B.i). The main effect of genotype for PG was evident across inoculation treatments and, across 7 and 10 DPI where Tx7000 had a significantly greater PG content than SC599 ($P = 0.0001$) (Fig. 6.3.B.ii). The galactolipids:phospholipids ratio was significantly decreased in SC599 after MP inoculation at 4 DPI ($P = 0.0125$) while it significantly increased the ratio in Tx7000 ($P = 0.0491$) (Fig. 6.3.C.i). Although *M. phaseolina* inoculation did not significantly affect the galactolipids:phospholipids ratio of SC599 ($P = 0.8377$) across 7 and 10 DPI, it significantly decreased the galactolipids:phospholipids ratio in Tx7000 ($P = 0.0074$) (Fig. 6.3.C.ii).

Analysis of lipid species

Out of 132 lipid species analyzed, 31 showed significant genotype × inoculation treatment interaction across the three post-inoculation stages (Table 6.3). Compared to control, *M. phaseolina* inoculation significantly increased the PG(34:3) content of SC599 while it significantly decreased the same in Tx7000. *M. phaseolina* significantly increased the PG (36:2) in Tx7000. *M. phaseolina* inoculation significantly increased PC(34:3), PC(36:6), and PC(36:1) content of SC599 while it significantly decreased PC(34:2). A significant PC(36:6) and PC(36:2) increase was also observed in Tx7000 after *M. phaseolina* inoculation. *M. phaseolina* inoculation significantly increased the PE(34:4), PE(34:3), and PE(36:6) species in SC599. These species were not significantly affected in Tx7000 after pathogen inoculation. However, PE(36:2) and PE(42:2) species were present in significantly greater quantities in *M. phaseolina*-inoculated Tx7000 although *M. phaseolina* did not significantly affect PE(36:2) and PE(42:2) of SC599. *M. phaseolina* inoculated Tx7000 had significantly greater amounts of PI(34:2), PI(36:4), and PI(36:2) species. *M. phaseolina* significantly reduced the PI(34:2) in SC599 while did not significantly affect the PI(36:4) and PI(36:2). *M. phaseolina* inoculation significantly increased the PS(36:3), PS(38:3), PS(40:3) species in SC599 although none of them were significantly

affected in Tx7000. PS(34:3) was significantly reduced in *M. phaseolina*-inoculated Tx7000. However, PS(34:3) was not significantly affected by *M. phaseolina* in SC599. Although *M. phaseolina* inoculation significantly increased the PA(34:3) and PA(36:6) species in both sorghum genotypes, there was a greater increase with SC599 compared to Tx7000. *M. phaseolina* significantly decreased campesterol-glc(18:2) in SC599 but not in Tx7000. The stigmasterol-glc:sitosterol-glc ratio was significantly greater in pathogen-inoculated Tx7000. However, pathogen inoculation did not significantly affect the ratio of SC599. Although *M. phaseolina* significantly increased TAG(18:3/36:9) and TAG(16:0/36:6) in both sorghum genotypes, there was a greater increase in SC599. SC599 had significantly lower DAG(34:2) content after *M. phaseolina* inoculation although the same was not significantly affected in Tx7000. The ox-lipid species MGDG(18:4-O/18:3), MGDG(18:3-2O/18:3), PE(16:0/18:3-2O), PE(18:2/18:2-2O), and PC(16:0/18:3-2O) were found to be significantly greater in SC599 after *M. phaseolina* inoculation. Except for the significantly reduced PE(18:2/18:2-2O), *M. phaseolina* did not affected the aforementioned ox-lipid species in Tx7000.

DISCUSSION

This study enabled the elucidation of underlying lipid alterations which condition charcoal rot resistance and susceptibility in grain sorghum. At the lipid class level, MGDG:DGDG ratio, PS, sterol glucosides, total ox-lipids, and PA in sorghum stalk tissues appeared to be the key lipid determinants associated with charcoal rot disease reaction.

The enzyme digalactosyldiacylglycerol (DGD) synthase transfers a galactose from UDP-galactose onto MGDG to form DGDG (Boudière *et al*., 2014). MGDG does not form bilayers in mixtures with water while DGDG is a bilayer-forming lipid (Webb & Green, 1991). The ratio of non-bilayer-forming to bilayer-forming lipids is critical for protein folding and insertion (Gounaris & Barber, 1983; Bogdanov & Dowhan, 1999) as well as for intracellular protein trafficking (Kusters *et al*., 1994). Therefore, the MGDG:DGDG ratio in chloroplasts must be tightly regulated to maintain a stable physical phase and for the proper functioning of the thylakoid membranes. The decreased ratio of MGDG:DGDG enhances the stability of the membrane under various stresses (Moellering *et al*, 2010; Chen *et al.*, 2006; Hazei & Williams, 1990; Welti *et al*., 2002). In the current study, DGD synthase gene was significantly down-

regulated in Tx7000 after *M. phaseolina* inoculation which contributed to impeded MGDG to DGDG conversion. This was evident with the increased MGDD:DGDG ratio observed in Tx7000 upon *M. phaseolina* inoculation. Therefore, *M. phaseolina* may promote charcoal rot susceptibility through a negative impact on thylakoid membrane stability and function.

The two most abundant classes of phospholipids in plant mitochondria and cell membrane are phosphatidylcholine (PC) and phosphatidylethanolamine (PE) (Horvath & Daum, 2013). Maintaining a lower PE:PC ratio is important to enhance the stability of membranes under various stresses (Moellering *et al*., 2010; Chen *et al*., 2006; Hazei & Williams, 1990; Welti *et al*., 2002). In the current study, we did not observe a significant alteration in this ratio after pathogen inoculation in either genotype. However, phosphatidylserine (PS) is also considered an important lipid constituent in cell and mitochondria membranes (Horvath & Daum, 2013). Although a relatively minor plant cell lipid class (Devaiah *et al*., 2006; Nakamura & Ohta, 2007), PS plays an important role in cell death signaling, vesicular trafficking, lipid–protein interactions, and membrane lipid metabolism (Vance, 2008). We observed a significant reduction in PS in Tx7000 as a lipid class and three PS species (PS(36:3), PS(38:3), and PS(40:3)) increment in SC599 after *M. phaseolina* inoculation. The significantly up-regulated phosphatidylserine synthase gene in Tx7000 after *M. phaseolina* inoculation may be an indication of Tx7000's need to produce extra PS. Therefore, despite the unaltered PE:PC ratio, the current study provided some evidence for the potential negative impacts of *M. phaseolina* on mitochondrial and cell membrane stability and functioning in the charcoal-rot-susceptible genotype, Tx7000.

Phytosterols (campesterol, stigmasterol, and sitosterol) represent the most abundant sterols in plants (Benveniste, 2004). They are integral constituents of membrane lipid bilayer and regulators of membrane fluidity and permeability, and influence membrane properties, functions, and structure (Demel & De Kruyff, 1976; Bloch, 1983; Schuler *et al*., 1991; Schaller, 2003; Roche *et al*., 2008). Phytosterols also play a crucial role in plant innate immunity against phytopathogens. For instance, silencing of *N. benthamiana* squalene synthase, a key gene in phytosterol biosynthesis, compromised non-host resistance to a few pathovars of *Pseudomonas syringae* and *Xanthomonas campestris* while an *Arabidopsis* sterol methyltransferase mutant (sterol methyltransferase2) involved in sterol biosynthesis also compromised plant innate

immunity against bacterial pathogens (Wang *et al*., 2012). In the current study, we observed significant down-regulation of prenyltransferase, para-hydroxybenzoate-polyprenyl transferase, and polyprenyl synthetase genes in Tx7000 after MP inoculation, which may have limited trans, trans-farnesyl diphosphate biosynthesis. Trans, trans-farnesyl diphosphate is essentially the primary precursor for the biosynthesis of all phytosterols (http://pathway.gramene.org/gramene/sorghumcyc.shtml). Moreover, important genes involved in phytosterol biosynthesis such as cycloartenol synthase, 24-methylenesterol C-methyltransferase 2, cycloeucalenol cycloisomerase, and cytochrome P450 51 were significantly down-regulated in Tx7000 after *M. phaseolina* inoculation. Confirming the gene expression data, significantly lower sterol glucoside (∑ campesterol, stigmasterol, sitosterol) content was observed in Tx7000 after *M. phaseolina* inoculation. Therefore, *M. phaseolina* inoculation associated phytosterol reduction in Tx7000 could result in cell membrane destabilization and compromised plant immunity that could contribute to enhanced charcoal rot susceptibility.

The stigmasterol to sitosterol ratio was found to be significantly greater in *M. phaseolina* inoculated Tx7000. The sitosterol to stigmasterol conversion is triggered through perception of pathogen-associated molecular patterns such as flagellin and lipopolysaccharides, and the generation of reactive oxygen species (ROS) (Griebel & Zeier, 2010). Therefore, the increased stigmasterol to sitosterol ratio observed in the current study provided a clue about the strong oxidative stress experienced by Tx7000 after *M. phaseolina* inoculation. Previous studies provided evidence for *M. phaseolina*'s ability to create oxidative stress responses in charcoal-rot-susceptible sorghum genotypes such as Tx7000 and BTx3042 through induced host nitric oxide (NO) and ROS biosynthesis (see Chapter 3). Moreover, through mutant analysis and exogenous sterol application, Griebel & Zeier (2010) have shown that an increased stigmasterol to sitosterol ratio in *Arabidopsis* leaves weakens specific plant defence responses, which results in enhanced susceptibility against *Pseudomonas syringae*. Therefore, it is possible that *M. phaseolina* inoculation associated stigmasterol to sitosterol ratio increase could contribute to enhanced charcoal rot disease susceptibility in Tx7000.

The biosynthetic pathway for phytosterols also provides precursors for brassinosteroids, phytohormones involved in the regulation of plant growth and development (Fujioka *et al*.,

2002). In the current study, genes involved in brassinosteroid biosynthesis such as steroid 22-alpha hydroxylase and 3-oxo-5-alpha-steroid 4-dehydrogenase were significantly down-regulated in Tx7000 after *M. phaseolina* inoculation. Therefore, although host brassinosteroid content was not directly measured in this study, the significantly lower sterol glucosides (precursors for brassinosteroids biosynthesis) content as well as the down-regulation of key genes involved in brassinosteroid biosynthesis suggested the bottleneck that could be faced by Tx7000 in synthesizing brassinosteroid after *M. phaseolina* inoculation. Perhaps, impeded brassinosteroid biosynthesis could be a mechanism through which Tx7000 attenuates further upsurge of ROS mediated oxidative stress after *M. phaseolina* inoculation. Brassinosteroids are reported to induce ROS accumulation and programmed cell death in plants (Fukuda, 2000; Kuriyama *et al*., 2001; Roberts *et al*., 2000; Xia *et al*., 2009)

Like oxylipins, ox-lipids may also function as signaling molecules that initiate stress responses in plants (Andersson *et al*., 2006). Plants can produce ox-lipids in response to a variety of stresses including pathogen attacks (Thoma *et al*., 2003). Ox-lipids are produced enzymatically through the action of lipoxygenase or non-enzymatically through the action of reactive oxygen species (ROS) (Zoeller *et al*., 2012). The primary product of lipoxygenase mediated lipid oxidation is lipid hydroperoxides while phytoprostanes are the primary product of ROS-mediated oxidation (Christensen & Kolomiets, 2011). The precursor lipid hydroperoxides can further be subjected to various enzymatic reactions which results in the generation of a variety of oxylipins including 12- oxo-phytodienoic acid (OPDA) and jasmonic acid (JA) (Imbusch & Mueller, 2000; Gobel *et al*., 2002; Mosblech *et al*., 2009). In the current study, compared to control, we observed significantly higher ox-lipid content in the charcoal-rot-resistant genotype, SC599, after *M. phaseolina* inoculation. Although not directly measured, the presence of ox-lipids in higher quantities (particularly PC(16:0/18:3-O) and PC(16:0/18:3-2O) species) along with the net up-regulation of phospholipase A2 and lipoxygenase genes (phospholipase A2 and lipoxygenase are necessary to produce lipid hydroperoxides which are essential precursors for JA biosynthesis) suggested SC599's potential to produce ample amounts of jasmonic acid under *M. phaseolina* inoculation. JA is an important plant hormone which confers resistance against necrotrophic pathogens (McDowell & Dangl, 2000; Glazebrook, 2005). On the other hand, although genes involve in the latter steps of JA biosynthesis such as cytochrome P450 74A3 and 12-

oxophytodienoate reductase are highly up-regulated in Tx7000 after *M. phaseolina* inoculation, the net down-regulation of the phospholipase A2 and lipoxygenase genes (needed for initial steps in JA biosynthesis) may hinder JA synthesis in Tx7000 after *M. phaseolina* infection. The impeded potential of Tx7000 to produce JA under *M. phaseolina* infection is also supported by its significantly lower ox-lipid content. As described earlier, Tx7000 appeared to experience a strong oxidative stress after *M. phaseolina* infection. Oxidative stress results in the biosynthesis of phytoprostanes from the available polyunsaturated fatty acid (PUFA, particularly linolenate), which reduces available linolenate pools to be utilized in the JA production. Therefore, Tx7000 appeared to suffer with the major precursor (linolenate) shortage to produce JA under *M. phaseolina* infection, which in turn could make Tx7000 more susceptible to this important necrotrophic fungus.

The phosphatidic acid (PA) involved in cell signaling is produced via two phospholipase pathways. It can be generated directly through the hydrolysis of structural phospholipids through phospholipase D (PLD) activity (Testerink & Munnik, 2005; Munnik, 2001; Wang, 2004). It is also synthesized via the successive action of phospholipase C (PLC) and diacylglycerol kinase (DAGK) (Testerink & Munnik, 2005; Munnik, 2001; Wang, 2004). In this pathway, PLC hydrolyzes phosphatidylinositol (PI) into inositol-1,4,5-trisphosphate and diacylglycerol (DAG). The resulting DAG is rapidly phosphorylated to PA by DAGK (Testerink & Munnik, 2005). In the current study, both genotypes contained significantly higher PA(34:3) and PA(36:6) upon *M. phaseolina* inoculation. However, compared to control, the resistant genotype had increased PA(34:3) and PA(36:6) after pathogen inoculation. The PLC/DAGK pathway contributes to this increase. The net log2 fold down-regulation of PLD in *M. phaseolina* inoculated Tx7000 was -3.4 while that of SC599 was -2.4. Therefore, the PLD pathway may not contribute to enhanced PA synthesis in both genotypes after *M. phaseolina* infection. The significantly lower PI(34:2) and DAG (34:2) content of *M. phaseolina*-inoculated SC599 indicated their contribution to enhanced PA content under pathogen infection through the PLC/DAGK pathway. The significantly up-regulated PLC gene (*Sb09g002320*) and non-significantly differentially expressed DAGK genes in SC599 bolsters this observation. The contribution of PLC/DAGK pathway to increased PA biosynthesis under *M. phaseolina* inoculation agree with previous reports that, pathogenic elicitors, in general, activate the PLC/DAGK pathway (de Jong *et al*.,

2004; Laxalt & Munnik, 2002; Van der Luit *et al*., 2000; Den Hartog *et al*., 2003; Yamaguchi *et al*., 2003). On the other hand, the significantly higher PI(34:2), PI(36:4), and PI(36:2) content in inoculated Tx7000 is in agreement with the observed down-regulation of PLC genes. Therefore, although many DAGK genes are significantly up-regulated in Tx7000, the amount of PA generated through the PLC/DAGK pathway is comparatively lower compared to that of SC599 after pathogen infection.

Although PA plays an important role in plant defense against pathogens (Laxalt & Munnik, 2002; Munnik, 2001; Wang, 2004), the increased level of PA could contribute to destabilizing membrane bilayers that result in membrane fusion and cell death (Welti *et al*., 2002). Moreover, a hike in PA is likely to be upstream of an oxidative burst while exogenously applied PA can induce a partial oxidative burst in plants (de Jong *et al*., 2004). These studies suggest the potential downsides of excess PA to normal cellular function. The significantly higher total PA content in Tx7000 compared to SC599 (across 7 and 10 DPI and across two treatments) suggested that Tx7000 may be more vulnerable to PA-hike-associated retardation of cell function.

Plants tend to synthesize additional galactolipids to replace phospholipids under conditions of phosphate deprivation, which results in an increased galactolipid:phospholipid ratio (Andersson *et al*., 2003; Hartel *et al*., 2000). However, low temperature stress increases the proportion of phospholipids and results in a decreased galactolipid:phospholipid ratio (Li *et al*., 2008; Uemura *et al*., 1995). In the current study, we observed a significantly greater galactolipid:phospholipid ratio in Tx7000 after *M. phaseolina* inoculation at 4 DPI. It may be possible that Tx7000 undergoes phosphate deprivation at the initial stages of pathogen infection. Interestingly, the exact opposite phenomenon was observed across 7 and 10 DPI. This indicates that the potential phosphate deprivation experienced by Tx7000 at the initial stages of infection would only be transient. The potential relationship between the galactolipid:phospholipid ratio and charcoal rot disease reaction deserves further investigation.

CONCLUSIONS

Lipids are of paramount importance for normal cellular function. Their contribution extends from structural building blocks to signaling molecules. Lipids are also important determinants of the outcome of host-pathogen interactions. Here, by using gene expression and functional lipidomic investigations, we provide evidence for *M. phaseolina*'s ability to significantly decrease phosphatidylserine and phytosterol in a charcoal-rot-susceptible sorghum genotype (Tx7000). Additionally, the monogalactosyldiacylglycerol to digalactosyldiacylglycerol ratio was significantly increased in the susceptible genotype (Tx7000) after *M. phaseolina* inoculation. These findings suggest there are potential negative impacts of *M. phaseolina* inoculation on plastid- and cell membrane integrity. Moreover, Tx7000 had significantly lower ox-lipid content, which suggests that the pathogen can impede the host's lipid-based signaling capacity including jasmonic acid biosynthesis. Furthermore, the enhanced stigmasterol to sitosterol ratio observed in Tx7000 after *M. phaseolina* inoculation provides additional evidence that Tx7000 is under oxidative stress after *M. phaseolina* infection. Except for higher ox-lipid content, the above mentioned lipid classes and ratios of the resistant genotype (SC599) were not significantly affected by *M. phaseolina*. Therefore, SC599 appears to be resilient to *M. phaseolina* inoculation-associated lipid profile changes that were observed in Tx7000. In summary, this study revealed the underlying lipid alterations that contribute to induced charcoal rot disease susceptibility in grain sorghum.

REFERENCES

Andersson MX, Hamberg M, Kourtchenko O, Brunnstrom A, McPhail KL, Gerwick WH, Göbel C, Feussner I, Ellerström M. 2006. Oxylipin profiling of the hypersensitive response in *Arabidopsis thaliana*. Formation of a novel oxo-phytodienoic acid-containing galactolipid, arabidopside E. *The Journal of Biological Chemistry* 281: 31528-31537.

Andersson MX, Stridh MH, Larsson KE, Liljenberg C, Sandelius AS. 2003. Phosphate-deficient oat replaces a major portion of the plasma membrane phospholipids with the galactolipid digalactosyldiacylglycerol. *FEBS Letters* 537: 128-132.

Benjamini Y, Hochberg Y. 1995. Controlling the false discovery rate: a practical and powerful approach to multiple testing. *Journal of the Royal Statistical Society series B* (Methodological) 57: 289-300.

Benveniste P. 2004. Biosynthesis and accumulation of sterols. *Annual Review of Plant Biology* 55: 429-457.

Bloch KE. 1983. Sterol, structure and membrane function. *Critical Reviews in Biochemistry* 14: 47-92.

Bogdanov M, Dowhan W. 1999. Lipid-assisted protein folding. *Journal of Biological Chemistry.* 274: 36827-36830.

Boudière L, Michaud M, Petroutsos D, Rébeillé F, Falconet D, Bastien O, Roy S, Finazzi G, Rolland N, Jouhet J *et al*. 2014. Glycerolipids in photosynthesis: composition, synthesis and trafficking. *Biochimica et Biophysica Acta* 1837: 470-480.

Chen J, Burke JJ, Xin Z, Xu C, Velten J. 2006. Characterization of the *Arabidopsis* thermo sensitive mutant atts02 reveals an important role for galactolipids in thermotolerance. *Plant Cell & Environment* 29: 1437-1448.

Christensen SA, Kolomiets MV. 2011. The lipid language of plant–fungal interactions. *Fungal Genetics and Biology* 48: 4-14.

De Jong CF, Laxalt AM, Bargmann BO, De Wit PJ, Joosten MH, Munnik T. 2004. Phosphatidic acid accumulation is an early response in the Cf-4/Avr4 interaction. *Plant Journal* 39: 1-12

Demel RA, De Kruyff B. 1976. The function of sterols in membranes. The function of sterols in membranes. *Biochimica et Biophysica Acta* 457: 109-132.

den Hartog M, Verhoef N, Munnik T. 2003. Nod factor and elicitors activate different phospholipid signaling pathways in suspension-cultured alfalfa cells. *Plant Physiology* 132: 311-317.

Devaiah SP, Roth MR, Baughman E, Li M, Tamura P, Jeannotte R, Welti R, Wang X. 2006. Quantitative profiling of polar glycerolipid species from organs of wild-type Arabidopsis and a PHOSPHOLIPASE Da1 knockout mutant. *Phytochemistry* 67: 1907-1924.

Fujii S, Kobayashi K, Nakamura Y, Wada H. 2014. Inducible knockdown of MONOGALACTOSYLDIACYLGLYCEROL SYNTHASE1 reveals roles of galactolipids in organelle differentiation in Arabidopsis cotyledons. *Plant Physiology* 166: 1436-1449.

Fujioka S, Takatsuto S, Yoshida S. 2002. An early C-22 oxidation branch in the brassinosteroid biosynthetic pathway. *Plant Physiology* 130: 930-939.

Fukuda H. 2000. Programmed cell death of tracheary elements as a paradigm in plants. *Plant Molecular Biology* 44: 245-253.

Funk CD. 2001. Prostaglandins and leukotrienes: advances in eicosanoid biology. *Science* 294: 1871-1875.

Glazebrook J. 2005. Contrasting mechanisms of defense against biotrophic and necrotrophic pathogens. *Annual Review of Phytopathology* 43: 205-227

Gobel C, Feussner I, Hamberg M, Rosahl S. 2002. Oxylipin profiling in pathogen-infected potato leaves. *Biochimica et Biophysica Acta* 1584: 55-64.

Gounaris K, Barber J. 1983. Monogalactosyldiacylglycerol: the most abundant polar lipid in nature. *Trends in Biochemical Sciences* 8: 378-381

Griebel T, Zeier J. 2010. A role for β-sitosterol to stigmasterol conversion in plant–pathogen interactions. *Plant Journal* 63: 254-268.

Hartel H, Dormann P, Benning C. 2000. DGD1-independent biosynthesis of extraplastidic galactolipids after phosphate deprivation in Arabidopsis. *Proceedings of the National Academy of Sciences USA* 97: 10649-10654.

Hazei JR, Williams EE. 1990. The role of alterations in membrane lipid composition in enabling physiological adaptation of organisms to their physical environment. *Progress in Lipid Research* 29: 167-227.

Horvath SE, Daum G. 2013. Lipids of mitochondria. *Progress in Lipid Research* 52: 590-614.

Howe LR. 2007. Inflammation and breast cancer: cyclooxygenase/prostaglandin signaling and breast cancer. *Breast Cancer Research* 9: 210.

Imbusch R. Mueller MJ. 2000. Analysis of oxidative stress and wound-inducible dinor isoprostanes F(1) (phytoprostanes F(1)) in plants. *Plant Physiology* 124: 1293-1304.

Islam MS, Haque MS, Islam MM, Emdad EM, Halim A, Hossen QM, Hossain MZ, Ahmed B, Rahim S, Rahman MS *et al*. 2012. Tools to kill: genome of one of the most destructive plant pathogenic fungi *Macrophomina phaseolina*. *BMC Genomics* 13: 1.

Jenks MA, Joly RA, Rich PJ, Axtell JD, Ashworth EN. 1994. Chemically induced cuticle mutation affecting epidermal conductance to water vapor and disease susceptibility in *Sorghum bicolor* (L.) Moench. *Plant Physiology 105:* 1239-1245.

Joyard J. Ferro M, Masselon C, Seigneurin-Berny D, Salvi D, Garin J, Rolland N. 2010. Chloroplast proteomics highlights 230 The Plant Cell the subcellular compartmentation of lipid metabolism. *Progress in Lipid Research* 49: 128-158.

Kachroo A, Kachroo P. 2009. Fatty acid-derived signals in plant defense. *Annual Review of Phytopathology* 47: 153-176.

Khangura, R. and Aberra, M. (2009). First report of charcoal rot on canola caused by *Macrophomina phaseolina* in Western Australia. *Plant Disease* 93: 666-666.

Kolattukudy PE. 2001. Polyesters in higher plants. *Advances in Biochemical Engineering / Biotechnology* 71:1-49.

Kusters R, Breukink E, Gallusser A, Kuhn A, De Kruijff B. 1994. A dual role for phosphatidylglycerol in protein translocation across the *Escherichia coli* inner membrane. *Journal of Biological Chemistry* 269: 1560-1563.

Kuriyama H, Fukuda H. 2001. Regulation of tracheary element differentiation. *Journal of Plant Growth Regulation* 20: 35-51.

Laxalt AM, Munnik T. 2002. Phospholipid signalling in plant defence. *Current Opinion in Plant Biology* 5: 332-338.

Li W, Wang R, Li M, Li L, Wang C, Welti R, Wang X. 2008. Differential degradation of extraplastidic and plastidic lipids during freezing and post-freezing recovery in *Arabidopsis thaliana*. *Journal of Biological Chemistry* 283: 461-468.

Mahmoud A, Budak H. 2011. First report of charcoal rot caused by *Macrophomina phaseolina* in sunflower in Turkey. *Plant Disease* 95: 223-223.

Martin M. 2011. Cutadapt removes adapter sequences from high-throughput sequencing reads. *EMBnet. Journal* 17: 10-12.

McDowell JM, Dangl JL. 2000. Signal transduction in the plant immune response. *Trends in Biochemical Sciences* 25: 79-82.

Moellering ER, Muthan B, Benning C. 2010. Freezing tolerance in plants requires lipid remodeling at the outer chloroplast membrane. *Science* 330: 226-228.

Mortazavi A, Williams BA, McCue K, Schaeffer L, Wold B. 2008. Mapping and quantifying mammalian transcriptomes by RNA-Seq. *Nature Methods* 5: 621-628.

Munnik T. 2001. Phosphatidic acid; an emerging plant lipid second messenger. *Trends in Plant Science* 6: 227-233.

Nakamura Y. Ohta H. 2007. The diacylglycerol forming pathways differ among floral organs of *Petunia hybrida*. *FEBS Letters* 581: 5475-5479.

Paterson AH, Bowers JE, Bruggmann R, Dubchak I, Grimwood J, Gundlach H, Haberer G, Hellsten U, Mitros T, Poliakov A. 2009. The *Sorghum bicolor* genome and the diversification of grasses. *Nature* 457: 551-556.

Reina-Pinto JJ, Yephremov A. 2009. Surface lipids and plant defenses. *Plant Physiology and Biochemistry* 47: 540-549.

Roberts K, McCann MC. 2000. Xylogenesis: the birth of a corpse. *Current Opinion of Plant Biology* 3: 517-522.

Roche Y, Gerbeau-Pissot P, Buhot B, Thomas D, Bonneau L, Gresti J, Mongrand S, Perrier-Cornet JM, Simon-Plas F. 2008. Depletion of phytosterols from the plant plasma membrane provides evidence for disruption of lipid rafts. *The FASEB Journal* 22: 3980-3991.

Sandhu A, Singh R, Sandhu A. 1999. Factors influencing susceptibility of cowpea to *M. phaseolina*. *Journal of Mycology and Plant Pathology* 29: 421-424.

Schaller H. 2003. The role of sterols in plant growth and development. *Progress in Lipid Research* 42: 163-175.

Schuler I, Milon A, Nakatani Y, Ourisson G, Albrecht AM, Benveniste P, Hartman MA. 1991. Differential effects of plant sterols on water permeability and on acyl chain ordering of soybean phosphatidylcholine bilayers. *Proceedings of the National Academy of Sciences USA* 88: 6926-6930.

Shah J. 2005. Lipids, lipases, and lipid-modifying enzymes in plant disease resistance. *Annual Review of Phytopathology* 43: 229-260.

Shea JM, Del Poeta M. 2006. Lipid signaling in pathogenic fungi. *Current Opinion in Microbiology* 9: 352-358.

Short G, Wyllie T, Bristow P. 1980. Survival of *Macrophomina phaseolina* in soil and in residue of soybean. *Phytopathology* 70: 13-17.

Sutton B.C. 1980. The coelomycetes, fungi imperfecti with pycnidia, acervuli and stromata. Commonwealth Mycological Institute. Kew, Surrey, UK.

Tarr, SAJ. 1962. Root and stalk diseases: Red stalk rot, Colletotrichum rot, anthracnose, and red leaf spot, in: Diseases of Sorghum, Sudan Grass and Brown Corn. Commonwealth Mycological Institute, Kew, Surrey, UK, pp. 58-73.

Tesso T, Claflin LE, Tuinstra MR. 2004. Estimation of combining ability for resistance to Fusarium stalk rot in grain sorghum. *Crop Science* 44: 1195-1199.

Tesso T, Perumal R, Little CR, Adeyanju A, Radwan GL, Prom LK, Magill CW. 2012. Sorghum pathology and biotechnology-a fungal disease perspective: Part II. Anthracnose, stalk rot, and downy mildew. *European Journal of Plant Science and Biotechnology* 6: 31-44.

Testerink C, Munnik T. 2005. Phosphatidic acid: a multifunctional stress signaling lipid in plants. *Trends in Plant Science* 10: 368-375.

Thoma I, Loeffler C, Sinha AK, Gupta M, Krischke M, Steffan B, Roitsch T, Mueller MJ. 2003. Cyclopentenone isoprostanes induced by reactive oxygen species trigger defense gene activation and phytoalexin accumulation in plants. *Plant Journal* 34: 363-375

Uemura M, Joseph RA, Steponkus PL. 1995. Cold acclimation of *Arabidopsis thaliana* (Effect on plasma membrane lipid composition and freeze-induced lesions). *Plant Physiology* 109: 15-30.

van der Luit AH, Piatti T, van Doorn A, Musgrave A, Felix G, Boller T, Munnik T. 2000. Elicitation of suspension-cultured tomato cells triggers the formation of phosphatidic acid and diacylglycerol pyrophosphate. *Plant Physiology* 123: 1507-1516.

van Leeuwen W, Okresz L, Bogre L, Munnik T. 2004. Learning the lipid language of plant signalling. *Trends in Plant Science* 9: 378-384.

van Meer G, Voelker DR, Feigenson GW. 2008. Membrane lipids: where they are and how they behave. *Nature Reviews Molecular Cell Biology* 9: 112-124.

Vance JE. 2008. Phosphatidylserine and phosphatidylethanolamine in mammalian cells: two metabolically related aminophospholipids. *Journal of Lipid Research* 49: 1377-1387.

Vu HS, Shiva S, Roth MR, Tamura P, Zheng L, Li M, Sarowar S, Honey S, McEllhiney D, Hinkes P *et al*. 2014. Lipid changes after leaf wounding in *Arabidopsis thaliana*: expanded lipidomic data form the basis for lipid co-occurrence analysis. *Plant Journal* 80: 728-743.

Vu HS, Tamura P, Galeva NA, Chaturvedi R, Roth M.R, Williams TD, Wang X, Shah J, Welti R. 2012. Direct infusion mass spectrometry of oxylipin-containing *Arabidopsis* membrane lipids reveals varied patterns in different stress responses. *Plant Physiology* 158: 324-339.

Walley JW, Kliebenstein DJ, Bostock RM, Dehesh K. 2013. Fatty acids and early detection of pathogens. *Current Opinion in Plant Biology* 16: 520-526.

Wallis JG, Browse J. 2002. Mutants of Arabidopsis reveal many roles for membrane lipids. *Progress in Lipid Research* 41: 254-278.

Wang K, Senthil-Kumar M, Ryu, CM, Kang L, Mysore KS. 2012. Phytosterols play a key role in plant innate immunity against bacterial pathogens by regulating nutrient efflux into the apoplast. *Plant Physiology* 158: 1789-1802.

Wang X, 2004. Lipid signalling. *Current Opinion in Plant Biology* 7: 329-336.

Webb M. Green BR. 1991. Biochemical and biophysical properties of thylakoid acyl lipids. *Biochimica et Biophysica Acta* 1060: 133-158.

Welti R, Li W, Li M, Sang Y, Biesiada H, Zhou HE, Rajashekar CB, Williams TD, Wang X. 2002. Profiling membrane lipids in plant stress responses. Role of phospholipase D alpha in freezing-induced lipid changes in Arabidopsis. *Journal of Biological Chemistry* 277: 31994-32002.

Welti R, Shah J, Li W, Li M, Chen J, Burke JJ, Fauconnier ML, Chapman K, Chye ML, Wang X. 2007. Plant lipidomics: Discerning biological function by profiling plant complex lipids using mass spectrometry. *Frontiers in Bioscience* 12: 2494-2506.

Wu TD, Watanabe CK. 2005. GMAP: a genomic mapping and alignment program for mRNA and EST sequences. *Bioinformatics* 21: 1859-1875.

Xia XJ, Wang YJ, Zhou YH, Tao Y, Mao WH, Shi K, Asami T, Chen Z, Yu JQ. 2009. Reactive oxygen species are involved in brassinosteroid-induced stress tolerance in cucumber. *Plant Physiology* 150: 801-814.

Xiao S, Gao W, Chen QF, Chan SW, Zheng SX, Ma J, Wang M, Welti R, Chye ML. 2010. Overexpression of Arabidopsis acyl-CoA binding protein ACBP3 promotes starvation-induced and age-dependent leaf senescence. *Plant Cell* 22: 1463-1482.

Yamaguchi T, Minami E, Shibuya N. 2003. Activation of phospholipases by N-acetylchitooligosaccharide elicitor in suspension-cultured rice cells mediates reactive oxygen generation. *Physiologia Plantarum* 118: 361-370.

Zheng G, Tian B, Zhang F, Tao F, Li W. 2011. Plant adaptation to frequent alterations between high and low temperatures: remodelling of membrane lipids and maintenance of unsaturation levels. *Plant Cell & Environment* 34: 1431-1442.

Zoeller M, Stingl N, Krischke M, Fekete A, Waller F, Berger S, Mueller MJ. 2012. Lipid profiling of the *Arabidopsis* hypersensitive response reveals specific lipid peroxidation and fragmentation processes: biogenesis of pimelic and azelaic acid. *Plant Physiology* 160: 365-378.

TABLES AND FIGURES

Table 6.1. Significantly ($q < 0.05$) differentially expressed genes (related to lipid associated metabolic pathways) between SC599 (charcoal-rot-resistant) and Tx7000 (charcoal-rot-susceptible) sorghum genotypes in response to *Macrophomina phaseolina* inoculation at 7 days post-inoculation.

Metabolic pathway	Gene annotation	Gene	Geno × Trt* q-value	SC599 (MP-CON)†		Tx7000 (MP-CON)	
				log2 DE‡	q-value	log2 DE	q-value
Jasmonic acid biosynthesis	Phospholipase A2	*Sb07g028890*	3.13E-12	-	-	-9.028	8.36E-16
		Sb01g010640	2.01E-15	0.916	0.4214	-6.590	9.57E-11
		Sb03g037150	2.44E-02	0.534	0.9013	-3.442	3.12E-05
		Sb01g040430	4.76E-05	2.527	0.0037	-1.772	1.03E-01
		Sb06g021680	1.67E-10	1.468	0.0006	-1.373	2.97E-03
		Sb03g003310	4.84E-02	-0.093	0.9880	3.415	2.47E-03
		Sb01g031910	2.52E-02	-	-	4.694	1.84E-03
	Lypoxygenase	*Sb06g031350*	6.88E-04	1.344	0.4897	-4.604	2.55E-14
		Sb01g011040	1.01E-03	0.147	0.9583	-2.357	1.06E-06
		Sb01g011050	5.99E-04	2.331	0.0001	-0.300	6.10E-01
		Sb06g018040	1.23E-04	-0.294	0.9368	2.816	3.14E-23
	Cytochrome P450 74A3	*Sb01g007000*	6.35E-04	-0.498	0.8491	2.467	1.96E-13
		Sb01g042270	6.01E-02	1.053	0.1592	2.245	4.58E-20
	12-oxophytodienoate reductase	*Sb06g017670*	1.46E-02	-1.040	0.4414	1.091	1.48E-02
		Sb06g017680	5.68E-03	-0.803	0.3192	1.092	2.19E-02
		Sb10g007300	3.08E-02	-	-	2.111	1.89E-03
		Sb10g007310	2.84E-04	-0.988	0.5635	3.048	1.15E-06
		Sb10g007330	3.20E-04	-0.940	0.6610	3.144	1.31E-09
		Sb09g000520	3.09E-06	-0.473	0.8539	5.201	2.72E-04

		Sb10g007320	7.34E-04	-	-	5.990	2.56E-16
Trans, trans-farnesyl diphosphate biosynthesis	Prenyltransferase	*Sb01g044560*	3.52E-03	0.927	0.3933	-1.370	4.07E-02
	Para-hydroxybenzoate-polyprenyl transferase	*Sb04g038180*	8.36E-06	0.248	0.8750	-1.489	4.66E-07
	Polyprenyl synthetase	*Sb07g005530*	4.17E-03	0.548	0.7654	-1.670	2.55E-03
Phytosterol biosynthesis	Cycloartenol synthase	*Sb06g015960*	3.29E-06	0.945	0.5760	-3.084	8.64E-10
		Sb08g019310	1.89E-04	-0.047	0.9905	-3.041	6.67E-09
		Sb08g019300	2.54E-05	0.131	0.9668	-3.021	6.09E-10
		Sb08g019290	1.32E-06	0.127	0.9583	-2.306	1.27E-11
		Sb07g006300	2.93E-02	0.820	0.5426	-0.979	5.57E-02
	24-methylenesterol C-methyltransferase 2	*Sb01g004280*	7.02E-03	-	-	-1.857	1.13E-02
		Sb01g004290	2.01E-04	-	-	-2.015	1.41E-02
		Sb01g004295	4.33E-14	0.201	0.9583	-6.755	1.78E-18
		Sb01g004300	3.62E-19	0.268	0.9289	-6.791	1.40E-52
		Sb01g004310	2.65E-09	-0.789	0.3990	-7.238	4.64E-19
		Sb09g029600	2.46E-04	1.086	0.4261	-2.199	9.95E-05
	Cycloeucalenol cycloisomerase	*Sb09g002170*	9.42E-03	-	-	-2.151	1.04E-02
	Cytochrome P450 51	*Sb05g022370*	4.60E-02	-	-	-4.138	9.47E-03
		Sb08g002250	1.75E-03	-0.207	0.9143	-1.780	5.35E-09
	C-14 sterol reductase (sterol delta-7 reductase)	*Sb04g017400*	4.87E-02	-0.465	0.8393	0.964	2.56E-07
	3-beta-hydroxysteroid-delta-isomerase	*Sb03g008970*	4.79E-09	0.463	0.8161	6.624	1.69E-07
Brassinosteroid biosynthesis	Steroid 22-alpha hydroxylase	*Sb03g002870*	1.83E-08	0.927	0.3667	-4.279	3.16E-13
		Sb05g002580	5.42E-03	0.964	0.2168	-0.906	4.39E-02
	3-oxo-5-alpha-steroid 4-dehydrogenase	*Sb03g040050*	1.79E-04	0.178	0.9559	-2.153	3.25E-07
		Sb02g003510	3.82E-02	-	-	-2.154	9.89E-02
Phosphatidic acid (PA) biosynthesis	Diacylglycerol kinase	*Sb04g032990*	1.13E-06	-0.947	0.4938	3.129	1.58E-24
		Sb03g036560	5.99E-04	0.603	0.7489	3.579	3.66E-16
		Sb07g020990	3.98E-04	-0.540	0.5124	0.878	6.08E-06
		Sb07g020990	3.98E-04	-0.540	0.5124	0.878	6.08E-06
		Sb07g025680	6.55E-04	-0.612	0.2243	0.430	3.77E-02
		Sb04g035410	1.28E-02	-0.454	0.4325	0.322	2.04E-01

		Sb05g024160	5.16E-03	0.996	0.3236	-0.968	1.32E-02
		Sb07g029110	1.07E-02	0.134	0.9484	-1.133	9.94E-04
	phospholipase C	*Sb09g002320*	1.20E-07	1.296	0.0113	-4.020	7.24E-09
		Sb02g044010	3.13E-03	0.645	0.4053	-0.630	8.53E-03
		Sb06g020050	3.34E-02	0.364	0.7953	-0.630	1.33E-02
	phospholipase D	*Sb02g024910*	6.80E-13	0.805	0.7224	-7.983	1.66E-26
		Sb02g008130	3.83E-06	0.741	0.5370	-2.123	8.72E-10
		Sb10g025660	4.28E-03	-1.021	0.0322	0.388	3.94E-01
		Sb03g012720	3.76E-04	-0.524	0.1612	0.752	1.66E-02
		Sb01g031100	6.38E-13	-0.552	0.1446	1.078	7.36E-08
		Sb01g033480	3.05E-05	-0.932	0.4264	2.247	1.56E-08
Phosphatidylserine (PS) biosynthesis	Phosphatidylserine synthase	*Sb09g027850*	3.48E-09	-0.779	0.5593	3.136	1.25E-55
MGDG˚ to DGDG conversion	Digalactosyldiacylglycerol synthase	*Sb05g003730*	2.60E-03	0.545	0.5608	-1.102	1.62E-03
Phospholipid and Glycolipid desaturation	Omega-6/-3 fatty acid desaturase	*Sb07g021640*	1.23E-06	0.753	0.5296	-2.490	1.99E-14
		Sb01g042150	1.42E-03	0.756	0.6311	-2.001	7.86E-05
		Sb02g043980	4.83E-02	0.004	0.9988	-0.912	1.58E-02
		Sb06g004770	6.52E-03	-0.482	0.6500	0.921	3.72E-03
		Sb01g038500	5.69E-03	-0.598	0.5541	1.216	4.30E-03
		Sb08g000460	9.18E-07	-1.891	0.0870	2.785	9.53E-08
		Sb05g000400	4.89E-03	-	-	3.470	9.70E-04

***** Geno × Trt = genotype by treatment interaction where treatment consists of *M. phaseolina* and Control inoculations. †MP = *M. phaseolina,* CON = control. ‡ log2 DE = log2 fold differential expression. ˚MGDG = Monogalactosyldiacylglycerol, DGDG = Digalactosyldiacylglycerol.

Table 6.2. F-statistic *P*-values from analysis of variance (ANOVA) for different sorghum stalk lipid classes isolated from charcoal-rot-resistant (SC599) and susceptible (Tx7000) sorghum genotypes after inoculation with *M. phaseolina* and phosphate buffered saline (mock-inoculated control) at three post-inoculation time points (4, 7, and 10 days post-inoculation) ($\alpha = 0.05$). Lipids were analyzed using an electrospray ionization-triple quadrupole mass spectrometer.

Lipid class / effect	*P*-value						
	Genotype (G)	Time (T)	G × T	Trt* (I)	G × I	T × I	G × T × I
DGDG†	0.0002	0.1330	0.3049	0.0302	0.6788	0.2693	0.0275
MGDG	0.1025	0.0048	0.6768	0.9439	0.9147	0.4966	0.0638
MGDG/DGDG	<0.0001	0.0106	0.2427	0.0042	**0.0143**	0.5874	0.9198
SQDG	0.8342	0.1793	0.8570	0.4282	0.8711	0.2635	0.0213
PG	<0.0001	0.0278	0.0022	0.8903	0.0284	0.9771	0.0214
PC	0.8012	0.1981	0.5463	0.0695	0.6494	0.2462	0.2508
PE	0.0266	0.2560	0.1483	0.2908	0.4520	0.4450	0.2195
PE/PC	0.0005	0.4360	0.0482	0.8763	0.0735	0.6460	0.3786
PI	0.0110	0.0085	0.3554	0.0204	0.3264	0.3787	0.2057
PS	0.1392	0.0118	0.1097	0.2378	**0.0190**	0.2142	0.0765
PA	<0.0001	0.0211	0.2362	0.0002	0.9484	0.5027	0.0243
Galactolipids˚/Phospholipids¨	0.0288	0.0081	0.1794	0.0142	0.9596	0.8798	0.0009
LysoPC	<0.0001	0.0521	0.6556	0.1929	0.4753	0.0848	0.3285
LysoPE	0.0936	0.1601	0.5967	0.2781	0.5530	0.3353	0.9535
Sterol Glucosides	0.0019	0.5439	0.7711	0.0145	**0.0464**	0.9666	0.8195
Acyl(18:2)Sterol Glucosides	<0.0001	0.0811	0.5158	0.0218	**0.0152**	0.6307	0.0624
Acyl(16:0)Sterol Glucosides	<0.0001	0.1510	0.0657	0.3174	0.3141	0.1602	0.0803
NL297(18:2)containing TAG	<0.0001	0.3251	0.0473	0.0023	0.7659	0.9300	0.1361
NL295(18:3)containing DAG,TAG	<0.0001	0.4359	0.3500	<0.0001	0.1266	0.9599	0.1738
NL273(16:0)containing DAG,TAG	<0.0001	0.1934	0.0976	0.0004	0.5034	0.7124	0.1367
HexCer	0.7335	0.7213	0.3913	0.0464	0.9281	0.2743	0.4609
Prec291(18:3-2O)or18:4-O (A)	<0.0001	0.0026	0.5462	0.0128	**0.0013**	0.0136	0.7611
Prec293(18:2-2O)or18:3-O (B)	0.9411	<0.0001	0.0151	0.1397	**0.0165**	0.6564	0.2161
Total ox-lipids (A+B)	0.0043	<0.0001	0.1882	0.2308	**0.0020**	0.0585	0.9105

*Trt = Inoculation treatment. † DGDG = digalactosyldiacylglycerol; MGDG = Monogalactosyldiacylglycerol; SQGD = Sulfoquinovosyl diacylglycerol; PG = Phosphatidylglycerol; PC = Phosphatidylcholine; PE = Phosphatidylethanolamine; PI = Phosphatidylinositol; PS = Phosphatidylserine; PA = Phosphatidic acid; LysoPC = Lysophosphatidylcholine; LysoPE = Lysophosphatidylethanolamine; TAG = Triacylglycerol; DAG = Diacylglycerol; HexCer = Hexosylceramide. ˚Galactolipids = (DGDG + MGDG + SQDG). ¨Phospholipids = (PG + PC + PE + PI + PS + PA).

Table 6.3. Lipid species with significant genotype × inoculation treatment interactions across three post- inoculation stages (4, 7, and 10 days post-inoculation). Mean lipid content (normalized signal in % basis) and *P*-values for mean difference between control and *Macrophomina phaseolina* are given (α = 0.05).

Lipid species	P-value G × I*	SC599		*P*-value	Tx7000		*P*-value
		Mean			Mean		
		CON‡	MP•		CON	MP	
PG(34:3)†	0.0006	0.519	0.654	0.0127	0.699	0.626	0.0015
PG(36:2)	0.0038	0.007	0.008	0.7542	0.014	0.024	0.0005
PC(34:3)	0.0003	6.164	7.540	<0.0001	4.074	4.358	0.1321
PC(34:2)	0.0127	9.554	8.667	0.0178	10.544	11.010	0.2234
PC(36:6)	0.0001	0.899	1.405	<.0001	0.434	0.531	0.0288
PC(36:2)	0.0026	0.392	0.413	0.4497	0.516	0.733	0.0003
PC(36:1)	0.0115	0.058	0.081	0.0047	0.063	0.054	0.3268
PE(34:4)	0.0485	0.010	0.014	0.0018	0.007	0.008	0.0905
PE(34:3)	0.0013	1.953	2.553	<.0001	1.548	1.597	0.6338
PE(36:6)	0.0006	0.181	0.319	<.0001	0.105	0.127	0.0869
PE(36:2)	0.0002	0.072	0.077	0.2534	0.101	0.153	<.0001
PE(42:2)	0.0380	0.131	0.140	0.1744	0.151	0.182	0.0003
PI(34:2)	0.0130	4.591	4.154	0.0435	4.848	5.399	0.0347
PI(36:4)	0.0290	0.178	0.162	0.4206	0.230	0.278	0.0218
PI(36:2)	<0.0001	0.061	0.065	0.2765	0.080	0.144	<.0001
PS(34:3)	0.0190	0.330	0.356	0.2664	0.248	0.198	0.0206
PS(36:3)	0.0010	0.036	0.047	<.0001	0.035	0.032	0.3687
PS(38:3)	0.0020	0.061	0.080	0.0004	0.066	0.060	0.2986
PS(40:3)	0.0095	0.102	0.126	0.0172	0.134	0.115	0.1361
PA(34:3)	0.0041	0.700	1.122	<.0001	0.817	0.981	<.0001
PA(36:6)	0.0002	0.070	0.144	<.0001	0.060	0.080	0.0002
Campesterol-Glc(18:2)	0.0276	0.155	0.132	0.0078	0.066	0.069	0.7538
Stigmasterol-Glc/Sitosterol-Glc	0.0162	0.393	0.392	0.9907	0.559	0.830	0.0062
TAG(18:3/36:9)	0.0006	0.076	0.190	<.0001	0.016	0.037	0.0050
TAG(16:0/36:6)	0.0016	0.067	0.140	<.0001	0.016	0.032	0.0051
DAG(34:2)	0.0026	0.021	0.015	<.0001	0.017	0.017	0.6329
MGDG(18:4-O/18:3)	0.0188	0.016	0.025	0.0302	0.009	0.007	0.3356
MGDG(18:3-2O/18:3)	0.0056	0.014	0.025	0.0063	0.011	0.009	0.4408
PE(16:0/18:3-2O)	0.0008	0.009	0.026	0.0014	0.009	0.006	0.2419
PE(18:2/18:2-2O)	0.0001	0.021	0.030	0.0144	0.036	0.026	0.0011
PC(16:0/18:3-O)	0.0418	0.013	0.010	0.0321	0.008	0.010	0.4566
PC(16:0/18:3-2O)	0.0006	0.008	0.021	0.0003	0.007	0.006	0.6307

*G×I = Genotype by Inoculation treatment interaction. ‡CON = Mock inoculated control treatment. •MP = *Macrophomina phaseolina* inoculation. †PG = Phosphatidylglycerol; PC = Phosphatidylcholine; PE = Phosphatidylethanolamine; PI = Phosphatidylinositol; PS = Phosphatidylserine; PA = Phosphatidic acid; TAG = Triacylglycerol; DAG = Diacylglycerol; MGDG = Monogalactosyldiacylglycerol.

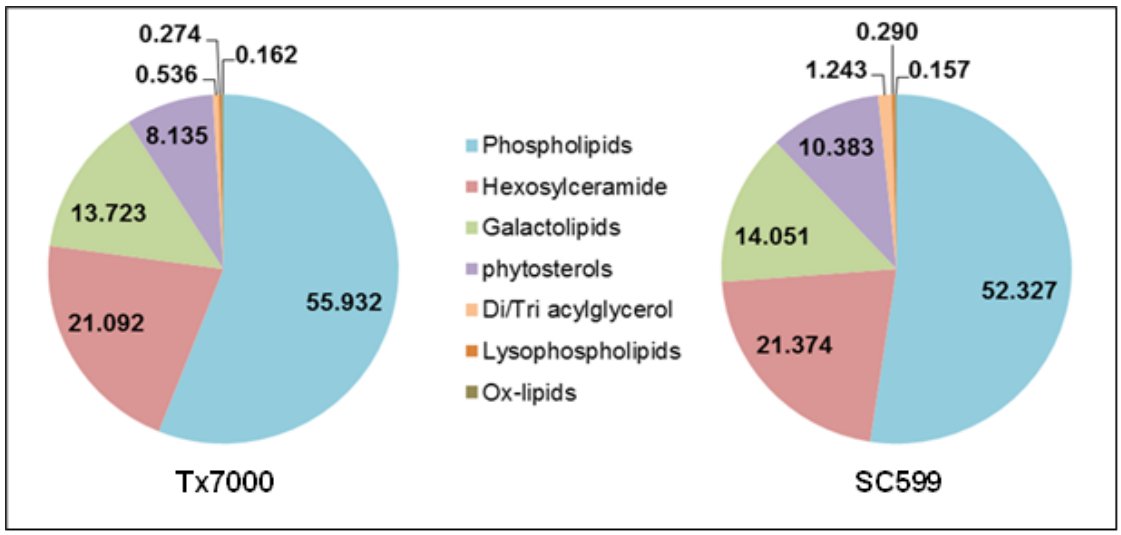

Figure 6.1. Stalk lipid composition (%) of two tested sorghum genotypes (SC599 and Tx7000) after control treatment across three time points (4, 7, 10 days post-inoculation). Phospholipids = ∑ (PG, PC, PE, PI, PS, PA); galactolipids = ∑ (DGDG, MGDG, SQDG); phytosterols = ∑ (sterol glucosides, acyl(18:2) sterol glucosides, acyl(16:0) sterol glucosides); Di/Triacylglycerol = ∑ (NL297(18:2) containing TAG, NL295 (18:3) containing DAG/TAG, NL273 (16:0) containing DAG/TAG); lysophospholipids = ∑ (LysoPC, LysoPE), and Ox-lipids = ∑ (prec291 (18:3-2O) or 18:4-O, prec293 (18:2-2O) or 18:3-O)). ∑ = sum.

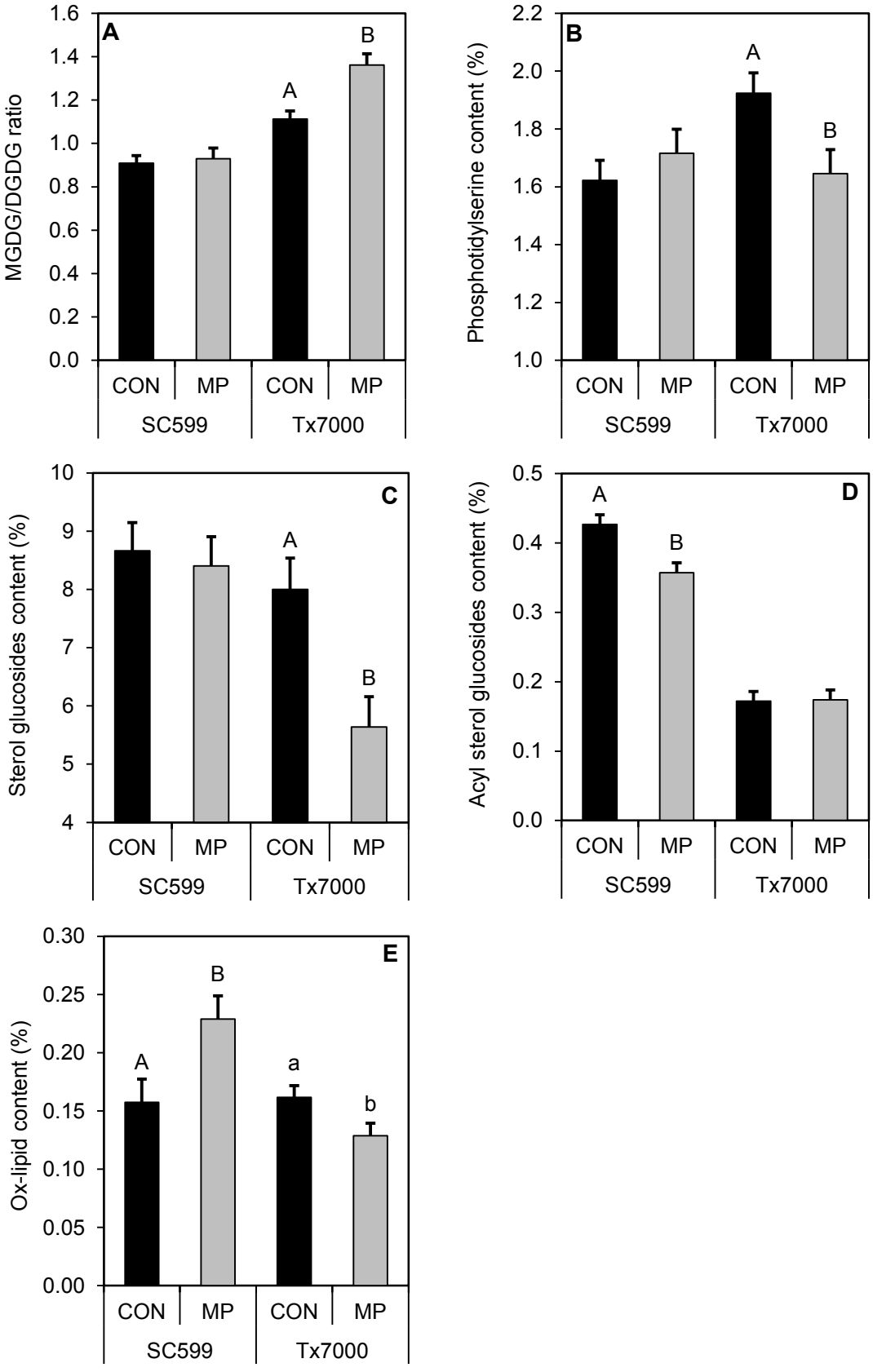
A
MGDG/DGDG ratio
1.6
1.4
1.2
1.0
0.8
0.6
0.4
0.2
0.0
A
B
CON
MP
CON
MP
SC599
Tx7000
B
Phosphotidylserine content (%)
2.2
2.0
1.8
1.6
1.4
1.2
1.0
A
B
CON
MP
CON
MP
SC599
Tx7000
C
Sterol glucosides content (%)
10
9
8
7
6
5
4
A
B
CON
MP
CON
MP
SC599
Tx7000
D
Acyl sterol glucosides content (%)
0.5
0.4
0.3
0.2
0.1
0.0
A
B
CON
MP
CON
MP
SC599
Tx7000
E
Ox-lipid content (%)
0.30
0.25
0.20
0.15
0.10
0.05
0.00
A
B
a
b
CON
MP
CON
MP
SC599
Tx7000

Figure 6.2. Comparison of the mean values (normalized mass spectral signal per mg of stalk tissue) among inoculation treatments for (A) monogalactosyldiacylglycerol(MGDG)/digalactosyldiacylglycerol (DGDG) ratio, (B) phosphatidylserine, (C) sterol glucoside, (D) acyl(18:2) sterol glucoside, and (E) ox-lipid content at each genotype across three time points (4, 7, and 10 days post-inoculation). Means followed by different letters within each genotype are significantly different while the treatments without letter designations within each genotype are not significantly different at $\alpha = 0.05$. Error bars represent standard errors. CON = phosphate-buffered saline mock-inoculated control, MP = *Macrophomina phaseolina*.

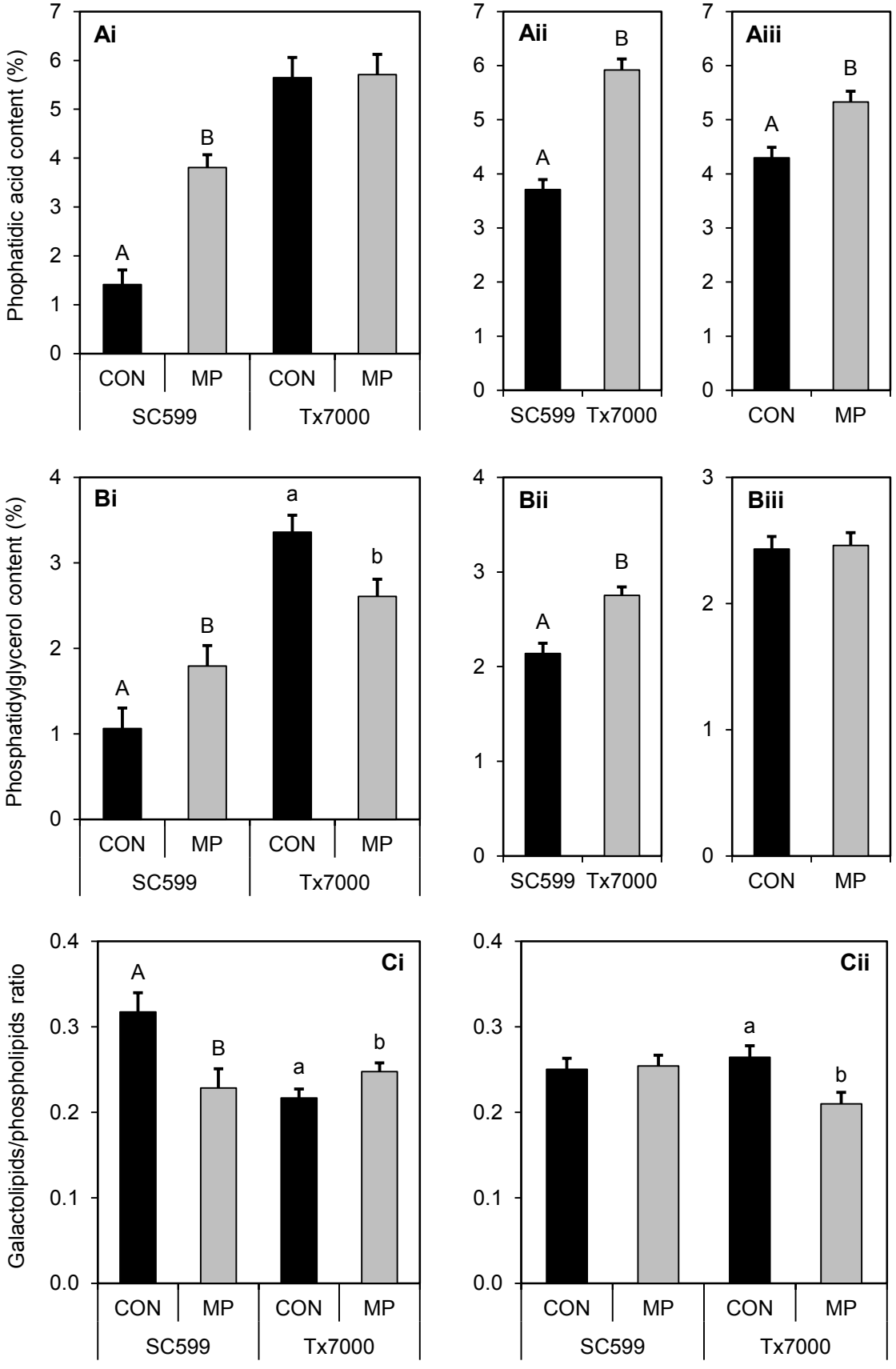
Phophatidic acid content (%)
Ai
A
B
CON
MP
CON
MP
SC599
Tx7000
Aii
A
B
SC599
Tx7000
Aiii
A
B
CON
MP
Phosphatidylglycerol content (%)
Bi
A
B
a
b
CON
MP
CON
MP
SC599
Tx7000
Bii
A
B
SC599
Tx7000
Biii
CON
MP
Galactolipids/phospholipids ratio
Ci
A
B
a
b
CON
MP
CON
MP
SC599
Tx7000
Cii
a
b
CON
MP
CON
MP
SC599
Tx7000

Figure 6.3. Comparison of the mean (normalized mass spectral signal per mg of stalk tissue) phosphatidic acid content (Ai) at 4 days post-inoculation (DPI) (Aii) across 7 and 10 DPI and inoculation treatments (Aiii) across 7 and 10 DPI and two genotypes; phosphatidylglycerol content (Bi) at 4 DPI (Bii) across 7 and 10 DPI and inoculation treatments (Biii) across 7 and 10 DPI and two genotypes; and the galactolipids/phospholipid ratio (Ci) at 4 DPI and (Cii) across 7 and 10 DPI. Means followed by different letters (within each letter case) are significantly different while the treatments without letter designations are not significantly different at $\alpha = 0.05$. Error bars represent standard errors. CON = phosphate-buffered saline mock-inoculated control, MP = *Macrophomina phaseolina*.

Appendix A - Significantly overrepresented gene ontology (GO) terms in sets of genes obtained by comparing differentially expressed genes between control and *Macrophomina phaseolina* treatments.

GO term	P-value	Annotation	Classification
		SC599 at 2 days post-inoculation	
GO:0009738	0.0060	abscisic acid-activated signaling pathway	BP
GO:0048830	0.0088	adventitious root development	BP
GO:0010230	0.0198	alternative respiration	BP
GO:0006865	0.0320	amino acid transport	BP
GO:0009058	0.0142	biosynthetic process	BP
GO:0016132	0.0201	brassinosteroid biosynthetic process	BP
GO:0010268	0.0052	brassinosteroid homeostasis	BP
GO:0016131	0.0167	brassinosteroid metabolic process	BP
GO:0010120	0.0025	camalexin biosynthetic process	BP
GO:0009756	0.0130	carbohydrate mediated signaling	BP
GO:0005975	0.0001	carbohydrate metabolic process	BP
GO:0015976	0.0257	carbon utilization	BP
GO:0016117	0.0102	carotenoid biosynthetic process	BP
GO:0006520	0.0496	cellular amino acid metabolic process	BP
GO:0030643	0.0332	cellular phosphate ion homeostasis	BP
GO:0030007	0.0063	cellular potassium ion homeostasis	BP
GO:0016036	0.0007	cellular response to phosphate starvation	BP
GO:0009855	0.0291	determination of bilateral symmetry	BP
GO:0006855	0.0429	drug transmembrane transport	BP
GO:0045184	0.0426	establishment of protein localization	BP
GO:0009835	0.0225	fruit ripening	BP
GO:0019375	0.0052	galactolipid biosynthetic process	BP
GO:0006542	0.0438	glutamine biosynthetic process	BP
GO:0006868	0.0009	glutamine transport	BP
GO:0006071	0.0012	glycerol metabolic process	BP
GO:0005978	0.0126	glycogen biosynthetic process	BP
GO:0009247	0.0161	glycolipid biosynthetic process	BP
GO:0006096	0.0063	glycolytic process	BP
GO:0010286	0.0112	heat acclimation	BP
GO:0015817	0.0243	histidine transport	BP
GO:0048527	0.0342	lateral root development	BP
GO:0009809	0.0261	lignin biosynthetic process	BP
GO:0030259	0.0034	lipid glycosylation	BP
GO:0006629	0.0047	lipid metabolic process	BP
GO:0006869	0.0041	lipid transport	BP
GO:0009094	0.0485	L-phenylalanine biosynthetic process	BP
GO:0030539	0.0242	male genitalia development	BP
GO:0007112	0.0014	male meiosis cytokinesis	BP
GO:0019593	0.0241	mannitol biosynthetic process	BP
GO:0010014	0.0282	meristem initiation	BP
GO:0008152	0.0129	metabolic process	BP
GO:0007018	0.0229	microtubule-based movement	BP
GO:0006741	0.0271	NADP biosynthetic process	BP
GO:0009788	0.0002	negative regulation of abscisic acid-activated signaling pathway	BP
GO:0043086	0.0020	negative regulation of catalytic activity	BP
GO:0043508	0.0376	negative regulation of JUN kinase activity	BP
GO:0048579	0.0206	negative regulation of long-day photoperiodism, flowering	BP
GO:0006997	0.0407	nucleus organization	BP
GO:0018131	0.0234	oxazole or thiazole biosynthetic process	BP
GO:0055114	0.0366	oxidation-reduction process	BP
GO:0031408	0.0017	oxylipin biosynthetic process	BP
GO:0009698	0.0221	phenylpropanoid metabolic process	BP
GO:0010205	0.0012	photoinhibition	BP
GO:0009765	0.0004	photosynthesis, light harvesting	BP
GO:0009768	0.0057	photosynthesis, light harvesting in photosystem I	BP
GO:0019684	0.0408	photosynthesis, light reaction	BP
GO:0009773	0.0042	photosynthetic electron transport in photosystem I	BP
GO:0000914	0.0461	phragmoplast assembly	BP
GO:0009828	0.0396	plant-type cell wall loosening	BP
GO:0016973	0.0190	poly(A)+ mRNA export from nucleus	BP

GO:0009963	0.0087	positive regulation of flavonoid biosynthetic process	BP
GO:0010072	0.0306	primary shoot apical meristem specification	BP
GO:0006606	0.0139	protein import into nucleus	BP
GO:0006468	0.0297	protein phosphorylation	BP
GO:0010325	0.0386	raffinose family oligosaccharide biosynthetic process	BP
GO:0010017	0.0286	red or far-red light signaling pathway	BP
GO:0009585	0.0413	red, far-red light phototransduction	BP
GO:0019253	0.0001	reductive pentose-phosphate cycle	BP
GO:0009934	0.0043	regulation of meristem structural organization	BP
GO:0010119	0.0005	regulation of stomatal movement	BP
GO:0009737	0.0001	response to abscisic acid	BP
GO:0009646	0.0307	response to absence of light	BP
GO:0009733	0.0051	response to auxin	BP
GO:0009637	0.0153	response to blue light	BP
GO:0010036	0.0461	response to boron-containing substance	BP
GO:0009741	0.0026	response to brassinosteroid	BP
GO:0046686	0.0111	response to cadmium ion	BP
GO:0009409	0.0001	response to cold	BP
GO:0009735	0.0493	response to cytokinin	BP
GO:0009723	0.0068	response to ethylene	BP
GO:0009739	0.0002	response to gibberellin	BP
GO:0009408	0.0235	response to heat	BP
GO:0042542	0.0112	response to hydrogen peroxide	BP
GO:0009753	0.0001	response to jasmonic acid	BP
GO:0009416	0.0007	response to light stimulus	BP
GO:0010038	0.0301	response to metal ion	BP
GO:0009624	0.0069	response to nematode	BP
GO:0006970	0.0200	response to osmotic stress	BP
GO:0051707	0.0212	response to other organism	BP
GO:0010193	0.0307	response to ozone	BP
GO:0010114	0.0114	response to red light	BP
GO:0009751	0.0030	response to salicylic acid	BP
GO:0009651	0.0003	response to salt stress	BP
GO:0006950	0.0145	response to stress	BP
GO:0010224	0.0377	response to UV-B	BP
GO:0009414	0.0001	response to water deprivation	BP
GO:0009611	0.0015	response to wounding	BP
GO:0048765	0.0010	root hair cell differentiation	BP
GO:0048767	0.0055	root hair elongation	BP
GO:0010223	0.0020	secondary shoot formation	BP
GO:0007172	0.0232	signal complex assembly	BP
GO:0019252	0.0113	starch biosynthetic process	BP
GO:0005983	0.0130	starch catabolic process	BP
GO:0010118	0.0468	stomatal movement	BP
GO:0005986	0.0131	sucrose biosynthetic process	BP
GO:0046506	0.0161	sulfolipid biosynthetic process	BP
GO:0009627	0.0188	systemic acquired resistance	BP
GO:0007169	0.0365	transmembrane receptor protein tyrosine kinase signaling pathway	BP
GO:0006810	0.0095	transport	BP
GO:0005992	0.0028	trehalose biosynthetic process	BP
GO:0006569	0.0123	tryptophan catabolic process	BP
GO:0006833	0.0001	water transport	BP
GO:0009501	0.0040	amyloplast	CC
GO:0031225	0.0001	anchored component of membrane	CC
GO:0048046	0.0062	apoplast	CC
GO:0009986	0.0018	cell surface	CC
GO:0005618	0.0116	cell wall	CC
GO:0009707	0.0265	chloroplast outer membrane	CC
GO:0030093	0.0300	chloroplast photosystem I	CC
GO:0009570	0.0217	chloroplast stroma	CC
GO:0009535	0.0004	chloroplast thylakoid membrane	CC
GO:0009512	0.0232	cytochrome b6f complex	CC
GO:0005576	0.0047	extracellular region	CC
GO:0016021	0.0003	integral component of membrane	CC
GO:0016328	0.0252	lateral plasma membrane	CC
GO:0030076	0.0012	light-harvesting complex	CC
GO:0016020	0.0069	membrane	CC
GO:0005875	0.0062	microtubule associated complex	CC
GO:0009522	0.0001	photosystem I	CC
GO:0009782	0.0366	photosystem I antenna complex	CC

GO:0009538	0.0034	photosystem I reaction center	CC
GO:0009523	0.0002	photosystem II	CC
GO:0009783	0.0284	photosystem II antenna complex	CC
GO:0009505	0.0002	plant-type cell wall	CC
GO:0005886	0.0042	plasma membrane	CC
GO:0030094	0.0160	plasma membrane-derived photosystem I	CC
GO:0010287	0.0001	plastoglobule	CC
GO:0008287	0.0201	protein serine/threonine phosphatase complex	CC
GO:0010245	0.0014	radial microtubular system formation	CC
GO:0012506	0.0448	vesicle membrane	CC
GO:0004497	0.0104	(+)-abscisic acid 8'-hydroxylase activity	MF
GO:0004553	0.0040	1,2-diacylglycerol 3-beta-galactosyltransferase activity	MF
GO:0009055	0.0249	1,4-alpha-glucan branching enzyme activity	MF
GO:0015250	0.0346	1-phosphatidylinositol-4-phosphate 5-kinase activity	MF
GO:0016168	0.0304	2,3-bisphosphoglycerate-independent phosphoglycerate mutase activity	MF
GO:0018298	0.0137	9-cis-epoxycarotenoid dioxygenase activity	MF
GO:0020037	0.0260	acid phosphatase activity	MF
GO:0043169	0.0100	alpha-amylase activity	MF
GO:0015293	0.0379	amino acid binding	MF
GO:0009926	0.0329	amino acid transmembrane transporter activity	MF
GO:0019825	0.0264	ammonia ligase activity	MF
GO:0008171	0.0248	arogenate dehydratase activity	MF
GO:0015186	0.0347	auxin efflux transmembrane transporter activity	MF
GO:0008889	0.0312	auxin influx transmembrane transporter activity	MF
GO:0046983	0.0006	auxin polar transport	MF
GO:0046509	0.0141	calcium ion binding	MF
GO:0016165	0.0309	carboxy-lyase activity	MF
GO:0008649	0.0001	cation binding	MF
GO:0004713	0.0001	chlorophyll binding	MF
GO:0000156	0.0062	chlorophyll catabolite transmembrane transporter activity	MF
GO:0008281	0.0417	cinnamoyl-CoA reductase activity	MF
GO:0010290	0.0103	copper ion binding	MF
GO:0015431	0.0253	dihydroorotate oxidase activity	MF
GO:0004805	0.0001	electron carrier activity	MF
GO:0004674	0.0272	ethylene binding	MF
GO:0004556	0.0187	ferric iron binding	MF
GO:0045735	0.0275	ferroxidase activity	MF
GO:0005507	0.0397	flavin adenine dinucleotide binding	MF
GO:0010295	0.0403	galactinol-sucrose galactosyltransferase activity	MF
GO:0008289	0.0148	gibberellin 3-beta-dioxygenase activity	MF
GO:0000155	0.0062	glutathione S-conjugate-exporting ATPase activity	MF
GO:0003777	0.0017	glycerophosphodiester phosphodiesterase activity	MF
GO:0004722	0.0242	glycogen phosphorylase activity	MF
GO:0045549	0.0001	heme binding	MF
GO:0046592	0.0001	hydrolase activity, hydrolyzing O-glycosyl compounds	MF
GO:0005509	0.0262	L-allo-threonine aldolase activity	MF
GO:0003700	0.0300	L-amino acid transmembrane transporter activity	MF
GO:0016707	0.0176	L-ascorbate oxidase activity	MF
GO:0008395	0.0009	L-glutamine transmembrane transporter activity	MF
GO:0008447	0.0042	linoleate 13S-lipoxygenase activity	MF
GO:0008199	0.0105	lipid binding	MF
GO:0009496	0.0446	long-chain fatty acid-CoA ligase activity	MF
GO:0004525	0.0119	microtubule motor activity	MF
GO:0008184	0.0001	monooxygenase activity	MF
GO:0047769	0.0100	nutrient reservoir activity	MF
GO:0003844	0.0008	O-methyltransferase activity	MF
GO:0004158	0.0006	oxygen binding	MF
GO:0003993	0.0264	phenylalanine ammonia-lyase activity	MF
GO:0008732	0.0054	phosphorelay response regulator activity	MF
GO:0016211	0.0111	phosphorelay sensor kinase activity	MF
GO:0045548	0.0232	plastoquinol--plastocyanin reductase activity	MF
GO:0051740	0.0138	polyamine oxidase activity	MF
GO:0004322	0.0485	prephenate dehydratase activity	MF
GO:0043565	0.0020	protein dimerization activity	MF
GO:0016757	0.0085	protein serine/threonine kinase activity	MF
GO:0015179	0.0120	protein serine/threonine phosphatase activity	MF
GO:0046537	0.0051	protein tyrosine kinase activity	MF
GO:0016831	0.0001	protein-chromophore linkage	MF
GO:0010328	0.0398	pyridoxal phosphate binding	MF
GO:0015171	0.0241	ribonuclease III activity	MF

GO:0016308	0.0049	rRNA methyltransferase activity	MF
GO:0010329	0.0280	sequence-specific DNA binding	MF
GO:0004837	0.0143	sequence-specific DNA binding transcription factor activity	MF
GO:0016597	0.0163	steroid hydroxylase activity	MF
GO:0016758	0.0062	sulfonylurea receptor activity	MF
GO:0050660	0.0002	symporter activity	MF
GO:0030170	0.0288	transferase activity, transferring glycosyl groups	MF
GO:0047274	0.0394	transferase activity, transferring hexosyl groups	MF
GO:0016621	0.0084	trehalose-phosphatase activity	MF
GO:0004467	0.0377	tyrosine decarboxylase activity	MF
GO:0004664	0.0001	water channel activity	MF
		SC599 at 7 days post-inoculation	
GO:0006833	1.00E-04	water transport	BP
GO:0006071	0.0002	glycerol metabolic process	BP
GO:0006857	0.0002	oligopeptide transport	BP
GO:0008643	0.0002	carbohydrate transport	BP
GO:0006468	0.0004	protein phosphorylation	BP
GO:0009624	0.0004	response to nematode	BP
GO:0009832	0.0004	plant-type cell wall biogenesis	BP
GO:0009637	0.0011	response to blue light	BP
GO:0009414	0.0019	response to water deprivation	BP
GO:0055085	0.0022	transmembrane transport	BP
GO:0031408	0.0033	oxylipin biosynthetic process	BP
GO:0009834	0.0056	plant-type secondary cell wall biogenesis	BP
GO:0008361	0.0058	regulation of cell size	BP
GO:0006637	0.0068	acyl-CoA metabolic process	BP
GO:0043481	0.0079	anthocyanin accumulation in tissues in response to UV light	BP
GO:0000304	0.0107	response to singlet oxygen	BP
GO:0009958	0.0107	positive gravitropism	BP
GO:0009644	0.0139	response to high light intensity	BP
GO:0009698	0.0156	phenylpropanoid metabolic process	BP
GO:0010099	0.0191	regulation of photomorphogenesis	BP
GO:0047496	0.0227	vesicle transport along microtubule	BP
GO:0009756	0.0229	carbohydrate mediated signaling	BP
GO:0048497	0.0244	maintenance of floral organ identity	BP
GO:0005993	0.0247	trehalose catabolic process	BP
GO:0006021	0.0250	inositol biosynthetic process	BP
GO:0009612	0.0251	response to mechanical stimulus	BP
GO:0016998	0.0293	cell wall macromolecule catabolic process	BP
GO:0016887	0.0295	ATPase activity	BP
GO:0048527	0.0296	lateral root development	BP
GO:0006950	0.0315	response to stress	BP
GO:0010260	0.0325	organ senescence	BP
GO:0006073	0.0333	cellular glucan metabolic process	BP
GO:0019685	0.0442	photosynthesis, dark reaction	BP
GO:0015720	0.0460	allantoin transport	BP
GO:0006655	0.0471	phosphatidylglycerol biosynthetic process	BP
GO:0046345	0.0471	abscisic acid catabolic process	BP
GO:0048838	0.0471	release of seed from dormancy	BP
GO:0010196	0.0476	nonphotochemical quenching	BP
GO:0018125	0.0481	peptidyl-cysteine methylation	BP
GO:0007263	0.0497	nitric oxide mediated signal transduction	BP
GO:0042542	0.0497	response to hydrogen peroxide	BP
GO:0009505	0.0028	plant-type cell wall	CC
GO:0046658	0.0031	anchored component of plasma membrane	CC
GO:0016021	0.0054	integral component of membrane	CC
GO:0042651	0.0081	thylakoid membrane	CC
GO:0009986	0.0102	cell surface	CC
GO:0009535	0.0114	chloroplast thylakoid membrane	CC
GO:0005886	0.0219	plasma membrane	CC
GO:0035062	0.0226	omega speckle	CC
GO:0016020	0.0256	membrane	CC
GO:0009570	0.0356	chloroplast stroma	CC
GO:0005773	0.0385	vacuole	CC
GO:0010368	0.0462	chloroplast isoamylase complex	CC
GO:0048046	0.0465	apoplast	CC
GO:0005642	0.0468	annulate lamellae	CC
GO:0015250	0.0001	water channel activity	MF
GO:0008889	0.0002	glycerophosphodiester phosphodiesterase activity	MF
GO:0005355	0.0006	glucose transmembrane transporter activity	MF

GO:0004713	0.0013	protein tyrosine kinase activity	MF
GO:0004674	0.0014	protein serine/threonine kinase activity	MF
GO:0005365	0.0017	myo-inositol transmembrane transporter activity	MF
GO:0015148	0.0017	D-xylose transmembrane transporter activity	MF
GO:0015168	0.0017	glycerol transmembrane transporter activity	MF
GO:0015575	0.0017	mannitol transmembrane transporter activity	MF
GO:0015576	0.0017	sorbitol transmembrane transporter activity	MF
GO:0015591	0.0017	D-ribose transmembrane transporter activity	MF
GO:0005354	0.0021	galactose transmembrane transporter activity	MF
GO:0015198	0.0025	oligopeptide transporter activity	MF
GO:0010329	0.0038	auxin efflux transmembrane transporter activity	MF
GO:0004181	0.0049	metallocarboxypeptidase activity	MF
GO:0004698	0.0061	calcium-dependent protein kinase C activity	MF
GO:0016813	0.0075	linear amidines	MF
GO:0009815	0.0112	1-aminocyclopropane-1-carboxylate oxidase activity	MF
GO:0005524	0.0191	ATP binding	MF
GO:0050738	0.0217	fructosyltransferase activity	MF
GO:0051738	0.0246	xanthophyll binding	MF
GO:0004555	0.0247	alpha,alpha-trehalase activity	MF
GO:0004512	0.0250	inositol-3-phosphate synthase activity	MF
GO:0046406	0.0252	magnesium protoporphyrin IX methyltransferase activity	MF
GO:0016165	0.0286	linoleate 13S-lipoxygenase activity	MF
GO:0000062	0.0291	fatty-acyl-CoA binding	MF
GO:0016209	0.0315	antioxidant activity	MF
GO:0016706	0.0328	incorporation of one atom each of oxygen into both donors	MF
GO:0016762	0.0375	xyloglucan:xyloglucosyl transferase activity	MF
GO:0047100	0.0436	activity	MF
GO:0016630	0.0442	protochlorophyllide reductase activity	MF
GO:0030612	0.0450	arsenate reductase (thioredoxin) activity	MF
GO:0005274	0.0460	allantoin uptake transmembrane transporter activity	MF
GO:0030156	0.0460	benzodiazepine receptor binding	MF
GO:0030547	0.0460	receptor inhibitor activity	MF
GO:0004419	0.0462	hydroxymethylglutaryl-CoA lyase activity	MF
GO:0015362	0.0472	high-affinity sodium:dicarboxylate symporter activity	MF
GO:0005516	0.0478	calmodulin binding	MF
GO:0004612	0.0481	phosphoenolpyruvate carboxykinase (ATP) activity	MF
GO:0016301	0.0482	kinase activity	MF
GO:0008281	0.0483	sulfonylurea receptor activity	MF
GO:0010290	0.0483	chlorophyll catabolite transmembrane transporter activity	MF
GO:0015431	0.0483	glutathione S-conjugate-exporting ATPase activity	MF
GO:0005222	0.0497	intracellular cAMP activated cation channel activity	MF
		SC599 at 30 days post-inoculation	
GO:0006268	1.00E-04	DNA unwinding involved in DNA replication	BP
GO:0006629	1.00E-04	lipid metabolic process	BP
GO:0006869	1.00E-04	lipid transport	BP
GO:0009813	1.00E-04	flavonoid biosynthetic process	BP
GO:0030174	1.00E-04	regulation of DNA-dependent DNA replication initiation	BP
GO:0042538	1.00E-04	hyperosmotic salinity response	BP
GO:0048653	1.00E-04	anther development	BP
GO:0009414	0.0002	response to water deprivation	BP
GO:0009611	0.0002	response to wounding	BP
GO:0009788	0.0002	negative regulation of abscisic acid-activated signaling pathway	BP
GO:0009651	0.0003	response to salt stress	BP
GO:0006572	0.0004	tyrosine catabolic process	BP
GO:0000084	0.0006	mitotic S phase	BP
GO:0015746	0.0006	citrate transport	BP
GO:0009737	0.0007	response to abscisic acid	BP
GO:0048448	0.0008	stamen morphogenesis	BP
GO:0010117	0.0009	photoprotection	BP
GO:0009624	0.0010	response to nematode	BP
GO:0009744	0.0024	response to sucrose	BP
GO:0015743	0.0025	malate transport	BP
GO:0048451	0.0025	petal formation	BP
GO:0006979	0.0026	response to oxidative stress	BP
GO:0010205	0.0028	photoinhibition	BP
GO:0006561	0.0031	proline biosynthetic process	BP
GO:0010119	0.0032	regulation of stomatal movement	BP
GO:0006267	0.0039	replication	BP
GO:0015744	0.0041	succinate transport	BP
GO:0030865	0.0046	cortical cytoskeleton organization	BP

GO:0031115	0.0046	negative regulation of microtubule polymerization	BP
GO:0009416	0.0047	response to light stimulus	BP
GO:0005975	0.0051	carbohydrate metabolic process	BP
GO:0042391	0.0055	regulation of membrane potential	BP
GO:0006334	0.0059	nucleosome assembly	BP
GO:0006559	0.0064	L-phenylalanine catabolic process	BP
GO:0051453	0.0064	regulation of intracellular pH	BP
GO:0009626	0.0068	plant-type hypersensitive response	BP
GO:0006857	0.0073	oligopeptide transport	BP
GO:0048544	0.0086	recognition of pollen	BP
GO:0010223	0.0096	secondary shoot formation	BP
GO:0048504	0.0099	regulation of timing of organ formation	BP
GO:0009051	0.0111	pentose-phosphate shunt, oxidative branch	BP
GO:0043090	0.0127	amino acid import	BP
GO:0007263	0.0134	nitric oxide mediated signal transduction	BP
GO:0009753	0.0137	response to jasmonic acid	BP
GO:0010115	0.0140	regulation of abscisic acid biosynthetic process	BP
GO:0016121	0.0157	carotene catabolic process	BP
GO:0016124	0.0157	xanthophyll catabolic process	BP
GO:0010053	0.0159	root epidermal cell differentiation	BP
GO:0006071	0.0162	glycerol metabolic process	BP
GO:0010200	0.0171	response to chitin	BP
GO:0010025	0.0185	wax biosynthetic process	BP
GO:0006633	0.0191	fatty acid biosynthetic process	BP
GO:0006825	0.0197	copper ion transport	BP
GO:0055114	0.0199	oxidation-reduction process	BP
GO:0006097	0.0209	glyoxylate cycle	BP
GO:0009247	0.0218	glycolipid biosynthetic process	BP
GO:0046506	0.0218	sulfolipid biosynthetic process	BP
GO:0009718	0.0220	anthocyanin-containing compound biosynthetic process	BP
GO:0010072	0.0225	primary shoot apical meristem specification	BP
GO:0010345	0.0228	suberin biosynthetic process	BP
GO:0046369	0.0253	galactose biosynthetic process	BP
GO:0031536	0.0260	positive regulation of exit from mitosis	BP
GO:0030418	0.0261	nicotianamine biosynthetic process	BP
GO:0006083	0.0283	acetate metabolic process	BP
GO:0015802	0.0283	basic amino acid transport	BP
GO:0010189	0.0308	vitamin E biosynthetic process	BP
GO:0015804	0.0382	neutral amino acid transport	BP
GO:0006810	0.0389	transport	BP
GO:0009688	0.0389	abscisic acid biosynthetic process	BP
GO:0046466	0.0396	membrane lipid catabolic process	BP
GO:0048444	0.0396	floral organ morphogenesis	BP
GO:0015810	0.0397	aspartate transport	BP
GO:0015827	0.0397	tryptophan transport	BP
GO:0016126	0.0401	sterol biosynthetic process	BP
GO:0046688	0.0410	response to copper ion	BP
GO:0006970	0.0418	response to osmotic stress	BP
GO:0006821	0.0451	chloride transport	BP
GO:0045493	0.0490	xylan catabolic process	BP
GO:0007034	0.0491	vacuolar transport	BP
GO:0009856	0.0493	pollination	BP
GO:0006468	0.0498	protein phosphorylation	BP
GO:0005656	0.0001	nuclear pre-replicative complex	CC
GO:0042555	0.0001	MCM complex	CC
GO:0005773	0.0003	vacuole	CC
GO:0031225	0.0003	anchored component of membrane	CC
GO:0008287	0.0032	protein serine/threonine phosphatase complex	CC
GO:0005886	0.0035	plasma membrane	CC
GO:0048046	0.0135	apoplast	CC
GO:0009517	0.0141	PSII associated light-harvesting complex II	CC
GO:0010330	0.0155	cellulose synthase complex	CC
GO:0000786	0.0165	nucleosome	CC
GO:0005775	0.0183	vacuolar lumen	CC
GO:0005618	0.0210	cell wall	CC
GO:0001520	0.0236	outer dense fiber	CC
GO:0012505	0.0284	endomembrane system	CC
GO:0009505	0.0324	plant-type cell wall	CC
GO:0005637	0.0373	nuclear inner membrane	CC
GO:0009341	0.0416	beta-galactosidase complex	CC

GO:0005576	0.0433	extracellular region	CC
GO:0009833	0.0451	plant-type primary cell wall biogenesis	CC
GO:0004722	0.0001	protein serine/threonine phosphatase activity	MF
GO:0005507	0.0001	copper ion binding	MF
GO:0008171	0.0001	O-methyltransferase activity	MF
GO:0009055	0.0001	electron carrier activity	MF
GO:0015137	0.0001	citrate transmembrane transporter activity	MF
GO:0016210	0.0001	naringenin-chalcone synthase activity	MF
GO:0016298	0.0001	lipase activity	MF
GO:0020037	0.0002	heme binding	MF
GO:0043169	0.0008	cation binding	MF
GO:0008289	0.0011	lipid binding	MF
GO:0008194	0.0020	UDP-glycosyltransferase activity	MF
GO:0004601	0.0021	peroxidase activity	MF
GO:0046983	0.0031	protein dimerization activity	MF
GO:0015140	0.0033	malate transmembrane transporter activity	MF
GO:0019825	0.0040	oxygen binding	MF
GO:0015362	0.0046	high-affinity sodium:dicarboxylate symporter activity	MF
GO:0004567	0.0047	beta-mannosidase activity	MF
GO:0030410	0.0047	nicotianamine synthase activity	MF
GO:0043508	0.0050	negative regulation of JUN kinase activity	MF
GO:0015172	0.0065	acidic amino acid transmembrane transporter activity	MF
GO:0004867	0.0076	serine-type endopeptidase inhibitor activity	MF
GO:0008889	0.0076	glycerophosphodiester phosphodiesterase activity	MF
GO:0004739	0.0091	pyruvate dehydrogenase (acetyl-transferring) activity	MF
GO:0015175	0.0091	neutral amino acid transmembrane transporter activity	MF
GO:0004713	0.0097	protein tyrosine kinase activity	MF
GO:0051010	0.0111	microtubule plus-end binding	MF
GO:0042626	0.0115	ATPase activity, coupled to transmembrane movement of substances	MF
GO:0051101	0.0126	regulation of DNA binding	MF
GO:0035264	0.0128	multicellular organism growth	MF
GO:0005222	0.0134	intracellular cAMP activated cation channel activity	MF
GO:0008047	0.0135	enzyme activator activity	MF
GO:0045551	0.0139	cinnamyl-alcohol dehydrogenase activity	MF
GO:0010301	0.0140	xanthoxin dehydrogenase activity	MF
GO:0045735	0.0141	nutrient reservoir activity	MF
GO:0009974	0.0153	zeinoxanthin epsilon hydroxylase activity	MF
GO:0010291	0.0153	carotene beta-ring hydroxylase activity	MF
GO:0016758	0.0168	transferase activity, transferring hexosyl groups	MF
GO:0043138	0.0172	3'-5' DNA helicase activity	MF
GO:0008094	0.0175	DNA-dependent ATPase activity	MF
GO:0008794	0.0186	arsenate reductase (glutaredoxin) activity	MF
GO:0003700	0.0188	sequence-specific DNA binding transcription factor activity	MF
GO:0003993	0.0189	acid phosphatase activity	MF
GO:0005247	0.0208	voltage-gated chloride channel activity	MF
GO:0016702	0.0226	oxidoreductase activity, acting on single donors with incorporation of molecular oxygen, incorporation of two atoms of oxygen	MF
GO:0008233	0.0227	peptidase activity	MF
GO:0008146	0.0243	sulfotransferase activity	MF
GO:0031176	0.0243	endo-1,4-beta-xylanase activity	MF
GO:0004197	0.0244	cysteine-type endopeptidase activity	MF
GO:0043167	0.0245	ion binding	MF
GO:0005242	0.0247	inward rectifier potassium channel activity	MF
GO:0003842	0.0255	1-pyrroline-5-carboxylate dehydrogenase activity	MF
GO:0015926	0.0255	glucosidase activity	MF
GO:0000252	0.0258	C-3 sterol dehydrogenase (C-4 sterol decarboxylase) activity	MF
GO:0045549	0.0262	9-cis-epoxycarotenoid dioxygenase activity	MF
GO:0004338	0.0265	glucan exo-1,3-beta-glucosidase activity	MF
GO:0050662	0.0268	coenzyme binding	MF
GO:0016847	0.0274	1-aminocyclopropane-1-carboxylate synthase activity	MF
GO:0015399	0.0283	primary active transmembrane transporter activity	MF
GO:0042972	0.0293	licheninase activity	MF
GO:0009809	0.0299	lignin biosynthetic process	MF
GO:0004674	0.0300	protein serine/threonine kinase activity	MF
GO:0016491	0.0312	oxidoreductase activity	MF
GO:0030551	0.0340	cyclic nucleotide binding	MF
GO:0015398	0.0355	activity	MF
GO:0004040	0.0379	amidase activity	MF
GO:0030599	0.0397	pectinesterase activity	MF
GO:0018456	0.0401	aryl-alcohol dehydrogenase (NAD+) activity	MF

GO:0004565	0.0416	beta-galactosidase activity	MF
GO:0005262	0.0433	calcium channel activity	MF
GO:0004439	0.0463	phosphatidylinositol-4,5-bisphosphate 5-phosphatase activity	MF
GO:0016884	0.0468	carbon-nitrogen ligase activity, with glutamine as amido-N-donor	MF
GO:0004497	0.0477	monooxygenase activity	MF
GO:0005509	0.0484	calcium ion binding	MF
GO:0000062	0.0491	fatty-acyl-CoA binding	MF
GO:0015105	0.0491	arsenite transmembrane transporter activity	MF
GO:0016157	0.0499	sucrose synthase activity	MF
		Tx7000 at 2 days post-inoculation	
GO:0009414	0.0120	abscisic acid biosynthetic process	BP
GO:0048448	0.0090	actin filament polymerization	BP
GO:0006468	0.0494	aging	BP
GO:0009741	0.0188	allantoin transport	BP
GO:0048451	0.0226	anisotropic cell growth	BP
GO:0048653	0.0012	anther development	BP
GO:0009408	0.0078	auxin polar transport	BP
GO:0006857	0.0285	barrier septum assembly	BP
GO:0051707	0.0157	brassinosteroid metabolic process	BP
GO:0019761	0.0206	carbohydrate mediated signaling	BP
GO:0009644	0.0073	carbohydrate metabolic process	BP
GO:0006355	0.0362	carbohydrate transport	BP
GO:0005986	0.0040	cell tip growth	BP
GO:0009932	0.0404	cell wall mannoprotein biosynthetic process	BP
GO:0009863	0.0346	chaperone-mediated protein complex assembly	BP
GO:0006952	0.0441	chondroitin sulfate biosynthetic process	BP
GO:0030856	0.0305	citrate transport	BP
GO:0015706	0.0320	cuticle development	BP
GO:0055085	0.0044	defense response	BP
GO:0007616	0.0124	defense response to bacterium	BP
GO:0008152	0.0164	defense response to fungus	BP
GO:0005975	0.0385	diaminopimelate biosynthetic process	BP
GO:0009926	0.0226	embryonic pectoral fin morphogenesis	BP
GO:0009272	0.0169	flavonol biosynthetic process	BP
GO:0030041	0.0084	fungal-type cell wall biogenesis	BP
GO:0009624	0.0252	ganglioside catabolic process	BP
GO:0009646	0.0023	glucosinolate biosynthetic process	BP
GO:0009626	0.0191	glycosaminoglycan metabolic process	BP
GO:0009737	0.0441	biosynthetic process	BP
GO:0005992	0.0188	high-affinity copper ion transport	BP
GO:0009688	0.0273	integrin-mediated signaling pathway	BP
GO:0042742	0.0303	lactate transport	BP
GO:0055114	0.0357	lateral root formation	BP
GO:0010161	0.0336	leucine biosynthetic process	BP
GO:0006044	0.0068	long-term memory	BP
GO:0016131	0.0252	male courtship behavior	BP
GO:0031347	0.0376	maltose biosynthetic process	BP
GO:0042542	0.0245	mannitol biosynthetic process	BP
GO:0050832	0.0069	metabolic process	BP
GO:0051555	0.0404	mitotic cell size control checkpoint	BP
GO:0002240	0.0155	N-acetylglucosamine metabolic process	BP
GO:0009651	0.0252	neuromuscular process controlling balance	BP
GO:0009617	0.0056	nitrate transport	BP
GO:0015678	0.0016	oligopeptide transport	BP
GO:0015720	0.0252	oligosaccharide catabolic process	BP
GO:0030203	0.0261	organelle fusion	BP
GO:0009756	0.0131	oxidation-reduction process	BP
GO:0030516	0.0252	penetration of zona pellucida	BP
GO:0035118	0.0245	peptidyl-histidine phosphorylation	BP
GO:0045743	0.0009	petal formation	BP
GO:0051211	0.0416	photosynthesis, dark reaction	BP
GO:0009751	0.0483	pinocytosis	BP
GO:0018106	0.0109	plant-type hypersensitive response	BP
GO:0019593	0.0406	polytene chromosome puff	BP
GO:0006689	0.0226	positive regulation of fibroblast growth factor receptor signaling pathway	BP
GO:0007341	0.0004	protein phosphorylation	BP
GO:0008049	0.0283	protein-tetrapyrrole linkage	BP
GO:0009313	0.0479	raffinose family oligosaccharide biosynthetic process	BP
GO:0050885	0.0358	recognition of pollen	BP
GO:0006567	0.0147	red light signaling pathway	BP

GO:0010025	0.0226	regulation of axon extension	BP
GO:0048284	0.0365	regulation of cell proliferation	BP
GO:0007229	0.0479	regulation of circadian rhythm	BP
GO:0017006	0.0160	regulation of defense response	BP
GO:0000917	0.0045	regulation of epithelial cell differentiation	BP
GO:0009753	0.0372	regulation of response to stimulus	BP
GO:0035071	0.0027	regulation of transcription, DNA-templated	BP
GO:0015727	0.0112	response to abscisic acid	BP
GO:0015746	0.0101	response to absence of light	BP
GO:0009620	0.0186	response to bacterium	BP
GO:0010200	0.0005	response to brassinosteroid	BP
GO:0042335	0.0314	response to chitin	BP
GO:0016126	0.0405	response system	BP
GO:0009098	0.0493	response to freezing	BP
GO:0051131	0.0309	response to fungus	BP
GO:0010311	0.0015	response to heat	BP
GO:0048544	0.0024	response to high light intensity	BP
GO:0008643	0.0161	response to hydrogen peroxide	BP
GO:0042127	0.0286	response to jasmonic acid	BP
GO:0048583	0.0177	response to molecule of oomycetes origin	BP
GO:0000024	0.0101	response to nematode	BP
GO:0019877	0.0017	response to other organism	BP
GO:0010016	0.0244	response to salicylic acid	BP
GO:0000032	0.0177	response to salt stress	BP
GO:0031567	0.0405	response to very low fluence red light stimulus	BP
GO:0010201	0.0001	response to water deprivation	BP
GO:0010203	0.0418	ribonucleoprotein complex biogenesis	BP
GO:0005703	0.0043	salicylic acid mediated signaling pathway	BP
GO:0019685	0.0296	salivary gland cell autophagic cell death	BP
GO:0022613	0.0394	shoot system morphogenesis	BP
GO:0010136	0.0003	stamen morphogenesis	BP
GO:0010103	0.0329	sterol biosynthetic process	BP
GO:0006805	0.0425	stomatal complex morphogenesis	BP
GO:0015014	0.0033	sucrose biosynthetic process	BP
GO:0030206	0.0255	threonine catabolic process	BP
GO:0010325	0.0060	transmembrane transport	BP
GO:0042752	0.0117	trehalose biosynthetic process	BP
GO:0006907	0.0419	ureide catabolic process	BP
GO:0050826	0.0259	wax biosynthetic process	BP
GO:0007568	0.0428	xenobiotic metabolic process	BP
GO:0009505	0.0027	anchored component of membrane	CC
GO:0031225	0.0104	apoplast	CC
GO:0005618	0.0035	cell wall	CC
GO:0009570	0.0058	chloroplast stroma	CC
GO:0018444	0.0221	cortical microtubule, transverse to long axis	CC
GO:0048046	0.0339	extracellular region	CC
GO:0001520	0.0383	extrinsic component of vacuolar membrane	CC
GO:0010005	0.0438	gravitropism	CC
GO:0005576	0.0181	outer dense fiber	CC
GO:0000306	0.0435	phragmoplast	CC
GO:0009524	0.0002	plant-type cell wall	CC
GO:0009630	0.0440	SCAR complex	CC
GO:0031209	0.0078	translation release factor complex	CC
GO:0004713	0.0001	protein tyrosine kinase activity	MF
GO:0009055	0.0001	electron carrier activity	MF
GO:0004674	0.0002	protein serine/threonine kinase activity	MF
GO:0020037	0.0002	heme binding	MF
GO:0004857	0.0003	enzyme inhibitor activity	MF
GO:0043169	0.0013	cation binding	MF
GO:0003700	0.0015	sequence-specific DNA binding transcription factor activity	MF
GO:0008794	0.0020	arsenate reductase (glutaredoxin) activity	MF
GO:0004028	0.0021	3-chloroallyl aldehyde dehydrogenase activity	MF
GO:0004805	0.0021	trehalose-phosphatase activity	MF
GO:0004553	0.0023	hydrolase activity, hydrolyzing O-glycosyl compounds	MF
GO:0019825	0.0028	oxygen binding	MF
GO:0004497	0.0029	monooxygenase activity	MF
GO:0043565	0.0032	sequence-specific DNA binding	MF
GO:0015089	0.0045	high-affinity copper ion transmembrane transporter activity	MF
GO:0043023	0.0046	ribosomal large subunit binding	MF
GO:0004564	0.0074	beta-fructofuranosidase activity	MF

GO:0005366	0.0076	myo-inositol:proton symporter activity	MF
GO:0030599	0.0079	pectinesterase activity	MF
GO:0035251	0.0082	UDP-glucosyltransferase activity	MF
GO:0045735	0.0084	nutrient reservoir activity	MF
GO:0018456	0.0113	aryl-alcohol dehydrogenase (NAD+) activity	MF
GO:0004854	0.0119	xanthine dehydrogenase activity	MF
GO:0051087	0.0141	chaperone binding	MF
GO:0047793	0.0168	cycloeucalenol cycloisomerase activity	MF
GO:0003959	0.0173	NADPH dehydrogenase activity	MF
GO:0005274	0.0188	allantoin uptake transmembrane transporter activity	MF
GO:0005365	0.0188	myo-inositol transmembrane transporter activity	MF
GO:0015148	0.0188	D-xylose transmembrane transporter activity	MF
GO:0015168	0.0188	glycerol transmembrane transporter activity	MF
GO:0015575	0.0188	mannitol transmembrane transporter activity	MF
GO:0015576	0.0188	sorbitol transmembrane transporter activity	MF
GO:0015591	0.0188	D-ribose transmembrane transporter activity	MF
GO:0003785	0.0205	actin monomer binding	MF
GO:0008922	0.0206	long-chain fatty acid [acyl-carrier-protein] ligase activity	MF
GO:0008453	0.0227	alanine-glyoxylate transaminase activity	MF
GO:0016757	0.0231	transferase activity, transferring glycosyl groups	MF
GO:0004965	0.0233	G-protein coupled GABA receptor activity	MF
GO:0004855	0.0245	xanthine oxidase activity	MF
GO:0016231	0.0252	beta-N-acetylglucosaminidase activity	MF
GO:0043022	0.0261	ribosome binding	MF
GO:0004557	0.0267	alpha-galactosidase activity	MF
GO:0010294	0.0295	abscisic acid glucosyltransferase activity	MF
GO:0005354	0.0298	galactose transmembrane transporter activity	MF
GO:0010293	0.0302	abscisic aldehyde oxidase activity	MF
GO:0050302	0.0302	indole-3-acetaldehyde oxidase activity	MF
GO:0015129	0.0303	lactate transmembrane transporter activity	MF
GO:0004794	0.0352	L-threonine ammonia-lyase activity	MF
GO:0008061	0.0355	chitin binding	MF
GO:0047631	0.0359	ADP-ribose diphosphatase activity	MF
GO:0004328	0.0371	formamidase activity	MF
GO:0004740	0.0380	pyruvate dehydrogenase (acetyl-transferring) kinase activity	MF
GO:0009922	0.0385	fatty acid elongase activity	MF
GO:0043015	0.0396	gamma-tubulin binding	MF
GO:0004647	0.0401	phosphoserine phosphatase activity	MF
GO:0043508	0.0403	negative regulation of JUN kinase activity	MF
GO:0004475	0.0404	mannose-1-phosphate guanylyltransferase activity	MF
GO:0031405	0.0411	lipoic acid binding	MF
GO:0016630	0.0416	protochlorophyllide reductase activity	MF
GO:0004623	0.0423	phospholipase A2 activity	MF
GO:0003852	0.0431	2-isopropylmalate synthase activity	MF
GO:0010177	0.0431	2-(2'-methylthio)ethylmalate synthase activity	MF
GO:0004485	0.0450	methylcrotonoyl-CoA carboxylase activity	MF
		Tx7000 at 7 days post-inoculation	
GO:0006468	1.00E-04	protein phosphorylation	BP
GO:0009407	1.00E-04	toxin catabolic process	BP
GO:0009753	1.00E-04	response to jasmonic acid	BP
GO:0055085	1.00E-04	transmembrane transport	BP
GO:0006096	0.0002	glycolytic process	BP
GO:0009409	0.0002	response to cold	BP
GO:0009751	0.0002	response to salicylic acid	BP
GO:0015692	0.0002	lead ion transport	BP
GO:0009737	0.0004	response to abscisic acid	BP
GO:0006805	0.0005	xenobiotic metabolic process	BP
GO:0009416	0.0005	response to light stimulus	BP
GO:0009723	0.0005	response to ethylene	BP
GO:0007169	0.0006	transmembrane receptor protein tyrosine kinase signaling pathway	BP
GO:0010150	0.0006	leaf senescence	BP
GO:0015979	0.0006	photosynthesis	BP
GO:0016998	0.0006	cell wall macromolecule catabolic process	BP
GO:0000302	0.0007	response to reactive oxygen species	BP
GO:0006108	0.0007	malate metabolic process	BP
GO:0006032	0.0008	chitin catabolic process	BP
GO:0006099	0.0009	tricarboxylic acid cycle	BP
GO:0009630	0.0009	gravitropism	BP
GO:0006865	0.0011	amino acid transport	BP
GO:0009414	0.0011	response to water deprivation	BP

GO:0009826	0.0012	unidimensional cell growth	BP
GO:0005975	0.0015	carbohydrate metabolic process	BP
GO:0009611	0.0018	response to wounding	BP
GO:0009556	0.0019	microsporogenesis	BP
GO:0010227	0.0020	floral organ abscission	BP
GO:0010158	0.0023	abaxial cell fate specification	BP
GO:0009956	0.0027	radial pattern formation	BP
GO:0030104	0.0027	water homeostasis	BP
GO:0050832	0.0029	defense response to fungus	BP
GO:0009269	0.0031	response to desiccation	BP
GO:0010200	0.0036	response to chitin	BP
GO:0009813	0.0038	flavonoid biosynthetic process	BP
GO:0009610	0.0045	response to symbiotic fungus	BP
GO:0009607	0.0046	response to biotic stimulus	BP
GO:0009856	0.0047	pollination	BP
GO:0010117	0.0047	photoprotection	BP
GO:0009831	0.0052	plant-type cell wall modification involved in multidimensional cell growth	BP
GO:0009944	0.0052	polarity specification of adaxial/abaxial axis	BP
GO:0009734	0.0054	auxin-activated signaling pathway	BP
GO:0010047	0.0058	fruit dehiscence	BP
GO:0000038	0.0059	very long-chain fatty acid metabolic process	BP
GO:0005986	0.0065	sucrose biosynthetic process	BP
GO:0042752	0.0069	regulation of circadian rhythm	BP
GO:0006809	0.0070	nitric oxide biosynthetic process	BP
GO:0009816	0.0079	defense response to bacterium, incompatible interaction	BP
GO:0009747	0.0080	hexokinase-dependent signaling	BP
GO:0031347	0.0080	regulation of defense response	BP
GO:0005978	0.0082	glycogen biosynthetic process	BP
GO:0006071	0.0087	glycerol metabolic process	BP
GO:0009809	0.0087	lignin biosynthetic process	BP
GO:0015995	0.0093	chlorophyll biosynthetic process	BP
GO:0006814	0.0098	sodium ion transport	BP
GO:0006749	0.0108	glutathione metabolic process	BP
GO:0010114	0.0108	response to red light	BP
GO:0055114	0.0113	oxidation-reduction process	BP
GO:0006820	0.0115	anion transport	BP
GO:0009637	0.0119	response to blue light	BP
GO:0016758	0.0123	transferase activity, transferring hexosyl groups	BP
GO:0010154	0.0127	fruit development	BP
GO:0010229	0.0130	inflorescence development	BP
GO:0048765	0.0132	root hair cell differentiation	BP
GO:0009651	0.0139	response to salt stress	BP
GO:0010268	0.0141	brassinosteroid homeostasis	BP
GO:0046274	0.0141	lignin catabolic process	BP
GO:0006629	0.0142	lipid metabolic process	BP
GO:0019252	0.0143	starch biosynthetic process	BP
GO:0019593	0.0160	mannitol biosynthetic process	BP
GO:0042538	0.0163	hyperosmotic salinity response	BP
GO:0006857	0.0165	oligopeptide transport	BP
GO:0042335	0.0171	cuticle development	BP
GO:0000162	0.0173	tryptophan biosynthetic process	BP
GO:0010325	0.0173	raffinose family oligosaccharide biosynthetic process	BP
GO:0010119	0.0176	regulation of stomatal movement	BP
GO:0015014	0.0187	biosynthetic process	BP
GO:0030206	0.0187	chondroitin sulfate biosynthetic process	BP
GO:0009735	0.0188	response to cytokinin	BP
GO:0042631	0.0188	cellular response to water deprivation	BP
GO:0009835	0.0197	fruit ripening	BP
GO:0006567	0.0203	threonine catabolic process	BP
GO:0010017	0.0206	red or far-red light signaling pathway	BP
GO:0009854	0.0208	oxidative photosynthetic carbon pathway	BP
GO:0009855	0.0216	determination of bilateral symmetry	BP
GO:0009626	0.0220	plant-type hypersensitive response	BP
GO:0005992	0.0221	trehalose biosynthetic process	BP
GO:0010042	0.0226	response to manganese ion	BP
GO:0010050	0.0228	vegetative phase change	BP
GO:0010161	0.0232	red light signaling pathway	BP
GO:0012501	0.0235	programmed cell death	BP
GO:0048767	0.0237	root hair elongation	BP
GO:0010189	0.0241	vitamin E biosynthetic process	BP

GO:0009926	0.0244	auxin polar transport	BP
GO:0030951	0.0248	establishment or maintenance of microtubule cytoskeleton polarity	BP
GO:0008643	0.0250	carbohydrate transport	BP
GO:0009399	0.0251	nitrogen fixation	BP
GO:0010044	0.0260	response to aluminum ion	BP
GO:0006552	0.0263	leucine catabolic process	BP
GO:0009341	0.0275	beta-galactosidase complex	BP
GO:0010254	0.0286	nectary development	BP
GO:0010014	0.0303	meristem initiation	BP
GO:0010072	0.0303	primary shoot apical meristem specification	BP
GO:0019253	0.0304	reductive pentose-phosphate cycle	BP
GO:0009863	0.0312	salicylic acid mediated signaling pathway	BP
GO:0009624	0.0317	response to nematode	BP
GO:0009765	0.0319	photosynthesis, light harvesting	BP
GO:0010310	0.0319	regulation of hydrogen peroxide metabolic process	BP
GO:0015996	0.0329	chlorophyll catabolic process	BP
GO:0000160	0.0330	phosphorelay signal transduction system	BP
GO:0009727	0.0340	detection of ethylene stimulus	BP
GO:0010218	0.0341	response to far red light	BP
GO:0006548	0.0342	histidine catabolic process	BP
GO:0006855	0.0342	drug transmembrane transport	BP
GO:0009733	0.0353	response to auxin	BP
GO:0009555	0.0355	pollen development	BP
GO:0000753	0.0359	cell morphogenesis involved in conjugation with cellular fusion	BP
GO:0016121	0.0359	carotene catabolic process	BP
GO:0016124	0.0359	xanthophyll catabolic process	BP
GO:0016126	0.0361	sterol biosynthetic process	BP
GO:0005982	0.0374	starch metabolic process	BP
GO:0010187	0.0383	negative regulation of seed germination	BP
GO:0009116	0.0387	nucleoside metabolic process	BP
GO:0006979	0.0392	response to oxidative stress	BP
GO:0051707	0.0397	response to other organism	BP
GO:0000303	0.0402	response to superoxide	BP
GO:0007015	0.0409	actin filament organization	BP
GO:0009744	0.0412	response to sucrose	BP
GO:0043481	0.0414	anthocyanin accumulation in tissues in response to UV light	BP
GO:0006564	0.0416	L-serine biosynthetic process	BP
GO:0006633	0.0444	fatty acid biosynthetic process	BP
GO:0009850	0.0447	auxin metabolic process	BP
GO:0009567	0.0458	double fertilization forming a zygote and endosperm	BP
GO:0009851	0.0458	auxin biosynthetic process	BP
GO:0009913	0.0461	epidermal cell differentiation	BP
GO:0015893	0.0471	drug transport	BP
GO:0009081	0.0479	branched-chain amino acid metabolic process	BP
GO:0010005	0.0482	cortical microtubule, transverse to long axis	BP
GO:0016131	0.0482	brassinosteroid metabolic process	BP
GO:0002240	0.0484	response to molecule of oomycetes origin	BP
GO:0006952	0.0486	defense response	BP
GO:0006869	0.0497	lipid transport	BP
GO:0045493	0.0066	xylan catabolic process	BP
GO:0005886	0.0001	plasma membrane	CC
GO:0009505	0.0001	plant-type cell wall	CC
GO:0009507	0.0001	chloroplast	CC
GO:0016021	0.0001	integral component of membrane	CC
GO:0009514	0.0003	glyoxysome	CC
GO:0031225	0.0003	anchored component of membrane	CC
GO:0005576	0.0005	extracellular region	CC
GO:0009543	0.0009	chloroplast thylakoid lumen	CC
GO:0048046	0.0063	apoplast	CC
GO:0010287	0.0104	plastoglobule	CC
GO:0012505	0.0171	endomembrane system	CC
GO:0016020	0.0175	membrane	CC
GO:0030096	0.0181	plasma membrane-derived thylakoid photosystem II	CC
GO:0042742	0.0182	defense response to bacterium	CC
GO:0009570	0.0255	chloroplast stroma	CC
GO:0009706	0.0264	chloroplast inner membrane	CC
GO:0045298	0.0287	tubulin complex	CC
GO:0008287	0.0342	protein serine/threonine phosphatase complex	CC
GO:0004364	0.0001	glutathione transferase activity	MF
GO:0004674	0.0001	protein serine/threonine kinase activity	MF

GO:0004713	0.0001	protein tyrosine kinase activity	MF
GO:0005351	0.0001	sugar:proton symporter activity	MF
GO:0009055	0.0001	electron carrier activity	MF
GO:0019825	0.0001	oxygen binding	MF
GO:0042626	0.0001	ATPase activity, coupled to transmembrane movement of substances	MF
GO:0015171	0.0002	amino acid transmembrane transporter activity	MF
GO:0020037	0.0002	heme binding	MF
GO:0004568	0.0003	chitinase activity	MF
GO:0043169	0.0003	cation binding	MF
GO:0008061	0.0007	chitin binding	MF
GO:0043565	0.0008	sequence-specific DNA binding	MF
GO:0004497	0.0011	monooxygenase activity	MF
GO:0050660	0.0012	flavin adenine dinucleotide binding	MF
GO:0003700	0.0014	sequence-specific DNA binding transcription factor activity	MF
GO:0016210	0.0018	naringenin-chalcone synthase activity	MF
GO:0005315	0.0024	inorganic phosphate transmembrane transporter activity	MF
GO:0005355	0.0024	glucose transmembrane transporter activity	MF
GO:0009011	0.0025	starch synthase activity	MF
GO:0016597	0.0025	amino acid binding	MF
GO:0004857	0.0026	enzyme inhibitor activity	MF
GO:0005365	0.0030	myo-inositol transmembrane transporter activity	MF
GO:0015148	0.0030	D-xylose transmembrane transporter activity	MF
GO:0015168	0.0030	glycerol transmembrane transporter activity	MF
GO:0015575	0.0030	mannitol transmembrane transporter activity	MF
GO:0015576	0.0030	sorbitol transmembrane transporter activity	MF
GO:0015591	0.0030	D-ribose transmembrane transporter activity	MF
GO:0030060	0.0046	L-malate dehydrogenase activity	MF
GO:0004867	0.0053	serine-type endopeptidase inhibitor activity	MF
GO:0008289	0.0057	lipid binding	MF
GO:0004807	0.0060	triose-phosphate isomerase activity	MF
GO:0015250	0.0060	water channel activity	MF
GO:0004029	0.0064	aldehyde dehydrogenase (NAD) activity	MF
GO:0005509	0.0069	calcium ion binding	MF
GO:0005354	0.0073	galactose transmembrane transporter activity	MF
GO:0004340	0.0080	glucokinase activity	MF
GO:0004030	0.0088	aldehyde dehydrogenase [NAD(P)+] activity	MF
GO:0008865	0.0091	fructokinase activity	MF
GO:0030599	0.0098	pectinesterase activity	MF
GO:0050662	0.0105	coenzyme binding	MF
GO:0035251	0.0108	UDP-glucosyltransferase activity	MF
GO:0004028	0.0122	3-chloroallyl aldehyde dehydrogenase activity	MF
GO:0004805	0.0148	trehalose-phosphatase activity	MF
GO:0004629	0.0182	phospholipase C activity	MF
GO:0046983	0.0185	protein dimerization activity	MF
GO:0015078	0.0188	hydrogen ion transmembrane transporter activity	MF
GO:0004553	0.0207	hydrolase activity, hydrolyzing O-glycosyl compounds	MF
GO:0003779	0.0208	actin binding	MF
GO:0004084	0.0232	branched-chain-amino-acid transaminase activity	MF
GO:0009931	0.0242	calcium-dependent protein serine/threonine kinase activity	MF
GO:0008514	0.0250	organic anion transmembrane transporter activity	MF
GO:0030246	0.0257	carbohydrate binding	MF
GO:0005522	0.0260	profilin binding	MF
GO:0008891	0.0265	glycolate oxidase activity	MF
GO:0000220	0.0275	vacuolar proton-transporting V-type ATPase, V0 domain	MF
GO:0004565	0.0275	beta-galactosidase activity	MF
GO:0008964	0.0288	phosphoenolpyruvate carboxylase activity	MF
GO:0042389	0.0299	omega-3 fatty acid desaturase activity	MF
GO:0004161	0.0300	dimethylallyltranstransferase activity	MF
GO:0015200	0.0317	methylammonium transmembrane transporter activity	MF
GO:0003993	0.0328	acid phosphatase activity	MF
GO:0047066	0.0333	phospholipid-hydroperoxide glutathione peroxidase activity	MF
GO:0051537	0.0345	2 iron, 2 sulfur cluster binding	MF
GO:0019199	0.0356	transmembrane receptor protein kinase activity	MF
GO:0050661	0.0377	NADP binding	MF
GO:0004806	0.0387	triglyceride lipase activity	MF
GO:0003997	0.0395	acyl-CoA oxidase activity	MF
GO:0008889	0.0410	glycerophosphodiester phosphodiesterase activity	MF
GO:0046556	0.0410	alpha-L-arabinofuranosidase activity	MF
GO:0046910	0.0422	pectinesterase inhibitor activity	MF
GO:0010486	0.0437	manganese:proton antiporter activity	MF

GO:0016829	0.0462	lyase activity	MF
GO:0004776	0.0472	succinate-CoA ligase (GDP-forming) activity	MF
GO:0004601	0.0499	peroxidase activity	MF
GO:0010326	0.0499	methionine-oxo-acid transaminase activity	MF
GO:0016491	0.0351	oxidoreductase activity	MF
		Tx7000 at 30 days post-inoculation	
GO:0001503	1.00E-04	ossification	BP
GO:0006334	1.00E-04	nucleosome assembly	BP
GO:0006833	1.00E-04	water transport	BP
GO:0006857	1.00E-04	oligopeptide transport	BP
GO:0007018	1.00E-04	microtubule-based movement	BP
GO:0007169	1.00E-04	transmembrane receptor protein tyrosine kinase signaling pathway	BP
GO:0009408	1.00E-04	response to heat	BP
GO:0009826	1.00E-04	unidimensional cell growth	BP
GO:0016321	1.00E-04	female meiosis chromosome segregation	BP
GO:0009414	0.0002	response to water deprivation	BP
GO:0009644	0.0002	response to high light intensity	BP
GO:0010114	0.0002	response to red light	BP
GO:0042335	0.0002	cuticle development	BP
GO:0009934	0.0003	regulation of meristem structural organization	BP
GO:0010480	0.0003	microsporocyte differentiation	BP
GO:0048015	0.0003	phosphatidylinositol-mediated signaling	BP
GO:0009611	0.0004	response to wounding	BP
GO:0048765	0.0004	root hair cell differentiation	BP
GO:0051085	0.0004	chaperone mediated protein folding requiring cofactor	BP
GO:0007172	0.0005	signal complex assembly	BP
GO:0009648	0.0006	photoperiodism	BP
GO:0030002	0.0006	cellular anion homeostasis	BP
GO:0001666	0.0007	response to hypoxia	BP
GO:0010068	0.0008	protoderm histogenesis	BP
GO:0009932	0.0009	cell tip growth	BP
GO:0010075	0.0010	regulation of meristem growth	BP
GO:0010103	0.0010	stomatal complex morphogenesis	BP
GO:0042542	0.0011	response to hydrogen peroxide	BP
GO:0008356	0.0013	asymmetric cell division	BP
GO:0009628	0.0013	response to abiotic stimulus	BP
GO:0010167	0.0013	response to nitrate	BP
GO:0030041	0.0014	actin filament polymerization	BP
GO:0010218	0.0016	response to far red light	BP
GO:0009860	0.0019	pollen tube growth	BP
GO:0048645	0.0024	organ formation	BP
GO:0009228	0.0029	thiamine biosynthetic process	BP
GO:0009828	0.0030	plant-type cell wall loosening	BP
GO:0006986	0.0032	response to unfolded protein	BP
GO:0009735	0.0044	response to cytokinin	BP
GO:0009909	0.0052	regulation of flower development	BP
GO:0030154	0.0054	cell differentiation	BP
GO:0048229	0.0055	gametophyte development	BP
GO:0000024	0.0056	maltose biosynthetic process	BP
GO:0006869	0.0057	lipid transport	BP
GO:0019593	0.0058	mannitol biosynthetic process	BP
GO:0010440	0.0062	stomatal lineage progression	BP
GO:0031535	0.0064	plus-end directed microtubule sliding	BP
GO:0051300	0.0064	spindle pole body organization	BP
GO:0010325	0.0069	raffinose family oligosaccharide biosynthetic process	BP
GO:0010162	0.0070	seed dormancy process	BP
GO:0010025	0.0077	wax biosynthetic process	BP
GO:0015727	0.0079	lactate transport	BP
GO:0006312	0.0084	mitotic recombination	BP
GO:0006808	0.0084	regulation of nitrogen utilization	BP
GO:0009501	0.0086	amyloplast	BP
GO:0048579	0.0089	negative regulation of long-day photoperiodism, flowering	BP
GO:0009737	0.0095	response to abscisic acid	BP
GO:0005945	0.0097	6-phosphofructokinase complex	BP
GO:0006096	0.0099	glycolytic process	BP
GO:0007052	0.0101	mitotic spindle organization	BP
GO:0042753	0.0118	positive regulation of circadian rhythm	BP
GO:0000056	0.0126	ribosomal small subunit export from nucleus	BP
GO:0009269	0.0130	response to desiccation	BP
GO:0009831	0.0130	plant-type cell wall modification involved in multidimensional cell growth	BP

GO:0048366	0.0141	leaf development	BP
GO:0009740	0.0162	gibberellic acid mediated signaling pathway	BP
GO:0007568	0.0164	aging	BP
GO:0006597	0.0171	spermine biosynthetic process	BP
GO:0007100	0.0171	mitotic centrosome separation	BP
GO:0018131	0.0173	oxazole or thiazole biosynthetic process	BP
GO:0012505	0.0179	endomembrane system	BP
GO:0006821	0.0180	chloride transport	BP
GO:0005978	0.0191	glycogen biosynthetic process	BP
GO:0044403	0.0195	symbiosis, encompassing mutualism through parasitism	BP
GO:0005985	0.0204	sucrose metabolic process	BP
GO:0008608	0.0204	attachment of spindle microtubules to kinetochore	BP
GO:0010376	0.0235	stomatal complex formation	BP
GO:0009744	0.0239	response to sucrose	BP
GO:0000914	0.0240	phragmoplast assembly	BP
GO:0010074	0.0242	maintenance of meristem identity	BP
GO:0007080	0.0245	mitotic metaphase plate congression	BP
GO:0042116	0.0255	macrophage activation	BP
GO:0006952	0.0267	defense response	BP
GO:0006463	0.0268	steroid hormone receptor complex assembly	BP
GO:0031503	0.0268	protein complex localization	BP
GO:0046661	0.0268	male sex differentiation	BP
GO:0009641	0.0291	shade avoidance	BP
GO:0006950	0.0316	response to stress	BP
GO:0030155	0.0333	regulation of cell adhesion	BP
GO:0006532	0.0350	aspartate biosynthetic process	BP
GO:0006533	0.0350	aspartate catabolic process	BP
GO:0019266	0.0350	asparagine biosynthetic process from oxaloacetate	BP
GO:0010038	0.0352	response to metal ion	BP
GO:0008295	0.0359	spermidine biosynthetic process	BP
GO:0030497	0.0367	fatty acid elongation	BP
GO:0042545	0.0371	cell wall modification	BP
GO:0010158	0.0374	abaxial cell fate specification	BP
GO:0019953	0.0376	sexual reproduction	BP
GO:0015804	0.0384	neutral amino acid transport	BP
GO:0016046	0.0389	detection of fungus	BP
GO:0009624	0.0409	response to nematode	BP
GO:0009116	0.0410	nucleoside metabolic process	BP
GO:0009755	0.0412	hormone-mediated signaling pathway	BP
GO:0055046	0.0419	microgametogenesis	BP
GO:0045184	0.0421	establishment of protein localization	BP
GO:0045010	0.0422	actin nucleation	BP
GO:0000395	0.0424	mRNA 5'-splice site recognition	BP
GO:0030951	0.0427	establishment or maintenance of microtubule cytoskeleton polarity	BP
GO:0009051	0.0434	pentose-phosphate shunt, oxidative branch	BP
GO:0009753	0.0438	response to jasmonic acid	BP
GO:0006629	0.0442	lipid metabolic process	BP
GO:0051289	0.0446	protein homotetramerization	BP
GO:0006521	0.0447	regulation of cellular amino acid metabolic process	BP
GO:0010069	0.0447	zygote asymmetric cytokinesis in embryo sac	BP
GO:0006468	0.0456	protein phosphorylation	BP
GO:0048367	0.0480	shoot system development	BP
GO:0010053	0.0481	root epidermal cell differentiation	BP
GO:0009960	0.0488	endosperm development	BP
GO:0009409	0.0026	response to cold	BP
GO:0000786	0.0001	nucleosome	CC
GO:0005875	0.0001	microtubule associated complex	CC
GO:0009505	0.0001	plant-type cell wall	CC
GO:0035059	0.0001	RCAF complex	CC
GO:0001740	0.0002	Barr body	CC
GO:0016324	0.0035	apical plasma membrane	CC
GO:0005871	0.0046	kinesin complex	CC
GO:0010317	0.0066	pyrophosphate-dependent phosphofructokinase complex, alpha-subunit	CC
GO:0005700	0.0079	polytene chromosome	CC
GO:0005911	0.0086	cell-cell junction	CC
GO:0010287	0.0110	plastoglobule	CC
GO:0005811	0.0138	lipid particle	CC
GO:0005634	0.0155	nucleus	CC
GO:0005576	0.0191	extracellular region	CC
GO:0005740	0.0192	mitochondrial envelope	CC

GO:0005874	0.0251	microtubule	CC
GO:0005618	0.0312	cell wall	CC
GO:0045169	0.0375	fusome	CC
GO:0003700	0.0001	sequence-specific DNA binding transcription factor activity	MF
GO:0003777	0.0001	microtubule motor activity	MF
GO:0015250	0.0001	water channel activity	MF
GO:0009055	0.0003	electron carrier activity	MF
GO:0003677	0.0005	DNA binding	MF
GO:0004857	0.0005	enzyme inhibitor activity	MF
GO:0047334	0.0012	diphosphate-fructose-6-phosphate 1-phosphotransferase activity	MF
GO:0015198	0.0013	oligopeptide transporter activity	MF
GO:0016818	0.0016	hydrolase activity	MF
GO:0030599	0.0018	pectinesterase activity	MF
GO:0016538	0.0028	cyclin-dependent protein serine/threonine kinase regulator activity	MF
GO:0043565	0.0028	sequence-specific DNA binding	MF
GO:0009011	0.0042	starch synthase activity	MF
GO:0005524	0.0049	ATP binding	MF
GO:0003842	0.0055	1-pyrroline-5-carboxylate dehydrogenase activity	MF
GO:0009924	0.0059	octadecanal decarbonylase activity	MF
GO:0005247	0.0064	voltage-gated chloride channel activity	MF
GO:0005089	0.0065	Rho guanyl-nucleotide exchange factor activity	MF
GO:0016175	0.0073	superoxide-generating NADPH oxidase activity	MF
GO:0009922	0.0079	fatty acid elongase activity	MF
GO:0015129	0.0079	lactate transmembrane transporter activity	MF
GO:0015293	0.0080	symporter activity	MF
GO:0016174	0.0085	NAD(P)H oxidase activity	MF
GO:0003872	0.0097	6-phosphofructokinase activity	MF
GO:0015362	0.0105	high-affinity sodium:dicarboxylate symporter activity	MF
GO:0004373	0.0109	glycogen (starch) synthase activity	MF
GO:0046863	0.0125	ribulose-1,5-bisphosphate carboxylase/oxygenase activator activity	MF
GO:0003883	0.0135	CTP synthase activity	MF
GO:0047274	0.0138	galactinol-sucrose galactosyltransferase activity	MF
GO:0004674	0.0158	protein serine/threonine kinase activity	MF
GO:0004713	0.0162	protein tyrosine kinase activity	MF
GO:0045330	0.0169	aspartyl esterase activity	MF
GO:0004014	0.0171	adenosylmethionine decarboxylase activity	MF
GO:0045551	0.0195	cinnamyl-alcohol dehydrogenase activity	MF
GO:0016887	0.0210	ATPase activity	MF
GO:0008131	0.0232	primary amine oxidase activity	MF
GO:0008017	0.0234	microtubule binding	MF
GO:0008574	0.0237	ATP-dependent microtubule motor activity, plus-end-directed	MF
GO:0016984	0.0256	ribulose-bisphosphate carboxylase activity	MF
GO:0016987	0.0263	sigma factor activity	MF
GO:0008559	0.0279	xenobiotic-transporting ATPase activity	MF
GO:0015112	0.0297	nitrate transmembrane transporter activity	MF
GO:0051536	0.0313	iron-sulfur cluster binding	MF
GO:0008967	0.0337	phosphoglycolate phosphatase activity	MF
GO:0004350	0.0355	glutamate-5-semialdehyde dehydrogenase activity	MF
GO:0017084	0.0355	delta1-pyrroline-5-carboxylate synthetase activity	MF
GO:0015079	0.0360	potassium ion transmembrane transporter activity	MF
GO:0005522	0.0394	profilin binding	MF
GO:0015171	0.0399	amino acid transmembrane transporter activity	MF
GO:0004103	0.0404	choline kinase activity	MF
GO:0005351	0.0427	sugar:proton symporter activity	MF
GO:0015175	0.0438	neutral amino acid transmembrane transporter activity	MF
GO:0004737	0.0440	pyruvate decarboxylase activity	MF
GO:0008289	0.0449	lipid binding	MF
GO:0016298	0.0464	lipase activity	MF
GO:0051082	0.0478	unfolded protein binding	MF
GO:0051219	0.0484	phosphoprotein binding	MF
GO:0010328	0.0487	auxin influx transmembrane transporter activity	MF
GO:0016161	0.0487	beta-amylase activity	MF
GO:0035259	0.0487	glucocorticoid receptor binding	MF

BP = biological process, CC = cellular component, MF = molecular function

Appendix B - Significantly enriched metabolic pathways from Z-score enrichment analysis of SorghumCyc pathways for differentially expressed genes between resistant (SC599) and susceptible (Tx7000) sorghum genotypes in response to *M. phaseolina* inoculation at 2 and 7 days post inoculation.

Pathway	Observed gene count	Expected gene count	Z-score
2 days post-inoculation			
Betanidin degradation	33	3.5	50.4
Fructose degradation to pyruvate and lactate (anaerobic)	28	3.0	42.8
Cytokinins-glucoside biosynthesis	27	2.9	41.3
Triacylglycerol degradation	22	2.3	33.6
Gamma glutamyl cycle	21	2.2	32.1
Cellulose biosynthesis	19	2.0	28.9
Jasmonic acid biosynthesis	18	1.9	27.5
NAD salvage pathway II	16	1.7	24.4
Starch degradation	15	1.6	22.9
Phospholipid biosynthesis II	14	1.5	21.4
Beta alanine betaine biosynthesis	11	1.2	16.8
Aerobic respiration - electron donor III	11	1.2	16.8
Brassinosteroid biosynthesis II	11	1.2	16.8
Nicotine degradation III	11	1.2	16.8
7 days post-inoculation			
Fructose degradation to pyruvate and lactate (anaerobic)	100	30.9	53.5
Betanidin degradation	92	28.8	49.8
Triacylglycerol degradation	64	19.8	34.2
Cytokinins-glucoside biosynthesis	62	19.2	33.2
Gamma glutamyl cycle	55	17.0	29.4
Jasmonic acid biosynthesis	43	13.3	23.0
Aerobic respiration -electron donor II	40	12.4	21.4
Glutathione-mediated detoxification	40	12.4	21.4
Starch degradation	40	12.4	21.4
NAD salvage pathway II	34	10.5	18.2
Aerobic respiration -electron donor III	30	9.3	16.1
Cellulose biosynthesis	29	9.0	15.5
Methionine biosynthesis II	28	8.7	15.0
Brassinosteroid biosynthesis II	27	8.3	14.4
Phospholipid biosynthesis 1 & II	27	8.3	14.4
Purine nucleotides-de novo biosynthesis I	27	8.3	14.4
tRNA charging pathway	26	8.0	13.9
Homogalacturonan degradation	23	7.1	12.3
Tetrahydrofolate biosynthesis I	22	6.8	11.8
Nicotine degradation II & III	21	6.5	11.2
Chorismate biosynthesis	21	6.5	11.2
Salvage pathways of purine and pyrimidine nucleotides	20	6.2	10.7
Calvin cycle	19	5.9	10.2
Glycerol degradation I & IV	19	5.9	10.2
Gibberellin biosynthesis I, II, III, & IV	18	5.6	9.6
Phospholipases	16	4.9	8.6
Chlorophyllide biosynthesis	14	4.3	7.5
Aerobic respiration - electron donors reaction list	13	4.0	7.0
Beta alanine betaine biosynthesis	13	4.0	7.0
dTDP-L-rhamnose biosynthesis I	13	4.0	7.0
Mevalonate pathway	13	4.0	7.0
Beta alanine biosynthesis III	12	3.7	6.4
Branched-chain & alpha-keto acid dehydrogenase complex	12	3.7	6.4
Ethylene biosynthesis from methionine	12	3.7	6.4
Salvage pathways of pyrimidine ribonucleotides	12	3.7	6.4
UDP-glucose conversion	12	3.7	6.4
Sterol biosynthesis	11	3.4	5.9
TCA cycle	11	3.4	5.9
Pentose phosphate pathway (oxidative branch)	10	3.1	5.4
Tryptophan biosynthesis	10	3.1	5.4
UDP-acetylgalactosamine biosynthesis	10	3.1	5.4
Galactosylcyclitol biosynthesis	9	2.8	4.8

Leucine biosynthesis	9	2.8	4.8
Starch biosynthesis	9	2.8	4.8
Trehalose biosynthesis I	9	2.8	4.8
Tyrosine degradation I	9	2.8	4.8
De novo biosynthesis of pyrimidine ribonucleotides	8	2.5	4.3
Fatty acid elongation-unsaturated II	8	2.5	4.3
Isoflavonoid biosynthesis II	8	2.5	4.3
Lysine degradation II	8	2.5	4.3
Nitrate reduction II (assimilatory)	8	2.5	4.3
Sucrose degradation to ethanol and lactate (anaerobic)	8	2.5	4.3
Threonine degradation III (to methylglyoxal)	8	2.5	4.3
Glutathione redox reactions I	7	2.2	3.7
Photorespiration	7	2.2	3.7
Anthocyanin biosynthesis (pelargonidin 3-O-glucoside, cyanidin 3-O-glucoside)	7	2.2	3.7
Biotin biosynthesis II	7	2.2	3.7
Isoleucine degradation II	7	2.2	3.7
Phylloquinone biosynthesis	7	2.2	3.7
Pyridoxal 5'-phosphate salvage pathway	7	2.2	3.7
Tetrapyrrole biosynthesis I	7	2.2	3.7
Valine degradation II	7	2.2	3.7
Ascorbate glutathione cycle	6	1.9	3.2
Choline biosynthesis III	6	1.9	3.2
Cytokinins degradation	6	1.9	3.2
Dolichyl-diphosphooligosaccharide biosynthesis	6	1.9	3.2
Ethanol fermentation to acetate	6	1.9	3.2
Fatty acid elongation - saturated	6	1.9	3.2
Flavonoid biosynthesis	6	1.9	3.2
Galactose degradation II	6	1.9	3.2
Glycogen biosynthesis II (from UDP-D-Glucose)	6	1.9	3.2
Glycolipid desaturation	6	1.9	3.2
Lysine biosynthesis I	6	1.9	3.2
Menaquinone biosynthesis	6	1.9	3.2
Phenylalanine biosynthesis I	6	1.9	3.2
Phenylpropanoid biosynthesis	6	1.9	3.2
Proline biosynthesis I	6	1.9	3.2
Proline degradation II	6	1.9	3.2
Superpathway of gluconate degradation	6	1.9	3.2
TCA cycle variation I	6	1.9	3.2
Tryptophan degradation III (eukaryotic)	6	1.9	3.2
Chlorophyll a degradation	5	1.5	2.7
Citrulline-nitric oxide cycle	5	1.5	2.7
Cyanate degradation	5	1.5	2.7
Cysteine biosynthesis I	5	1.5	2.7
Fatty acid biosynthesis - initial steps	5	1.5	2.7
Flavin biosynthesis	5	1.5	2.7
Gluconeogenesis	5	1.5	2.7
Heme biosynthesis II	5	1.5	2.7
Leucopelargonidin and leucocyanidin biosynthesis	5	1.5	2.7
Respiration (anaerobic)	5	1.5	2.7
salvage pathways of adenine, hypoxanthine, and their nucleosides	5	1.5	2.7
Stachyose biosynthesis	5	1.5	2.7
Sucrose degradation I	5	1.5	2.7
Xylulose-monophosphate cycle	5	1.5	2.7
Arginine biosynthesis II (acetyl cycle)	4	1.2	2.1
Ascorbate biosynthesis	4	1.2	2.1
Canavanine degradation	4	1.2	2.1
Carotenoid biosynthesis	4	1.2	2.1
Cyclopropane fatty acid (CFA) biosynthesis	4	1.2	2.1
Histidine biosynthesis I	4	1.2	2.1
Phenylalanine degradation III	4	1.2	2.1
Reductive TCA cycle I	4	1.2	2.1
Secologanin and strictosidine biosynthesis	4	1.2	2.1
Trans,trans-farnesyl diphosphate biosynthesis	4	1.2	2.1

Appendix C - Differentially expressed genes between resistant (SC599) and susceptible (Tx7000) sorghum genotypes in response to *M. phaseolina* inoculation, their annotations, and accompanied meatabolic pathways at 7 days post-inoculation.

Metabolic pathway	Gene annotation	Gene ID	Geno × Trt*	SC599 (MP-CON)†		Tx7000 (MP-CON)	
			q-value	log2 DE‡	q-value	log2 DE	q-value
Trehalose biosynthesis I	CPuORF22 - conserved peptide uORF-containing transcript	*Sb04g032740*	1.26E-08	-1.933	7.2E-04	1.206	1.2E-03
		Sb01g029590	1.85E-05	-0.487	8.7E-01	2.990	8.2E-14
	Lissencephaly type-1-like homology motif	*Sb03g009770*	2.21E-01	-0.036	9.9E-01	0.672	3.3E-02
		Sb07g004180	7.69E-02	-0.381	7.2E-01	-1.205	1.8E-06
	Trehalase precursor	*Sb01g031280*	4.75E-02	-1.215	3.2E-02	-0.377	2.9E-01
	Trehalose phosphatase	*Sb02g033420*	8.21E-13	-	-	6.503	4.4E-14
	Trehalose synthase	*Sb03g034640*	3.72E-01	0.055	9.9E-01	0.669	8.3E-02
		Sb09g025660	2.58E-03	0.325	8.6E-01	2.231	1.0E-09
		Sb03g033590	1.24E-02	0.675	1.7E-01	-0.422	2.5E-01
	Trehalose-6-phosphate synthase	*Sb07g021920*	5.79E-09	-0.843	6.5E-01	4.655	1.1E-20
		Sb07g020270	1.48E-01	0.678	7.1E-01	2.253	3.6E-06
		Sb02g023610	5.65E-03	0.376	7.9E-01	2.379	1.4E-07
	Uncharacterized glycosyl hydrolase Rv2006/MT2062	*Sb01g033800*	2.54E-03	-0.065	9.9E-01	3.160	1.3E-16
UDP-glucose conversion	60S ribosomal protein L18a-1	*Sb09g028580*	4.07E-02	0.580	4.2E-01	-0.285	3.1E-01
		Sb03g030610	4.74E-02	-0.096	9.7E-01	0.801	5.2E-03
	Casein kinase II subunit beta-4	*Sb01g028740*	1.07E-02	-0.418	7.4E-01	0.858	3.4E-03
	Expressed protein	*Sb02g019490*	2.51E-04	-	-	6.632	2.2E-13
		Sb07g002570	1.35E-05	-0.461	6.5E-01	1.329	5.3E-11
	Inorganic H+ pyrophosphatase	*Sb04g036230*	2.48E-05	0.948	6.0E-01	-3.626	5.1E-12
		Sb10g005250	4.13E-03	-0.211	9.7E-01	2.882	1.9E-15
		Sb10g025280	1.05E-08	-0.526	5.1E-01	1.665	9.7E-16
	Methyltransferase small domain containing protein	*Sb01g002920*	6.95E-03	-0.132	9.5E-01	0.930	5.5E-04
	Phosphoglucomutase	*Sb03g028080*	1.31E-02	0.404	6.2E-01	-0.885	2.5E-02
	Soluble inorganic pyrophosphatase	*Sb03g040910*	3.05E-11	2.384	7.2E-04	-3.618	2.9E-08
	ThiF family domain containing protein	*Sb03g027840*	3.41E-09	-0.729	3.5E-01	2.169	3.8E-15
dTDP-L-rhamnose biosynthesis I	Glucose-1-phosphate adenylyltransferase large subunit	*Sb03g028850*	8.42E-03	0.388	7.3E-01	-0.926	4.9E-03
		Sb07g024240	5.95E-04	0.166	9.8E-01	-6.131	4.7E-06
	Male sterility protein	*Sb01g046030*	1.48E-03	0.321	7.2E-01	-0.792	2.8E-03
		Sb05g005330	3.05E-02	-	-	-3.540	1.1E-02
	Mannose-1-phosphate guanyltransferase	*Sb01g043370*	2.60E-06	-0.277	7.8E-01	1.296	2.1E-07
		Sb01g039220	1.64E-04	-0.062	9.8E-01	1.147	1.5E-06
	NAD dependent epimerase	*Sb03g039180*	3.31E-02	-0.183	8.8E-01	0.473	5.4E-02
		Sb09g018070	1.46E-03	-0.213	9.4E-01	1.608	5.3E-10
	Oxidoreductase, short chain dehydrogenase/reductase family	*Sb07g018840*	4.06E-03	0.217	9.3E-01	-1.352	5.0E-06
		Sb01g038050	2.19E-02	-0.662	8.6E-01	3.693	2.1E-13
		Sb08g022850	1.22E-02	-	-	5.504	8.8E-05
	Reductase	*Sb10g024490*	3.88E-08	-0.616	7.6E-01	3.590	1.6E-33
	UDP-glucuronate 4-epimerase	*Sb02g029130*	3.99E-03	-0.733	7.9E-01	3.040	3.4E-07
Fructose degradation to pyruvate and lactate	2,3-bisphosphoglycerate-independent phosphoglycerate mutase	*Sb03g038020*	3.20E-03	-0.374	7.4E-01	0.814	1.6E-05
	6-phosphofructokinase	*Sb03g034060*	4.84E-03	-0.157	9.5E-01	1.136	1.6E-08
		Sb09g006030	1.39E-04	-0.100	9.8E-01	3.594	6.8E-16
	Aspartic proteinase nepenthesin-2 precursor	*Sb10g011110*	6.37E-12	0.312	9.2E-01	-4.776	2.1E-16

	Sb04g029680	1.45E-07	-0.641	5.6E-01	1.920	1.3E-12
	Sb02g027990	4.12E-03	-	-	2.096	2.6E-01
	Sb04g029400	1.01E-06	-1.626	1.5E-01	3.276	1.2E-14
	Sb04g029670	3.16E-06	-2.191	1.1E-01	4.193	1.2E-14
	Sb02g028000	3.12E-16	0.224	9.6E-01	4.911	4.3E-40
	Sb03g006630	9.70E-03	0.950	6.1E-01	-2.089	1.5E-03
Aspartic proteinase	*Sb03g026970*	4.18E-02	2.517	2.9E-02	0.254	7.9E-01
	Sb10g023970	3.68E-14	0.207	8.8E-01	3.686	8.7E-25
CBS domain containing membrane protein	*Sb06g002220*	2.01E-08	-1.214	2.1E-01	2.598	8.1E-33
	Sb02g000670	3.93E-07	-	-	-6.194	2.3E-06
	Sb02g000700	6.74E-03	-	-	-5.767	2.5E-05
	Sb05g005200	4.24E-02	-	-	-3.889	3.1E-03
	Sb05g008800	1.86E-03	-	-	5.580	6.8E-07
Dirigent	*Sb05g008780*	6.26E-04	-1.402	4.5E-01	5.638	6.4E-05
	Sb05g008770	2.16E-04	-	-	6.306	1.5E-06
	Sb02g010230	2.82E-09	-	-	6.530	4.3E-14
	Sb05g008790	7.99E-03	-	-	6.827	1.8E-07
Dirigent-like protein Pdir17	*Sb06g032050*	1.07E-02	-0.586	8.3E-01	-3.350	7.5E-07
	Sb05g006060	8.13E-04	-0.152	9.6E-01	-2.000	6.3E-12
DUF803 domain containing	*Sb09g021300*	5.57E-03	0.531	8.2E-01	-1.653	5.4E-04
	Sb04g020130	1.21E-02	0.161	9.6E-01	-1.447	1.4E-05
	Sb06g034190	3.37E-02	-0.032	9.8E-01	-0.570	1.7E-02
Endonuclease	*Sb01g050650*	1.03E-02	0.351	7.8E-01	-0.714	5.2E-04
Endonuclease/exonuclease/phosphatase domain containing protein	*Sb01g024860*	4.08E-02	-0.071	9.8E-01	-1.299	4.1E-05
Enolase	*Sb10g002460*	1.56E-02	-0.156	9.6E-01	1.424	1.5E-05
	Sb02g023480	2.56E-03	-0.253	8.7E-01	1.455	2.2E-04
Expressed protein	*Sb07g000730*	8.91E-05	-0.525	5.2E-01	1.201	1.6E-05
	Sb01g043800	5.94E-09	-0.492	8.2E-01	3.717	1.6E-41
	Sb05g004590	5.48E-16	0.227	9.3E-01	-4.459	2.9E-70
Fructose-bisphospate aldolase isozyme	*Sb10g023850*	2.19E-02	1.193	5.6E-01	-3.507	1.1E-02
	Sb08g004500	2.72E-06	1.661	2.6E-02	-2.887	1.5E-06
	Sb03g008050	1.16E-05	0.034	9.9E-01	1.990	2.4E-12
Glutamine synthetase, catalytic domain containing protein	*Sb01g042450*	3.75E-03	0.817	6.8E-01	-2.157	2.0E-08
	Sb06g018880	6.15E-04	0.810	5.0E-01	-2.555	3.1E-05
Glyceraldehyde-3-phosphate dehydrogenase	*Sb04g004750*	3.63E-05	-0.295	6.1E-01	0.801	5.2E-04
	Sb04g025120	2.32E-06	-0.691	7.8E-01	4.756	5.1E-28
Glycerol-3-phosphate acyltransferase	*Sb03g040260*	7.78E-04	0.242	9.6E-01	-4.961	2.8E-06
	Sb03g003190	5.27E-03	0.915	3.1E-01	-0.816	1.5E-02
Hexokinase	*Sb09g026080*	1.33E-02	-0.034	9.9E-01	1.080	6.8E-05
	Sb03g033200	3.43E-04	-	-	2.978	7.6E-05
Homeobox and START domains containing protein	*Sb06g025750*	2.93E-03	-0.154	9.7E-01	-3.266	3.5E-03
	Sb06g029270	1.33E-02	-0.216	9.2E-01	-1.858	1.2E-05
	Sb04g023410	1.18E-05	2.340	1.2E-02	-3.210	2.3E-02
Homeobox associated leucine zipper	*Sb01g029000*	1.79E-04	0.945	4.6E-01	-2.778	6.5E-05
	Sb01g042030	1.75E-03	1.395	9.0E-03	-1.051	7.6E-02
	Sb02g000560	1.25E-02	-	-	-3.475	4.0E-02
Kinesin motor domain containing protein	*Sb06g029500*	6.56E-03	0.244	9.3E-01	-1.599	8.8E-05
	Sb09g029240	3.23E-03	-0.397	5.0E-01	0.499	4.0E-02
Lactate/malate dehydrogenase	*Sb08g022770*	1.75E-03	-0.101	9.7E-01	1.423	2.5E-07
	Sb06g024610	2.10E-03	-	-	4.103	2.2E-07

		Sb04g000590	2.20E-03	-	-	5.415	5.4E-09
	Maf	*Sb01g041990*	2.34E-03	0.814	3.2E-01	-0.722	1.7E-02
		Sb05g021370	8.64E-03	0.423	6.8E-01	-0.636	3.4E-02
	Membrane associated DUF588 domain containing protein	*Sb08g018660*	1.32E-02	-0.731	7.5E-01	2.213	1.7E-04
	Peptidyl-prolyl cis-trans isomerase	*Sb01g043790*	1.44E-02	0.003	1.0E+00	1.075	8.8E-04
	Phenylalanine ammonia-lyase	*Sb06g022750*	1.32E-05	-1.949	1.8E-01	5.078	1.2E-31
	Phosphate/phosphate translocator	*Sb06g034090*	2.26E-04	0.764	3.9E-01	-1.358	7.0E-05
	Phosphofructokinase	*Sb01g022370*	1.79E-02	-0.519	3.2E-01	0.837	7.2E-02
		Sb07g021500	2.32E-02	0.384	8.9E-01	2.137	7.0E-10
	Phosphoglycerate kinase protein	*Sb09g024340*	2.01E-03	0.491	7.8E-01	-1.917	1.3E-05
	Polygalacturonase	*Sb07g025130*	2.05E-02	-	-	4.551	2.8E-03
	Pyridoxal biosynthesis protein PDX2	*Sb04g002510*	4.17E-02	-0.019	1.0E+00	-0.888	1.4E-03
	Pyrophosphate-fructose 6-phosphate 1-phosphotransferase subunit alpha	*Sb07g012720*	5.05E-11	0.116	9.5E-01	-1.821	1.8E-15
	Pyruvate kinase	*Sb02g004550*	1.75E-02	0.129	9.6E-01	-1.056	7.6E-03
		Sb03g030110	7.72E-04	-0.356	7.6E-01	1.102	3.2E-05
		Sb01g005200	5.49E-07	-0.481	3.7E-01	1.354	9.6E-06
		Sb05g008760	1.20E-04	-0.428	8.6E-01	2.414	1.2E-16
		Sb10g008380	1.38E-02	-0.417	8.9E-01	-2.548	2.2E-12
	Ras-related protein	*Sb09g025400*	1.78E-02	0.895	7.2E-01	-2.408	3.8E-03
		Sb09g007420	6.18E-04	0.607	6.4E-01	-1.844	6.1E-03
	S1 RNA binding domain containing protein	*Sb04g001123*	2.36E-07	0.461	4.2E-01	-0.955	2.7E-05
	SOR/SNZ family protein	*Sb02g000720*	7.61E-03	0.495	6.0E-01	-1.058	6.9E-03
	Sucrose-phosphate synthase	*Sb09g028570*	1.45E-05	0.522	3.7E-01	-0.852	1.9E-05
	Terpene synthase	*Sb07g004470*	4.12E-04	-1.654	3.0E-01	3.750	1.0E-13
	Toc64	*Sb01g010650*	3.25E-02	-0.209	8.4E-01	0.391	8.3E-02
		Sb06g018610	1.95E-02	0.469	7.6E-01	-1.139	6.0E-03
		Sb03g009310	2.68E-02	0.157	9.6E-01	-1.074	1.1E-04
		Sb09g029520	3.99E-04	0.044	9.8E-01	0.942	9.7E-06
	Transporter family protein	*Sb10g002770*	4.89E-03	0.549	8.5E-01	3.456	6.6E-09
		Sb05g023140	1.28E-02	-	-	4.098	7.1E-05
		Sb02g000650	2.24E-15	-1.057	4.3E-01	4.941	1.3E-51
		Sb06g018540	1.62E-04	-	-	5.727	2.5E-05
	Triosephosphate isomerase, chloroplast precursor	*Sb02g031030*	2.42E-02	0.069	9.8E-01	-0.945	7.2E-05
		Sb03g039480	1.36E-02	-0.090	9.9E-01	2.064	1.0E-04
	tRNA methyltransferase	*Sb01g020930*	2.30E-03	0.957	2.4E-01	-0.653	1.3E-01
	Tubulin/FtsZ domain containing protein	*Sb06g033640*	1.37E-02	0.055	9.8E-01	-0.726	4.5E-03
Sucrose degradation to ethanol and lactate	Glucose-6-phosphate isomerase	*Sb01g006480*	1.89E-04	-0.273	6.7E-01	0.871	6.9E-04
		Sb02g009280	1.19E-03	-	-	4.017	2.0E-04
		Sb02g036310	6.08E-04	-0.204	9.6E-01	2.975	2.8E-08
		Sb02g037570	2.66E-15	-2.168	1.6E-03	4.586	7.4E-20
	Transporter family protein	*Sb03g007080*	4.09E-02	0.158	9.4E-01	1.034	9.9E-06
		Sb08g016530	8.18E-06	-0.587	7.7E-01	3.040	4.1E-16
		Sb09g028810	3.13E-06	-1.648	7.7E-05	1.479	4.1E-03
		Sb07g003750	1.26E-04	-0.747	4.7E-01	1.589	3.3E-08
Sucrose degradation I	Glycosyl hydrolases	*Sb04g000620*	1.68E-04	4.312	1.1E-07	-1.656	1.8E-01
	Neutral/alkaline invertase	*Sb03g013420*	1.47E-08	-0.672	5.6E-01	2.681	1.3E-15
		Sb04g002180	2.19E-02	-0.537	7.3E-01	-2.412	4.4E-04
	Plant neutral invertase domain containing protein	*Sb04g022350*	2.44E-13	-0.674	1.4E-01	1.270	7.0E-11
		Sb05g004770	3.21E-02	-0.332	7.6E-01	0.709	5.0E-02
Starch degradation	Alpha amylase, catalytic domain containing protein	*Sb06g001540*	4.38E-02	0.422	9.1E-01	-1.826	1.7E-02

		Sb03g032830	9.39E-04	-0.718	6.7E-01	1.976	2.9E-07
	Alpha-amylase precursor	*Sb02g023250*	2.43E-04	0.512	8.7E-01	4.748	7.6E-31
		Sb02g023790	4.88E-14	-0.605	7.3E-01	5.186	1.1E-38
	alpha-glucan phosphorylast isozyme	*Sb03g040060*	2.21E-02	-0.962	6.1E-01	1.663	1.3E-03
		Sb04g028170	1.27E-07	0.012	1.0E+00	-5.424	6.0E-59
	Auxin efflux carrier component	*Sb10g008290*	3.21E-04	-0.449	8.6E-01	-3.595	4.3E-23
		Sb02g029210	3.36E-02	-0.148	9.7E-01	-2.906	1.1E-03
	Beta-amylase	*Sb04g002450*	6.12E-03	0.569	5.2E-01	-0.678	1.9E-02
	Dehydrogenase	*Sb06g028240*	1.87E-02	0.265	9.6E-01	-2.432	5.6E-03
		Sb10g006300	2.41E-03	-	-	5.583	1.7E-08
	Diacylglycerol O-acyltransferase	*Sb10g012770*	6.49E-08	-0.134	9.7E-01	3.425	4.9E-38
		Sb05g027506	4.98E-02	-	-	-2.794	1.8E-02
	Expressed protein	*Sb05g027390*	5.77E-03	-0.285	9.2E-01	1.636	4.4E-03
		Sb05g027400	1.09E-05	-0.535	6.7E-01	1.763	3.6E-05
	Glycogen operon protein glgX	*Sb02g027280*	1.16E-12	1.619	8.3E-04	-1.610	2.1E-10
	Glycosyl hydrolase, family 31	*Sb03g007230*	7.95E-03	-0.325	9.0E-01	-3.059	1.5E-05
		Sb03g007960	6.63E-03	-	-	2.375	4.6E-04
		Sb03g008020	1.51E-03	-0.285	9.0E-01	-2.329	7.1E-09
	Glycosyltransferase	*Sb10g018300*	4.73E-05	-0.832	2.0E-02	0.702	2.8E-02
		Sb10g002800	8.16E-03	-1.009	5.8E-01	1.646	1.6E-02
		Sb03g008010	4.84E-10	-	-	6.650	6.0E-11
	Hexokinase	*Sb04g035100*	5.59E-08	-	-	6.703	2.4E-11
		Sb09g005840	1.05E-05	0.650	7.6E-01	4.773	5.4E-47
		Sb01g043480	6.79E-04	1.673	1.8E-01	-2.986	4.3E-02
	Membrane associated DUF588 domain containing protein	*Sb01g006950*	5.34E-03	0.052	9.9E-01	-2.844	6.9E-06
		Sb02g015330	3.16E-03	-	-	-2.035	2.2E-02
		Sb09g022380	1.21E-02	-0.692	5.4E-01	0.667	2.2E-02
	M-phase phosphoprotein 10	*Sb02g031250*	1.18E-02	0.075	9.8E-01	-1.225	2.6E-03
	Papain family cysteine protease domain containing protein	*Sb02g034490*	1.43E-12	-0.588	5.5E-01	2.873	7.6E-32
	Poly synthetase 2-A	*Sb03g013840*	3.63E-16	0.670	3.9E-01	-3.512	1.9E-24
		Sb07g021760	1.13E-07	0.320	9.3E-01	-4.723	3.1E-22
		Sb04g035780	1.53E-03	-	-	-4.670	6.4E-05
		Sb02g024990	3.52E-07	1.708	5.0E-02	-4.523	2.3E-08
		Sb03g005870	2.59E-07	-0.304	9.1E-01	-4.264	1.9E-08
	Transferase family protein	*Sb07g021750*	9.79E-05	0.774	6.0E-01	-2.740	1.2E-04
		Sb02g022440	5.68E-03	1.358	3.7E-01	-2.653	2.1E-03
		Sb02g031580	2.65E-02	-	-	3.355	5.1E-02
		Sb10g005760	7.32E-05	-	-	4.919	1.8E-05
		Sb10g005770	1.87E-10	-	-	6.460	9.3E-14
Starch biosynthesis	1,4-alpha-glucan-branching enzyme, chloroplast precursor	*Sb06g015360*	6.79E-03	-0.001	1.0E+00	-1.894	1.5E-07
	Alpha amylase, catalytic domain containing protein	*Sb07g027200*	4.06E-04	-0.091	9.8E-01	-3.339	7.2E-10
	Glucose-6-phosphate isomerase	*Sb02g027000*	2.14E-10	-0.464	5.8E-01	1.753	4.0E-21
	soluble starch synthase 3, chloroplast precursor	*Sb06g029050*	5.18E-11	0.559	5.8E-01	-2.521	3.3E-33
	Starch synthase	*Sb02g009870*	7.66E-07	0.133	9.8E-01	-5.681	3.0E-28
		Sb09g026570	5.36E-03	0.093	9.7E-01	-1.315	1.8E-04
		Sb02g037590	5.51E-03	-	-	2.353	2.7E-02
	Transporter family protein	*Sb09g028820*	3.31E-05	0.788	5.2E-01	-2.506	1.3E-05
		Sb01g016730	1.46E-02	-0.046	9.9E-01	2.448	8.8E-08
Glycerol degradation	Dihydrolipoyl dehydrogenase 1, mitochondrial precursor	*Sb03g013290*	5.89E-03	-0.043	9.8E-01	0.855	1.2E-04
	DNA binding protein	*Sb10g026430*	6.00E-03	-0.291	9.3E-01	2.026	8.1E-06

	FAD dependent oxidoreductase domain containing protein	*Sb03g037590*	7.13E-05	0.460	7.9E-01	-1.855	1.1E-10
	FGGY family of carbohydrate kinases	*Sb06g030600*	5.24E-06	-0.184	9.4E-01	2.008	3.1E-24
	GDSL-like lipase/acylhydrolase	*Sb02g020850*	1.23E-04	0.270	9.1E-01	-2.319	1.3E-05
	Glycerol-3-phosphate dehydrogenase	*Sb03g045390*	2.18E-06	0.271	9.4E-01	-4.022	2.2E-20
		Sb04g021010	3.25E-80	-3.210	1.2E-19	6.427	5.9E-110
		Sb06g014320	8.89E-23	-3.093	1.6E-05	6.106	3.6E-35
		Sb07g026000	2.41E-11	-2.384	2.1E-02	4.219	3.5E-24
	Glycerophosphoryl diester phosphodiesterase family protein	*Sb01g015000*	2.99E-10	-1.945	9.7E-04	2.740	6.7E-09
		Sb03g035370	5.89E-07	-0.426	5.7E-01	1.446	1.8E-08
		Sb04g024440	1.64E-02	-0.789	6.1E-01	1.182	3.5E-04
		Sb02g039350	3.24E-02	0.424	8.2E-01	-0.953	4.8E-02
	Lycopene epsilon cyclase, chloroplast precursor	*Sb03g026020*	1.48E-05	1.098	2.5E-01	-1.780	5.2E-08
	Protein kinase domain containing protein	*Sb04g007620*	2.21E-02	-	-	-1.016	2.9E-01
	Protein kinase family protein	*Sb06g017260*	1.98E-07	-1.369	9.7E-02	2.365	3.1E-09
	SET domain-containing protein	*Sb04g029430*	1.02E-02	0.907	3.3E-01	-0.507	8.7E-02
	Alpha-1,4-glucan-protein synthase	*Sb01g015090*	2.06E-06	-0.680	3.8E-01	1.671	1.1E-08
	Cellulase	*Sb09g008170*	9.88E-05	1.431	3.5E-01	-3.793	2.1E-10
		Sb01g024390	2.00E-06	-1.406	3.9E-01	4.382	4.6E-44
	CESA7 - cellulose synthase	*Sb01g019720*	1.33E-02	0.830	7.8E-01	-6.707	1.2E-09
	CESA4 - cellulose synthase	*Sb03g034680*	1.28E-02	0.520	9.1E-01	-6.215	1.4E-06
	CESA9 - cellulose synthase	*Sb02g025020*	6.15E-03	0.842	7.8E-01	-6.022	3.7E-06
	CESA3 - cellulose synthase	*Sb02g010110*	2.98E-03	1.602	2.1E-01	-1.712	4.5E-04
	CESA2 - cellulose synthase	*Sb03g047220*	1.39E-26	-1.602	2.6E-02	5.231	1.1E-64
	CSLE2 - cellulose synthase-like family E	*Sb04g029420*	4.18E-07	-1.262	6.7E-02	2.343	1.0E-06
	CSLF6 - cellulose synthase-like family F; beta1,3;1,4 glucan synthase	*Sb07g004110*	1.09E-03	1.738	1.4E-02	-2.313	8.4E-03
		Sb02g035980	5.94E-03	-0.649	8.5E-01	3.463	2.7E-05
	CSLH1 - cellulose synthase-like family H	*Sb06g016750*	8.58E-05	-0.337	9.3E-01	-4.503	3.0E-14
		Sb02g030990	7.04E-29	1.849	8.0E-11	-2.227	5.4E-15
Cellulose biosynthesis	Endoglucanase, putative	*Sb01g008860*	2.69E-07	0.621	3.5E-01	-1.631	9.9E-09
		Sb04g028520	1.50E-03	0.057	9.9E-01	3.062	5.7E-08
	Eukaryotic translation initiation factor	*Sb01g019730*	1.60E-02	-0.473	6.8E-01	0.746	7.0E-03
	Glucan endo-1,3-beta-glucosidase precursor	*Sb05g027690*	7.30E-09	-0.326	8.5E-01	3.328	3.5E-17
		Sb02g035490	2.78E-19	-1.529	8.7E-02	5.818	6.4E-33
		Sb10g023710	3.30E-03	-0.403	6.5E-01	-1.644	1.5E-09
		Sb01g009770	3.27E-04	0.560	5.4E-01	-1.623	1.7E-04
		Sb03g040630	9.96E-09	-0.929	1.9E-01	1.959	8.7E-12
	Glycosyl hydrolases family 17	*Sb09g024320*	1.56E-02	0.099	9.8E-01	2.148	2.5E-08
		Sb09g021800	1.14E-04	-1.555	2.1E-01	2.423	1.2E-08
		Sb03g045480	5.59E-05	-	-	2.888	2.0E-03
		Sb03g045630	4.35E-02	0.611	8.6E-01	4.007	1.9E-14
		Sb03g045460	3.29E-03	-0.722	8.2E-01	6.477	6.3E-08
	peptidyl-prolyl cis-trans isomerase	*Sb02g024520*	3.47E-02	-0.258	8.9E-01	0.671	6.4E-04
	Ribulose-1,5 bisphosphate carboxylase	*Sb02g024510*	2.06E-03	0.680	5.1E-01	-1.560	1.8E-02
		Sb01g017520	8.14E-06	-	-	-5.465	7.6E-05
		Sb07g000850	1.85E-03	-	-	2.794	7.4E-07
	Invertase/pectin methylesterase inhibitor family protein	*Sb07g000870*	1.29E-08	-1.279	1.7E-01	4.164	1.6E-09
Homogalacturonan degradation		*Sb06g000550*	2.19E-09	-1.200	2.2E-01	4.514	8.3E-13
		Sb07g000860	4.32E-06	-	-	6.286	1.8E-06
	Pectinesterase inhibitor domain containing protein	*Sb04g021920*	9.49E-08	0.572	6.9E-01	4.225	1.8E-29
	Pectinesterase	*Sb07g022090*	4.13E-03	-	-	-4.046	1.2E-02

		Sb03g036790	9.57E-05	-1.371	2.2E-01	1.727	1.6E-03
		Sb01g022290	5.94E-08	-0.789	3.4E-01	1.870	2.8E-13
		Sb02g012560	5.77E-08	-0.774	6.6E-01	3.293	1.2E-15
		Sb09g017920	4.45E-04	-0.168	9.8E-01	4.741	5.8E-21
		Sb03g012820	1.32E-08	-	-	6.741	1.9E-07
	PME/invertase inhibitor	*Sb06g017880*	1.23E-09	-	-	-2.498	1.9E-04
		Sb01g004220	3.47E-04	1.252	5.4E-01	-5.882	1.4E-10
		Sb03g013310	1.11E-02	-	-	-3.766	2.1E-02
		Sb01g002550	7.66E-14	0.348	5.7E-01	-2.002	1.2E-12
		Sb04g035020	1.32E-02	0.581	5.7E-01	-0.881	6.6E-02
	Polygalacturonase	*Sb02g025730*	2.00E-02	-0.006	1.0E+00	0.935	2.8E-04
		Sb02g028280	4.81E-15	-0.427	6.2E-01	2.731	1.8E-22
		Sb09g027150	9.15E-04	0.531	6.8E-01	2.915	2.7E-12
		Sb07g000740	1.78E-07	-0.756	5.2E-01	2.920	1.6E-13
		Sb03g042350	1.08E-09	-	-	6.262	3.6E-09
	ATBET9	*Sb07g002270*	4.36E-02	0.181	9.1E-01	-0.678	2.5E-02
	Ethylene-insensitive protein	*Sb01g011025*	3.03E-03	0.754	1.6E-01	-0.564	1.1E-01
Phenylalanine biosynthesis I	Glycosyltransferase family 43 protein	*Sb03g030990*	3.82E-02	-0.492	4.0E-01	0.353	3.6E-01
		Sb06g000430	1.51E-05	-0.583	4.7E-01	1.444	2.3E-05
	OsAPx6 - Stromal Ascorbate Peroxidase encoding gene 5,8	*Sb08g004880*	3.04E-02	-0.275	8.6E-01	0.731	1.7E-02
	P-protein	*Sb01g038740*	1.85E-05	-0.734	4.5E-01	1.475	2.4E-12
	Dehydrogenase	*Sb06g001430*	9.12E-03	-0.920	6.2E-01	-4.268	1.6E-14
		Sb07g006090	1.75E-02	0.016	1.0E+00	-2.586	6.5E-05
Phenylpropanoid biosynthesis	Caffeoyl-CoA O-methyltransferase	*Sb07g028530*	1.06E-02	0.488	8.1E-01	-1.476	4.6E-05
		Sb07g003580	1.36E-02	0.355	7.9E-01	-0.798	5.6E-02
	Phenylalanine ammonia-lyase	*Sb04g026560*	2.98E-03	-1.423	3.8E-01	2.046	1.5E-05
	Cytochrome P450	*Sb04g017460*	4.06E-05	-1.175	5.9E-01	6.282	1.9E-14
Coumarin biosynthesis (via 2-coumarate)	Os5bglu20 - beta-glucosidase homologue	*Sb09g018160*	3.55E-07	1.120	2.4E-01	-3.581	1.2E-10
	Os3bglu6 - beta-glucosidase/beta-fucosidase/beta-galactosidase	*Sb01g043030*	7.13E-03	0.103	9.8E-01	-3.403	4.3E-03
	Os4bglu18 - monolignol beta-glucoside homologue	*Sb06g022510*	7.22E-04	-0.247	9.6E-01	3.018	7.7E-11
	CXE carboxylesterase	*Sb07g025010*	3.05E-02	-0.608	7.9E-01	1.671	3.5E-02
		Sb02g026550	1.79E-02	-0.597	7.4E-01	-2.703	2.2E-08
		Sb02g003580	1.13E-02	0.632	7.3E-01	-2.032	2.1E-03
Isoflavonoid biosynthesis		*Sb02g026816*	3.76E-03	0.738	5.3E-01	-1.475	1.4E-02
	Gibberellin receptor GID1L2	*Sb03g005590*	5.30E-04	-0.260	9.4E-01	2.561	3.7E-07
		Sb03g005570	2.28E-02	0.720	6.3E-01	2.902	2.6E-05
		Sb01g005720	9.47E-03	0.689	7.6E-01	3.647	1.8E-08
		Sb01g040580	6.45E-08	-0.213	9.5E-01	4.296	2.9E-16
		Sb07g024270	6.31E-08	-0.713	7.6E-01	-7.811	5.3E-11
		Sb05g008830	1.21E-04	1.702	2.8E-01	-6.135	5.3E-06
		Sb09g025570	5.14E-04	-0.516	8.8E-01	-5.362	1.2E-04
		Sb09g025510	3.64E-31	4.027	2.0E-20	-4.279	1.3E-23
Lignin biosynthesis	O-methyltransferase	*Sb07g005970*	1.28E-02	-	-	-3.549	3.5E-02
		Sb04g036900	1.30E-02	0.142	9.8E-01	-2.100	9.8E-03
		Sb04g037820	3.18E-06	2.324	1.3E-09	-2.072	5.8E-03
		Sb10g027340	9.98E-03	-1.463	3.9E-01	3.450	2.5E-02
		Sb10g027360	1.08E-02	-0.614	8.0E-01	5.882	1.7E-05
		Sb10g030970	5.91E-05	1.278	3.7E-01	-2.836	4.3E-19
Aerobic respiration -- electron donor II	1,3-beta-glucan synthase component domain containing protein	*Sb03g023490*	3.71E-03	0.133	9.7E-01	-1.741	8.6E-08
		Sb10g005550	2.74E-09	0.755	6.1E-02	-1.607	1.1E-05

		Sb04g008830	1.57E-02	-0.602	7.3E-01	1.304	5.8E-04
		Sb03g030800	1.14E-03	-0.887	2.3E-01	0.907	1.1E-02
	Autophagy protein 9	*Sb01g041090*	2.94E-04	-0.301	8.2E-01	1.160	3.2E-07
	COX VIIa	*Sb02g041360*	3.34E-03	-0.074	9.8E-01	1.015	1.7E-06
	Cytochrome b6-f complex iron-sulfur subunit, chloroplast precursor	*Sb09g020820*	2.29E-02	0.614	5.4E-01	-1.715	1.6E-02
		Sb01g004390	3.98E-02	0.007	1.0E+00	0.905	7.4E-05
	Cytochrome b-c1 complex subunit 7	*Sb01g008560*	8.59E-03	-0.216	9.1E-01	0.914	1.4E-05
		Sb10g005110	3.25E-03	-0.239	9.1E-01	1.324	3.9E-05
		Sb05g002090	1.55E-03	-0.029	9.9E-01	1.479	3.8E-10
	cytochrome c oxidase assembly protein COX11	*Sb01g010010*	4.42E-02	-0.339	7.4E-01	0.446	1.5E-01
	cytochrome c oxidase polypeptide Vc	*Sb08g018180*	2.56E-04	-0.082	9.8E-01	1.583	1.0E-12
	Cytochrome c oxidase subunit 5B, mitochondrial precursor	*Sb09g030230*	4.60E-03	0.167	9.4E-01	-1.281	1.3E-03
		Sb03g027710	9.35E-03	0.073	9.7E-01	0.842	2.6E-04
	Cytochrome c oxidase subunit	*Sb02g039590*	1.92E-02	0.556	8.9E-01	4.555	2.6E-03
		Sb01g006750	2.57E-05	-0.198	9.1E-01	1.380	5.2E-12
		Sb09g021110	4.43E-02	2.253	6.6E-02	-0.799	5.8E-01
		Sb09g028410	3.37E-02	1.492	1.1E-01	-0.308	5.9E-01
	DnaJ domain containing protein	*Sb09g002340*	2.63E-03	0.152	9.6E-01	-1.357	1.3E-03
		Sb03g041460	9.42E-03	0.762	6.1E-01	-1.311	3.2E-04
		Sb07g014620	9.97E-04	-	-	6.005	7.5E-06
	DUF617 domain containing protein	*Sb02g026900*	1.34E-05	1.616	3.3E-01	-6.015	1.9E-08
	DUF617 domain containing protein	*Sb04g030260*	8.71E-09	-0.050	9.9E-01	-5.638	9.4E-21
	ELMO/CED-12 family protein	*Sb01g036800*	7.41E-03	-0.129	9.5E-01	0.783	2.5E-04
	ELMO/CED-12 family protein	*Sb05g001780*	2.70E-02	-0.239	9.1E-01	0.962	3.1E-03
		Sb06g024240	3.56E-03	0.186	9.3E-01	-1.080	2.7E-04
	Expressed protein	*Sb08g020220*	4.45E-02	0.313	8.4E-01	-0.639	1.1E-02
		Sb02g038790	5.95E-04	-0.212	9.0E-01	1.750	2.7E-04
	Histone-lysine N-methyltransferase, H3 lysine-9 specific SUVH1	*Sb06g001340*	2.69E-02	0.029	9.9E-01	-0.767	2.9E-03
	Histone-lysine N-methyltransferase	*Sb06g024160*	3.07E-04	0.350	6.5E-01	-0.674	3.0E-03
	Nodulin	*Sb06g013900*	2.84E-02	-0.734	7.1E-01	1.423	6.2E-03
	PPR repeat domain containing protein	*Sb06g024190*	2.02E-04	0.512	7.5E-01	-2.174	7.7E-05
		Sb01g021270	4.06E-02	1.356	6.0E-02	-0.277	6.8E-01
	Sodium/calcium exchanger protein	*Sb03g008600*	1.90E-03	-0.275	6.4E-01	0.588	2.6E-02
		Sb08g022240	4.37E-02	1.818	2.9E-03	3.673	1.6E-11
	Ubiquinol-cytochrome c reductase complex 6.7 kDa protein	*Sb02g043020*	1.17E-02	-0.128	9.6E-01	1.094	5.0E-06
	Ubiquinol-cytochrome C reductase hinge protein	*Sb04g022156*	1.58E-03	-0.405	7.3E-01	0.947	1.6E-06
	YDG/SRA domain containing protein	*Sb07g019860*	1.28E-02	0.354	8.9E-01	-1.461	2.1E-03
		Sb02g023620	1.22E-02	0.800	1.5E-01	-0.205	4.8E-01
	Potassium transporter	*Sb06g028380*	3.91E-02	0.903	1.9E-01	-0.390	4.0E-01
	Transmembrane 9 superfamily member	*Sb04g029570*	4.25E-02	-0.043	9.8E-01	0.335	7.4E-02
		Sb03g024550	3.00E-07	-0.844	5.3E-01	-6.449	1.7E-26
	Auxin-induced protein 5NG4	*Sb02g035040*	1.38E-07	0.777	5.9E-01	-4.623	3.0E-14
		Sb07g023970	2.98E-10	-0.450	7.2E-01	-4.456	3.6E-31
Aerobic respiration -- electron donor III		*Sb10g000830*	2.03E-02	-1.743	4.5E-02	-4.006	9.3E-26
	Nodulin	*Sb02g025210*	2.17E-03	1.066	4.2E-01	-1.860	5.7E-03
		Sb07g022685	8.88E-05	0.618	7.3E-01	-3.742	5.8E-08
	Potassium transporter	*Sb02g000340*	5.17E-03	-0.553	7.8E-01	-3.630	7.5E-07
		Sb06g028130	5.96E-05	0.092	9.5E-01	-0.858	2.7E-04
		Sb03g045180	5.07E-04	0.474	5.8E-01	-1.018	1.3E-04
	Transmembrane 9 superfamily member	*Sb07g024530*	1.56E-02	-0.063	9.8E-01	-0.882	1.3E-04

	integral membrane protein	*Sb01g033660*	8.26E-07	-1.159	1.2E-01	2.278	1.0E-07
		Sb10g029500	2.99E-02	-0.072	9.9E-01	2.345	1.3E-05
		Sb02g042430	1.65E-05	-0.537	4.3E-01	0.915	6.8E-06
		Sb10g009770	1.74E-03	0.004	1.0E+00	1.880	4.5E-06
	Potassium transporter	*Sb07g006000*	2.38E-09	-0.659	1.8E-01	2.481	4.1E-10
		Sb03g044780	2.68E-09	-1.431	9.8E-02	3.533	2.8E-10
		Sb03g044790	4.12E-08	0.239	9.3E-01	4.092	9.4E-20
		Sb10g000940	2.24E-03	-0.217	8.9E-01	0.869	2.3E-05
	RNA recognition motif containing protein	*Sb01g008070*	3.37E-02	-0.209	9.0E-01	0.984	1.3E-02
		Sb01g010170	1.92E-10	-0.947	5.2E-01	4.282	9.1E-32
		Sb08g004730	1.11E-02	-0.091	9.4E-01	0.484	2.9E-02
		Sb01g041650	7.13E-07	-0.309	4.9E-01	0.602	9.9E-04
		Sb02g032530	6.30E-10	-0.540	2.1E-01	1.172	8.6E-08
	Transmembrane 9 superfamily member	*Sb07g016310*	6.61E-05	-0.409	6.7E-01	1.253	2.7E-06
		Sb04g029560	3.93E-16	-1.006	1.6E-03	1.862	3.3E-11
		Sb10g025700	9.21E-09	-0.864	5.9E-01	3.909	1.5E-33
		Sb10g025690	1.27E-10	-1.640	6.2E-02	4.106	9.6E-19
Nitrate reduction I	Laccase precursor protein	*Sb08g011530*	2.07E-11	-1.372	4.5E-01	9.344	2.9E-76
		Sb04g027860	1.30E-02	-0.420	9.1E-01	7.480	2.1E-31
	Laccase-23 precursor	*Sb05g000680*	2.96E-03	-	-	3.995	7.0E-05
Chlorophyll a degradation	Chlorophyllase-2, chloroplast precursor	*Sb02g012300*	1.28E-02	-	-	7.654	1.1E-10
	NBS-LRR disease resistance protein	*Sb05g003950*	3.79E-03	-0.743	5.4E-01	1.474	3.4E-03
		Sb09g003990	2.53E-02	-	-	3.037	8.4E-02
	Resistance protein LR10	*Sb02g002770*	1.20E-02	-0.335	6.8E-01	0.762	3.8E-02
	Stripe rust resistance protein Yr10	*Sb05g024900*	9.73E-05	0.459	5.6E-01	-1.128	2.1E-04
Calvin cycle	ABC transporter, ATP-binding protein	*Sb10g028530*	5.70E-04	0.169	9.0E-01	-1.459	6.9E-04
	ADP-ribosylation factor	*Sb01g033450*	2.20E-03	-0.581	4.3E-01	0.750	2.1E-02
	Histidine triad family protein	*Sb08g002160*	1.12E-02	-0.457	4.6E-01	0.352	2.5E-01
		Sb09g025640	1.45E-07	0.443	7.2E-01	-2.949	3.4E-06
		Sb10g030070	1.77E-02	-	-	-2.260	3.0E-02
		Sb06g017650	2.02E-02	-	-	2.248	9.0E-02
		Sb02g005790	4.25E-02	-0.221	8.9E-01	0.637	1.6E-02
		Sb01g002980	3.12E-02	-0.179	9.2E-01	0.675	2.4E-03
		Sb04g033160	2.87E-02	-0.324	8.3E-01	0.759	7.2E-03
		Sb10g021730	1.89E-03	-0.230	8.7E-01	0.841	1.6E-05
	Ras-related protein	*Sb03g030650*	1.25E-03	-0.647	3.6E-01	0.945	1.1E-02
		Sb03g025350	1.34E-03	-0.154	9.3E-01	1.015	9.2E-06
		Sb03g001085	4.80E-03	-0.348	8.2E-01	1.067	8.8E-05
		Sb07g026600	5.20E-05	-0.476	5.8E-01	1.089	6.8E-06
		Sb09g028560	2.68E-03	-0.313	7.8E-01	1.101	1.5E-03
		Sb09g000550	1.23E-02	-0.317	8.8E-01	1.375	6.3E-04
		Sb06g019620	4.08E-05	-0.217	9.1E-01	1.518	8.8E-14
		Sb01g044440	4.02E-29	-1.633	1.6E-02	5.389	1.3E-38
	Ribulose bisphosphate carboxylase small chain	*Sb05g003480*	3.14E-03	0.948	3.9E-01	-1.655	1.6E-03
Gamma glutamyl cycle	AAA family ATPase	*Sb03g029270*	7.88E-04	0.069	9.9E-01	2.139	2.1E-09
	AAA-type ATPase family protein	*Sb01g016970*	3.32E-03	0.944	1.6E-01	3.000	2.9E-12
	Aspartyl protease family protein	*Sb09g028060*	8.40E-03	-	-	2.987	5.5E-03
	ATPase 3	*Sb08g023150*	4.17E-02	-2.375	1.7E-02	-0.243	7.7E-01
		Sb08g023140	4.63E-02	-2.166	4.9E-02	-0.028	9.8E-01
	ATPase	*Sb01g034560*	2.24E-02	0.933	4.6E-01	-1.062	2.9E-02

		Sb02g005600	8.62E-03	-1.470	6.2E-02	0.747	2.0E-01
	BCS1 protein	*Sb02g034790*	1.68E-14	-2.214	5.8E-04	4.035	1.0E-07
	Chaperone protein dnaJ	*Sb01g013390*	1.00E-03	0.462	6.6E-01	-0.977	6.1E-07
		Sb01g005860	2.63E-02	0.484	7.2E-01	-0.689	2.5E-04
	Dual specificity protein phosphatase	*Sb10g003660*	3.64E-03	0.424	5.6E-01	-0.655	5.7E-02
	FGGY family of carbohydrate kinases	*Sb06g030210*	2.01E-02	0.418	3.7E-01	-0.354	2.4E-01
	Gamma-glutamyltranspeptidase 1 precursor	*Sb06g018740*	1.51E-07	-0.491	7.8E-01	2.849	5.3E-19
		Sb01g041250	4.70E-08	1.004	1.1E-01	-2.080	1.1E-07
	Heat shock protein DnaJ	*Sb03g009120*	3.49E-02	0.217	9.6E-01	-1.603	2.9E-05
		Sb02g023210	4.08E-03	-	-	5.068	4.3E-04
	Homeobox and START domains containing protein	*Sb07g002780*	3.70E-04	-0.412	8.5E-01	-2.980	7.1E-12
		Sb01g022420	4.51E-03	-	-	-3.187	6.4E-02
		Sb02g030660	8.92E-03	0.896	9.9E-02	-0.637	1.6E-01
		Sb06g024480	1.14E-06	1.246	4.7E-01	-6.119	3.0E-10
	Homeobox associated leucine zipper	*Sb02g027300*	2.38E-07	-0.232	9.2E-01	-4.594	1.1E-15
		Sb02g026150	5.91E-05	-0.128	9.8E-01	-3.905	9.6E-12
		Sb07g029150	6.78E-07	-0.156	9.6E-01	-3.196	3.4E-20
		Sb01g044620	2.28E-03	-0.664	6.3E-01	1.465	6.0E-05
	OsSub52 - Putative Subtilisin homologue	*Sb10g028870*	3.75E-02	0.038	9.9E-01	-1.635	5.7E-04
		Sb03g002260	2.29E-02	-	-	-3.251	2.2E-02
	Peptide-N4-asparagine amidase A	*Sb03g002270*	8.25E-04	1.490	2.7E-01	-3.057	8.8E-05
		Sb09g019510	3.96E-07	0.858	2.6E-01	-2.071	1.8E-05
		Sb10g007520	1.24E-02	-	-	-6.678	2.9E-07
		Sb04g028940	2.27E-02	0.384	9.4E-01	-3.364	4.8E-02
		Sb04g027290	1.00E-03	0.092	9.8E-01	-2.817	3.7E-08
		Sb02g012910	6.54E-07	-1.547	1.2E-01	2.812	1.2E-11
	Plastocyanin-like domain containing protein	*Sb01g010500*	1.32E-08	0.181	9.4E-01	3.844	6.7E-21
		Sb06g018350	5.09E-05	-	-	4.315	7.1E-09
		Sb02g012920	1.20E-19	-1.990	6.4E-02	5.085	1.6E-30
		Sb01g010510	8.57E-16	-0.766	7.1E-01	7.606	1.1E-85
		Sb10g009630	1.02E-14	-	-	8.503	1.0E-18
	Polygalacturonase	*Sb04g002530*	1.53E-02	1.919	8.2E-02	-0.618	4.7E-01
		Sb03g004360	7.80E-03	-0.159	9.3E-01	1.453	5.6E-02
	Purine permease	*Sb09g028020*	4.36E-02	-	-	-4.873	8.3E-04
		Sb03g031210	2.75E-07	0.390	8.5E-01	-3.727	5.0E-09
	Puromycin-sensitive aminopeptidase	*Sb04g007610*	8.03E-04	-0.435	7.2E-01	1.252	7.1E-06
	WRKY10	*Sb03g003360*	1.57E-02	0.667	7.5E-01	-1.670	1.0E-04
	WRKY102	*Sb03g003640*	2.85E-02	0.365	8.7E-01	-1.336	3.7E-03
	WRKY11	*Sb03g028530*	5.48E-07	-0.994	5.0E-01	3.653	5.0E-12
	WRKY16	*Sb03g030480*	4.23E-02	-0.375	8.4E-01	0.825	2.0E-02
	WRKY26	*Sb03g032800*	7.71E-04	-0.199	9.8E-01	5.623	8.0E-39
	WRKY3	*Sb01g007570*	2.17E-02	-1.196	3.1E-01	1.029	2.4E-01
	WRKY36	*Sb06g024220*	4.56E-05	0.363	9.0E-01	-2.774	1.8E-05
		Sb04g033240	1.27E-02	-	-	-1.627	7.7E-02
	WRKY67	*Sb09g005700*	4.72E-03	-0.646	7.8E-01	2.424	2.0E-06
	WRKY72	*Sb05g017130*	1.79E-09	-0.676	6.1E-01	3.130	9.5E-24
	WRKY77	*Sb03g026170*	8.31E-03	-	-	3.043	1.4E-03
	Zinc finger C-x8-C-x5-C-x3-H type family protein	*Sb03g009930*	6.89E-04	0.166	8.3E-01	-0.543	1.3E-02
Glutathione-mediated detoxification	Glutathione S-transferase, N-terminal domain containing protein	*Sb02g003090*	2.25E-20	-0.940	6.2E-01	7.878	2.1E-89
		Sb05g007005	2.40E-04	-0.637	3.3E-01	1.033	2.2E-03

		Sb03g025210	3.74E-05	0.629	8.3E-01	-5.179	4.7E-11
		Sb01g030800	3.03E-11	1.552	2.1E-02	-2.410	6.4E-11
		Sb01g030810	6.85E-03	0.914	6.2E-01	-2.058	6.0E-05
		Sb08g007310	3.50E-02	0.147	9.6E-01	-1.320	3.0E-03
		Sb09g003700	4.16E-02	-1.415	1.7E-01	0.294	6.8E-01
		Sb09g003750	5.00E-04	-	-	4.463	2.1E-04
		Sb03g015070	4.27E-02	-	-	0.811	6.7E-01
		Sb04g023210	2.75E-02	-0.253	9.0E-01	0.930	1.5E-03
		Sb09g003690	1.22E-06	-1.221	4.1E-02	1.052	4.2E-05
		Sb01g005990	3.13E-02	-0.252	9.4E-01	1.395	1.4E-06
		Sb01g006010	7.49E-03	-0.160	9.7E-01	2.069	8.4E-07
		Sb03g045840	8.83E-04	-1.241	4.3E-01	2.164	5.3E-05
		Sb08g006690	1.25E-05	-1.070	2.7E-01	2.174	5.7E-07
		Sb05g001525	3.60E-02	-0.898	7.3E-01	2.244	8.0E-03
		Sb01g031030	7.76E-05	-1.035	4.2E-01	2.437	7.4E-09
		Sb08g007300	1.10E-04	-1.001	4.2E-01	2.608	4.2E-07
	Glutathione S-transferase	*Sb01g030930*	4.84E-05	-	-	3.231	3.6E-16
		Sb01g006000	6.19E-08	-0.113	9.8E-01	3.350	5.3E-17
		Sb02g027080	3.75E-09	-0.322	8.6E-01	3.793	1.6E-09
		Sb01g030870	6.19E-04	-0.061	9.9E-01	3.825	3.0E-10
		Sb01g030790	1.27E-02	0.095	9.9E-01	3.902	2.8E-07
		Sb03g031780	6.48E-04	-0.284	9.5E-01	4.035	2.9E-11
		Sb03g045830	4.29E-09	-0.966	4.4E-01	4.178	1.3E-13
		Sb04g022250	1.57E-04	-0.014	1.0E+00	4.591	6.0E-26
		Sb01g030980	2.09E-20	-0.040	9.9E-01	5.577	7.1E-89
		Sb01g030830	5.52E-03	0.703	8.4E-01	5.988	6.7E-06
		Sb01g031040	2.43E-07	-	-	6.583	2.3E-15
		Sb01g030990	5.25E-17	-	-	6.826	4.5E-08
		Sb01g031020	3.11E-03	-	-	7.167	9.4E-09
		Sb01g031000	2.48E-35	-2.419	1.1E-03	7.237	2.8E-40
		Sb01g031010	5.80E-14	-	-	7.480	3.9E-10
		Sb01g031050	4.03E-06	-	-	8.004	1.3E-11
		Sb02g038130	2.30E-34	-	-	9.543	1.0E-35
		Sb01g038900	7.40E-05	-1.399	3.2E-01	3.575	1.9E-09
	IN2-1 protein	*Sb01g038910*	2.34E-04	-1.216	1.1E-01	1.013	4.8E-04
		Sb09g002800	1.78E-03	1.195	8.8E-02	-0.486	5.4E-02
	Microsomal glutathione S-transferase 3	*Sb01g010540*	3.03E-02	-0.035	9.9E-01	1.163	5.8E-06
	Puromycin-sensitive aminopeptidase	*Sb07g019810*	3.29E-02	0.221	8.0E-01	1.048	4.0E-04
Flavonoid biosynthesis	AMP-binding domain containing protein	*Sb01g048390*	2.17E-02	-1.263	4.3E-01	-4.693	7.8E-23
		Sb07g022040	1.40E-06	-0.407	9.3E-01	6.187	4.5E-20
	AMP-binding enzyme	*Sb04g001460*	1.57E-02	0.006	1.0E+00	1.900	7.4E-08
	Chalcone synthase	*Sb05g020160*	6.71E-06	-2.168	1.2E-01	8.847	3.3E-15
		Sb05g020220	6.08E-03	-	-	7.051	1.2E-14
		Sb05g020230	3.70E-03	-0.825	7.1E-01	6.264	1.5E-07
Betanidine degradation	Acetyl-CoA carboxylase	*Sb06g003090*	8.72E-06	0.615	4.0E-01	-1.265	2.2E-07
	Atypical receptor-like kinase MARK	*Sb01g042480*	4.18E-02	0.434	9.2E-01	-2.979	9.3E-04
	Auxin response factor 5	*Sb04g003240*	3.33E-02	0.312	9.3E-01	-1.704	1.1E-07
	Bromodomain domain containing protein	*Sb04g025160*	3.15E-02	-0.059	9.7E-01	0.712	2.1E-02
	Copine	*Sb03g043290*	1.33E-04	-0.148	9.6E-01	1.972	2.9E-14
	Copine-1	*Sb10g023860*	6.54E-07	-0.698	3.0E-01	1.751	5.2E-08

Copine-6	*Sb07g002700*	6.42E-06	-0.806	3.6E-01	1.476	1.0E-07
	Sb01g034710	5.58E-08	0.982	5.2E-01	-6.415	9.2E-07
	Sb01g034460	1.72E-05	-0.422	9.0E-01	-5.320	1.2E-17
	Sb01g034470	2.77E-02	-	-	-5.186	3.2E-04
	Sb01g016900	3.09E-04	0.662	8.2E-01	-4.083	1.4E-11
Cytochrome P450	*Sb02g025840*	2.47E-03	-0.484	8.7E-01	-3.986	1.2E-12
	Sb02g007420	2.58E-03	-0.031	1.0E+00	-2.788	2.3E-07
	Sb01g034730	3.40E-02	-	-	-1.856	3.1E-01
	Sb04g024710	2.92E-08	-	-	5.641	2.7E-12
	Sb04g024730	1.13E-20	-	-	6.414	1.9E-31
Ethylene-insensitive protein	*Sb03g001440*	2.48E-02	-0.085	9.7E-01	-1.118	8.9E-05
Expressed protein	*Sb04g020200*	9.28E-16	1.145	1.2E-03	-1.942	3.5E-08
Glycerol-3-phosphate dehydrogenase	*Sb03g037280*	1.07E-02	-0.198	9.4E-01	1.347	1.0E-04
Glycosyltransferase family 43 protein	*Sb03g011010*	1.35E-05	-0.716	6.2E-01	2.436	7.8E-07
	Sb03g007030	9.11E-06	-	-	-3.883	5.6E-04
Inactive receptor kinase At2g26730 precursor	*Sb09g030250*	1.98E-02	0.135	9.8E-01	-2.206	3.3E-06
	Sb02g024230	5.13E-06	-0.702	7.2E-01	3.712	3.0E-08
	Sb04g028850	4.52E-03	-0.265	9.6E-01	-4.579	1.4E-07
	Sb02g030900	6.61E-05	-0.031	1.0E+00	-3.502	3.9E-13
	Sb02g024640	8.86E-05	-0.333	8.8E-01	-3.155	6.5E-07
	Sb05g027360	1.22E-03	0.414	8.8E-01	-2.161	1.2E-14
	Sb07g024970	6.48E-06	0.713	5.5E-01	-2.031	2.9E-07
MYB family transcription factor	*Sb08g018370*	5.10E-03	-0.567	7.8E-01	1.693	4.1E-05
	Sb05g026820	4.71E-26	-0.876	2.8E-02	2.342	4.7E-22
	Sb01g047450	2.05E-02	-	-	2.467	1.2E-01
	Sb04g026210	2.10E-02	-	-	2.931	5.8E-05
	Sb03g012310	3.07E-03	0.383	9.4E-01	6.210	1.2E-27
OsSub51 - Putative Subtilisin homologue	*Sb10g024550*	2.04E-12	0.084	9.8E-01	-5.155	4.9E-17
OsSub28 - Putative Subtilisin homologue	*Sb01g041350*	2.50E-04	1.242	5.4E-01	-5.118	3.3E-04
OsSub56 - Putative Subtilisin homologue	*Sb07g022170*	1.39E-02	1.737	2.7E-01	-2.279	2.2E-01
OsSub45 - Putative Subtilisin homologue	*Sb06g025980*	3.60E-02	1.211	5.3E-01	-2.082	2.7E-02
OsSub61 - Putative Subtilisin homologue	*Sb01g031090*	5.13E-03	2.440	5.8E-02	-1.388	1.8E-01
OsSub41 - Putative Subtilisin homologue	*Sb06g016860*	2.81E-05	0.000	1.0E+00	1.624	3.3E-09
OsSub59 - Putative Subtilisin homologue	*Sb02g030760*	4.59E-07	0.071	9.8E-01	1.913	4.0E-09
OsSub35 - Putative Subtilisin homologue	*Sb06g001140*	4.36E-02	-	-	2.181	8.3E-02
OsSub3 - Putative Subtilisin homologue	*Sb03g033440*	4.96E-02	0.033	1.0E+00	3.496	2.7E-06
OsFBX390 - F-box domain containing protein	*Sb04g007355*	2.35E-02	-	-	5.096	4.1E-04
	Sb03g004380	1.13E-03	-	-	-6.322	3.9E-27
	Sb10g010040	2.21E-02	-0.055	1.0E+00	-4.847	9.3E-04
	Sb09g024590	1.96E-06	0.224	9.6E-01	-4.310	2.2E-08
	Sb10g021610	3.99E-05	0.103	9.8E-01	-4.143	6.1E-16
	Sb01g031740	2.19E-02	-	-	-4.082	1.0E-02
	Sb08g016840	3.30E-03	-	-	-3.584	3.3E-05
Peroxidase precursor	*Sb05g009400*	1.75E-02	-	-	-3.329	5.4E-02
	Sb04g008590	2.72E-02	-	-	-2.895	1.0E-01
	Sb10g027490	3.49E-02	0.342	9.4E-01	-2.663	2.8E-03
	Sb06g027520	5.02E-04	0.928	2.2E-01	-2.078	1.3E-03
	Sb02g037840	4.94E-03	1.552	2.4E-01	-1.964	8.4E-02
	Sb03g010740	2.62E-02	0.113	9.8E-01	-1.619	1.6E-04
	Sb03g024460	7.89E-03	1.924	2.0E-02	-1.288	3.5E-01

		Sb04g038610	3.10E-02	1.669	2.1E-01	-1.221	2.6E-01
		Sb01g049140	2.15E-02	1.092	4.3E-01	-0.999	4.2E-02
		Sb03g010250	7.64E-03	1.582	1.4E-01	-0.796	2.9E-01
		Sb05g001030	3.40E-02	-0.385	8.3E-01	1.078	2.2E-02
		Sb09g004650	3.30E-03	-1.060	4.2E-01	1.574	9.0E-05
		Sb09g004660	3.48E-02	-	-	1.724	3.1E-01
		Sb10g028500	4.84E-02	0.360	9.0E-01	2.291	3.2E-07
		Sb03g036760	1.78E-07	-1.329	1.9E-01	2.916	2.8E-05
		Sb09g020960	3.77E-02	-	-	3.354	2.2E-02
		Sb03g046760	1.41E-06	-0.600	8.3E-01	3.940	1.5E-64
		Sb06g030940	1.19E-04	-	-	5.274	1.9E-04
		Sb05g001000	2.57E-10	-	-	6.071	1.4E-08
		Sb09g021000	5.30E-04	-	-	6.133	4.5E-06
		Sb01g020830	2.92E-08	-0.562	8.1E-01	6.170	1.1E-21
		Sb03g013200	4.21E-04	-	-	7.646	1.0E-10
		Sb03g013210	9.52E-10	0.762	7.9E-01	9.079	1.1E-86
		Sb01g041760	3.43E-04	-	-	9.278	8.2E-27
	Prephenate dehydratase domain containing protein	*Sb02g011470*	3.17E-02	-0.148	9.5E-01	0.836	2.3E-03
		Sb04g023710	3.08E-03	-	-	-4.858	8.7E-04
		Sb01g044010	1.07E-03	0.019	1.0E+00	-2.956	5.0E-09
		Sb06g018600	3.35E-02	0.682	7.8E-01	-1.793	3.2E-03
		Sb02g024060	7.94E-07	0.921	1.6E-01	-1.406	1.4E-06
	Transporter family protein	*Sb08g016520*	1.93E-02	-0.152	9.6E-01	1.248	7.2E-05
		Sb01g044000	1.89E-08	-1.060	3.5E-02	1.268	7.7E-06
		Sb05g025290	9.02E-03	-0.452	8.8E-01	2.053	2.0E-05
		Sb06g023360	2.77E-03	-0.400	8.8E-01	2.431	6.4E-06
		Sb0391s002020	2.04E-11	-	-	4.848	1.5E-22
		Sb06g032120	5.13E-05	0.428	6.1E-01	-1.132	1.2E-06
		Sb09g022600	1.04E-02	0.538	7.3E-01	-1.047	8.6E-10
		Sb06g026250	4.71E-02	0.245	9.1E-01	-0.960	1.1E-01
		Sb02g037390	8.24E-03	0.274	8.4E-01	-0.739	1.0E-02
	Ubiquitin-conjugating enzyme	*Sb09g007410*	3.11E-02	0.143	9.2E-01	-0.568	2.8E-02
		Sb03g030840	3.98E-04	-0.459	3.6E-01	0.583	1.4E-02
		Sb01g030580	1.46E-02	-0.272	8.2E-01	0.653	8.8E-03
		Sb02g021080	4.37E-02	-0.292	8.7E-01	0.655	3.3E-03
		Sb04g001680	2.13E-05	-0.939	4.6E-01	2.420	3.5E-15
Salicylate biosynthesis	Phenylalanine ammonia-lyase	*Sb06g022750*	1.32E-05	-1.949	1.8E-01	5.078	1.2E-31
		Sb04g026560	2.98E-03	-1.423	3.8E-01	2.046	1.5E-05
Chorismate biosynthesis	3-phosphoshikimate 1-carboxyvinyltransferase, chloroplast precursor	*Sb10g002230*	1.06E-02	-0.044	9.9E-01	1.234	5.6E-05
	Adenylate kinase	*Sb06g000495*	1.16E-02	0.182	9.4E-01	-1.113	4.3E-05
	Anthranilate phosphoribosyltransferase	*Sb06g034070*	1.47E-05	1.604	8.0E-03	-2.180	3.5E-04
		Sb02g033370	1.86E-02	-0.682	2.5E-01	0.290	3.4E-01
	Bifunctional 3-dehydroquinate dehydratase/shikimate dehydrogenase	*Sb03g018040*	4.96E-02	0.145	9.4E-01	1.020	5.3E-04
	Chorismate synthase 2, chloroplast precursor	*Sb01g040790*	7.60E-03	-0.176	9.0E-01	1.091	2.4E-03
	CS domain containing protein	*Sb01g027930*	4.52E-03	0.522	8.0E-01	-1.782	2.3E-04
	Disease resistance protein RPM1	*Sb10g028720*	2.36E-05	-0.640	6.4E-01	1.936	5.2E-06
	MCM9 - Putative minichromosome maintenance MCM family subunit 9	*Sb10g007540*	2.23E-02	-	-	-2.298	1.1E-01
	NB-ARC domain containing protein	*Sb09g004240*	1.69E-02	0.166	9.7E-01	2.084	1.7E-05
	NBS-LRR disease resistance protein	*Sb05g003930*	5.94E-04	-0.797	3.9E-01	1.230	3.1E-04
		Sb05g003920	4.74E-05	-0.853	3.5E-01	1.418	2.1E-05

	Phospho-2-dehydro-3-deoxyheptonate aldolase, chloroplast precursor	*Sb01g033590*	6.01E-03	-0.885	4.4E-01	1.170	3.3E-03
		Sb02g039660	4.59E-04	-1.150	3.2E-01	1.804	3.1E-06
	Shikimate/quinate 5-dehydrogenase	*Sb06g030160*	2.80E-06	1.076	1.9E-01	-1.931	1.1E-07
	Signal recognition particle receptor subunit beta	*Sb05g000300*	4.21E-03	0.160	9.5E-01	-1.212	2.2E-03
	Stripe rust resistance protein Yr10	*Sb05g027240*	7.30E-03	-0.182	9.7E-01	-2.766	8.5E-17
		Sb05g024910	4.31E-03	-	-	1.998	3.3E-06
		Sb08g001580	6.17E-06	0.071	9.8E-01	-1.615	1.5E-09
	Transporter-related	*Sb01g019150*	1.93E-03	-0.869	2.5E-01	0.792	1.4E-02
		Sb02g037520	6.89E-08	-0.241	7.8E-01	1.089	2.5E-08
		Sb04g032940	4.56E-02	-	-	-2.999	8.8E-02
		Sb10g028110	3.71E-03	0.790	3.2E-01	-1.044	6.3E-02
	AP2 domain containing protein	*Sb06g024530*	1.16E-02	-	-	3.992	1.9E-08
		Sb07g023030	2.54E-02	-	-	4.162	2.7E-06
		Sb09g021540	1.68E-03	-	-	4.254	7.1E-04
		Sb04g027180	1.85E-06	-0.330	9.5E-01	5.844	4.4E-33
	Dehydration-responsive element-binding protein	*Sb01g031140*	3.66E-02	-	-	4.441	6.0E-04
		Sb10g001620	6.94E-03	0.487	9.0E-01	5.009	5.6E-14
	Ethylene-responsive transcription factor	*Sb06g024355*	1.07E-02	0.028	9.9E-01	1.784	7.4E-05
		Sb08g004260	6.96E-04	-	-	4.277	2.1E-06
	Expressed protein	*Sb02g012630*	2.18E-02	-	-	2.596	3.0E-02
Tetrahydrofolate biosynthesis I	Formate--tetrahydrofolate ligase	*Sb02g026140*	3.75E-02	0.085	9.8E-01	1.070	3.7E-08
	Formyl transferase	*Sb01g050510*	2.94E-10	1.010	5.9E-02	-1.402	5.9E-07
	GTP cyclohydrolase I 1	*Sb06g031800*	2.75E-12	-0.573	2.9E-01	1.942	2.8E-13
		Sb01g020570	3.19E-03	-1.216	1.2E-01	0.994	3.9E-02
		Sb06g002560	4.57E-02	-	-	2.519	4.8E-02
	Inorganic phosphate transporter	*Sb06g002800*	7.03E-05	-0.031	1.0E+00	2.741	5.1E-12
		Sb01g020580	4.07E-06	-	-	3.726	6.1E-08
		Sb07g023780	5.78E-18	-1.944	1.8E-01	6.645	3.4E-45
		Sb01g023950	6.32E-05	-0.524	3.2E-01	-1.772	8.9E-17
	Transporter family protein	*Sb02g032700*	2.61E-03	-0.336	6.8E-01	0.724	9.7E-03
		Sb01g020990	8.70E-06	-0.197	8.6E-01	1.256	6.8E-06
		Sb02g026280	3.28E-09	-1.413	1.3E-02	1.380	9.0E-05
	1-aminocyclopropane-1-carboxylate oxidase protein	*Sb09g003800*	1.02E-03	-1.924	1.5E-01	1.698	3.6E-08
		Sb09g003790	1.57E-04	-2.034	1.5E-01	3.879	5.8E-08
	26S proteasome non-ATPase regulatory subunit 4	*Sb01g026350*	1.94E-02	-	-	3.321	1.6E-03
Ethylene biosynthesis	Aminotransferase, classes I and II	*Sb02g000780*	4.03E-04	0.506	6.4E-01	-1.307	2.1E-06
from methionine	BTBN10 - Bric-a-Brac, Tramtrack	*Sb01g006980*	2.82E-02	0.755	5.2E-01	-1.513	1.9E-01
	BTBN17 - Bric-a-Brac, Tramtrack	*Sb01g013680*	1.12E-02	-0.087	9.9E-01	-2.806	1.4E-10
	BTBN2 - Bric-a-Brac, Tramtrack	*Sb06g001450*	3.93E-02	-0.501	7.8E-01	-2.141	1.8E-06
	Oxidoreductase, short chain dehydrogenase	*Sb02g042120*	4.11E-02	-	-	0.871	1.7E-01
	Single myb histone	*Sb03g026470*	2.88E-02	0.059	9.8E-01	-0.594	7.8E-03
		Sb01g016630	1.25E-06	-	-	-4.219	1.9E-18
	AMP-binding domain containing protein	*Sb03g042910*	1.83E-06	0.770	4.7E-01	-2.489	6.9E-07
		Sb01g048050	3.01E-02	1.279	1.4E-01	-0.654	3.8E-01
		Sb07g007810	3.16E-04	-1.447	4.8E-02	0.935	5.3E-02
Methionine biosynthesis II	Anthranilate phosphoribosyltransferase	*Sb01g013120*	4.48E-03	-	-	-3.773	2.1E-02
	Cysteine synthase, chloroplast precursor	*Sb03g037860*	3.23E-03	-0.079	9.8E-01	-1.452	1.2E-04
	Cysteine synthase, mitochondrial precursor	*Sb03g009260*	1.02E-03	-0.719	2.6E-01	0.656	1.2E-02
	Dehydrogenase	*Sb07g025220*	1.39E-04	0.247	9.4E-01	3.164	6.8E-16
	GHMP kinases ATP-binding protein	*Sb03g037310*	2.18E-02	0.325	7.4E-01	-0.450	2.4E-02

	Homocysteine S-methyltransferase protein	*Sb03g036040*	4.31E-04	-	-	2.077	1.6E-02
		Sb01g042580	1.55E-04	-	-	3.696	1.3E-05
	Mitochondrial carrier protein	*Sb10g023470*	2.13E-02	0.132	9.5E-01	-0.793	1.2E-03
		Sb01g036806	1.70E-02	-0.334	8.5E-01	0.821	5.8E-02
		Sb03g025740	7.19E-04	-0.229	8.1E-01	0.628	1.5E-03
		Sb04g008020	3.85E-05	-0.387	7.6E-01	1.616	2.1E-08
		Sb03g032590	6.15E-13	-0.559	4.5E-01	2.106	3.8E-16
		Sb01g023070	5.90E-03	0.447	8.7E-01	3.149	4.4E-10
	OsClp11 - Putative Clp protease homologue	*Sb01g027680*	3.77E-02	0.361	7.2E-01	-0.558	9.1E-02
	Pleckstrin homology domain-containing protein	*Sb02g041730*	2.08E-02	0.396	7.3E-01	-0.617	1.1E-02
		Sb05g003310	3.58E-02	0.293	9.0E-01	-1.102	4.3E-02
	rhoGAP domain containing protein	*Sb06g026110*	4.09E-02	-1.043	2.4E-01	0.282	5.0E-01
		Sb04g031870	5.56E-05	-0.420	4.6E-01	0.954	1.1E-03
	Serine esterase	*Sb10g029410*	4.71E-02	-0.007	1.0E+00	-0.663	2.0E-02
	Stromal membrane-associated protein	*Sb04g006690*	7.75E-03	0.526	7.6E-01	-1.270	6.7E-05
		Sb09g022100	2.53E-02	1.380	4.5E-01	-2.121	1.5E-02
	Transporter family protein	*Sb02g037580*	4.96E-20	-0.906	2.6E-02	2.697	6.4E-21
		Sb01g042690	1.05E-14	-2.280	1.4E-05	4.284	3.2E-15
	YCF37	*Sb04g037030*	1.34E-04	1.467	5.3E-02	-3.064	3.6E-02
Brassinosteroid biosynthesis II	3-beta hydroxysteroid dehydrogenase/isomerase family protein	*Sb08g005500*	2.34E-07	0.620	6.2E-01	-3.263	2.3E-11
	3-oxo-5-alpha-steroid 4-dehydrogenase	*Sb03g040050*	1.79E-04	0.178	9.6E-01	-2.153	3.3E-07
		Sb02g003510	3.82E-02	-	-	-2.154	9.9E-02
	Aldose 1-epimerase	*Sb06g018830*	3.93E-04	-	-	4.645	3.2E-13
	Astaxanthin synthase KC28	*Sb05g002420*	8.56E-05	0.652	4.6E-01	-2.210	2.0E-05
	Cell division inhibitor	*Sb04g038640*	1.11E-06	0.920	1.5E-01	-1.713	5.9E-06
	Cinnamoyl-CoA reductase-related	*Sb09g029490*	1.16E-02	-0.576	7.2E-01	1.090	5.1E-03
	Cysteine proteinase A494 precursor	*Sb02g033270*	8.70E-03	-	-	5.313	1.6E-04
	Cytochrome P450	*Sb03g002870*	1.83E-08	0.927	3.7E-01	-4.279	3.2E-13
		Sb05g002580	5.42E-03	0.964	2.2E-01	-0.906	4.4E-02
	Isoflavone reductase	*Sb03g008760*	7.30E-03	-1.036	2.2E-01	-3.953	2.4E-04
		Sb03g029820	7.04E-07	1.427	4.7E-04	-1.456	5.9E-03
	leucoanthocyanidin reductase	*Sb06g029550*	1.48E-16	-	-	6.565	3.3E-30
	NAD dependent epimerase	*Sb06g028720*	8.52E-04	-0.400	6.5E-01	1.045	3.2E-04
		Sb07g023080	1.11E-05	0.763	5.9E-01	-2.739	4.8E-11
		Sb01g035100	1.07E-02	1.001	2.4E-01	-1.098	6.5E-02
		Sb05g022890	6.93E-03	-0.302	8.2E-01	0.731	2.8E-04
		Sb10g025740	6.94E-05	-0.421	7.8E-01	1.518	2.0E-08
		Sb02g038530	2.86E-02	-	-	2.269	1.4E-03
		Sb01g021890	5.94E-11	-1.097	1.0E-01	2.381	2.6E-15
		Sb02g038520	3.26E-05	-1.006	4.4E-01	2.638	1.3E-09
		Sb01g035380	1.52E-07	-0.178	9.5E-01	3.575	1.1E-16
	Oryzain beta chain precursor	*Sb06g030800*	2.30E-05	-1.058	3.4E-01	2.172	3.2E-11
	Os1bglu1 - beta-mannosidase/glucosidase homologue	*Sb03g008350*	3.88E-02	-1.954	7.0E-02	0.920	6.0E-01
	Os4bglu14 - monolignol beta-glucoside homologue	*Sb06g022450*	1.67E-03	-0.707	4.4E-01	-3.250	2.6E-05
	Os6bglu24 - beta-glucosidase homologue	*Sb10g012220*	1.65E-02	-	-	-1.952	9.0E-03
	Sterol-4-alpha-carboxylate 3-dehydrogenase	*Sb02g029890*	2.69E-04	0.041	9.8E-01	-1.101	1.1E-05
Sterol biosynthesis	Cycloartenol synthase	*Sb06g015960*	3.29E-06	0.945	5.8E-01	-3.084	8.6E-10
		Sb08g019310	1.89E-04	-0.047	9.9E-01	-3.041	6.7E-09
		Sb08g019300	2.54E-05	0.131	9.7E-01	-3.021	6.1E-10
		Sb08g019290	1.32E-06	0.127	9.6E-01	-2.306	1.3E-11

		Sb07g006300	2.93E-02	0.820	5.4E-01	-0.979	5.6E-02
	Cycloartenol-C-24-methyltransferase 1	*Sb01g004300*	3.62E-19	0.268	9.3E-01	-6.791	1.4E-52
	Cycloeucalenol cycloisomerase	*Sb09g002170*	9.42E-03	-	-	-2.151	1.0E-02
		Sb05g022370	4.60E-02	-	-	-4.138	9.5E-03
	Cytochrome P450 51	*Sb08g002250*	1.75E-03	-0.207	9.1E-01	-1.780	5.4E-09
		Sb02g036650	2.23E-02	-	-	5.130	6.0E-04
	Delta14-sterol reductase	*Sb04g017400*	4.87E-02	-0.465	8.4E-01	0.964	2.6E-07
	Prenyltransferase	*Sb01g044560*	3.52E-03	0.927	3.9E-01	-1.370	4.1E-02
Trans, trans-farnesyl diphosphate biosynthesis	Para-hydroxybenzoate--polyprenyltransferase	*Sb04g038180*	8.36E-06	0.248	8.8E-01	-1.489	4.7E-07
	polyprenyl synthetase	*Sb07g005530*	4.17E-03	0.548	7.7E-01	-1.670	2.6E-03
		Sb10g027240	3.06E-03	-0.255	7.6E-01	0.757	1.0E-02
	1-aminocyclopropane-1-carboxylate oxidase 2	*Sb01g000660*	1.47E-02	-0.136	9.8E-01	1.780	3.6E-04
	DANA2	*Sb01g000680*	3.27E-04	0.091	9.6E-01	-1.058	3.7E-05
		Sb06g032090	1.04E-02	0.865	4.4E-01	-1.050	4.1E-02
	Flavonol synthase/flavanone 3-hydroxylase	*Sb10g004340*	2.12E-03	0.122	9.4E-01	1.049	8.5E-05
		Sb03g038880	4.75E-07	-0.105	9.8E-01	5.527	5.3E-25
		Sb01g029140	2.52E-08	-0.312	9.4E-01	5.932	3.6E-19
		Sb09g020760	2.98E-02	-	-	-4.085	1.4E-03
	Gibberellin 20 oxidase 2	*Sb01g014540*	8.87E-04	1.268	3.1E-01	-2.268	2.0E-03
		Sb02g012470	2.77E-02	-0.577	5.6E-01	1.771	2.2E-02
Gibberellin biosynthesis	Gibberellin 2-beta-dioxygenase 7	*Sb02g000460*	1.70E-02	0.819	7.2E-01	-3.678	2.8E-02
	Gibberellin 3-beta-dioxygenase 2-2	*Sb03g004020*	1.14E-06	-0.585	8.4E-01	3.574	1.6E-14
	Hydroxylase	*Sb10g005170*	1.81E-05	1.946	6.2E-03	-0.988	4.3E-03
	Leucoanthocyanidin dioxygenase	*Sb06g014550*	2.28E-03	1.449	1.0E-01	-0.867	6.7E-02
		Sb01g038520	1.13E-07	-	-	4.050	5.8E-17
		Sb06g026350	6.71E-03	-2.311	7.6E-02	1.273	1.6E-01
	Naringenin,2-oxoglutarate 3-dioxygenase	*Sb06g026330*	4.40E-06	-	-	3.671	1.9E-12
		Sb06g026340	2.58E-04	-	-	5.311	2.6E-08
	Oxidoreductase	*Sb01g031160*	1.73E-03	0.029	9.9E-01	1.336	6.4E-09
		Sb07g022500	2.85E-02	-0.756	1.0E-02	0.104	8.1E-01
		Sb06g017670	1.46E-02	-1.040	4.4E-01	1.091	1.5E-02
		Sb06g017680	5.68E-03	-0.803	3.2E-01	1.092	2.2E-02
	12-oxophytodienoate reductase	*Sb10g007300*	3.08E-02	-	-	2.111	1.9E-03
		Sb10g007310	2.84E-04	-0.988	5.6E-01	3.048	1.1E-06
		Sb10g007330	3.20E-04	-0.940	6.6E-01	3.144	1.3E-09
		Sb09g000520	3.09E-06	-0.473	8.5E-01	5.201	2.7E-04
		Sb10g007320	7.34E-04	-	-	5.990	2.6E-16
	14-3-3 protein	*Sb07g025680*	6.55E-04	-0.612	2.2E-01	0.430	3.8E-02
	Cysteine proteinase 1 precursor	*Sb04g017830*	1.05E-09	-1.711	4.6E-03	1.665	8.5E-13
Jasmonic acid biosynthesis	Cytochrome P450	*Sb01g007000*	6.35E-04	-0.498	8.5E-01	2.467	2.0E-13
		Sb06g017700	3.30E-02	0.395	6.1E-01	-0.617	1.0E-01
	Expressed protein	*Sb03g026050*	1.17E-03	0.095	9.8E-01	3.414	1.4E-14
		Sb03g039130	1.97E-02	-	-	5.099	5.4E-04
	lipoxygenase protein	*Sb06g018040*	1.23E-04	-0.294	9.4E-01	2.816	3.1E-23
		Sb01g011050	5.99E-04	2.331	8.5E-05	-0.300	6.1E-01
	Lipoxygenase	*Sb06g031350*	6.88E-04	1.344	4.9E-01	-4.604	2.5E-14
		Sb01g011040	1.01E-03	0.147	9.6E-01	-2.357	1.1E-06
	NAC domain transcription factor	*Sb03g037940*	1.79E-04	-0.183	9.7E-01	3.469	7.7E-24
	NAC domain-containing protein 67	*Sb02g006680*	4.11E-02	-0.643	7.7E-01	1.355	9.0E-04
		Sb01g003710	9.02E-03	0.381	8.9E-01	3.163	2.2E-08

		Sb05g003400	6.54E-03	-	-	2.349	6.2E-02
		Sb07g001400	2.79E-05	-1.186	4.9E-02	0.702	7.4E-02
		Sb01g028450	9.36E-03	-1.653	2.1E-02	0.057	9.2E-01
		Sb08g022560	4.93E-02	-	-	0.850	3.2E-01
		Sb07g001550	6.92E-12	0.745	6.0E-01	-6.064	7.1E-09
		Sb10g002120	2.20E-02	-	-	-5.240	2.3E-04
		Sb04g026440	3.82E-05	1.692	2.9E-01	-5.160	2.8E-04
	no apical meristem protein	*Sb03g042210*	1.88E-02	0.409	8.5E-01	-1.486	1.1E-02
		Sb01g036590	1.88E-02	-0.082	9.8E-01	1.444	1.2E-03
		Sb03g041920	4.38E-02	0.220	9.5E-01	1.837	1.1E-08
		Sb06g017190	1.39E-02	0.255	9.4E-01	2.237	5.0E-17
		Sb05g001590	9.52E-06	-1.161	3.5E-01	2.243	7.9E-15
		Sb08g021080	6.52E-04	-0.218	8.7E-01	2.400	2.1E-05
		Sb06g028800	1.45E-04	-0.507	8.7E-01	3.426	3.9E-10
		Sb10g027100	1.06E-06	-0.769	6.1E-01	4.406	2.3E-13
		Sb03g001520	1.75E-05	1.314	5.1E-01	-6.489	6.0E-10
	Nodulin MtN3 family protein	*Sb03g041740*	3.76E-06	0.044	9.9E-01	-4.031	3.3E-20
		Sb03g024250	7.20E-17	-0.145	9.6E-01	3.842	7.8E-44
		Sb02g029430	1.46E-02	-	-	5.247	2.3E-04
	Phospholipase A2	*Sb01g040430*	4.76E-05	2.527	3.7E-03	-1.772	1.0E-01
		Sb01g010640	2.01E-15	0.916	4.2E-01	-6.590	9.6E-11
	Thiol protease SEN102 precursor	*Sb05g021550*	1.57E-02	0.182	9.8E-01	3.604	1.8E-14
	ABC-2 type transporter domain containing protein	*Sb03g042560*	3.91E-06	1.021	6.2E-01	-4.978	3.8E-09
	Anthocyanidin 3-O-glucosyltransferase	*Sb03g040840*	1.42E-05	-1.612	1.7E-01	2.435	1.2E-04
		Sb10g006140	1.37E-04	-	-	5.402	8.7E-09
		Sb09g026260	1.63E-03	-	-	-4.950	6.2E-04
		Sb09g026270	4.71E-04	0.105	9.8E-01	-3.561	2.2E-04
		Sb05g017280	2.54E-03	-0.573	7.3E-01	-3.353	1.9E-04
		Sb03g033890	9.78E-04	0.638	6.9E-01	-2.471	2.0E-04
	Anthocyanidin 5,3-O-glucosyltransferase	*Sb03g033810*	1.21E-03	0.133	9.7E-01	-2.371	3.5E-09
		Sb03g033830	3.03E-03	0.385	8.5E-01	-1.892	5.4E-05
		Sb08g019890	2.69E-02	0.374	8.7E-01	-1.166	1.3E-03
		Sb09g026250	2.77E-03	-0.460	6.0E-01	0.757	1.3E-02
		Sb03g033833	1.46E-02	-0.039	9.9E-01	1.595	5.8E-03
		Sb03g033880	2.97E-04	-	-	2.037	8.1E-03
Cytokinins glucoside biosynthesis		*Sb10g010343*	5.05E-03	-	-	-2.959	5.0E-04
	Anthocyanin 3-O-beta-glucosyltransferase	*Sb02g038560*	2.57E-02	0.639	7.8E-01	-1.809	6.6E-03
		Sb03g029060	1.13E-02	-0.323	9.1E-01	1.719	1.4E-05
		Sb05g002710	1.79E-06	-0.763	7.3E-01	3.789	1.8E-21
		Sb03g002810	5.83E-05	-	-	-6.954	5.7E-08
		Sb09g018640	2.20E-07	-0.325	9.2E-01	-4.934	3.0E-18
	Cytokinin dehydrogenase precursor	*Sb01g019000*	2.19E-02	-0.102	9.8E-01	-2.836	5.9E-04
		Sb03g045410	1.34E-02	-1.087	5.1E-01	1.702	1.1E-03
		Sb03g003280	4.23E-03	-	-	1.852	4.1E-04
		Sb03g036160	1.10E-02	0.296	9.6E-01	4.019	2.4E-13
	cytokinin-N-glucosyltransferase 1	*Sb02g007090*	4.32E-02	-	-	3.426	7.0E-09
		Sb07g028920	2.10E-06	-0.882	6.1E-01	3.733	5.9E-08
	Cytokinin-O-glucosyltransferase 1	*Sb01g001220*	1.69E-02	2.033	1.5E-01	-1.597	3.2E-01
		Sb06g018460	9.73E-06	2.888	1.3E-03	-2.778	1.0E-02
		Sb04g023930	1.58E-03	-0.127	9.8E-01	1.839	3.7E-10

	Sb04g023530	1.81E-02	0.220	9.3E-01	1.884	2.4E-05
	Sb07g021090	9.96E-06	-0.798	4.9E-01	2.421	1.4E-09
	Sb04g027420	2.00E-05	0.528	8.7E-01	5.296	6.1E-24
	Sb04g023920	5.34E-13	-0.694	8.0E-01	7.949	8.2E-57
	Sb07g002470	4.25E-03	1.035	2.7E-01	-2.469	1.1E-01
	Sb10g007060	1.96E-03	0.143	9.8E-01	-3.562	6.5E-06
Digalactosyldiacylglycerol synthase, chloroplast precursor	*Sb05g003730*	2.60E-03	0.545	5.6E-01	-1.102	1.6E-03
	Sb04g007220	2.81E-06	1.021	2.3E-01	-2.234	3.0E-05
Flavonol-3-O-glycoside-7-O-glucosyltransferase 1	*Sb03g004130*	6.89E-08	-1.318	2.3E-02	1.959	3.4E-06
	Sb03g004140	7.77E-07	-	-	6.582	8.8E-13
Glucosyltransferase	*Sb02g005940*	9.00E-03	-	-	5.816	1.9E-05
Hydroquinone glucosyltransferase	*Sb03g028190*	5.26E-03	1.588	9.5E-02	-1.175	1.7E-01
	Sb09g006910	3.04E-02	-0.569	8.9E-01	2.647	1.1E-09
Indole-3-acetate beta-glucosyltransferase	*Sb06g030880*	6.99E-03	-	-	1.738	2.9E-03
	Sb02g033580	5.09E-11	-	-	7.840	2.1E-11
Limonoid UDP-glucosyltransferase	*Sb03g005340*	1.44E-04	-	-	-5.261	1.9E-04
	Sb04g005960	2.67E-02	-0.197	9.6E-01	1.339	9.3E-08
MGD2	*Sb07g027910*	2.36E-17	-3.515	4.5E-04	8.125	2.1E-35
Sucrose synthase	*Sb01g035890*	2.28E-03	0.953	2.4E-01	-1.003	9.0E-03
	Sb10g006330	5.40E-04	-0.018	1.0E+00	3.607	3.0E-26
	Sb02g023360	1.19E-02	-	-	1.087	2.7E-01
Transporter	*Sb02g023340*	2.85E-03	-0.797	5.9E-01	1.553	3.4E-06
	Sb01g004100	4.80E-11	-0.306	7.3E-01	1.564	3.5E-12
	Sb01g007620	2.99E-03	1.503	2.4E-01	-1.780	5.9E-02
	Sb10g023070	1.66E-03	-	-	-3.142	9.3E-04
	Sb02g007100	1.62E-05	2.019	5.4E-02	-2.920	4.1E-07
	Sb02g039670	3.04E-02	-	-	-2.825	1.8E-02
	Sb02g034130	9.29E-07	1.508	3.1E-02	-2.379	8.2E-03
	Sb01g007630	1.77E-05	1.255	9.1E-02	-1.851	1.3E-04
UDP-glucoronosyl and UDP-glucosyl transferase domain containing protein	*Sb03g032050*	1.05E-03	-0.810	4.4E-01	1.203	5.3E-04
	Sb04g008700	1.12E-04	-0.643	7.1E-01	2.121	2.6E-07
	Sb02g030020	1.79E-02	-	-	2.676	2.2E-05
	Sb06g020440	2.31E-06	-0.597	7.8E-01	2.930	7.6E-07
	Sb02g034110	1.53E-12	0.382	7.9E-01	4.672	8.4E-24
	Sb02g030050	1.68E-02	-	-	4.895	8.6E-04
	Sb02g030040	5.83E-09	-1.552	3.3E-01	7.161	2.7E-17
	Sb06g020400	2.19E-02	-	-	-2.538	9.3E-03
UDP-glucoronosyl/UDP-glucosyl transferase	*Sb01g031560*	8.41E-03	-	-	2.886	5.3E-12
	Sb06g002180	1.27E-02	-0.018	1.0E+00	3.400	7.1E-03
UNE2	*Sb07g020120*	1.97E-07	0.227	9.4E-01	3.582	1.3E-26

*Geno × Trt = genotype by treatment interaction where treatment consists of *M. phaseolina* and control inoculations. †MP = *M. phaseolina*, CON = control. ‡ log2 DE = log2 fold differential expression.